

**X-RAY, DIELECTRIC AND ELECTRO-OPTIC STUDIES
ON FLUORINATED ACHIRAL AND CHIRAL LIQUID
CRYSTALS**

A Thesis submitted to the University of North Bengal

For the Award of

Doctor of Philosophy

in

Physics

**BY
DEBASHIS SINHA**

**GUIDE
PROF. PRADIP KUMAR MANDAL**

**Department of Physics
University of North Bengal
Rajarammohunpur, Dist: Darjeeling, Pin: 734013
West Bengal, India**

September 2015

*DEDICATED TO MY PARENTS, MY ELDER
BROTHER AND MY ELDER SISTER*

DECLARATION

I declare that the thesis entitled "**X-ray, dielectric and electro-optic studies on fluorinated achiral and chiral liquid crystals**" has been prepared by me under the guidance of Dr. Pradip Kr. Mandal, Professor, Department of Physics, University of North Bengal. No part of this thesis has formed the basis for the award of any degree or fellowship previously.

Debashis Sinha

Debashis Sinha

Department of Physics
University of North Bengal
P.O.: North Bengal University
Siliguri, Dist.: Darjeeling

Date: 11.09.2015

DEPARTMENT OF PHYSICS
UNIVERSITY OF NORTH BENGAL

P.O. North Bengal University, Siliguri, Dist. Darjeeling, West Bengal, Pin - 734013, India

Website: www.nbu.ac.in



Phone: +91-(0) 353-2776338, Fax: +91-(0) 353-2699001

ENLIGHTENMENT TO PERFECTION

CERTIFICATE

I certify that Mr. Debashis Sinha has prepared the thesis entitled "**X-RAY, DIELECTRIC AND ELECTRO-OPTIC STUDIES ON FLUORINATED ACHIRAL AND CHIRAL LIQUID CRYSTALS**" for the award of Ph.D. degree of the University of North Bengal, under my guidance. He has carried out the work at the Department of Physics, University of North Bengal.

Prof. Pradip Kumar Mandal

Department of Physics
University of North Bengal
P.O.: North Bengal University
Siliguri, Dist.: Darjeeling
Pin: 734013

Date: 11.09.2015

ABSTRACT

LIQUID CRYSTAL is a thermodynamic stable phase characterized by anisotropy of properties, lying in between crystalline solid and isotropic liquid and hence termed as mesophase. As research into this field continues and applications for this special kind of materials are still being discovered, liquid crystals will play an important role in many areas of science and technology. The most common application of liquid crystal technology is liquid crystal displays (LCDs). Performance of a liquid crystal (LC) display device depends on the nature of the LC material and the construction of the device. Fluoro-substituted LC materials are found to be useful in large information content display devices. High birefringence liquid crystals are important for fast switching display and various other applications like laser beam steering, tunable color filters, focus tunable lens, electrically controlled phase shifter in GHz and THz region. Besides Ferroelectric liquid crystals (FLCs) are very promising due to their various interesting basic properties. FLCs are also effective for fast switching electro-optical displays with wide viewing angle. Keeping all this in view, nine fluorinated achiral and 3 fluorinated chiral (ferroelectric) liquid crystalline compounds have been selected for investigation. Various physical properties have been studied using optical polarizing microscopy, X-ray diffraction, optical birefringence, dielectric spectroscopy and electro-optic methods.

The first Chapter of this thesis contains a brief introduction to liquid crystal (LC) physics, which includes a description of different types of ordering as well as the effect of fluorination on liquid crystalline materials. In the second Chapter all relevant experimental procedures and theoretical back-grounds have been described in details.

Two doubly fluorinated (2TP-3',3F-4NCS, 4TP-3',3F-4NCS) and one singly fluorinated (2TP-3'F-4NCS) isothiocyanato terphenyl compounds exhibiting a broad range of nematic phase were investigated by X-ray, dielectric and optical methods and compared with their properties to see the effect of fluorination and chain flexibility. Contrary to common perception, weak antiparallel correlation of isothiocyanato molecules is observed in each compound both from X-ray and dielectric studies. All the compounds exhibit high birefringence (0.373 - 0.331). They also show high order parameters at low temperatures. These results have been described in Chapter 3.

Chapter four deals with dielectric behavior of six fluorinated bicyclohexyl compounds (3ccp-f, 3ccp-ff, 3ccp-fff and 5ccp-f, 5ccp-ff, 5ccp-fff) and crystal structure analysis of one of them (5ccp-fff). It is observed that as number of fluorine increases threshold voltage (V_{th}) as well as driving voltage (V_d) decrease considerably in both the series (3ccp series & 5ccp series) while with increasing chain length V_{th} and V_d increases slightly except in triply fluorinated compound. Dielectric anisotropy increases as number of fluorine atom increases in a particular series. The splay elastic constant (K_{11}) is found to exhibit similar decreasing trend with temperature as observed in dielectric anisotropy. Only one strong dielectric absorption process is exhibited by the compounds which were almost Debye type.

In Chapter five, two partially fluorinated ferroelectric liquid crystals (4F3R, 4F6R) are investigated by X-ray diffraction, dielectric relaxation spectroscopy and electrooptic techniques. One of the compounds possesses SmC^* phase and the other possesses SmC^* phase as well as SmC_A^* phase. Tilt angle, measured by X-ray and optical methods are found to be high. Only Goldstone mode relaxation process is observed. Increase of dielectric strength and critical frequency with temperature has been explained in the light of generalized Landau model. No soft mode is observed since the compound directly melts into isotropic phase. Both of them possess moderate value of spontaneous polarization and the data fitted nicely to mean-field model. Fitted critical exponent (0.29 and 0.33) suggests that SmC^*-I transition is first order which is supported by DSC measurements. The compound 4F3R induces ferroelectric phase even below room temperature when mixed in a proper host mixture.

In Chapter six, phase behavior, structure and molecular dynamics of a chiral liquid crystalline compound, which exhibits SmG^* , SmJ^* , SmF^* , SmI^* , SmC^* , SmA^* , N^* and BP^* , have been presented. Observed optical textures, synchrotron radiation diffraction data and frequency dependent dielectric spectroscopic study clearly depict the temperature evolution of the different hexatic smectic phases along with cholesteric and blue phase in a single compound. In hexatic phases dielectric absorption spectra show one low frequency relaxation process, related to the phase fluctuation of the bond orientational order, and one high frequency process related to amplitude fluctuation of the bond orientational order coupled with the polarization and tilt of the molecules. Goldstone and soft mode relaxation processes are detected, respectively, in SmC^* and SmA^* phases.

Conclusions of all the experimental results have been summarized in Chapter seven.

PREFACE

The present dissertation entitled “**X-RAY, DIELECTRIC AND ELECTRO-OPTIC STUDIES ON FLUORINATED ACHIRAL AND CHIRAL LIQUID CRYSTALS**” is submitted to fulfill the requirements for the degree of Doctor of Philosophy (Science) of University of North Bengal. This dissertation explores various fruitful results of different physical properties of a few fluorinated achiral and chiral liquid crystalline compounds investigated by different experimental techniques. The analysis presented in this dissertation evaluates the benefits of choosing such compounds for successful application of liquid crystals in many areas of science and technology. All the studies have been carried out in Liquid Crystal Research Laboratory, Department of Physics, University of North Bengal under the supervision of Prof. Pradip Kumar Mandal, Department of Physics, University of North Bengal, Siliguri-734013. A very small part of the research work has been performed in Deutsches Elektronen-Synchrotron (DESY), Hamburg, Germany.

The thesis consists of seven chapters. The first Chapter of this thesis contains a brief introduction to liquid crystal (LC) physics and the list of investigated compounds. The basic theory and experimental procedures followed for studying different properties of liquid crystalline materials is described in Chapter 2. In Chapter 3, two doubly fluorinated and one singly fluorinated isothiocyanato terphenyl compounds have been investigated by X-ray, dielectric and optical methods. Chapter 4 describes dielectric behavior of six fluorinated bicyclohexyl compounds (3ccp-f, 3ccp-ff, 3ccp-fff and 5ccp-f, 5ccp-ff, 5ccp-fff) and structure property of one of them (5ccp-fff) by crystal structure analysis. In Chapter 5, two partially fluorinated ferroelectric liquid crystals (4F3R, 4F6R) are investigated by X-ray diffraction, dielectric relaxation spectroscopy and electrooptic techniques. Phase behavior, structure and molecular dynamics of a chiral liquid crystalline compound, which exhibits SmG*, SmJ*, SmF*, SmI*, SmC*, SmA*, N* and BP* phases, have been investigated in Chapter 6. A brief summary of all the experimental results is given in Chapter 7.

A list of selected books and monographs on liquid crystals has been listed in **Appendix A**. All of the results incorporated in this dissertation have already been published in different international scientific journals, a list of which is given in **Appendix B**.

Debashis Sinha

Debashis Sinha

Department of Physics

University of North Bengal

ACKNOWLEDGEMENTS

This thesis is the outcome of the learning, education, guidance and inspiration I received from my supervisor Prof. P. K. Mandal, Department of Physics, University of North Bengal. I start by expressing my sincere thanks and deep gratitude to my supervisor Prof. P. K. Mandal, for his supervision and constant help throughout the period of my research work. His guidance, support, encouragement and keen physical insight in each and every step of experimental works, results and discussions have been invaluable to me.

I express my heartfelt gratitude to Prof. R. Dabrowski, Military University of Technology, Warsaw, Poland for supplying most of the liquid crystal samples of good quality. I also like to thank him for invaluable suggestions.

A large debt of gratitude is owed to Prof. W. Haase, Institute of Physical Chemistry, Darmstadt University of Technology, Darmstadt, Germany for giving us an opportunity to perform some of the works on ferroelectric materials in his laboratory.

I also express my sincere thanks to Dr. K. Goubitz and Prof. H. Schenk, Crystallography Laboratory, University of Amsterdam, Amsterdam, the Netherlands for their help in crystallographic analysis.

I would also like to thank DST, India for providing financial assistance to perform experiments at Deutsches Elektronen-Synchrotron (DESY), Hamburg, Germany. Technical assistance during the experiment provided by Martin V Zimmermann and Olof Gutowski, DESY Photon Science is gratefully acknowledged.

I also like to thank Dr. Sripada Halder, Department of Physics, University of North Bengal for his help during experiments and data analysis.

I must not forget to thank and acknowledge Mr. Debarghya Goswami, Mr. Asim Debnath, and Mr. Kartick Chandra Dey, Department of physics, University of North Bengal, Senior researchers in the laboratory, for their kind cooperation and helpful assistance. I am thankful to Mr. Rajat Biswas and Miss. Aparna Ghosh, Department of physics, University of North Bengal, present Ph.D. students in the laboratory, for their cooperation. I greatly appreciate all my friends for sharing happiness and sadness all these years together.

The staff members of USIC are gratefully acknowledged for their help in constructing and fabricating the different parts of experimental set up. I like to thank Mr. Subrata Hazra, Technical Assiatant, Department of Physics, NBU for his help during experiments and Mr. Rajesh Pradhan, Technical Assiatant, Department of Physics, NBU for helping in maintaining the computer systems.

I also express my sincere thanks to the Head, Department of Physics, University of North Bengal for his kind co-operation. My special thanks to all the members of the Faculty, Non-teaching staff and Research Scholars of the Department of Physics, University of North Bengal for their kind hearted co-operation.

Last, but not the least, nothing could have been accomplished without support of my family. My sincere thanks to my parents, my elder brother and my elder sister for their unconditional love, patience and faith on me and encouraging me to complete the Ph.D work. Thank you all for always being there for me.

Place: University of North Bengal

Date: 11. 09. 2015

Debashis Sinha

Debashis Sinha

TABLE OF CONTENTS

Table of Contents.....	I – IV
List of Tables.....	V – VI
List of Figures.....	VII – XIII
List of Appendices.....	XIV

CHAPTERS

1. INTRODUCTION	1
1.1 INTRODUCTION	2
1.2 HISTORY OF LIQUID CRYSTALS	3
1.3 MOLECULAR ORDERING IN LIQUID CRYSTALS	4
1.4 CLASSIFICATION OF LIQUID CRYSTALS	4
1.4.1 THERMOTROPIC LIQUID CRYSTALS	6
1.4.2 ACHIRAL CALAMATIC LIQUID CRYSTALS	6
1.4.3 CHIRAL CALAMATIC LIQUID CRYSTALS	13
1.4.4 DISCOTIC LIQUID CRYSTALS	21
1.5 APPLICATIONS OF LIQUID CRYSTALS	21
1.6 LIQUID CRYSTAL COMPOUNDS INVESTIGATED IN THE PRESENT	
DISSERTATION	23
1.7 REFERENCES	26
2. EXPERIMENTAL TECHNIQUES AND ALLIED THEORY	33
2.1 INTRODUCTION	34
2.2 THEORIES OF LIQUID CRYSTALLINE PHASES	34
2.2.1 ORDER PARAMETER	35
MAIER-SAUPE MEAN FIELD THEORY OF NEMATIC PHASE	36
ORIENTATIONAL DISTRIBUTION FUNCTION AND EVALUATION	
OF ORDER PARAMETERS	37

	<i>MC MILLAN'S THEORY OF SMECTIC A PHASE</i>	38
2.2.2	MESOPHASE STRUCTURE: X-RAY DIFFRACTION	41
2.2.3	IDENTIFICATION OF MESOPHASES AND TRANSITION TEMPERATURES	45
2.2.4	OPTICAL BIREFRINGENCE	52
2.2.5	DIELECTRIC ANISOTROPY	57
	<i>MAIER AND MEIER THEORY OF DIELECTRICS FOR LIQUID CRYSTALS</i>	57
	<i>DIPOLE-DIPOLE CORRELATION FACTOR</i>	59
2.2.6	FREQUENCY DOMAIN DIELECTRIC SPECTROSCOPY	63
	<i>DEBYE AND COLE-COLE MODEL</i>	63
	<i>DIFFERENT RELAXATION PROCESSES IN CHIRAL AND ACHIRAL LIQUID CRYSTAL PHASES</i>	66
2.2.7	ELASTIC CONSTANTS	71
2.2.8	MEASUREMENT OF TILT ANGLE	74
2.2.9	SPONTANEOUS POLARIZATION	74
2.2.10	MEASUREMENT OF RESPONSE TIME: ELECTRICAL METHOD	77
2.2.11	ROTATIONAL VISCOSITY	77
2.2.12	THEORY OF CRYSTAL STRUCTURE DETERMINATION	78
2.3	REFERENCES	87
3.	HIGH BIREFRINGENCE LATERALLY FLUORINATED TERPHENYL ISOTHIOCYANATES: STRUCTURAL, OPTICAL AND DYNAMICAL PROPERTIES	101
3.1	INTRODUCTION	102
3.2	COMPOUNDS STUDIED	104
3.3	EXPERIMENTAL METHODS	105
3.4	RESULTS AND DISCUSSIONS	106

3.5 CONCLUSION	137
3.6 REFERENCES	138
4. INFLUENCE OF MOLECULAR STRUCTURE, FLUORINATION AND CHAIN LENGTH ON THE DIELECTRIC PROPERTIES OF NEMATOGENIC BI-CYCLOHEXYL PHENYL DERIVATIVES	145
4.1 INTRODUCTION	146
4.2 COMPOUNDS STUDIED	147
4.3 EXPERIMENTAL DETAILS	150
4.3.1 STRUCTURE DETERMINATION AND REFINEMENT	150
4.4 RESULTS AND DISCUSSION	151
4.5 CONCLUSION	180
4.6 REFERENCES	182
5. MOLECULAR AND DYNAMICAL PROPERTIES OF TWO PERFLUORINATED LIQUID CRYSTAL WITH DIRECT TRANSITION FROM FERROELECTRIC SmC* PHASE TO ISOTROPIC PHASE	190
5.1 INTRODUCTION	191
5.2 COMPOUNDS STUDIED	193
5.3 EXPERIMENTAL METHODS	194
5.4 RESULTS AND DISCUSSIONS	195
5.5 ROOM TEMPERATURE MIXTURE FORMULATION	216
5.6 CONCLUSION	217
5.7 REFERENCES	218

6. OPM, SYNCHROTRON X-RAY DIFFRACTION AND DIELECTRIC STUDY ON A CHIRAL BIPHENYL CARBOXYLATE	226
6.1 INTRODUCTION	227
6.2 COMPOUND STUDIED	228
6.3 EXPERIMENTAL METHODS	229
6.4 RESULTS AND DISCUSSIONS	230
6.5 CONCLUSION	244
6.6 REFERENCES	245
7. SUMMARY AND CONCLUSIONS	248

LIST OF TABLES

1.1 Molecular structures and transition temperatures of the investigated compounds	23
3.1 Molecular structures and transition temperatures of 2TP-3'F-4NCS, 2TP-3',3F-4NCS and 4TP-3',3F-4NCS	104
3.2 Optimized length, dipole moment and moment of inertia	110
3.3 Selected static dielectric parameters of compounds	120
3.4 Effective value of dipole moments (μ_{eff}) and dipole correlation factors (g_{λ})	121
3.5 Selected dynamic dielectric parameters of the compounds	130
3.6 Selected refractive indices (n_e & n_o), optical birefringence (Δn), density (ρ), polarizability anisotropy ($\Delta\alpha$) and order parameters $\langle P_2 \rangle$	136
4.1 Molecular structures and transition temperatures of the studied compounds	148
4.2 Phase transition temperatures ($^{\circ}\text{C}$) of 3ccp-ff, 3ccp-fff and related compounds	149
4.3 Important Crystallographic data	152
4.4 Optimized length, dipole moment and moment of inertia of the investigated Compounds	152
4.5 Fractional co-ordinates and equivalent isotropic thermal parameters of the non- Hydrogen atoms with e.s.d's in parentheses of 5ccp-fff	154
4.6 Anisotropic thermal parameters of the non-Hydrogen atoms with the e.s.d's in parantheses	155
4.7 Bond lengths (\AA) of the non-Hydrogen atoms with standard deviations in parentheses	156
4.8 Bond angles ($^{\circ}$) involving non-Hydrogen atoms with standard deviations in Parentheses	157
4.9 Selected intermolecular short contact distances less than 4.0 \AA of 5ccp-fff	159
4.10 Threshold voltage, driving voltage and driving field of the compounds	162
4.11 Effective values of dipole moments and dipole correlation factors	172

4.12 Relaxation frequency and activation energy of the studied compounds	180
5.1 Molecular structures and transition temperatures of the compounds 4F3R and 4F6R	194
5.2 Optimized length, dipole moment and moment of inertia of 4F3R and 4F6R	197
5.3 Weight percentage and transition temperatures of host compounds	216
6.1 Molecular structure and phase transition temperatures of MPOBC	228

LIST OF FIGURES

1.1 Typical structure of a rod-like liquid crystal molecule	5
1.2 Molecular arrangement in nematic phase	7
1.3 Molecular arrangement in SmA phase	9
1.4 Molecular arrangement in SmC phase, z is layer normal	10
1.5 Molecular arrangement in smectic B phase	11
1.6 Molecular arrangement of smectic I phase	12
1.7 Molecular arrangement of smectic F phase	12
1.8 Molecular arrangement in (a) crystal J and (b) crystal G phase	13
1.9 Molecular arrangement of cholesteric liquid crystal	14
1.10 Molecular arrangement of liquid crystal possessing blue phase	15
1.11 Basic structure of ferroelectric liquid crystal	16
1.12 Spiralling of the director in SmC* phase showing layer normal \mathbf{Z} , tilt angle θ , azimuthal angle Φ , molecular director \mathbf{n} and dipole moment \mathbf{p}_i	17
1.13 Molecular arrangement of antiferroelectric, ferrielectric and ferroelectric SmC* liquid crystal	18
1.14 The basic construction of the SSFLC display device showing (a) off state and (b) on state	19
1.15 Molecular arrangement of discotic liquid crystal	21
2.1 Typical scattering geometry showing the incident and scattered wave vector	41
2.2 Typical scattering geometry showing the incident (\mathbf{K}_i) and scattered (\mathbf{K}_s) wave vector	43
2.3 Polarizing microscope	46

2.4 Experimental setup for DSC measurement	47
2.5 X-ray diffraction experimental setup and diffraction photographs	48
2.6 Schematic representation of the X-ray diffraction pattern of an oriented (a) nematic and (b) smectic A phase	49
2.7 Synchrotron X-ray diffraction set up at DESY, Hamburg, Germany	52
2.8 Schematic arrangement for the measurement of refractive indices	54
2.9 A typical dielectric spectra for a Debye type liquid crystal	64
2.10 Cole-Cole plot for a Debye-type spectrum	66
2.11 The molecular aspect of different dielectric absorption peaks	68
2.12 Molecular arrangement of tilt angle fluctuation and phase fluctuation	69
2.13 Schematic arrangement for the measurement of dielectric permittivity	71
2.14 Molecular configuration of Splay, Twist and Bend elastic constants	72
2.15 Experimental set up to measure the value of P_s	76
3.1 Selected textures observed in 2TP-3'F-4NCS	107
3.2 Optimized structure of the compounds (a) 2TP-3'F-4NCS, (b) 2TP-3',3F-4NCS and (c) 4TP-3',3F-4NCS	109
3.3 X-ray diffraction photographs in (a) SmA phase (110°C) and (b) nematic phase (125°C) of 2TP-3'F-4NCS	111
3.4 X-ray diffraction photographs in nematic phase (95°C) of 2TP-3',3F-4NCS	111
3.5 X-ray diffraction photographs in (a) SmA phase (60°C) and (b) nematic phase (100°C) of 4TP-3',3F-4NCS	111
3.6 Temperature dependence of average intermolecular distance (D), smectic layer spacing (d) and apparent molecular length (l) of 2TP-3'F-4NCS	113
3.7 Temperature dependence of average intermolecular distance (D) and apparent molecular length (l) of 2TP-3',3F-4NCS	113
3.8 Temperature dependence of average intermolecular distance (D), smectic layer spacing (d) and apparent molecular length (l) of 4TP-3',3F-4NCS	114

3.9 Real part of dielectric constant (ϵ') in nematic phase as a function of bias voltage at 10 kHz in ITO cell for (a) 2TP-3' F-4NCS, (b) 2TP-3',3F-4NCS and (c) 4TP-3',3F-4NCS	116
3.10 Variation of static dielectric constants as a function temperature at 10 KHz in ITO cell in 2TP-3'F-4NCS	118
3.11 Variation of static dielectric constants as a function temperature at 10 KHz in ITO cell in 2TP-3',3F-4NCS	118
3.12 Variation of static dielectric constants as a function temperature at 10 KHz in ITO cell in 4TP-3',3F-4NCS	119
3.13 Temperature dependence of dielectric anisotropy of the compounds	119
3.14 Dispersion (a) and absorption (b) spectra at some selected temperatures in 2TP-3'F-4NCS. Solid curves in (b) represent curves fitted to modified Cole-Cole function as described in text	123
3.15 Dispersion (a) and absorption (b) spectra at some selected temperatures in 2TP-3',3F-4NCS. Solid curves in (b) represent curves fitted to modified Cole-Cole function as described in text	123
3.16 Dispersion (a) and absorption (b) spectra at some selected temperatures in 4TP-3',3F-4NCS. Solid curves in (b) represent curves fitted to modified Cole-Cole function as described in text	124
3.17 Cole-Cole plot in 2TP-3'F-4NCS	125
3.18 Cole-Cole in 2TP-3',3F-4NCS	125
3.19 Cole-Cole plot in 4TP-3',3F-4NCS	126
3.20 Temperature variation of relaxation frequency of compound 2TP-3'F-4NCS	127
3.21 Temperature variation of relaxation frequency of compound 2TP-3',3F-4NCS	127
3.22 Temperature variation of relaxation frequency of compound 4TP-3',3F-4NCS	128
3.23 Variation of $\ln\tau$ against $1000/T$ showing Arrhenius behavior in 2TP-3'F-4NCS	128
3.24 Variation of $\ln\tau$ against $1000/T$ showing Arrhenius behavior in 2TP-3',3F-4NCS	129
3.25 Variation of $\ln\tau$ against $1000/T$ showing Arrhenius behavior in 4TP-3',3F-4NCS	129
3.26 Temperature variation of splay elastic constant (K_{11}) of the three compounds	131
3.27 Temperature dependence of refractive indices (n_e , n_o , n_{av}) of the three compounds	132
3.28 Temperature variation of Δn of 2TP-3'F-4NCS, 2TP-3',3F-4NCS and 4TP-3',3F-4NCS	133
3.29 Temperature variation of density of 2TP-3'F-4NCS, 2TP-3',3F-4NCS and 4TP-3',3F-4NCS	134

3.30 Temperature variation of order parameters of 2TP-3',3F-4NCS, 2TP-3',3F-4NCS and 4TP-3',3F-4NCS	135
4.1 A perspective view of 5ccp-fff molecule with atom numbering scheme. Meaning of figures I-IV has been discussed in the text	153
4.2 Partial packing of 5ccp-fff molecule in the crystallographic unit cell	158
4.3 Crystal structure of 5ccp-fff projected along <i>a</i> -axis	158
4.4 Crystal structure of 5ccp-fff projected along <i>c</i> -axis	159
4.5 Different types of molecular associations observed in the crystal structure of 5ccp-fff	160
4.6 Real part of dielectric constant (ϵ') as a function of bias voltage at 10 kHz in 3ccp-f	163
4.7 Real part of dielectric constant (ϵ') as a function of bias voltage at 10 kHz in 3ccp-ff	163
4.8 Real part of dielectric constant (ϵ') as a function of bias voltage at 10 kHz in 3ccp-fff	164
4.9 Real part of dielectric constant (ϵ') as a function of bias voltage at 10 kHz in 5ccp-f	164
4.10 Real part of dielectric constant (ϵ') as a function of bias voltage at 10 kHz in 5ccp-ff	165
4.11 Real part of dielectric constant (ϵ') as a function of bias voltage at 10 kHz in 5ccp-fff	165
4.12 Temperature dependence of dielectric permittivity of compound 3ccp-f	166
4.13 Temperature dependence of dielectric permittivity of compound 3ccp-ff	167
4.14 Temperature dependence of dielectric permittivity of compound 3ccp-fff	167
4.15 Temperature dependence of dielectric permittivity of compound 5ccp-f	168
4.16 Temperature dependence of dielectric permittivity of compound 5ccp-ff	168
4.17 Temperature dependence of dielectric permittivity of compound 5ccp-fff	169
4.18 Temperature dependence of dielectric anisotropy ($\Delta\epsilon$) of the compounds	170
4.19 Temperature variation of splay elastic constant (K_{11}) of the compounds	171
4.20 Temperature variation of (a) real and (b) imaginary part of dielectric permittivity of 3ccp-f	173
4.21 Temperature variation of (a) real and (b) imaginary part of dielectric permittivity of 3ccp-ff	174
4.22 Temperature variation of (a) real and (b) imaginary part of dielectric permittivity of 3ccp-fff	174
4.23 Temperature variation of (a) real and (b) imaginary part of dielectric permittivity of 5ccp-f	175

4.24 Temperature variation of (a) real and (b) imaginary part of dielectric permittivity of 5ccp-ff	175
4.25 Temperature variation of (a) real and (b) imaginary part of dielectric permittivity of 5ccp-fff	176
4.26 Cole-cole plot of 3ccp-f	176
4.27 Cole-cole plot of 3ccp-ff	177
4.28 Cole-cole plot of 3ccp-fff	177
4.29 Cole-cole plot of 5ccp-f	178
4.30 Cole-cole plot of 5ccp-ff	178
4.31 Cole-cole plot of 5ccp-fff	179
5.1 Textures in different phases of compound 4F3R and 4F6R	196
5.2(a) Optimized geometry of 4F3R	198
5.2(b) Optimized geometry of 4F6R	198
5.3 X-ray diffraction photographs in different chiral smectic phases of 4F3R and 4F6R	199
5.4 Variations of average intermolecular distance (D) and layer spacing (d) with temperature in 4F3R	200
5.5 Variations of average intermolecular distance (D) and layer spacing (d) with temperature in 4F6R	201
5.6 Temperature variation of X-ray and optical tilt of 4F3R	202
5.7 Temperature variation of X-ray and optical tilt of 4F6R	203
5.8 (a) Real (ϵ') and (b) imaginary part (ϵ'') of dielectric constant as function of frequency at selected temperatures of 4F3R	204
5.9 (a) Real (ϵ') and (b) imaginary part (ϵ'') of dielectric constant as function of frequency at selected temperatures of 4F6R	204
5.10 Fitted spectra in SmC* phase (106 ⁰ C) of 4F3R along with observed data. GM, ITO and σ curves are also shown separately along with fitted parameters	205
5.11 Cole-Cole plot of 4F3R	205

5.12 Variation of (a) dielectric increment ($\Delta\epsilon$) and (b) Goldstone mode relaxation frequency (f_c) as a function of temperature for 4F3R	208
5.13 Variation of (a) dielectric increment ($\Delta\epsilon$) and (b) Goldstone mode relaxation frequency (f_c) as a function of temperature for 4F6R	208
5.14 Input and output signals captured in a digital oscilloscope for (a) 4F3R and (b) 4F6R	210
5.15 Temperature dependence of P_s of 4F3R. Mean field fitted curve is also shown	211
5.16 Temperature dependence of P_s of 4F6R. Mean field fitted curve is also shown	211
5.17 Variation of rotational viscosity (γ_ϕ) with temperature of 4F3R	213
5.18 Variation of rotational viscosity (γ_ϕ) with temperature of 4F6R	214
5.19 Variation of response time with temperature of 4F3R	215
5.20 Variation of response time with temperature of 4F6R	215
6.1 Observed textures in MPOBC in different phases	232
6.2 Diffraction photographs in Crystal, SmG^* , SmJ^* , SmF^* , SmI^* , SmC^* , SmA^* , N^* , BP^* and isotropic phases	234
6.3 Profile of wide angle diffraction peak depicting ordering within smectic planes in hexatic phases at $55^\circ C$ (SmG^*), $64^\circ C$ (SmJ^*), $66^\circ C$ (SmF^*) and $68^\circ C$ (SmI^*)	234
6.4 Layer spacing in smectic phases and apparent molecular length in cholesteric, blue and isotropic phases	236
6.5 Temperature dependence of X-ray and optical tilt of MPOBC	237
6.6 Optimized structure of MPOBC	238
6.7 Temperature variation spontaneous polarization (P_s) and rotational viscosity γ_ϕ in SmC^* phase	239
6.8 Temperature variation of dielectric increment with and without bias field. Magnified views are shown in the inset for (a) in hexatic phases and (b) in cholesteric and blue phases (without bias)	240

6.9 Observed critical frequencies with and without bias field in different phases of MPOBC	242
6.10 Effect of bias voltage on GM critical frequency in SmC* phase (75°C)	243

LIST OF APPENDICES

APPENDIX A: LIST OF SELECTED BOOKS AND MONOGRAPHS ON

LIQUID CRYSTALS..... 254

APPENDIX B: LIST OF PUBLICATIONS..... 257

BIBLIOGRAPHY..... 259

INDEX..... 289

CHAPTER 1

INTRODUCTION

1.1 INTRODUCTION

Liquid Crystal is a beautiful and fascinating state of matter. There is a little bit of liquid crystals in everybody's life since it is used almost in all our everyday gadgets like desktop computers, TV screens, laptops, mobile phones, calculators, digital watches, etc and it has become a multi-billion dollar industry. The liquid crystal technology is one of the important inventions of twentieth century that has found many applications as a visualization tool today. Liquid crystals change their color on application of external stimulus, for example temperature and shear stress distributions and thus act as a measure of their change. Liquid crystal technology has a major effect in many areas of science and engineering. Applications for this special kind of material are still being discovered and continue to provide effective solutions to many different problems.

Materials in nature can be divided into three main phases – solid, liquid and gas, depending on the mobility and amounts of ordering of the individual atoms or molecules. In a solid, particles are strongly bound to each other, and are not able to move about freely so shape and volume do not change. In a liquid, particles have more energy than in the solid state so they are able to move over each other and can flow to take up the shape of the container they are in, but the volume is fixed. In a gas, particles have enough energy to escape the attractive forces between them, so they are free to move in all directions at high speed. Particles will move around and fill whatever container they are in.

Although the three categories seem very well defined, the borders between the different states are not always clear. Apart from these three familiar states, there exist a large number of other intermediate phases. Liquid crystals are one of the intermediate phases in which the fluid nature of a liquid coexists with a partially ordered crystalline structure. The advancement of liquid crystal science and technology has been a truly interdisciplinary effort which combines basic principles of physics, chemistry and engineering. The field of liquid crystals covers a wide area of chemical structures, physical properties and technical applications and thus has drawn considerable attention from all branches of science and technology [1].

1.2 HISTORY OF LIQUID CRYSTALS

Liquid crystals have been used by mankind since ancient times, when soap was first discovered without knowing about their nature. The story of liquid crystals starts with a few European investigators who observed some new and interesting phenomena but whom never fully realized exactly what was happening in their experiments. These early scientists are not given the credit for discovering liquid crystals. In 1853 one European biologist Rudolf Virchow observed the characteristic of the liquid-crystalline state in nerve myelin and in 1857 Mettenheimer had deduced that nerve myelin was both fluid and optically birefringent [2], but were not formally recognized for another three decades. In 1887, the German physicist Otto Lehmann [3] was investigating phase transitions in cholesteryl esters, when he noted that during heating one particular substance would change from a clear liquid to a cloudy liquid before crystallizing when viewed under a polarizing microscope, but dismissed this as simply an imperfect phase transition. The next year, Friedrich Reinitzer [4], Austrian botanist, observed that cholesteryl benzoate had two distinct melting points. In his experiments, Reinitzer increased the temperature of a solid sample and observed at 145.5°C it became a hazy liquid which on further heating changed into a clear, transparent liquid at 178.5°C. Because of this early work, Reinitzer is often credited with discovering the new phase of matter i.e. Liquid Crystal.

From the earliest days, there was controversy over the nomenclature of these materials, and even the very name 'liquid crystal' was opposed by a number of prominent scientists. The field was dominated until the early 1920s by the German school, joined after about 1910 by the French school. Lehmann himself continued to publish extensively in the field until his death in 1922. In that year, G. Friedel published his famous two-hundred page overview in the *Annales de Physique*, where he set out most of the basic classification of liquid crystals, although he himself preferred the term 'mesomorphic state', into nematic, smectic, and cholesteric types [5]. Thus from the very beginnings, liquid crystal research was an international and multidisciplinary field. The total number of registered synthesized liquid crystal compounds, till year 2000, was 80080, out of which 59000 were benzene derivatives, 9000 mesogenic derivatives of cyclohexanes [6]. The beauty of this field of research is that a large number of physicists, chemists, biologists, engineers and medical doctors from almost all of the industrialized countries of the world are

involved in liquid crystal research. The details of historical evidences and perspectives in liquid crystal research are available in the references [2,7-14].

1.3 MOLECULAR ORDERING IN LIQUID CRYSTALS

In a crystalline solid the molecules have fixed orientation and the centre of mass of the molecules are distributed on a 3-dimensional periodic lattice. The crystal, therefore, possess long range ordering in both position and orientation of the molecules. But in case of an isotropic liquid the molecules do not have positional or orientational order. Their positions and the directions they point are randomly distributed. In liquid crystalline phase molecular arrangement is intermediate between the above two phases and they possess some typical properties of a liquid (e. g. fluidity, inability to support shear, formation and coalescence of droplets) as well as some properties of the crystalline state (anisotropy in optical, electrical, and magnetic properties, etc).

1.4 CLASSIFICATION OF LIQUID CRYSTALS

The various liquid-crystal phases can be characterized on the basis of geometrical structures of the molecules and type of ordering. Depending on the molecular structures, the system can pass through one or more mesomorphic states before it is transformed into an isotropic liquid. Transitions to these intermediate states may be induced by purely thermal process or by the influence of the solvents. Molecular systems that show mesomorphic behavior in a definite temperature range are called thermotropic liquid crystals. Lyotropic liquid crystalline phases, on the other hand, show mesomorphism in solution. The temperature range in which these lyotropic liquid crystals exist is mainly determined by the amount of solvent.

The molecules of liquid crystals are mostly rigid non-spherical and rod like or disc like in shape. The liquid crystals which are derived from rod like molecules are called “Calamatic” (Greek word *colomos* = rod) and which are derived from disc like molecules are called “Discotic”. The discotic liquid crystals were discovered independently by Chandrashekar *et al.* [15] and Billard *et al.* [16].

Besides the above two molecular types, the molecules may be lath like which are intermediate between the rod like and the disc like molecules. However, the constituent molecules may be even banana-, bowl-, sofa-, Y-, H-, T-, crooked-shaped etc [14].

The molecular structure of a typical rod-like liquid crystal molecule is shown in the Figure 1.1. It consists of two or more ring systems connected by a central linkage group, with a terminal group at one end and a flexible chain on the other end or chains at both ends.



Figure 1.1: Typical structure of a rod-like liquid crystal molecule

The presence of the rings in the above provides the short range molecular forces needed to form the liquid crystalline phases, but also affects the optical, electrical and elastic properties. The chemical stability of a liquid crystalline compound depends strongly on the central linkage group. Compounds with a single bond at the center are among the most stable ones. The length of the side chain has a significant impact on the flexibility and phase transition temperatures of the liquid crystalline compounds and affects the elastic constant. It is also commonly found that introduction of a side chain (group) decreases the melting point. The aromatic rings that form the core of the basic liquid crystal molecular structure can be saturated cyclohexane, unsaturated phenyl rings, or a combination of both. The ring structures of a liquid crystal molecule have an intrinsic effect on the dielectric anisotropy, birefringence, elastic constant, viscosity, and absorption. Polar group substitution at a terminal position results in enhanced dipole moment along the long axis of the molecule and lateral polar group substitution can cause the dipole moment along the short axis to become larger than that along the long axis, thereby affecting the dielectric properties of the materials [17,18].

On the other hand lyotropic molecule contains a hydrophilic polar head group and one or more long hydrophobic alkyl chains. Solutions of soap and water and various phospholipids are typical examples of lyotropic liquid crystals. Like thermotropic liquid crystals, they are also fluid phases possessing considerable molecular order. Lyotropic liquid crystals are mainly of interest

in biological applications and exhibit a considerable number of different phases. The biological aspects of lyotropic liquid crystals have been reviewed by J. W. Goodby [19].

1.4.1 THERMOTROPIC LIQUID CRYSTALS

Thermotropic liquid crystals are basically organic compounds and they exhibit a variety of phases as temperature is varied. Along with low molecular mass molecules some polymers also show thermotropic mesomorphic behavior, known as polymeric liquid crystals. In the low molecular mass category the constituent molecules may be achiral or chiral. If a molecule is asymmetric to mirror reflections i.e; cannot be superimposed on its mirror image, it is called a *chiral* molecule. On the other hand a molecule is *achiral* if it is super imposable on its mirror image. The achiral thermotropic liquid crystals are broadly classified into two main categories viz. nematic and smectic.

1.4.2 ACHIRAL CALAMATIC LIQUID CRYSTALS

Nematic Liquid Crystals

In nematic phase the centre of mass of the molecules are randomly distributed but the molecules possess long range orientational order. The molecules tend to align parallel to each other with their long axes all pointing roughly in the same direction. The average direction along which the molecules point is called the director and is usually denoted by a unit vector \mathbf{n} (Figure 1.2).

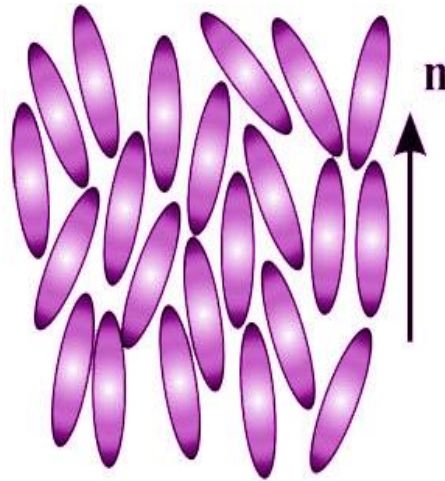


Figure 1.2: Molecular arrangement in nematic phase

The following characteristics of nematic phase are worth noting:

1. In the state of thermal equilibrium the nematic phase has symmetry $D_{\infty h}$ and is therefore uniaxial [20]. However some nematics are biaxial [21], meaning that in addition to orienting along their long axis, they also orient along a secondary axis.
2. There is long range orientational order i.e., the molecules tend to align parallel to each other.
3. There exists some preferential orientation of the molecules which is characterized by the axis of nematic order denoted by the unit vector \mathbf{n} .
4. The direction of \mathbf{n} is arbitrary in space and the preferred orientations \mathbf{n} and $-\mathbf{n}$ are indistinguishable.
5. When viewed under crossed polarized light microscope thread like structures appear from which nematics take their name (Greek “νημα” means thread). They also show schlieren; pseudo-isotropic; homogeneous textures.
6. Nematic phase are very sensitive to external fields, electric or magnetic and mechanical stress, which may be translated into visible optical effect, for which they find wide application in display devices.

From X-ray diffraction study [22,23], it is observed that some nematics possess a lamellar type of short-range order, i.e., they consist of clusters of molecules, called cybotactic groups, the

molecular centres in each cluster are arranged in layers and the molecules may either be arranged normal or tilted to the plane. The resulting phases are respectively called normal or skewed cybotactic nematic. Cladis [24] first observed that in a binary mixtures of two cyano compounds less ordered nematic phase reappears on cooling after more ordered smectic phase, such phases are called the re-entrant nematic. Re-entrant phenomena have been observed later in many pure systems.

Smectic Liquid Crystals

The smectic phases, which are found at lower temperatures than the nematic phase, form well-defined layers that can slide over one another in a manner similar to that of soap. The word "smectic" originates from the Latin word "smecticus", meaning cleaning, or having soap like properties. In general they are much more viscous than the nematics. The main characteristics of smectic phase are:

1. The elongated molecules exhibit orientational order as in the nematic phase but also align themselves in layers.
2. Molecules in this phase may show additional degrees of translational order within the layers.
3. Arrangement of the molecules may be normal to the plane of the layers or inclined to it.
4. The interlayer attractions are weaker than the lateral forces between molecules and hence the layers can easily slide over one another.

There are different types of packing of molecules in the layers, each of these types corresponds to different kinds of smectic phases [7,10,14,25-34]. The in plane positional ordering of the constituent molecules and the orientation of the molecules relative to the layer planes give rise to four sub-groups of smectic mesophases. The first two groups can be defined where the molecules have their long axes on an average normal to the layers with or without in plane ordering. The other two sub groups have their constituent molecules tilted relative to the layer planes. The smectic mesophases are Smectic **A**, Smectic **D**, Smectic **C**, Smectic **B**, Smectic **E**, Smectic **F**, Smectic **G**, Smectic **H**, Smectic **I**, Smectic **J**, Smectic **K**, Smectic **L**, Smectic **M**,

Smectic **O** and Smectic **Q**. The alphabetic order merely indicates the chronological order of discovery.

Smectic A Phase

Smectic A (SmA) is a phase in which the molecules are more or less parallel to one another and are arranged in layers with the long axes perpendicular to the layer plane. Within the layers, liquid-like structure remains (Figure 1.3). Thus, the structure may be defined as an orientationally ordered fluid on which a one dimensional density wave is superimposed. The molecules are free to rotate about their long axes [35,36]. SmA has infinite fold rotational symmetry (D_∞) about an axis parallel to the director, for which this phase is uniaxial [37]. This gives rise to characteristic textures like focal conic (fan-shaped or polygonal), stepped drops, pseudoisotropic, etc.

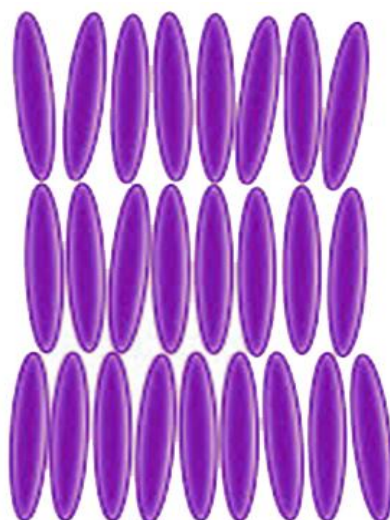


Figure 1.3: Molecular arrangement in SmA phase

Smectic A phase can further be divided into the following subphases. SmA₁ which is a conventional monolayer smectic A phase, where the molecules have random head to tail orientations, SmA₂ is a bilayer phase with antiferroelectric type ordering of the constituent molecules [38], SmA_d is a semi bilayer phase with partial molecular overlapping due to

associations [39,40] and $\text{Sm}\tilde{\text{A}}$ is called anti-phase [41-43] and SmA_{ic} is an incommensurate phase intermediate between SmA_{d} and SmA_2 [44].

Smectic C Phase

On decreasing temperature, the SmA phase may transform into a phase with the director \mathbf{n} is tilted with respect to the layer normal called smectic C (SmC) phase as shown in Figure 1.4. Tilting of the molecules, results in lower symmetry ($2/m$ symmetry). Due to the presence of pronounced tilt angles the phase is optically biaxial. The tilt angle provides a natural order parameter to distinguish it from smectic A phase. It shows broken focal-conic, schlieren and homogeneous textures.

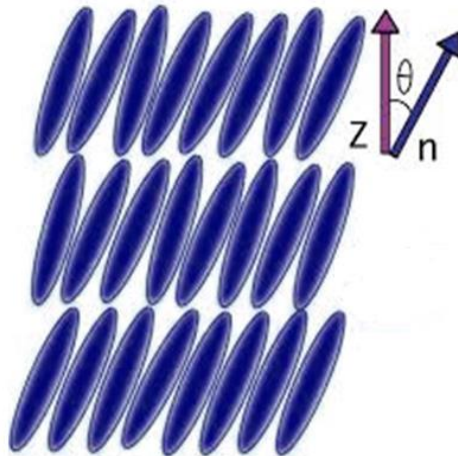


Figure 1.4: Molecular arrangement in SmC phase, z is layer normal

In SmC phase, when the constituent molecules are strongly axially polar, four sub phases are observed [45,46]; viz, SmC_1 , SmC_2 , SmC_{d} and SmC_{anti} are the analogues to A_1 , A_2 , A_{d} and $\tilde{\text{A}}$ phases respectively.

Smectic B Phase

In SmB phase, in addition to the layered structure ordering of the constituent molecules within the layers is also observed. Within a layer molecular long axes are perpendicular to the

plane of the layer and the centres of mass of the molecules are arranged in hexagonal symmetry ($6/m\bar{m}$ symmetry) [27,28,47-49]. Two different types of SmB phase have been observed – one is Crystal B (CrB) and another one is Hexatic B. Hexatic B phases have short range positional ordering as well as bond orientational ordering whereas Crystal B phases are smectic like soft crystal modifications [50,51] with the constituent molecules having long range positional ordering in 3-dimension. Thus the SmB phase is the most ordered of the three major smectic phase A, B and C. Under a microscope the SmB phase usually shows a mosaic texture.

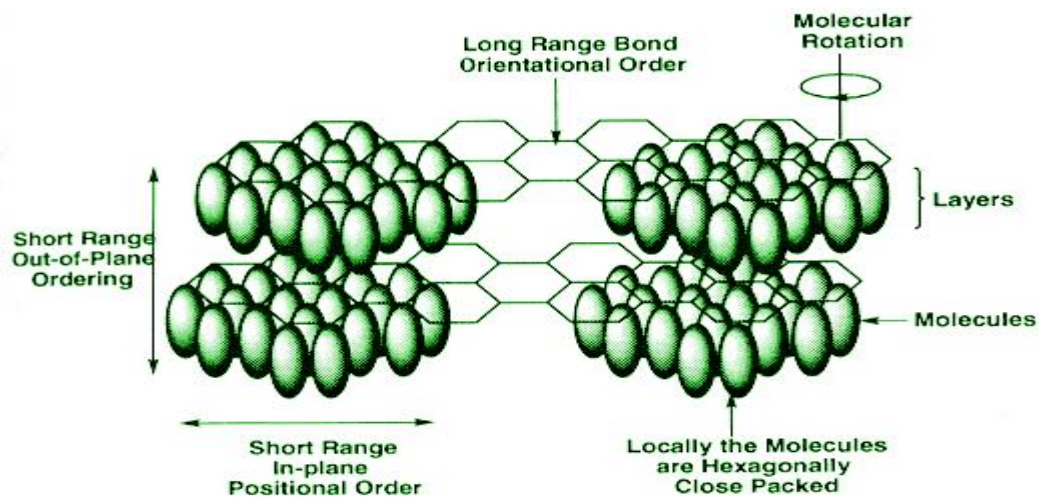


Figure 1.5: Molecular arrangement in smectic B phase [after reference 37]

Smectic I and Smectic F Phases

Smectic I (SmI) and Smectic F (SmF) phases are tilted analogues of hexatic SmB phase [52,53]. The tilt in the molecular long axis in SmI phase is directed towards an apex of the hexagonal packing net, whereas in SmF phase tilt is towards the edge of the hexagon (Figure 1.6 and Figure 1.7). SmF phase have slightly longer correlation length than SmI phase [54].

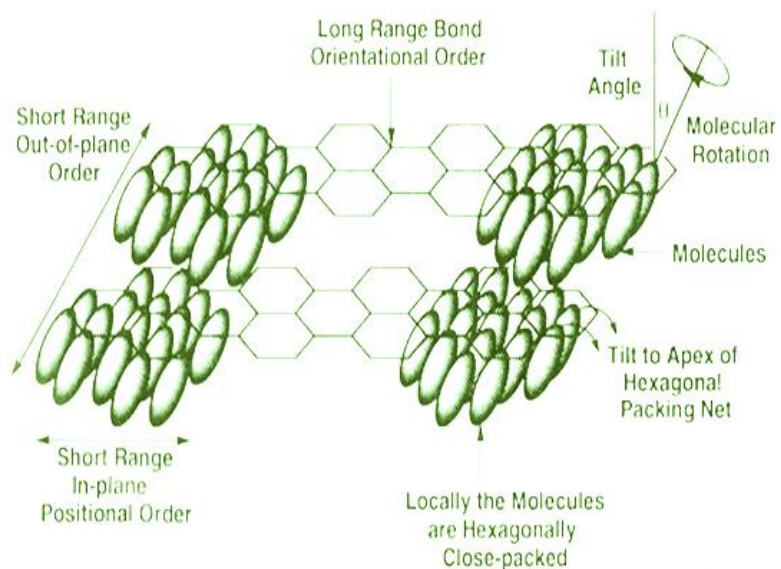


Figure 1.6: Molecular arrangement of smectic I phase [after reference 37]

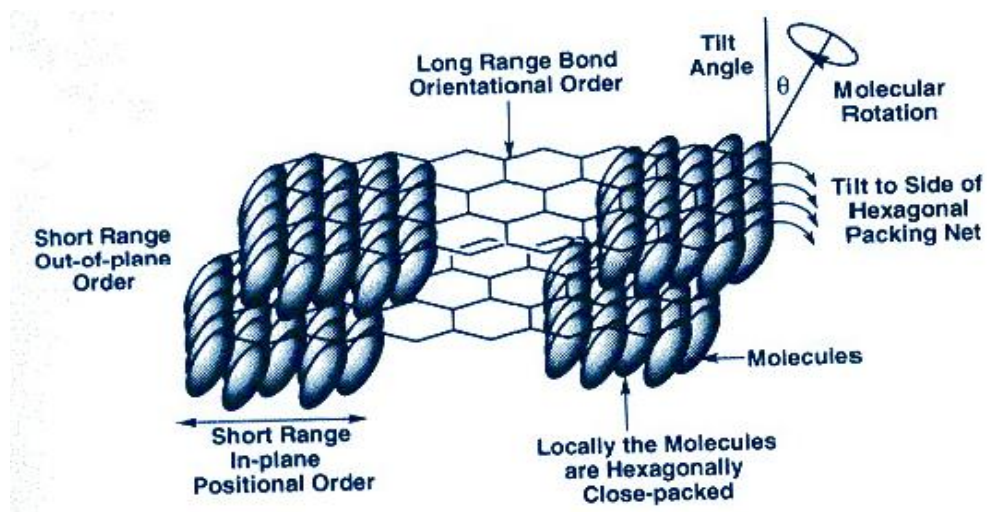


Figure 1.7: Molecular arrangement of smectic F phase [after reference 37]

Crystal J and G phases

The crystal J and G phases [55] are the crystalline analogues to smectic I and smectic F phases [27]. In crystal J phase the molecules are arranged in layer with their molecular long axes tilted relative to the layer planes. There is long range positional ordering within the layers and also between the layers [56]. The molecules in crystal J and G phases are packed in a pseudo-hexagonal structure when viewed down the tilt direction. The only difference between the two phases is the tilt direction. In the crystal G phase the tilt of the molecules is directed towards the edge of the hexagonal packing array whereas in J phase the tilt is towards the apex of the hexagonal net (Figure 1.8). The molecules undergo rapid re-orientational motion about their long axes [27,57].

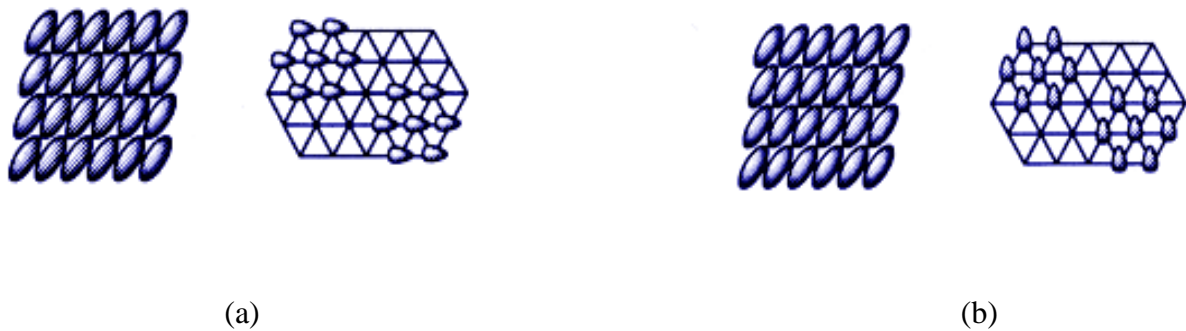


Figure 1.8: Molecular arrangement in (a) crystal J and (b) crystal G phase

1.4.3 CHIRAL CALAMATIC LIQUID CRYSTALS

Chiral calamitic compounds may form non-ferroelectric and ferroelectric phases which are discussed below.

Non Ferroelectric Phases

Cholesteric Liquid Crystals

A nematic liquid crystal when composed of chiral molecules or when mixed with chiral (optically active) molecules, the structure undergoes a helical distortion about an axis normal to the preferred molecular direction \mathbf{n} [58-62] as shown in Figure 1.9, giving rise to cholesteric or chiral nematic phase (Ch or N^*). The helix may be right handed or left handed depending on the molecular conformation. The pitch of the helix is usually of the order of several hundred nanometers, corresponds to the wave length of visible range of electromagnetic spectrum.

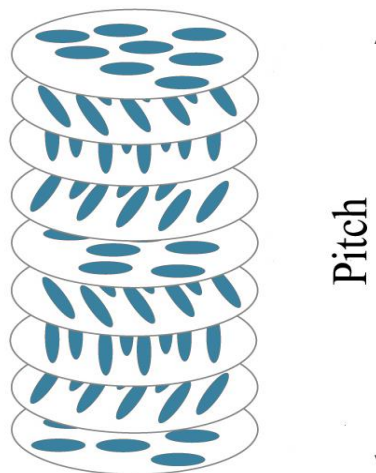


Figure 1.9: Molecular arrangement of cholesteric liquid crystal

In other words, a cholesteric liquid crystal with infinite pitch is nothing but a nematic liquid crystal. Pitch is highly sensitive to temperature, flow, chemical composition, and applied magnetic or electric field. The energy of twist forms a small part (10^{-5}) of the total energy associated with the parallel alignment of the molecules [63] so that even when a small amount of cholesteric substance or a non-mesogenic optically active substance is added to a nematic, the mixture adopts a helical conformation. In X-Ray diffraction patterns, both nematic and cholesteric phases show long-range positional order. The absence of Ch-N phase transition by variation of

temperature [64] and by application of strong magnetic field normal to the helical axis [65,66] confirm that the cholesteric phase may be regarded as a twisted nematic phase.

Blue Phases

Blue phases are liquid crystal phases that appear in the temperature range between a chiral nematic phase and an isotropic liquid phase and was first reported by Lehmann in 1906 [67]. The temperature region in which these blue phases are stable is often quite small, some tenths of a degree. Recently the stabilization of blue phases over a temperature range of more than 60 K including room temperature (260–326 K) has been demonstrated [68,69]. Blue phases have a regular three-dimensional cubic structure of defects with lattice periods of several hundred nanometers, and thus they exhibit selective Bragg reflections in the wavelength range of visible light. This phase possesses a relatively short pitch length ($< 5000 \text{ \AA}$). Three distinct blue phases (BPI, BPII and BPIII) have been identified and occur in that order with increasing temperature [70]. Although BPI and BPII, are cubic phases, BPIII is an amorphous phase which nevertheless reflects circularly polarized light. Under a microscope a texture of uniformly colored platelets is found in this phase. Blue phases are of interest for fast light modulators or tunable photonic crystals, blue phases stabilized at room temperature allow electro-optical switching with response times of the order of 10^{-4} s [71]. In 2008, the first Blue Phase Mode LCD panel had been developed by ‘Samsung Electronics’.

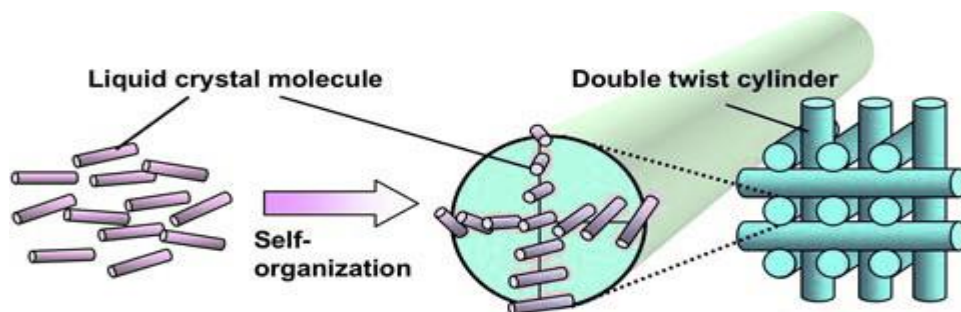


Figure 1.10: Molecular arrangement of liquid crystal possessing blue phase

Ferroelectric Liquid Crystals

All chiral smectic phases with tilted structure may exhibit ferroelectric properties if the molecules contain a transverse permanent dipole moment. The basic structure of a ferroelectric liquid crystal is shown in Figure 1.11. There are several types of smectic liquid crystal phases SmC^* , SmI^* and SmF^* and crystal smectic phases SmJ^* , SmG^* , SmK^* and SmH^* in which the constituent molecules are chiral and their long axes are tilted with respect to the layer planes. Due to their low symmetry they are able to exhibit spontaneous polarization (P_s) when molecules have permanent dipole moment and are known as ferroelectric liquid crystals [72]. The chiral smectic mesophases take the form of a helix, which is different from the helix in chiral nematic phase.

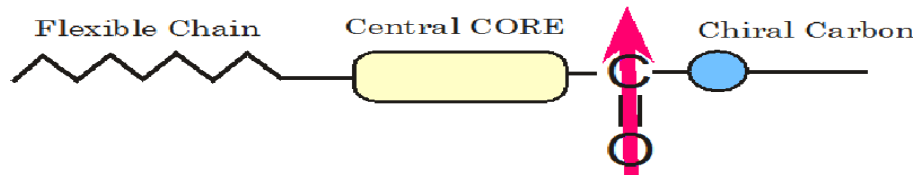


Figure 1.11: Basic structure of ferroelectric liquid crystal

The most commonly exhibited tilted chiral smectic phase is the SmC^* phase. In the SmC^* phase, where the molecules tilt with respect to the layer normal, the axis of the helix is along the layer normal. The director slowly rotates around the smectic cone progressively from layer to layer, preserving a constant azimuthal angle Φ within a single layer. This creates a helical structure with pitch being the distance along the layer normal needed to reach the same molecular orientation [73], as shown in Figure 1.12.

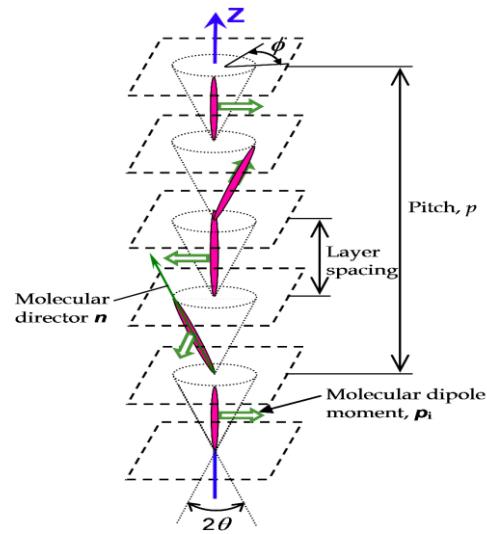


Figure 1.12: Spiralling of the director in SmC* phase showing layer normal \mathbf{Z} , tilt angle θ , azimuthal angle Φ , molecular director \mathbf{n} and dipole moment \mathbf{p}_i [after reference 74]

In addition to producing this helical structure, chirality results in a spontaneous molecular polarization. Since in every SmC* layer the vector of spontaneous polarization is in the plane of the layer and perpendicular to the plane which goes through the normal to the layers and the director \mathbf{n} , all possible directions of \mathbf{P}_s are tangent to the basis of the smectic cone. When there is no field applied across a SmC* sample, where the helical superstructure has developed, the spontaneous polarization will average to zero over one pitch, resulting in no macroscopic polarization of the system [74] thus ferroelectric liquid crystals are regarded as helielectric. Application of an external electric field (perpendicular to the helix axis) will couple the polarization vector to the field direction and unwind the helix which suggests that \mathbf{P}_s can be reoriented according to the direction of applied field. By virtue of their symmetry, ferroelectric liquid crystals are piezoelectric too, because polarisation in these materials can be induced by mechanical stress. Ferroelectricity in liquid crystals was first discovered in 1975 by R.B. Meyer and his co-workers [72,75] and the first developed liquid crystalline material was DOBAMBC. According to Meyer the symmetry argument is as follows: the smectic C phase has monoclinic symmetry (C_{2h}), the point group for which contains (i) only a two-fold rotation axis parallel to the layers and normal to the long molecular axis; (ii) a mirror plane normal to the two fold axis and the 'layer' and (iii) a centre of symmetry. When the constituent molecules are chiral, the

reflection plane normal to the two-fold axis and the centre of inversion are eliminated which reduces the symmetry to C_2 . The remaining single two-fold axis allows the existence of a permanent dipole moment parallel to this axis and if all the molecules are identical then a net polarization (a few Debye per molecule) will be produced. With these considerations Meyer was able to demonstrate ferroelectricity in the liquid crystalline material DOBAMBC.

There are other chiral smectic phases viz., antiferroelectric chiral smectic C^* (SmC^*_A) phase, the ferrielectric chiral smectic C^* (SmC^*_{ferri}) phase as shown in Figure 1.13. The constituent molecules of the antiferroelectric chiral smectic C^* (SmC^*_A) phase have the tilted lamellar structure as that of the ferroelectric SmC^* phase but the tilt direction alternates between the $+\theta$ and $-\theta$ positions from layer to layer to give a zig-zag structure resulting the spontaneous polarization of the phase to be zero (real materials may exhibit very small spontaneous polarization) [76]. This structure is evidenced by the fact that when a strong electric field is applied to this phase, the layer ordering is perturbed and the phase returns to a normal ferroelectric phase. The structure of ferroelectric SmC^* phase is repeated every 360° rotation of the helix, whereas the helical structure of the antiferroelectric phase repeats every 180° rotation. The first antiferroelectric liquid crystal (MHPOBC) was found by a Japanese group in 1989 [77,78]. The ferrielectric chiral smectic C (SmC^*_{ferri}) also has alternating tilted structure except that the alteration is not symmetrical and more layers are tilted in one direction than the other. This phase generates spontaneous polarization, the magnitude of which depends on the degree of alternation of tilt direction.

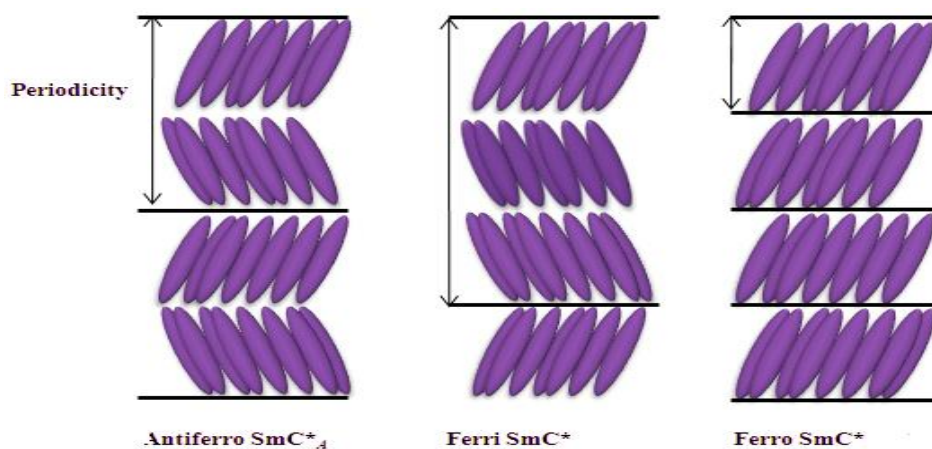


Figure 1.13: Molecular arrangement of antiferroelectric, ferrielectric and ferroelectric SmC^* liquid crystal

In some recent investigations three subphases of SmC^* phase, viz, SmC^*_α , SmC^*_β and SmC^*_γ - have also been found in many antiferroelectric liquid crystals [79]. The study of ferroelectric liquid crystals has become important for their variety of applications such as in large area, high information content colour display devices. The various applications of FLCs have been explored in references [80-83].

Surface Stabilized Ferroelectric Liquid Crystal Display Devices

In ferroelectric SmC^* phase the molecules in different layers create a helical structure. By suppressing the helix in FLCs, one can develop Surface Stabilized Ferroelectric liquid crystal (SSFLC). The way to suppress the helix was first proposed by Clark and Lagerwall [82], which resulted in the discovery of fast electrooptic switching. Although in solid ferroelectrics the macroscopic polarization is energetically stable in the absence of an external field, whereas due to helical structure bulk ferroelectric liquid crystals do not have any macroscopic polarization. In SmC^* phase there is no crystal lattice and its stable configuration is characterized by the helicoidal structure and the P_S changes gradually in the same way and so the P_S cancels to zero in the bulk phase. However, if the helix could be unwound, then the bulk phase would become ferroelectric.

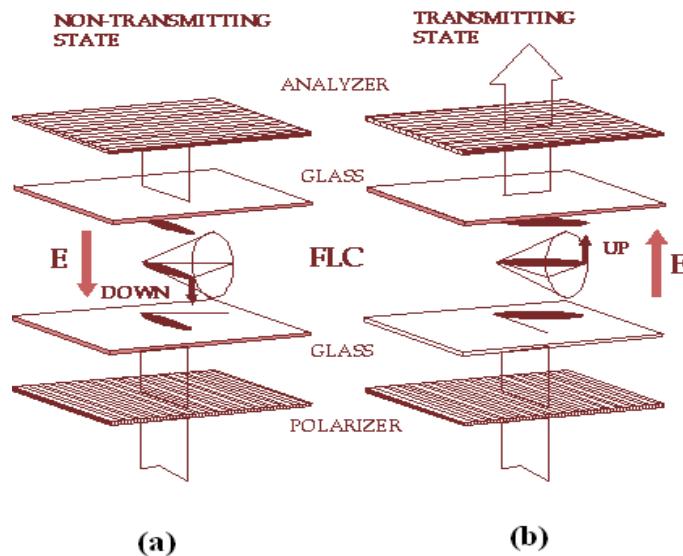


Figure 1.14: The basic construction of the SSFLC display device showing (a) off state and (b) on state [after reference 84]

In the surface-stabilized ferroelectric SmC^* phase the helix is inherently absent. For unwinding the helix, the FLC material is to be taken in a cell where the constituent molecules are to be aligned parallel to the cell surface. The surface forces generated in the constraints geometry of the cell effectively unwinds the helix. In a SSFLC display device, the FLC material is taken in between two ITO coated glass plates which were pre-treated with aligning materials (polyimide or silicon dioxide). The molecules are aligned in a unidirectional manner called bookshelf geometry. When the planar layers of FLC material are arranged perpendicular to the glass plates of the display, the directions of the permanent electric dipoles are perpendicular to the long axis of the molecule (the director \mathbf{n}). The cell is then placed in between polarizer and analyzer at the crossed position. The bottom polarizer is oriented in line with the molecular alignment direction. When a positive electric field is applied across the plates, the dipole wants to align toward one of the glass plates which make the director point to a particular direction. As soon as the field is reversed, the molecules will switch around an imaginary cone through an angle 2θ (θ is the tilt angle), as a result the dipole will rotate 180° to point the other direction. Now, since the entering light is polarized along the director in one of these states, no light will be able to penetrate a crossed polarizer on the other side and the cell appears dark which is called OFF state. The application of the electric field will cause molecular rotation through $2\theta = 45^\circ$ since θ is around 22.5° . Then the molecular alignment direction will be mid-way between the polarizer directions and hence the liquid crystal will be able to act as a half-wave retardation plate to allow light through. Thus the cell appears bright and it is called ON state. The device operation is clearly described in the article by Hird [84].

The main features of SSFLC display are that, it exhibits a fast response ($\sim \mu\text{s}$ order), wide viewing angle, high contrast ratio and bistable memory capability. Variety of novel FLC devices, including matrix-addressed arrays for displays and optical computing, linear arrays for printer applications, and single element switches for shuttering and light beam control are the targets in this research field.

1.4.4 DISCOTIC LIQUID CRYSTALS

Apart from the rod-like molecules, more advanced-shaped liquid crystals are possible such as disk-like liquid crystals which can give rise to another type of ordering. A discotic phase is one in which flat molecules typically with threefold or four fold symmetry that have a rigid core and several floppy side chains stacked with their planes lying roughly parallel to one another giving rise the director to be oriented roughly perpendicular to the plane of the molecule. There are two basic types of discotic mesophases that have been recognized viz., columnar and nematic. If the disks pack into stacks, the phase is called discotic columnar. On the other hand the nematic phase N_D exhibited by discotic materials shows similar optical textures as that of calamatic nematic phase N and has orientationally ordered arrangement of the disc without any long range positional order. Discotic mesophases have been reviewed by A. N. Cammidge, R J Bushby [85] and S. Kumar [86].



Figure 1.15: Molecular arrangement of discotic columnar liquid crystal

1.5 APPLICATIONS OF LIQUID CRYSTALS

From application point of view liquid crystal technology has a major effect in many areas of science and engineering, especially in device technology. Since liquid crystals are very sensitive to even weak external perturbations they are used in measurement of temperature, pressure and chemical contamination. Their dual nature and easy response to electric, magnetic and surface forces have generated innumerable applications in high-resolution TV displays,

projection systems, optical computing, etc which are the tool for fundamental and basic research in physics, chemistry, space, engineering, mathematics, biology and medical sciences. Originally, nematic liquid crystals were used in calculators or digital watches and had only a few black-and-white pixels. But nowadays, LCD's are widespread in all kinds of applications such as flat panel displays for desktop applications or notebooks, laptops, tablets, mobile phones, projectors. Relatively low power consumption, low operating voltage and light weight etc. are the main advantages of liquid crystal displays (LCD's) over other types of displays. Twisted nematic displays are still dominating the LCD field, as most of the displays produced today are either twisted nematic [87] or super-twisted [88] nematic displays. Recently, as a biomedical application, a simple, rapid and low-cost method has been reported for detecting *Escherichia coli* using a nematic liquid crystal (LC), 4-cyano-4'-pentylbiphenyl (5CB) [89].

Ferroelectric liquid crystal (FLC) technology [90,91] is enhanced broadly due to its fast switching and high resolution. These advantages and the possibility for dynamic gray scale and full color of SSFLC give it great potential for use in demanding applications such as high definition television (HDTV). The bistability offered by SSFLC devices makes them ideal where low energy consumption is concern. Polymer dispersed liquid crystals (PDLC) are also used in many types of displays [92].

Cholesteric liquid crystals are very useful for various applications. They are used in temperature sensitive devices, medical applications, thermometers, thermographs, visualization of RF (radio frequency) waves, tumor testing, battery testers, liquid crystal paints, mood rings, decoration and advertising. With the help of cholesteric liquid crystal technology skin infections and malignant skin tumours may be detected and located. It is possible due to the fact that the portion of the infected skin or tumor has higher temperature than the surrounding uninfected area. Liquid crystals are also used as anisotropic solvents for nuclear magnetic resonance (NMR) measurements, as solvents for the studies of infra red (IR) and ultra violet (UV) spectra of solute molecules in the form of liquid crystal films [92,93]. Lyotropic Liquid Crystals are important because of their role in biological applications [19]. Liquid crystals are used to detect electrically generated hot spots for failure analysis in the semiconductor industry. Liquid crystals are also used for lasing action. So a crucial contribution to this progress will be the design and synthesis of new liquid crystals having suitable applications.

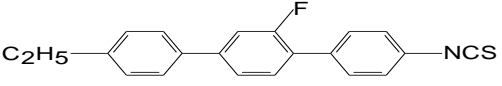
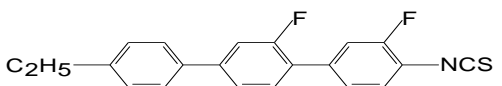
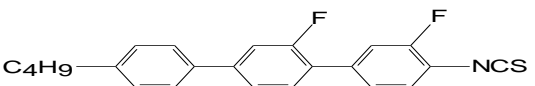
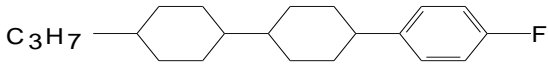
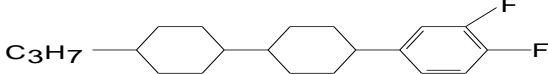
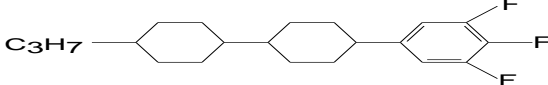
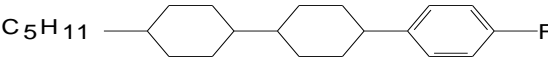
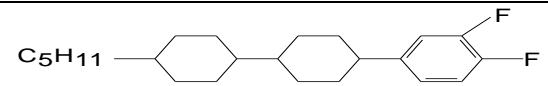
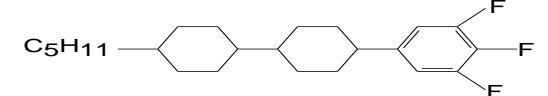
1.6 LIQUID CRYSTAL COMPOUNDS INVESTIGATED IN THE PRESENT DISSERTATION

In a liquid crystal the existence of different mesophases depend on the intermolecular association of the molecules constituting the liquid crystal. The existence as well as the thermal range of different mesophases can be modified by changing the degree of association between the molecules. One way of overcoming the strength of the pre-existing molecular association is by decreasing the melting temperature of the system so that different mesophases may arise before the isotropic phase is reached. Another way of modifying the molecular association is to introduce some substituents. The substituents are very limited and can be divided into two categories viz., multi-atomic (CH_3 , OH, CN, NH_2 , etc) and mono-atomic (F, Cl, B, I, etc). The substituents may increase or decrease the molecular association by increasing dipolar attraction or by increasing the separation of the molecules.

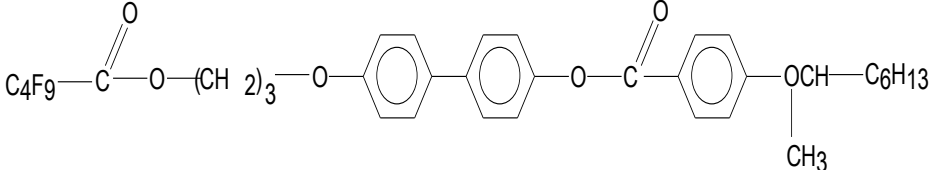
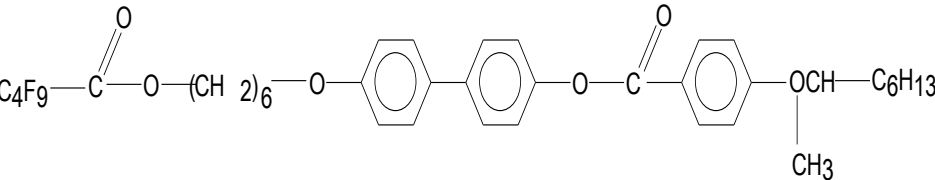
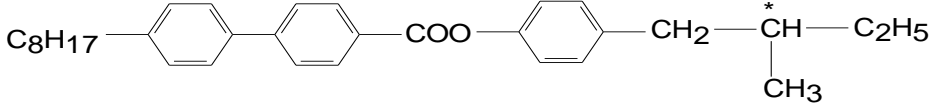
An effective mono-atomic substituent is fluorine (F). Fluorine is the most electronegative of all elements and its polarity is very high which produces a strong dipole moment thus affects the molecular association. For aliphatic or alicyclic compounds fluorine substitution causes a strong dipole moment which is introduced by the $\text{C}(\delta^+)\text{-F}(\delta^-)$ bond and the inductive effect arising from the high electro negativity of fluorine. The fluorine substitution can be introduced in different positions within a molecular structure to modify the properties of the parent system. Fluoro substitution at the terminal position enhances the dielectric anisotropy and elastic constants because of the introduction of high polarity C-F bond. Compounds having terminal fluoro substitution possess a high resistivity, high photo-chemical stability and low viscosity which is suitable for active matrix (thin-film transistor, TFT) displays. Another way of introducing fluorine is at the lateral position. Lateral fluoro substitution reduces the melting points of the compounds and also reduces the smectic phase stability. Additionally, fluoro substitution generates molecular tilting and thus produces smectic C phase which are essential for ferroelectric and antiferroelectric phase formation. Besides, fluoro substituted cyano compounds produce a large positive dielectric anisotropy which is used for low voltage switching in twisted nematic LCDs. Keeping these in view a number of achiral and chiral fluorinated compounds were therefore selected for investigation in the present dissertation. Their abbreviated names with molecular structures and transition temperatures are given in Table 1.1.

Table 1.1: Molecular structures and transition temperatures of the investigated compounds

ACHIRAL COMPOUNDS

Sl. No	Name	Molecular structure with transition temperature
1	2TP-3'F-4NCS	 <p style="text-align: center;">Cr 102.5°C SmA 120.5°C N 188.2°C I</p>
2	2TP-3',3F-4NCS	 <p style="text-align: center;">Cr 80.2°C N 188°C I</p>
3	4TP-3',3F-4NCS	 <p style="text-align: center;">Cr 58.1°C SmA 96.9°C N 181.8°C I</p>
4	3ccp-f	 <p style="text-align: center;">Cr 90.0 (71.0) N 158.0 I</p>
5	3ccp-ff	 <p style="text-align: center;">Cr 45.6 N 123.8 I</p>
6	3ccp-fff	 <p style="text-align: center;">Cr 64.7 N 93.7 I</p>
7	5ccp-f	 <p style="text-align: center;">Cr 68.0 SmB 75.0 N 157.0 I</p>
8	5ccp-ff	 <p style="text-align: center;">Cr 47.0 (26.8) N 125.2 I</p>
9	5ccp-fff	 <p style="text-align: center;">Cr 87.3 N 101.2 I</p>

CHIRAL COMPOUNDS

Sl. No	Name	Molecular structure with transition temperature
10	4F3R	 <p style="text-align: center;">Cr 79.8°C SmC* 134.1°C I</p>
11	4F6R	 <p style="text-align: center;">Cr₁ 46.7°C Cr₂ 60.0°C SmC_A* 86.5°C SmC* 128.3°C I</p>
12	MPOBC	 <p style="text-align: center;">Cr 48 SmG* 63 SmJ* 65 SmF* 67 SmI* 71 SmC* 81 SmA* 136 N* 139 BP* 140 Iso</p>

1.7 REFERENCES

- [1] G. Durand and J. D. Lister; *Ann. Rev. Mate. Sci.*, 23, 269 (1973), Recent advances in liquid crystals.
- [2] T. J. Sluckin, D. A. Dunmur and H. Stegemeyer, *Crystals That Flow: Classic Papers from the History of Liquid Crystals*, History of Physics Group Newsletter, Institute of Physics (2006).
- [3] O. Lehmann; *Z. physik. Chem.* 4, 462- 472 (1889), Fließende Kristalle.
- [4] F. Reinitzer; *Monatshefte für Chemie.*, 9, 421-441(1888), Beiträge Zur Kenntnis des Cholesterins.
- [5] G. Freidel; *Ann. Physique (Paris)*, 18, 273 (1922), Les états mésomorphes de la matière.
- [6] V. Vill; *Liq. Cryst 3.4 Database*, LC publisher GmbH, hamburg, May (2000).
- [7] H. Kelker and R. Hatz; *Verlag Chemie*, Chapter 1 (1980), *Hand Book of Liquid Crystals*.
- [8] H. Kelker; *Mol. Cryst. Liq. Cryst.*, 21, 1 (1973), History of liquid crystals.
- [9] H. Kelker and P. M. Knoll; *Liquid. Cryst.* 5(1), 19 (1989), Plenary Lecture: Some pictures of the history of liquid crystals.
- [10] G. W. Gray; *Mol. Cryst. Liq. Cryst.*, 63, 3 (1981), Comments on some recent development in the field of liquid crystals.
- [11] G. W. Gray; *Liq. Cryst.*, 24(1), 5 (1998), Reminiscences from a life with liquid crystals.
- [12] P. J. Coolings and M. Hird, *Introduction to Liquid Crystals Chemistry and Physics*, Taylor & Francis (1998).
- [13] G. W. Gray and H. Finkelmann in *Polymeric Liquid Crystals*, ed. A. Ciferri, W. R. Krigbaum and Robert B. Meyer, AP, chap-1 and chap-2 respectively (1982).
- [14] D. Demus; *Mol. Cryst. Liq. Cryst.*, 364, 25 (2001), One century liquid crystal chemistry: from Vorlander's rods to disks, stars and dendrites and G. W. Gray in *Handbook of Liquid Crystals. Vol. 1 (Fundamentals)*, Ed. D. Demus, J. W. Goodby, G. W. Gray, H.-W. Spiess and V. Vill, Introduction and Historical Development, WILEY-VCH, Verlag GmbH, Weinheim, FRG (1998).
- [15] S. Chandrasekhar, B. K. Sadashiva and K. A. Suresh; *Pramana*, 9, 471- 480 (1977), Liquid crystals of disc-like molecules.
- [16] J. Billard, J. C. Dubois, T. H. Nguyen and A. Zann; *Nouveau J. Chim.* 2, 535-540 (1978), Une mésophase disquotique.

- [17] Liquid Crystals Application and Uses Vol. 1-3. Ed. B. Bahadur, World Scientific, (1990-1992).
- [18] G. W. Brown, J. W. Doane and V. D. Neff, A Review of the Structure and Physical Properties of Liquid Crystals. CRC Press, Cleveland, Ohio (1971).
- [19] J. W. Goodby; *Liq. Cryst.* 24, 25-38 (1998), Liquid crystals and life.
- [20] P. G. de Gennes; "The Physics of Liquid Crystals", Clarendon Press, Oxford (1974); P. G. de Gennes and J. Prost, 2nd ed. Clarendon Press, Oxford (1993).
- [21] L. A. Madsen, T. J. Dingemans, M. Nakata, E. T. Samulski; *Phys. Rev. Lett.* 92 (14) (2004), Thermotropic Biaxial Nematic Liquid Crystals.
- [22] A. de Vries; *Mol. Cryst. Liq. Cryst.*, 10, 31 (1970), Evidence for the Existence of More Than One Type of Nematic Phase.
- [23] A. de Vries; *Mol. Cryst. Liq. Cryst.*, 10, 219 (1970), X-Ray Photographic Studies of Liquid Crystals I. A Cybotactic Nematic Phase and A. de Vries, in *Proc. of the International Liquid Crystal Conference, Bangalore, December, Pramana Supplement I*, 93 (1973), X-Ray Studies of Liquid Crystals: V. Classification of Thermotropic Liquid Crystals and Discussion of Intermolecular Distances.
- [24] P. E. Cladis; *Phys. Rev. Lett.*, 35, 48-51 (1975), New Liquid-Crystal Phase Diagram.
- [25] G. W. Gray, *Molecular Structure and the Properties of Liquid Crystals*, Academic Press, London (1962).
- [26] P. S. Pershan, *Structure of Liquid Crystals Phases*, World Scientific Lecture Note in Physics, Vol 23, World Scientific, Singapore (1988).
- [27] G. W. Gray and J. W. Goodby, Eds., *Smectic Liquid Crystals, Textures and Structures*, Leonard - Hill, Philadelphia (1984).
- [28] A. J. Leadbetter in *Thermotropic Liquid Crystals, Critical Reports on Applied Chemistry*, Vol. 22, G. W. Gray(Ed.),Wiley, Chichester, p1 (1987).
- [29] A. de Vries in *Liquid Crystals, The Fourth State of Matter* (Ed. F. D. Saeva), Marcell Dekker, New York, p1 (1972).
- [30] A. de Vries, *Mol. Cryst. Liq. Cryst.*, 63, 215(1981), A Structural Classification of Smectic Liquid Crystals.

- [31] J. Doucet in *The Molecular Physics of Liquid Crystals*, Eds. G. R. Luckhurst and G. W. Gray, Academic Press, London, p317 (1979).
- [32] L. V. Azaroff, *Mol. Cryst. Liq. Cryst.*, 60, 73(1980), X-Ray Diffraction by Liquid Crystals.
- [33] D. Demus, J. W. Goodby, G. W. Gray and H. Sackmann, *Mol. Cryst. Liq. Cryst.*, 56, 311(1980), Recommendation for The Use of The Code Letters G And H for Smectic Phases.
- [34] J. W. Goodby and G. W. Gray, *Mol. Cryst. Liq. Cryst.*, 41, 145-150 (1978), Some New Smectic F Materials.
- [35] R. M. Richardson, A. J. Leadbetter and J. C. Frost, *Mol. Phys.*, 45, 1163 (1982), A comparative study of the molecular motions in the three smectic phases of isobutyl 4(4' phenylbenzylideneamino) cinnamate using incoherent neutron scattering.
- [36] A. J. Leadbetter, J. C. Frost, J. P. Gaughan, and M. A. Mazid, *J. Phys. (Paris)*, 40, C3-185-C3-192 (1979), The structure of the crystal, smectic E and smectic B forms of IBPBAC.
- [37] J. W. Goodby in *Handbook of Liquid Crystals*, Eds. D. Demus, J. Goodby, G.W. Gray, H.-W. Spiess and V. Vill, Vol. 2A, Wiley-VCH, Verlag GmbH, Weinheim, FRG, p7 (1998).
- [38] F. Hardouin, A. M. Levelut, J. Bennattar and G. Sigaud; *Solid State Comm.*, 33, 337-340 (1980), X-rays investigations of the smectic A1 - smectic A2 transition.
- [39] A. J. Leadbetter, J. L. Durrant and M. Rugman; *Mol. Cryst. Liq. Cryst. Lett.*, 34, 231 (1977), The Density Of 4 n-Octyl-4-Cyano-Biphenyl (8CB).
- [40] A. J. Leadbetter, J. C. Frost, J.P. Gaughan, G.W. Gray and A. Mosley; *J. Phys. (Paris)*, 40, 375-380 (1979), The structure of smectic A phases of compounds with cyano end groups.
- [41] F. Hardouin, G. Sigaud, N. H. Tinh, A.F. Achard; *J. Phys. (Paris) Lett.*, 42, 63-66 (1981), A fluid smectic A antiphase in a pure nitro rod-like compound.
- [42] J. Prost; *Advances in Physics*, 33, 1-46 (1984), The smectic state.
- [43] P. S. Pershan, *Structure of Liquid crystals*, World Scientific, Singapore (1988).
- [44] B. R. Ratna, R. Shashidhar and V. N. Raja, *Phys. Rev. Lett.*; 55(14), 1476 (1985), Smectic-A phase with two collinear incommensurate density modulations.
- [45] S. T. Wang, S. L. Wang, X. F. Han, Z. Q. Liu, S. Findeisen, W. Weissflog and C. C. Huang; *Liq. Cryst.*, 32, 5, 609-617 (2005), Optical studies on two tilted smectic phases of meta-substituted three-ring liquid crystal compounds.
- [46] A. L. Tsykalo, *Thermophysical properties of liquid crystals*, Gordon and Breach Science Publishers (1991).

- [47] R. Pindak, D. E. Moncton, S. C. Davey and J. W. Goodby; *Phys. Rev. Lett.*, 46, 1135 (1981), X-Ray Observation of a Stacked Hexatic Liquid-Crystal B Phase.
- [48] D. E. Moncton and R. Pindak in *Ordering in Two Dimensions* (Ed. S. K. Sinha), North Holland, New York, p83 (1980).
- [49] A. J. Leadbetter, J. C. Frost, M. A. Mazid; *J. Phys. (Paris) Lett.*, 40, 325-329 (1979), Interlayer correlations in smectic B phases.
- [50] P. S. Pershan, G. Aeppli, J. D. Litster and R. J. Birgeneau; *Mol. Cryst. Liq. Cryst.*, 67, 205(1981), High-Resolution X-ray Study of the Smectic A-Smectic B Phase Transition and the Smectic B Phase in Butyloxybenzylidene Octylaniline.
- [51] D. E. Moncton, and R. Pindak; *Phys. Rev. Lett.*, 43, 701(1979), Long-Range Order in Two- and Three-Dimensional Smectic-B Liquid-Crystal Films.
- [52] P. A. C Gane, A. J. Leadbetter and P.G. Wrighton; *Mol. Cryst. Liq. Cryst.*, 66, 247-266 (1981), Structure and Correlations in Smectic B, F and I Phases.
- [53] S. Diele, D. Demus and H. Sackmann; *Mol. Cryst. Liq. Cryst. Lett.* , 56, 217 (1980), X-Ray Studies in the n-Pentyl 4-[4-n-Dodecyl-Oxybenzylidene-Amino]-Cinnamate in the S_I Phase.
- [54] J. J. Benattar, F. Moussa, M. Lambert; *J. Phys. (Paris) Lett.*, 42, 67-70 (1981), Two kinds of two-dimensional order : the SmF and SmI phases.
- [55] A. M. Levelut, J. Doucet and M. Lambert; *J. Phys.*, (Paris), 35, 773-779 (1974), X-ray study of the nature of the smectic B mesophases and of the solid-smectic B phase transition.
- [56] J. Doucet, P. Keller, A.M. Levelut and P. Porquet; *J. Phys. (Paris)*, 39, 548-553 (1978), Evidence of two new ordered smectic phases in ferroelectric liquid crystals.
- [57] A. J. Leadbetter, M. A. Mazid, R. M. Richardson, in *Liquid Crystals*, Ed. S. Chandrasekhar, Heyden, London, p65 (1980).
- [58] J. L. Fergason; *Sci. Am.*, 211, 76-85 (1964), Liquid Crystals.
- [59] D. Demus, J. Goodby, G.W. Gray, H.-W. Spiess and V. Vill, *Handbook of Liquid Crystals*, Ch. IV and V, Vol. 2A, Wiley-VCH, Verlag GmbH, Weinheim, FRG (1998).
- [60] F. D. Saeva; *Mol. Cryst. Liq. Cryst.*, 23, 171-177 (1973), On the Relationship between Cholesteric and Nematic Mesophases.
- [61] T. Nakagiri, H. Kodama and K.K. Kobayashi; *Phys. Rev. Lett.*, 27, 564-567 (1971), Helical Twisting Power in Mixtures of Nematic and Cholesteric Liquid Crystals*.
- [62] I. G. Chistiyakov; *Sov. Phys. Usp.*, 9, 551-573 (1967), Liquid Crystals.

- [63] A. Saupe; *Angew. Chem. Intl. Edn.* 7, 97-112 (1968), *Recent Results in the Field of Liquid Crystals*.
- [64] A. Hochbaum, *Fluorescent Guest-Host in Scattering Liquid crystals and New Physical Phenomena in Thin Liquid Crystal Films* (Ph.D. Thesis), Temple University, p.5 (1980).
- [65] J. J. Wysocki, J. Adams and W. Hasse; *Phys. Rev. Lett.*, 20, 1024-1025 (1968), *Electric-Field-Induced phase change in cholesteric liquid crystals*.
- [66] H. Baessler and M. M. Labes; *Phys. Rev. Lett.*, 21, 1791-1793 (1968), *Relationship Between Electric Field Strength and Helix Pitch in Induced Cholesteric-Nematic Phase Transitions*.
- [67] O. Lehmann; *Z Phys. Chem*, 56, 750 (1906).
- [68] Harry J Coles, Pivnenko, N. Mikhail; *Nature* 436 (7053), 997–1000 (2005), *Liquid crystal 'blue phases' with a wide temperature range*.
- [69] Jun Yamamoto, Isa Nishiyama, Miyoshi Inoue, Hiroshi Yokoyama; *Nature*, 437 (7058): 525 (2005), *Optical isotropy and iridescence in a smectic blue phase*.
- [70] R. M. Hornreich and S. Shtrikman; *J. Physique*, 41, 335-340 (1980), *A body-centered cubic structure for the cholesteric blue phase*.
- [71] H. Kikuchi, M. Yokota, Y. Hisakado, H Yang, T. Kajiyama; *Nature Materials*, 1 (1): 64–8 (2002), *Polymer-stabilized liquid crystal blue phases*.
- [72] R. B. Meyer, L. Liebert, L. Strzelecki and P. Keller; *J. Phys. Lett.* 36, L69-L71 (1975), *Ferroelectric liquid crystals*.
- [73] S. Pirke and M. Glogorova in *Ferroelectric – Physical Effects*; Ed, M. Lallart, INTECH, Rijeka, Croatia (2011).
- [74] S. Pirkl and M. Glogarova; *Intech, Croatia* (2011), *Ferroelectric liquid crystals with high spontaneous polarization*.
- [75] R. B. Meyer; *Mol. Cryst. Liq. Cryst.*, 40, 33-48 (1977), *Ferroelectric liquid crystals: A review*.
- [76] Yu. P. Panarin, O. Kalinovskaya & J. K. Vij; *Liquid Crystals*, Vol. 25, No. 2, 241- 252 (1998), *The investigation of the relaxation processes in antiferroelectric liquid crystals by broad band dielectric and electro-optic spectroscopy*.

- [77] A. D. L. Chandani, E. Gorecka, Y. Ouchi, H. Takezoe, and A. Fukuda; *Jpn. J. Appl. Phys.* 28(7), L1265 (1989), Antiferroelectric Chiral Smectic Phases Responsible for the Trislabile Switching in MHPOBC.
- [78] H. Hiraoka, A. D. L. Chandani, E. Gorecka, Y. Ouchi, H. Takezoe and A. Fukuda; *Jpn. J. Appl. Phys.* 29(8), L1473 (1990), Electric-Field-Induced Transitions among Antiferroelectric, Ferrielectric and Ferroelectric Phases in a Chiral Smectic MHPOBC.
- [79] J. P. F. Lagerwall, P. Rudquist, S. T. Lagerwall and F. Gießelmann; *Liq. Cryst.*, 30, 399-414 (2003), On the phase sequence of antiferroelectric liquid crystals and its relation to orientational and translational order.
- [80] K. Miyachi and A. Fukuda, in *Handbook of Liquid Crystals*, Eds. D. Demus, J. Goodby, G.W. Gray, H.-W. Spiess and V. Vill, Vol. 2B, Wiley-VCH, Verlag GmbH, Weinheim, FRG, Ch. 3 (1998).
- [81] J. Dijon in *Liquid Crystal Application and Uses* (Ed. B. Bahadur), Vol. I, World Scientific, Singapore, p 305 (1990).
- [82] N. A. Clark and S. T. Lagerwall; *Appl. Phys. Lett.*, 36, 899-901(1980), Submicrosecond bistable electrooptic switching in liquid crystals.
- [83] D. Armitage, J. I. Thakara and W. D. Eades; *Ferroelectrics*, 85, 291-302 (1988), Ferroelectric liquid-crystal devices and optical processing.
- [84] M. Hird; *Liq. Cryst.*, 38, 1467–1493 (2011), Invited topical review (Ferroelectricity in liquid crystals - materials, properties and applications).
- [85] A. N. Cammidge and R. J. Bushby in *Handbook of Liquid Crystals*, Eds. D. Demus, J. Goodby, G.W.Gray, H.-W. Spiess and V. Vill, Vol. 2B, Wiley-VCH, Verlag GmbH, Weinheim, FRG, Ch.VII (1998).
- [86] S. Kumar; *Liquid Crystals*, 31, 1037-1059 (2004), Recent developments in the chemistry of triphenylene-based discotic liquid crystals.
- [87] M. Schadt and W. Helfrich; *Appl. Phys. Lett.* 18(4), 127 (1971), Voltage-dependent optical activity of a twisted nematic liquid crystal.

- [88] T. J. Scheffer and J. Nehring; *Appl. Phys. Lett.* 45(10), 1021 (1984), A new, highly multiplexable liquid crystal display.
- [89] H. Xu, D. Hartono and K. -L. Yang, *Liquid Crystals*, 37 (10), 1269–1274 (2010), Detecting and differentiating *Escherichia coli* strain TOP10 using optical textures of liquid crystals.
- [90] J. Akaogi, Y. Koizumi, M. Ono and H. Furue; *Mol. Cryst. Liq. Cryst.*, 596, 106–112 (2014), Application of Ferroelectric Liquid Crystals to Optical Devices.
- [91] J. S. Patel and Seong-Woo Suh; *Journal of the Korean Physical Society*, 32, S1048-S1051 (1998), Ferroelectricity in Liquid Crystals and Its Applications.
- [92] C. L. Khetrapal in *Liquid Crystals in the Nineties and Beyond*, Ed. S. Kumar, World Scientific, p 435 (1995).
- [93] B. Bahadur in *Handbook of Liquid Crystals*, Eds. D. Demus, J. Goodby, G.W. Gray, H.-W. Spiess and V. Vill, Vol. 2A, Wiley-VCH, Verlag GmbH, Weinheim, FRG, p257 (1998).

CHAPTER 2

EXPERIMENTAL TECHNIQUES AND ALLIED THEORY

2.1 INTRODUCTION

Liquid crystals have very interesting physical and optical properties which have been established by scientists around the world and various theoretical models have been developed over the years to explain their physical properties. A large variety of liquid crystalline materials have been synthesized and their properties have been determined to establish the relationship between the molecular structures and the macroscopic properties of the materials. A systematic study of the experimental techniques is required for measuring the physical, chemical, electro-optical and dielectric parameters of the compounds. In this dissertation, various properties of selected mesogenic compounds have been studied using different experimental techniques. A brief theoretical background of these techniques along with the Maier-Saupe mean-field theories of nematic and smectic A phases have been described, since most of the materials possess these two phases.

2.2 THEORIES OF LIQUID CRYSTALLINE PHASES

Liquid crystals are an important subclass of soft condensed matter self-assembled on nano scale level and can be broadly described as ordered fluids formed from geometrically anisotropic molecules. The main feature of a liquid crystal is that it is anisotropic in nature and this anisotropic behaviour complicates the analysis of these materials to a great extent. However there are a number of fairly simple theories that can at least predict the general behaviour of the liquid crystal systems. The first molecular field theory of the nematic phase was proposed by M. Born in 1916 [1] where he considered that the nematic medium is an assembly of permanent electric dipoles although it is now well established that the liquid crystalline molecules need not possess permanent dipole moment as a pre-requisite. Various molecular statistical theories have been developed over the years which have been dealt in the books - "The Physics of Liquid Crystals" by de Gennes [2], "Thermophysical Properties of Liquid Crystals" by Tsykalo [3], "Liquid Crystals" by Chandrasekhar [4], "The Physics of Ferroelectric and Antiferroelectric Liquid Crystals" by Musevic, Blinc and Zeks [5] and in books and monographs by various other authors.

Properties of the nematic phase of a liquid crystal can be studied extensively by the molecular field theory. The well known Maier-Saupe (MS) theory [6,7] which is based on the molecular field approximations, explains effectively the nematic isotropic (N-I) transition in

terms of the orientational order parameters. The first molecular statistical treatment of the smectic-nematic transitions was developed by Kobayashi [8], where he introduced an additional isotropic paired intermolecular interaction in Maier-Saupe (MS) model. A simple but elegant description of SmA phase was proposed by McMillan [9,10] in which he extended MS theory to include additional translational and mixed order parameters and characterized the layered structure of SmA phase. In the Kobayashi-McMillan approach the effects of short range order and fluctuation of the order parameters are neglected. The details of the McMillan, Wulf and de Gennes theories on SmC liquid crystals and the Meyer-McMillan theory on of SmC, SmB, and SmH liquid crystals are given in reference [11,12].

2.2.1 Order Parameter

Order parameter is a quantity that measures the amount of order present in a system. In case of rod like liquid crystals, the long molecular axis tends to align in a preferred direction called the director \mathbf{n} . The orientational order parameter, in nematic phase, is basically used to describe the degree to which the liquid crystal molecules are oriented along that director. It can be described by averaged second order Legendre polynomial and is denoted by

$$S = \frac{1}{2}(3 \langle \cos^2 \theta \rangle - 1) \quad (2.1)$$

where $\langle \cos^2 \theta \rangle$ indicates a thermal average of all the molecules, θ being the angle between each molecule and the director. In crystalline state the molecules are perfectly oriented along the director and $\theta = 0$ for each molecule, so $S=1$ for crystalline state. On the other hand in an isotropic liquid the molecules are randomly oriented and the thermal average results in $S=0$. Therefore, within liquid crystalline state S can vary between 0 and 1. The higher values of order parameters correspond to a more ordered phase, as temperature decreases the molecules becomes more ordered. In the absence of an external electric field the most common values of order parameters observed are from 0.3 and 0.9. Strictly speaking order parameter in nematic phase is described by a traceless symmetric tensor of rank two. In order to identify appropriate order parameters of the nematic liquid crystal, it is important to note that it is the probability distribution of the orientations of the constituent molecules that undergoes qualitative change due to change in the symmetry of the system.

Nematic liquid crystals possess uniaxial symmetry, i.e., in a homogeneous medium a rotation around the director does not make a difference. The observed symmetry and structure of the nematic liquid has established that a single order parameter will be sufficient to describe the structure of the phase. In case of smectic liquid crystals, formation of layered structures decreases the symmetry of the medium with respect to the homogeneities of the density, and hence such order parameter should be obtained from probability distribution of the molecular positions in addition to orientational ordering within a plane.

Maier-Saupe (M-S) Mean Field Theory of Nematic Phase

Maier-Saupe theory [6,13-16] is a molecular theory that may be considered with the behavior of one molecule in the field of other molecules. In nematic phase the individual molecule is affected by the anisotropic part of the dispersion interaction energy due to other neighboring molecules. Each molecule is assumed to be in an average orienting field due to its environment. A macroscopic sample contains a huge number of molecules and it is impossible to account for all possible interactions between them. W. Maier and A. Saupe [6] used the concept of orientational order in the nematic phase and approximated the electrostatic interaction by the first term of its multipole expansion. They considered that as far as long range nematic order is concerned, the influence of the permanent dipoles can be neglected and only the induced dipole-dipole interactions need to be considered. They also considered that for a given molecule the distribution of the centers of mass of the remaining molecules may be assumed to be spherically symmetric and the molecules are rotationally symmetric with respect to their long molecular axes.

Thus Maier-Saupe theory is based on the concept of an average potential which is employed to all molecules since every molecule is embedded in a sea of many other molecules, the idea utilized in a thermodynamic system called mean-field theory. The degree of alignment of the molecules with respect to the director \mathbf{n} is described by an orientational order parameter given by (2.1).

It is noted that the potential energy corresponding to the alignment of the molecules is minimum when they are parallel to the director and maximum when they are perpendicular to the

director. The single molecule potential energy V_i should, therefore, be proportional to the function of $\cos^2\theta$ and the degree of order $\langle P_2 \rangle$ and can be represented as

$$V_i(\cos \theta) \propto -\langle P_2(\cos \theta) \rangle P_2(\cos \theta)$$

$$V_i(\cos \theta) = -\nu \langle P_2(\cos \theta) \rangle P_2(\cos \theta) \quad (2.2)$$

$$\text{i.e., } V_i(\cos \theta) = -\frac{A}{V_M} \langle P_2(\cos \theta) \rangle P_2(\cos \theta) \quad (2.3)$$

where ν is a factor represents the strength of intermolecular interaction, V_M is the molar volume of the sample and A is taken to be a constant independent of pressure, volume and temperature.

Humphries, James and Luckhurst [17] developed a more comprehensive concept by including higher order terms in the mean field potential for cylindrically symmetric molecules. Thus potential energy V was taken as

$$V_i(\cos \theta) = \sum_{L \text{ even}} V_L \langle P_L(\cos \theta) \rangle P_L(\cos \theta) \quad (L \neq 0)$$

where $P_L(\cos \theta)$ is the L^{th} order Legendre polynomial.

Orientational Distribution Function and Evaluation of Order Parameters

Once the potential energy of a single molecule in the nematic phase is derived, the orientational distribution function $[f(\cos\theta)]$ which gives the probability of finding a molecule at some prescribed angle θ from the director, can be obtained. According to classical statistical mechanics the orientational distribution function can be represented as

$$f(\cos \theta) = Z^{-1} \exp \left[\frac{-V(\cos \theta)}{kT} \right] \quad (2.4)$$

where k is the Boltzmann constant, T is temperature in absolute scale and Z being the partition function for a single molecule. Z is given by

$$Z = \int_0^1 \exp\left[\frac{-V(\cos\theta)}{kT}\right] d(\cos\theta)$$

The order parameter $\langle P_2 \rangle$ is the average value of the second order Legendre function for a given molecule and can be written as

$$\begin{aligned} S = \langle P_2 \rangle &= \int_0^1 P_2(\cos\theta) f(\cos\theta) d(\cos\theta) \\ &= \frac{\int_0^1 P_2(\cos\theta) \exp[v\langle P_2 \rangle P_2(\cos\theta)/kT] d(\cos\theta)}{\int_0^1 \exp[v\langle P_2 \rangle P_2(\cos\theta)/kT] d(\cos\theta)} \end{aligned} \quad (2.5)$$

This self-consistent equation can be solved numerically to find the temperature dependence of the order parameters. Out of several solutions, the equilibrium state is identified by the minimum value of free energy. For isotropic liquid $\langle P_2 \rangle = 0$, which is the disordered phase. For $T < 0.22284 v/k$, equation 2.5 gives two other solutions. At absolute zero the upper branch tends to unity which represents nematic phase and the lower branch tends to $-\frac{1}{2}$ at absolute zero represents an unstable phase where the molecules attempt to orient themselves perpendicular to the director. From $T = 0$ to $T = 0.22019 v/k$ the nematic phase is stable. Orientational order parameter varies from 1 at $T=0$ to 0.4289 at $T=0.22019 v/k$. Thus according to Maier-Saupe theory the nematic-isotropic transition is first order.

Exactly in a similar way one can find higher order orientational order parameter $\langle P_4 \rangle$ using the 4th order Legendre polynomial in equation (2.5).

McMillan's Theory of Smectic A Phase

The theory of smectic A liquid crystals have been investigated by a number of investigators. McMillan's Theory [9] is an extension of the Maier-Saupe mean field model of nematics in which an additional order parameter characterizing the 1-D translational periodicity of the layered structure is included. Since the smectic A liquid crystals possess both orientational and translational order, the molecular distribution function must therefore describe both the

tendency of the molecules to orient along \mathbf{n} and to form layers perpendicular to \mathbf{n} . Thus the distribution function will be a function of both $\cos\theta$ and z , and the normalised distribution function can be written as

$$f(z, \cos\theta) = \sum_{l \text{ even}} \sum_n A_{l,n} P_l(\cos\theta) \cos\left(\frac{2\pi n z}{d}\right) \quad (2.6)$$

with
$$\int_{-1}^1 \int_0^d f(z, \cos\theta) dz \cdot d(\cos\theta) = 1 \quad (2.7)$$

where d is the layer thickness.

The Kobayashi-McMillan (KM) description of the Sm_AN transition takes into account the effect of orientational order and an adhoc orientational interaction was introduced. In this theory the molecules are again assumed to be oriented along the z direction but the orientational ordering does not have to be ideal. With this concept McMillan developed [9] the theory of smectic A liquid crystals by assuming a model potential starting from the Kobayashi [18,19] form of potential. For simplicity, neglecting higher order terms, the mean field potential was expressed as

$$V_1(z, \cos\theta) = -v_0 \left[\delta \alpha \tau \cos\left(\frac{2\pi z}{d}\right) + \left\{ S + \sigma \alpha \cos\left(\frac{2\pi z}{d}\right) \right\} P_2(\cos\theta) \right] \quad (2.8)$$

where, $S = \frac{1}{2} \langle 3 \cos^2 \theta - 1 \rangle$ is the orientational order parameter,

$\tau = \langle \cos\left(\frac{2\pi z}{d}\right) \rangle$ is the translational order parameter, and

$\sigma = \langle P_2(\cos\beta) \cos\left(\frac{2\pi z}{d}\right) \rangle$ is the mixed order parameter

and v_0 and δ are constants characterising the strengths of the anisotropic and isotropic parts of the interaction respectively, α is a parameter which depends on the core length and the molecular length. The above potential function reduces to MS potential when the two adjustable parameters δ and α become zero.

Here the distribution function can be expressed as

$$f_1(z, \cos \theta) = Z^{-1} \exp \left[-\frac{V_1(z, \cos \theta)}{kT} \right] \quad (2.9)$$

where the single molecular partition function Z is given by

$$Z = \int_0^d dz \int_0^1 d(\cos \theta) \exp \left[-\frac{V_1(z, \cos \theta)}{kT} \right]$$

The various order parameters are, shown to be, given by

$$\left. \begin{aligned} S &= \int_0^1 \int_0^d P_2(\cos \theta) f_1(z, \cos \theta) dz d(\cos \theta) \\ \tau &= \int_0^1 \int_0^d \cos\left(\frac{2\pi z}{d}\right) f_1(z, \cos \theta) dz d(\cos \theta) \\ \sigma &= \int_0^1 \int_0^d P_2(\cos \theta) \cos\left(\frac{2\pi z}{d}\right) f_1(z, \cos \theta) dz d(\cos \theta) \end{aligned} \right\} \quad (2.10)$$

These self-consistent equations can be solved numerically to find the temperature dependence of the three order parameters.

Out of several solutions, the equilibrium state is identified by the minimum value of free energy. In general we get the following three cases with S , σ and τ :

- i) $\tau = \sigma = S = 0$, no order characteristic of the isotropic liquid phase;
- ii) $\tau = 0$, $\sigma = 0$, $S \neq 0$, orientational order only, the theory reduces to the Maier-Saupe theory for the nematic phase; and
- iii) $\tau \neq 0$, $\sigma \neq 0$, $S \neq 0$, orientational and translational order characteristic of the smectic A phase.

One can also predict the nature of the smectic to nematic phase transition observing McMillan ratio (T_{NA}/T_{NI}). If $(T_{NA}/T_{NI}) > 0.87$ then the SmA – N transition is of first order and if $(T_{NA}/T_{NI}) < 0.87$ then it is of the second order. Although the three quantities of equation 2.10 are sufficient

to parameterize simple mean field model, a good approximation to the true distribution function $f(\cos\theta, z)$ requires many terms in equation 2.6.

2.2.2 Mesophase Structure: X-Ray Diffraction

X-ray diffraction study provides one of the most definitive ways to determine the structure of different liquid crystalline phases. Structural investigations of the mesophases, identification of different mesophases and study of various microscopic physical quantities can be studied by this method. An X-ray diffraction experiment gives Fourier image of the electron density function and analysis of those scattering data yields information about the mutual arrangement of the molecules in a particular liquid crystalline phase as well as the specific features of the orientational and translational long range order. The details of this technique have been reviewed by many authors [20-23].

Consider a basic scattering experimental technique as shown in Figure 2.1. Bragg visualized the scattering of X-rays by a crystal in terms of reflections from sets of lattice planes, as shown in Figure 2.2.

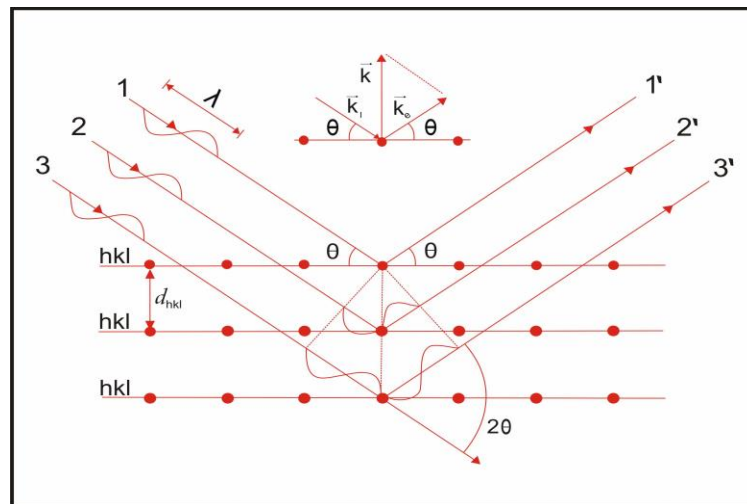


Figure 2.1: Typical scattering geometry showing the incident and scattered wave vector

For elastic scattering, the magnitude of incident and scattered wave vectors must be equal, i.e., $|\mathbf{K}_s| = |\mathbf{K}_i| = 2\pi / \lambda$, where λ is the wavelength of the incident radiation. The magnitude of the scattering wave vector is given by,

$$\mathbf{Q} = \mathbf{K}_s - \mathbf{K}_i, \quad Q = |\mathbf{Q}| = 4\pi\sin\theta/\lambda,$$

where 2θ is the angle between \mathbf{K}_s and \mathbf{K}_i . The scattering of incident radiation by a scattering centre at \mathbf{r} is described (relative to the initial amplitude) by the scattering amplitude $f \exp(i\mathbf{Q}\cdot\mathbf{r})$, where f is the scattering power of the scattering centre. Generalised to N such scattering centres the scattering amplitude can be expressed as

$$F(\mathbf{Q}) = \sum_{j=1}^N f_j \exp(i\mathbf{Q}\cdot\mathbf{r}_j) \quad (2.11)$$

where \mathbf{r}_j denotes the position of the j^{th} scattering centre. For a continuous distribution of scattering centers characterized by the electron density function $\rho(\mathbf{r})$ one writes

$$F(\mathbf{Q}) = \int \rho(\mathbf{r}) \exp(i\mathbf{Q}\cdot\mathbf{r}) d\mathbf{r} \quad (2.12)$$

If the integration is carried over all space then \mathbf{F} is Fourier transform of the electron density and provides the link between the real (\mathbf{r}) and the reciprocal (\mathbf{Q}) space.

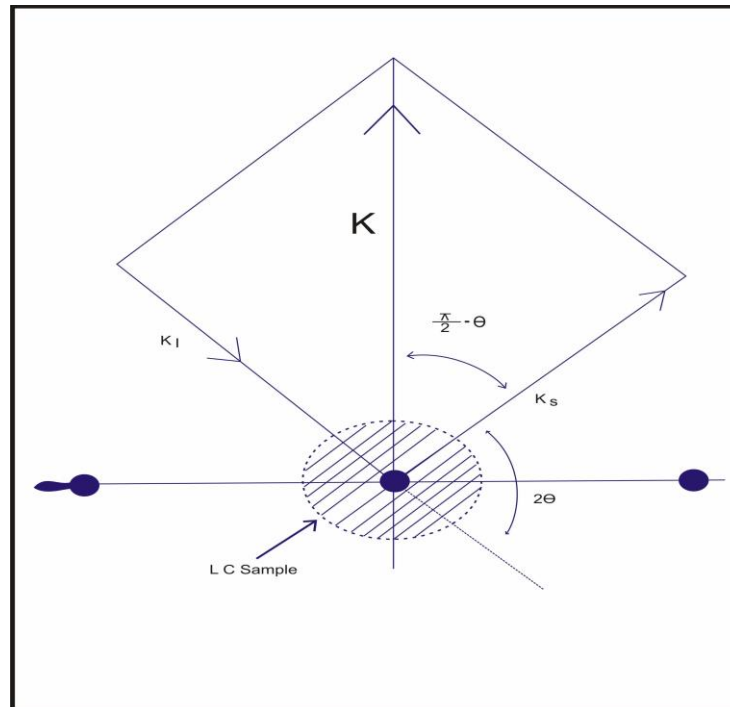


Figure 2.2: Typical scattering geometry showing the incident (K_i) and scattered (K_s) wave vector

For the case of isolated atom this assumes the form

$$f(\mathbf{Q}) = \int \rho_a(\mathbf{r}) \exp(i\mathbf{Q} \cdot \mathbf{r}) d\mathbf{r}$$

which is called the atomic scattering amplitude. For a group of atoms, for which

$$\rho(\mathbf{r}) = \sum_{j=1}^N \rho_j(\mathbf{r} - \mathbf{r}_j)$$

this leads to

$$F(\mathbf{Q}) = \sum_{j=1}^N f_j(\mathbf{Q}) \exp(i\mathbf{Q} \cdot \mathbf{r}_j) \quad (2.13)$$

This is almost identical to equation (2.11), but in this case the atoms are considered as extended object and the variation of the atomic scattering amplitude with \mathbf{Q} has been considered, i.e., the

diffraction by a set of atoms may be treated in terms of diffraction by a set of points, provided the variation of the atomic scattering amplitude is accounted for.

So far only scattering amplitudes have been considered. To get absolute value and hence the experimentally relevant intensity, the amplitude of a wave scattered by a single point electron must be known. With the help of classical electrodynamics expressing all intensities in terms of the scattering intensity of an electron we get expression for intensity

$$I(\mathbf{Q}) = |F(\mathbf{Q})|^2$$

For molecular liquids it is convenient to separate the amplitude due to the molecular structure from the total scattering amplitude [13]. Accordingly equation 2.11 can be written as

$$F(\mathbf{Q}) = \sum_{k,m} f_{km}(\mathbf{Q}) \exp[i\mathbf{Q} \cdot (\mathbf{r}_k - \mathbf{R}_{km})] \quad (2.14)$$

where \mathbf{r}_k gives the position of the centre of mass of the molecule 'k', and \mathbf{R}_{km} is the position of the atom 'm' within that molecule, f_{km} is the atomic scattering factor of the atom 'm' in the molecule 'k'. Using (2.14) the general scattering intensity from a set of molecules is

$$I(\mathbf{Q}) = \sum_{k,l,n,m} \langle f_{k,m}(\mathbf{Q}) f_{l,n}^*(\mathbf{Q}) \exp[i\mathbf{Q} \cdot (\mathbf{r}_k - \mathbf{r}_l)] \exp[i\mathbf{Q} \cdot (\mathbf{R}_{ln} - \mathbf{R}_{km})] \rangle \quad (2.15)$$

where the brackets indicate statistical average over the constituent molecules of the liquid. The intensity given in equation 2.15 can be written as

$$I(\mathbf{Q}) = I_m(\mathbf{Q}) + D(\mathbf{Q})$$

where $I_m(\mathbf{Q})$ is the molecular structure factor and $D(\mathbf{Q})$ is called the interference function which are respectively given by

$$I_m(\mathbf{Q}) = \sum_k \left\langle \sum_{m,n} f_{km}(\mathbf{Q}) f_{kn}^*(\mathbf{Q}) \exp[i\mathbf{Q} \cdot (\mathbf{R}_{kn} - \mathbf{R}_{km})] \right\rangle$$

$$= N \left\langle \left| \sum_m f_{km} \exp(-i \mathbf{Q} \cdot \mathbf{R}_{km}) \right|^2 \right\rangle \quad (2.16)$$

$$D(\mathbf{Q}) = \left\langle \sum_{k \neq l} \exp(i \mathbf{Q} \cdot \mathbf{r}_{kl}) \sum_{m,n} \langle f_{km}(\mathbf{Q}) f_{ln}^*(\mathbf{Q}) \exp[\mathbf{Q} \cdot (\mathbf{R}_{ln} - \mathbf{R}_{km})] \rangle \right\rangle \quad (2.17)$$

where $\mathbf{r}_{kl} = \mathbf{r}_k - \mathbf{r}_l$

The term $I_m(\mathbf{Q})$ gives the scattered intensity which would be observed from a random distribution of identical molecules. $D(\mathbf{Q})$ is the term containing information about correlation in both positional and orientation of different molecules. The parameters are (i) apparent molecular lengths in nematics, (ii) layer thickness in smectics, (iii) average lateral distance between the molecules, (iv) correlation lengths, (v) tilt angle, (vi) molecular packing, (vii) orientational distribution function, (viii) order parameters $\langle P_2 \rangle$, $\langle P_4 \rangle$... etc., (ix) bond orientational order parameter, (x) layer order parameters τ and $\langle z^2 \rangle$ in Sm-A and (xi) critical exponents.

2.2.3 Identification of Mesophases and Transition Temperatures

The existence of a liquid crystalline phase can be established by visual inspection of the compound while it is heated. The mesophase is distinguished from the isotropic liquid by its turbid appearance and from the crystalline solid by its flow properties. A liquid crystal may possess a variety of mesophases which is impossible to identify only by visual inspection. To study a liquid crystal it is very important to identify its phase behavior and the transition temperatures of each phase. In order to identify the liquid crystal phases and to determine the corresponding transition temperatures, several techniques can be used. We have used three techniques viz. (1) Optical polarization microscopy (OPM), (2) Differential scanning calorimetry (DSC), (3) X-ray diffraction method, which is described in subsequent sections. Other techniques used to find the nature of a mesophase include neutron scattering [24], nuclear magnetic resonance (NMR) [24-26], IR, Raman, UV-Visible spectroscopic studies [27], Fabry-Perot Etalon method [28] etc.

Optical Polarization Microscopy (OPM)

The polarizing microscope (Figure 2.3) is a classical and very useful tool for the investigation of liquid crystalline phases. In an optical microscope one looks at the object image of a thin mesomorphic layer (thickness $\sim 10\text{-}20\ \mu\text{m}$) between two glass plates under polarised light. The patterns so observed through the microscope are called textures which are due almost entirely to the defect structure that occurs in the long-range molecular order of the liquid crystals. Depending on the boundary conditions and the type of phase, specific textures are observed, that provide a means of classifying the different phases. The temperature of the liquid crystalline material is controlled usually between room temperature and 300°C by inserting the glass slide in a hot stage and placed between the polarisers which are crossed at 90° to each other. In isotropic phase the field of view appears dark, but beautiful texture appears if the material form liquid crystal phase on cooling. Observed texture type depends on the alignment of the sample viz., whether homeotropic or homogeneous (planar) and the involved phase structure.

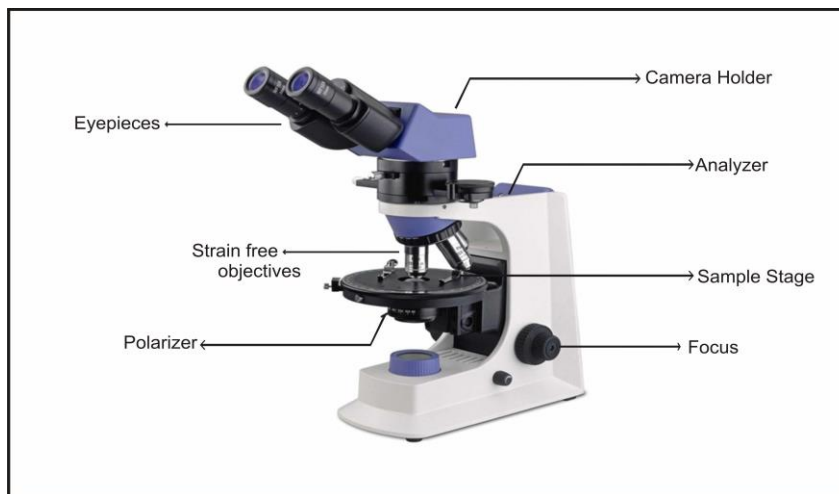


Figure 2.3: Polarizing microscope

Usually texture changes occur at the transitions between the various phases. A number of useful books with photographs of typical textures and explanations of their origins have been published by Demus and Richter (1978) [29], I. Dierking [30], Slaney *et al.* [31] and Bouligand [32]. The identification of the mesophases by this technique is often difficult because similar textures might be exhibited by different phases or sometimes very subtle changes in textures occur

at transitions and hence requires the support of other techniques to finalize the phase type present.

Differential Scanning Calorimetry (DSC)

Differential scanning calorimetry is the modern calorimetric method which is now very well-established tool for studying mesomorphic systems. The process reveals the transition temperatures of different phases by measuring the enthalpy change associated with a transition. The level of enthalpy change provides some indication of the types of phase involved. When a material melts, a change of state occurs from solid to liquid and this melting process requires energy (endothermic) from the surroundings. Converse is also true. Crystalline solid to liquid crystalline phase transition involves high enthalpy change ($\sim 30\text{-}40 \text{ kJmol}^{-1}$). But transition between two mesophases and mesophase to isotropic liquid transition are accompanied by much smaller enthalpy changes ($\sim 1\text{-}2 \text{ kJmol}^{-1}$). Mettler FP82 hot stage and FP84 thermosystem were used for texture and DSC studies. The DSC measurement setup is shown in Figure 2.4. A drawback of scanning calorimetric method is that the latent heat and the pretransitional increase in the specific heat near a phase transition are lumped together into one peak. In order to establish the nature of a phase transition the true latent heat must be measured. This can be done by adiabatic calorimetry, which is much more time consuming.

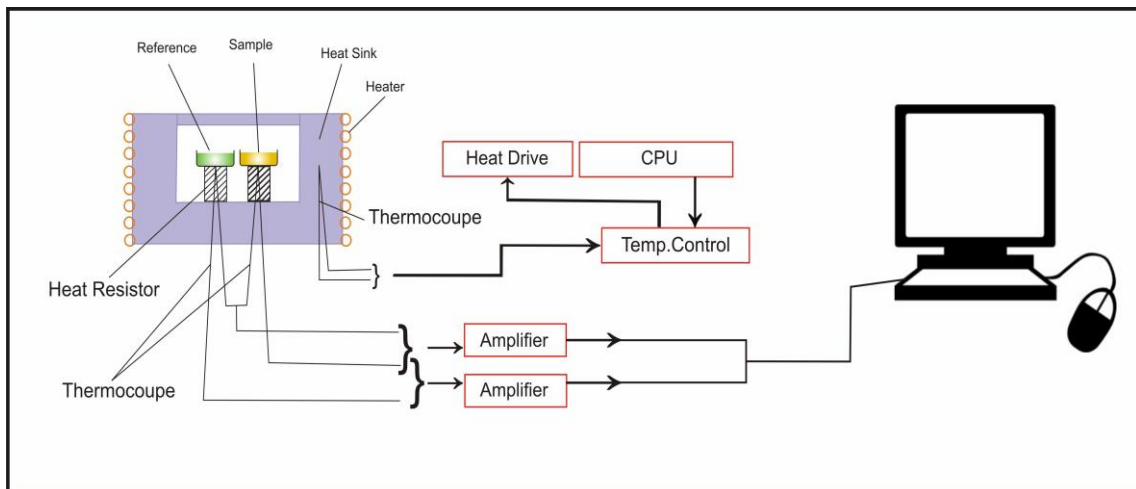


Figure 2.4: Experimental setup for DSC measurement

Experimental Techniques for X-ray Diffraction Studies and Method of Data Analysis

The basic experimental arrangement used for X-ray diffraction studies is shown in Figure 2.5 and similar experimental setup was designed and fabricated in our laboratory earlier [33,34], which I have used for the measurements.

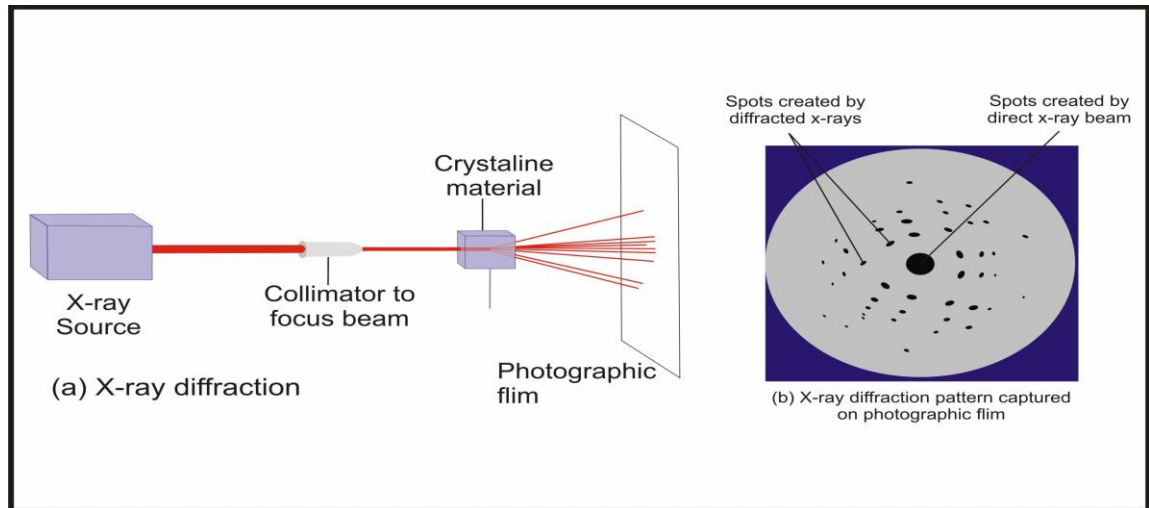


Figure 2.5: X-ray diffraction experimental setup and diffraction photographs

The x-ray diffraction photographs are taken using nickel filtered $\text{CuK}\alpha$ radiation, in a flat plate camera. By capillary action the sample is filled in a thin walled (~ 0.05 mm) Lindemann glass capillary of 1 mm diameter and is aligned by slow cooling from the isotropic phase to the desired temperature. X-ray photographs were taken at different temperatures by using a temperature controller, Indotherm 401- (India) within an accuracy of $\pm 0.5^\circ\text{C}$ and by the Eurotherm controller (2216e) with an accuracy $\pm 0.1^\circ\text{C}$.

Various types of diffraction patterns are obtained depending upon the type of the mesophases [34-43]. For the discussion of the experimental results for X-ray scattering by nematic and smectic liquid crystals, typical diffraction photographs of magnetically oriented samples are shown in Figure 2.6.

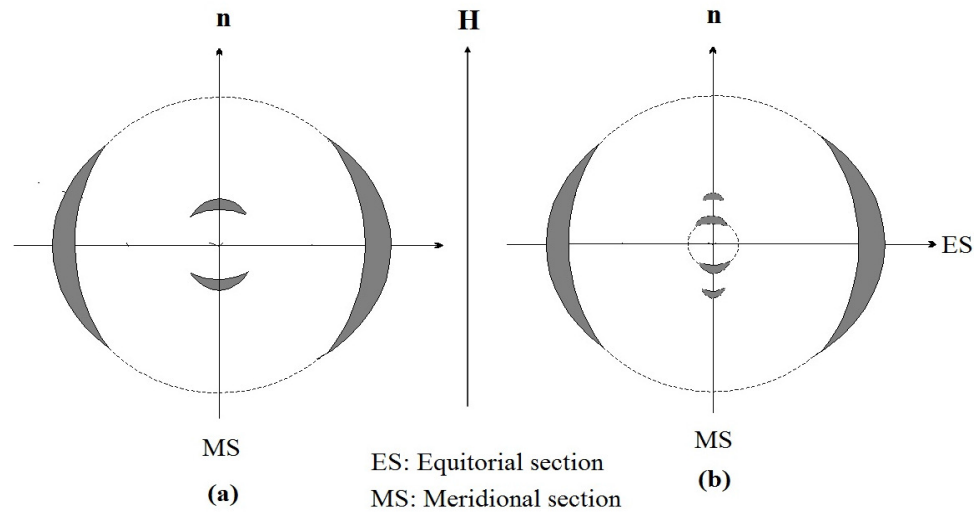


Figure 2.6: Schematic representation of the X-ray diffraction pattern of an oriented **(a)** nematic and **(b)** smectic A phase.

The diffraction pattern of nematic phase consists of a combination of meridional and equatorial maxima. However, an un-oriented nematic sample shows diffraction pattern as obtained from an isotropic liquid viz. two uniform halo, at low and high angles. This is due to the fact that, generally an un-oriented liquid crystal sample consists of a large number of domains and within each domain the molecules are aligned in a preferred direction, but there is no preferred direction for the sample as a whole and naturally, X-ray diffraction pattern will have a symmetry of revolution around the direction of X-ray beam. For an aligned nematic sample the outer circular halo is splitted into two crescents having maxima along the equatorial direction (\perp to \mathbf{n}) which are formed due to intermolecular scattering and the corresponding Bragg's angle is a measure of the lateral intermolecular distance (D). Generally the intermolecular distance (D) lie between 3.5\AA to 6.5\AA , lateral dimensions of a typical mesogenic molecule and the average intermolecular distance is found to be around 5\AA . Along the meridional direction (\parallel to \mathbf{n}), the inner halo also has two crescents with maxima at much lower angle. This diffraction peak must arise from correlations in the molecular arrangement along the director \mathbf{n} . So by measuring the corresponding diffraction angles one gets the value of the apparent molecular length (l) in the nematic phase and layer spacing in smectic phase. In case of smectic phases the inner pattern appears as sharp spots; sometimes second order spots are also found, translational order parameter can also be determined in such cases.

The average lateral distance between the neighboring molecules (D) was calculated from the x-ray diffraction photographs by using the Bragg formula

$$2D \sin\theta = k\lambda \quad (2.18)$$

where θ is the Bragg angle for the equatorial diffraction, λ is the wavelength of the x-ray beam and 'k' is a constant which comes from the cylindrical symmetry of the system. For perfectly ordered state $k = 1.117$ as given by de Vries [44,45]. As the variation of 'k' with $\langle P_2 \rangle$ is very small, the value of $k = 1.117$ is used for all our calculations. The apparent molecular length or the layer thickness 'd' is calculated from the equation

$$2d \sin \theta = \lambda \quad (2.19)$$

where θ is the Bragg angle for the meridional diffraction crescents for an aligned sample and inner halo for unaligned sample.

For the determination of the actual distance between the sample and the film, x-ray diffraction photograph of aluminium powder was taken. The Bragg's angle θ' corresponding to the (hkl) reflecting plane, is determined by using [46]

$$\sin \theta' = \frac{\lambda}{2a} \sqrt{h^2 + k^2 + l^2} \quad (2.20)$$

where a is the lattice constant. Measuring the diameter of the diffraction rings corresponding to (111) and (222) reflections, the actual distance between the sample and the film was found out from the relation

$$\tan 2\theta' = \frac{R}{2H} = \frac{\text{radius of the ring}}{\text{sample to film distance}} \quad (2.21)$$

Using this sample to film distance the Bragg angle (θ) for the peak corresponding to the parameters l, d and D of the liquid crystal sample were calculated using the above relation (2.21).

For the above analysis the diffraction photographs were first digitized in 24 bit RGB colour format by using HP scan jet 2200c scanner. The digitized images were analyzed using the colour values of the pixels to obtain the radii of the inner and outer diffraction rings and from that the apparent molecular length (l) or the smectic layer spacing (d) and the average intermolecular spacing (D) were obtained. Two softwares Adobe Photoshop 7.0 and origin 7.0 were used for analyzing the digital images. The uncertainties in calculated l and D values are $\pm 0.1, \pm 0.02 \text{ \AA}$ respectively.

Synchrotron X-ray Diffraction

In Synchrotron X-Ray Powder Diffraction technique, X-rays are generated by a synchrotron facility and it is an extremely powerful source of X-rays. A synchrotron uses powerful magnets and radio frequency waves to accelerate charged particles. The powerful magnet and radio frequency waves accelerate negatively charged electron along a stainless steel tube, where they reach high speed. As the magnets are turned on and off, electrons get pulled along the ring of tubes. Since the fast-moving electrons emit a continuous spectrum of light, with various wavelengths and strength, scientists can pick whatever wavelength they need for their experiments e.g. visible light, ultraviolet light or X-rays (soft or hard x-rays). The X-rays thus produced are at least 5 orders of magnitude more intense than the best X-ray laboratory sources. For studying the structures of different phases in the chiral compound (MPOBC), synchrotron radiation facility, PETRA III beamline at P07 Physics Hutch station at DESY, Hamburg was used (Figure 2.7). A sample was taken in a Lindemann glass capillary of diameter 1.0 mm and very slowly cooled down from isotropic phase to the desired temperature to get an aligned sample. 50 images of exposure time 0.2 s were grabbed and averaged to get one diffraction image and five such images were collected at a particular temperature. All the physical parameters were averaged over these five image data. A Perkin Elmer 2D detector of pixel size $200 \times 200 \mu\text{m}$ and total size $400 \times 400 \text{ mm}$ was used for image grabbing which was placed 3.3m away from the sample. QXRD program for PE Area Detectors (G Jennings, version 0.9.8, 64 bit) was used for data acquisition and also for analyzing the images. Images were integrated using a step size of 0.002 to get intensity versus wave vector (Q) distribution.

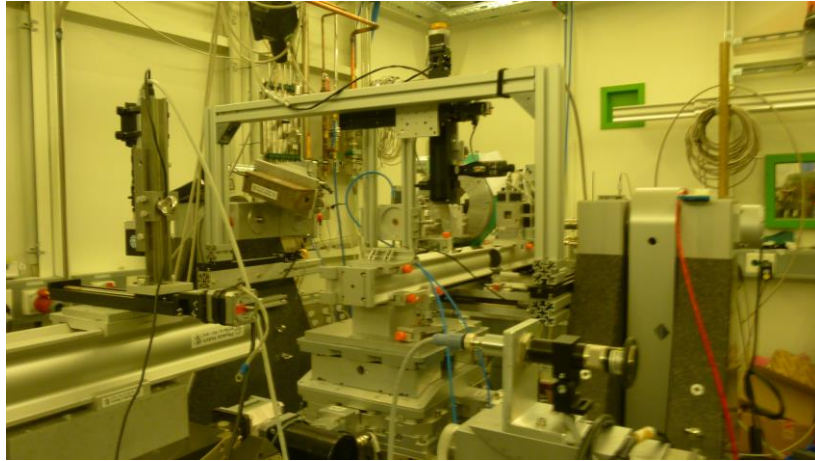


Figure 2.7: Synchrotron X-ray diffraction set up at DESY, Hamburg, Germany

2.2.4 Optical Birefringence

Liquid crystals are found to be birefringent due to their anisotropic nature i.e., they demonstrate double refraction. This is because of light polarized parallel to the director has a different index of refraction than light polarized perpendicular to the director. So, a uniaxial (liquid) crystal has two principal refractive indices, n_o and n_e . n_o is called the “ordinary” refractive index, associated with a light wave where the electric vector vibrates perpendicular to the optical axis. The “extraordinary” index n_e is observed for a linearly polarized light wave where the electric vector is parallel to the optical axis. The optical anisotropy or birefringence of a material is characterized by the difference ($\Delta n = n_e - n_o$) in the indices of refraction for the ordinary and extraordinary rays, which depends on the wavelength of the light used and the thermal state of the compounds [47]. Birefringence is a property usually associated with transparent crystals with a non-centrosymmetrical lattice structure. Physical origin of the optical properties of liquid crystal has been detailed by Dunmur [48].

Optical birefringence (Δn) is responsible for the appearance of interference colors in LCDs operating with plane-polarized light [49]. Interference between the extraordinary ray and the ordinary ray, gives rise to the colored appearance of these thin films. For a wave at normal incidence, the phase difference in radians between the o-ray and e-rays caused by traversing a

birefringent film of thickness d and birefringence Δn is referred to as the optical retardation δ given by

$$\delta = \frac{2\pi\Delta nd}{\lambda}$$

where λ is the wavelength of light in vacuum.

Measurement of Ordinary and Extraordinary Refractive Indices

The ordinary and extraordinary refractive indices (n_o , n_e) have been measured by constructing a thin prism in our laboratory. Geometry of the experimental set up is shown in Figure 2.8. To construct the prism a set of glass plates were taken and washed by concentrated nitric acid and clean water. After drying, plates were washed with acetone to clean oily substances present. The plates were then treated with a dilute (~1% aqueous) solution of polyvinyl alcohol (PVA) and then dried and rubbed several times on a tissue paper in the same direction to get a preferential direction on the substrates. A prism was then formed, by keeping the treated surfaces inside and the rubbing directions parallel to the refracting edge of the prism. The sides of the prism were then sealed by using a high temperature adhesive and it was baked for several hours. The angles of the prisms were kept less than 1° by using a thin glass spacer. The details of the preparation of the prism are already reported by Zeminder *et al.* [50]. The prism was filled with sample in isotropic phase from its top open side such that no air bubble was trapped inside. The system was heated to isotropic phase and cooled down slowly to the desired temperature so that liquid crystalline molecules were perfectly aligned with its optical axis parallel to the refracting edge of the prism. The prism was then placed inside a laboratory made thermostatic brass oven with a circular aperture. The temperature of the oven was controlled by a temperature controller (Eurotherm model 2216e with an accuracy of $\pm 0.1^\circ\text{C}$). The refractive indices were measured by using a Laser source (Jain Lasertech Pvt. Ltd., India), a collimator and a transparent scale as screen placed at a large distance. By measuring the deviation produced by the ordinary ray and extraordinary ray, the corresponding refractive indices were measured. The ordinary refractive index (n_o) is temperature dependent, increasing slightly over the nematic range and then rapidly increases as the temperature nears the phase transition. Conversely, the extraordinary refractive index (n_e) is particularly dependent on the molecular structure and can

vary in the visible region from 1.5 for saturated compounds up to 2.0 for highly conjugated compounds. At temperatures above the clearing point (T_c), liquid crystals become isotropic liquids and birefringence goes to zero as n_e and n_o coincide at their mean. Measured refractive indices were accurate within ± 0.001 .

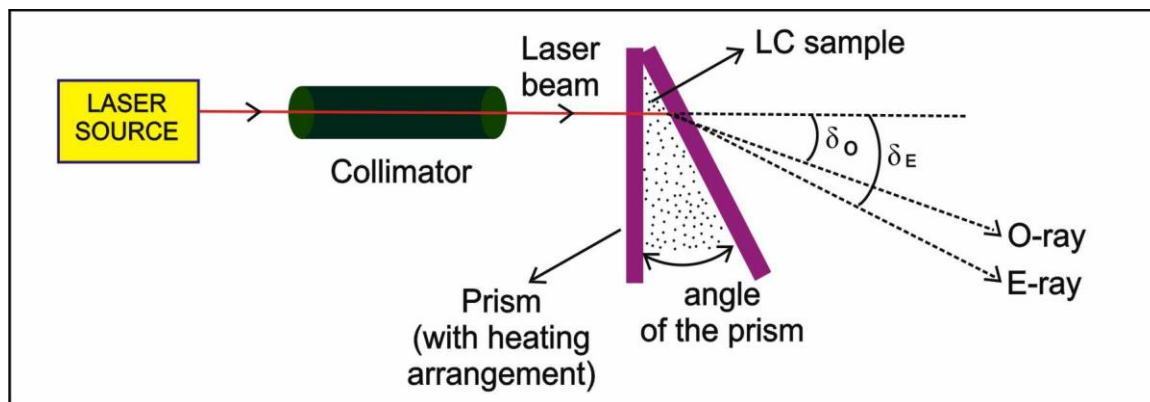


Figure 2.8: Schematic arrangement for the measurement of refractive indices

Measurement of Density

The density of the liquid crystalline samples were measured at different temperatures during both heating and cooling using a borosilicate glass tube dilatometer of capillary type, a travelling microscope and temperature controller. A weighed sample of the liquid crystal was introduced inside the dilatometer in isotropic state and was placed in a thermostated silica oil bath. The bulb of the dilatometer was filled with mercury. Sufficient time was allowed to reach the equilibrium at the desired temperature before taking each reading. The length of the liquid crystal column was measured at different temperatures with a travelling microscope. The densities were calculated after correction of glass expansion. Average value of the data obtained during heating and cooling are presented which are accurate within $\pm 0.1\%$.

Calculation of Optical Polarizabilities from Refractive Index and Density Measurements

The molecular polarizability (α) of the molecules and order parameter control the optical anisotropy. The linear molecules having a long and rigid core exhibit high order parameter. Molecules that consist of high polarizability units (having π and delocalized electrons) such as aromatic rings in the core, tolane linking groups and terminal cyano groups have a high birefringence. Conversely, a low birefringence is exhibited by molecules that are deficient in these types of groups and usually consist of alicyclic groups and terminal alkyl chains. The molecular polarizability ' α ' can be determined if the value of internal field, i.e., the average field acting on an individual molecule is known. Lorenz-Lorentz field, commonly known internal field valid for isotropic phase, is not applicable for mesogenic systems. Therefore, more realistic internal field, proposed by the Vuks' [51] and Neugebauer's [52] are usually applied in liquid crystalline systems.

Vuks' Method

Considering the internal field independent of molecular interaction, Vuks' derived the relations for polarizabilities associated with anisotropic molecules. In this case the effective molecular polarizabilities α_o and α_e , perpendicular and parallel to the direction of molecular axes, are related to n_o and n_e by the following equations

$$\alpha_o = \frac{3}{4\pi N} \frac{n_o^2 - 1}{n^2 + 2} \quad (2.22)$$

$$\alpha_e = \frac{3}{4\pi N} \frac{n_e^2 - 1}{n^2 + 2} \quad (2.23)$$

where N is the number of molecules per unit volume obtained from measured density and n is the mean refractive index and is given by

$$n^2 = \frac{1}{3}(2n_o^2 + n_e^2) \quad (2.24)$$

Neugebauer's Method

In this method internal field is calculated by representing the polarizability of a molecule by anisotropic point polarizability. Here the Lorenz-Lorentz equation for an isotropic system is extended to an anisotropic system. The relevant relations derived by Neugebauer are as follows:

$$n_e^2 - 1 = 4\pi N\alpha_e(1 - N\alpha_e\gamma_e)^{-1} \quad (2.25)$$

$$n_o^2 - 1 = 4\pi N\alpha_o(1 - N\alpha_o\gamma_o)^{-1} \quad (2.26)$$

where N is the number of molecules per unit volume and γ_e and γ_o are the respective internal field constants for extraordinary and ordinary rays. The equations necessary for calculating polarisabilities α_o and α_e obtained from the above equations are:

$$\frac{1}{\alpha_e} + \frac{2}{\alpha_o} = \frac{4\pi N}{3} \left[\frac{n_e^2 + 2}{n_e^2 - 1} + \frac{2(n_o^2 + 2)}{n_o^2 - 1} \right] \quad (2.27)$$

$$\alpha_e + 2\alpha_o = \frac{9}{4\pi N} \left[\frac{n^2 - 1}{n^2 + 2} \right] \quad (2.28)$$

Principal polarizabilities can be obtained by solving the above two equations.

Calculation of Orientational Order Parameter from Polarizability

The degree of order of the mesogenic molecule has been determined using polarizability values obtained from the above two methods. The principal polarizabilities, parallel and perpendicular to the direction of molecular axes, are related to the orientational order parameter [53-55] as

$$\alpha_e = \bar{\alpha} + \frac{2}{3}\Delta\alpha S$$

$$\alpha_o = \bar{\alpha} - \frac{1}{3}\Delta\alpha S$$

So,

$$S = \langle P_2 \rangle = \frac{\alpha_e - \alpha_o}{\alpha_{\parallel} - \alpha_{\perp}} \quad (2.29)$$

where $\bar{\alpha} = (2\alpha_o + \alpha_e)/3$, is the mean polarizability and $\Delta\alpha = \alpha_e - \alpha_o$ is the polarizability anisotropy. Here, S is the macroscopic order parameter and α_{\parallel} and α_{\perp} are the principal polarizabilities parallel and perpendicular to the long molecular axis in the perfectly ordered crystalline state where $S=1$. By using Haller's extrapolation procedure [56] one can get the values of $(\alpha_{\parallel} - \alpha_{\perp})$ in the solid state. In this method a graph is drawn by plotting $\log(\alpha_e - \alpha_o)$ against $\log(T_c - T)$ which should be a straight line. This line is extrapolated up to $\log(T_c)$, giving the value of $(\alpha_e - \alpha_o)_{T=0} = (\alpha_{\parallel} - \alpha_{\perp})$, T_c being the N-I transition temperature.

2.2.5 Dielectric Anisotropy

A material that does not conduct electricity but can essentially store the electric charges by means of polarization is called dielectric. The most common liquid crystal molecules are rod like and are axially symmetric about its long axis or the director \mathbf{n} . The dielectric constant along the long molecular axis (ϵ_{\parallel}) and perpendicular axis (ϵ_{\perp}) are different. The difference between this two is called the dielectric anisotropy ($\Delta\epsilon = \epsilon_{\parallel} - \epsilon_{\perp}$). Dielectric anisotropy is very important parameter because the threshold voltage (V_{th}) and other operational parameters of liquid crystal displays depend on the anisotropy of the permittivities [57]. The value of $\Delta\epsilon$ may be positive or negative depending on the angle between the permanent dipole moment and the molecular axis. The larger the dielectric anisotropy value is for a liquid crystal molecule, the weaker the electric field must be to reorient the dipole moment along the field direction. The dielectric anisotropy of liquid crystals is inversely proportional to temperature. As the temperature reaches the clearing point of a liquid crystal, the dielectric anisotropy abruptly approaches zero. Dielectric permittivities of nematic liquid crystals have extensively been studied both experimentally and theoretically [58-61].

Maier and Meier Theory of Dielectrics for Liquid Crystals

W. Maier and G. Meier [62] extended the Onsager theory [63] of isotropic dielectrics to nematics to correlate the dielectric properties to molecular parameters. According to Maier and

Meier theory, nematics are composed of molecules with polarizabilities α_{\parallel} , α_{\perp} and permanent dipole moment μ having components $\mu_{\parallel} = \mu \cos\theta$, $\mu_{\perp} = \mu \sin\theta$ along and perpendicular to molecular long axis. The molecule is considered to be in a spherical cavity surrounded by a continuum with macroscopic properties of the dielectric. The dielectric permittivities ε_{\parallel} and ε_{\perp} along and perpendicular to the molecular long axis in a static field are then given by

$$\varepsilon_{\parallel} = 1 + 4\pi N h F \left\{ \bar{\alpha} + \frac{2}{3} \Delta\alpha S + F \frac{\langle \mu_{\parallel}^2 \rangle}{kT} \right\} \quad (2.30)$$

$$\varepsilon_{\perp} = 1 + 4\pi N h F \left\{ \bar{\alpha} - \frac{1}{3} \Delta\alpha S + F \frac{\langle \mu_{\perp}^2 \rangle}{kT} \right\} \quad (2.31)$$

with

$$\langle \mu_{\parallel}^2 \rangle = \frac{\mu^2}{3} [1 - (1 - 3\cos^2\theta)S]$$

$$\langle \mu_{\perp}^2 \rangle = \frac{\mu^2}{3} \left[1 + \frac{1}{2}(1 - 3\cos^2\theta)S \right]$$

Therefore,

$$\Delta\varepsilon = \varepsilon_{\parallel} - \varepsilon_{\perp} = 4\pi N h F \left\{ \Delta\alpha - F \frac{\mu^2}{2kT} (1 - 3\cos^2\theta) \right\} S \quad (2.32)$$

$$\bar{\varepsilon} = \frac{\varepsilon_{\parallel} + 2\varepsilon_{\perp}}{3} = 1 + 4\pi N h F \left\{ \bar{\alpha} + F \frac{\mu^2}{3kT} \right\} \quad (2.33)$$

For isotropic phase (order parameter $S=0$), the permittivity becomes

$$\varepsilon_{\text{iso}} = 1 + 4\pi N h F \left\{ \alpha_{\text{iso}} + F \frac{\mu^2}{3kT} \right\} \quad (2.34)$$

where $N =$ the particle density $= \rho N_A / M$; $\rho =$ mass density, $N_A =$ Avogadro No., $M =$ Molecular weight and $\bar{\alpha} =$ mean polarizability given by

$$\bar{\alpha} = \frac{\alpha_{\parallel} + 2\alpha_{\perp}}{3} \quad (2.35)$$

$\Delta\alpha =$ polarizability anisotropy $= \alpha_{\parallel} - \alpha_{\perp}$; h and F are respectively the cavity field factor and the reaction field factor and are given by

$$\mathbf{h} = \frac{3\bar{\epsilon}}{2\bar{\epsilon} + 1} \quad \text{and} \quad F = \frac{1}{(1 - \alpha f)}$$

Here the factor f , called Onsager factor, is given by

$$f = \frac{8\pi}{3} N \frac{\bar{\epsilon} - 1}{2\bar{\epsilon} + 1}$$

The above equation 2.30 and 2.31 for $\epsilon_{||}$ and ϵ_{\perp} are used to find effective dipole moment of the molecules in nematic phase and its orientation with molecular long axis. Alternatively, one may find the order parameter S when all remaining quantities are known. Maier-Maier's equations satisfactorily explain many essential features of the permittivity of liquid crystals consisting of polar molecules.

Dipole-Dipole Correlation Factor

The Onsager–Kirkwood–Fröhlich (OKF) equation occupies a central place in the study of liquid crystals because it allows the estimation of dipole-dipole correlation factor (g_{λ}) from measurable physical properties and thus to probe into the molecular organization of liquid crystals and their mixtures. In a liquid crystal constituted by polar molecules, the correlation factor expresses the deviation from randomness of the orientation of a dipole with respect to its neighbours. The ensemble averages of the parallel ($||$) and perpendicular (\perp) components of the molecular dipole moments are calculated following the procedure of Bata and Buka [64]. The dipole-dipole correlation factor (g_{λ}) can be expressed as

$$g_{\lambda} = \frac{\langle \sum_{i \neq j} (\mu_{\lambda})_i (\mu_{\lambda})_j \rangle}{\langle \mu_{\lambda}^2 \rangle} \quad (2.36)$$

where the subscript λ refers to axes $||$ and \perp to the nematic director.

Although the short-range dipole-dipole interactions are not considered in Maier-Meier theory [63], the Kirkwood-Fröhlich theory for isotropic liquid dielectrics [60,65] provides a formula in which these short-range effects are considered. Bordewijk and de Jeu [66-69] extended this idea to anisotropic media with uniaxial symmetry and used it to find dipole-dipole

correlation factor for nematic liquid crystals. Their model was based on experimentally observed proportionality between the square of birefringence (Δn^2) and the product of the density (ρ) and order parameter (S). Bata and Buka [64] later obtained the following relation between the low and high frequency dielectric permittivity components and the molecular parameters as

$$\varepsilon_\lambda - \varepsilon_{\infty\lambda} = \frac{4\pi N}{9kT} \frac{\varepsilon_\lambda (\varepsilon_{\infty\lambda} + 2)^2}{(2\varepsilon_\lambda + \varepsilon_{\infty\lambda})} \langle \mu_\lambda^2 \rangle f_\lambda(\varepsilon, \Omega_\lambda^\varepsilon) g_\lambda \quad (2.37)$$

where

$$f_\lambda(\varepsilon, \Omega_\lambda^\varepsilon) = \frac{2\varepsilon_\lambda + \varepsilon_{\infty\lambda}}{\varepsilon_\lambda - (\varepsilon_\lambda - \varepsilon_{\infty\lambda})\Omega_\lambda^\varepsilon} \quad (2.38)$$

Here $\Omega_\lambda^\varepsilon$ is a factor which depends on the dielectric anisotropy of the system. For positive dielectric anisotropy [67] one has

$$\Omega_\parallel^\varepsilon = \frac{\varepsilon_\parallel}{\varepsilon_\parallel - \varepsilon_\perp} - \frac{\varepsilon_\parallel \varepsilon_\perp^{\frac{1}{2}}}{(\varepsilon_\parallel - \varepsilon_\perp)^{\frac{3}{2}}} \tan^{-1} \left(\frac{\varepsilon_\parallel - \varepsilon_\perp}{\varepsilon_\perp} \right)^{\frac{1}{2}} \quad (2.39)$$

and

$$\Omega_\perp^\varepsilon = \frac{\varepsilon_\parallel \varepsilon_\perp^{\frac{1}{2}}}{2(\varepsilon_\parallel - \varepsilon_\perp)^{\frac{3}{2}}} \tan^{-1} \left(\frac{\varepsilon_\parallel - \varepsilon_\perp}{\varepsilon_\perp} \right)^{\frac{1}{2}} - \frac{\varepsilon_\perp}{2(\varepsilon_\parallel - \varepsilon_\perp)} \quad (2.40)$$

For negative dielectric anisotropy

$$\Omega_\parallel^\varepsilon = \frac{\varepsilon_\parallel \varepsilon_\perp^{\frac{1}{2}}}{2(\varepsilon_\perp - \varepsilon_\parallel)^{\frac{3}{2}}} \left(\ln \frac{\varepsilon_\perp^{\frac{1}{2}} + (\varepsilon_\perp - \varepsilon_\parallel)^{\frac{1}{2}}}{\varepsilon_\perp^{\frac{1}{2}} - (\varepsilon_\perp - \varepsilon_\parallel)^{\frac{1}{2}}} \right) - \frac{\varepsilon_\parallel}{\varepsilon_\perp - \varepsilon_\parallel} \quad (2.41)$$

$$\Omega_\perp^\varepsilon = \frac{\varepsilon_\perp}{2(\varepsilon_\perp - \varepsilon_\parallel)} + \frac{\varepsilon_\parallel \varepsilon_\perp^{\frac{1}{2}}}{4(\varepsilon_\perp - \varepsilon_\parallel)^{\frac{3}{2}}} \left(\ln \frac{\varepsilon_\perp^{\frac{1}{2}} - (\varepsilon_\perp - \varepsilon_\parallel)^{\frac{1}{2}}}{\varepsilon_\perp^{\frac{1}{2}} + (\varepsilon_\perp - \varepsilon_\parallel)^{\frac{1}{2}}} \right) \quad (2.42)$$

Therefore

$$\Omega_{\perp}^{\epsilon} = \frac{1}{2}(1 - \Omega_{\parallel}^{\epsilon})$$

The average components of the effective dipole moment, $\langle \mu_{\parallel}^2 \rangle$ and $\langle \mu_{\perp}^2 \rangle$, appearing in equation (2.37) are evaluated as

$$\langle \mu_{\parallel}^2 \rangle = \frac{1}{3} \left\{ (2S+1) \left[\frac{\epsilon_{\infty\parallel} + (1 - \epsilon_{\infty\parallel})\Omega_{\parallel}^{\text{sh}}}{\epsilon_{\infty\parallel}} \right]^2 \mu_{\text{m}\parallel}^2 + (1-S) \left[\frac{\epsilon_{\infty\perp} + (1 - \epsilon_{\infty\perp})\Omega_{\perp}^{\text{sh}}}{\epsilon_{\infty\perp}} \right]^2 \mu_{\text{m}\perp}^2 \right\} \quad (2.43)$$

$$\langle \mu_{\perp}^2 \rangle = \frac{2}{3} \left\{ (1-S) \left[\frac{\epsilon_{\infty\parallel} + (1 - \epsilon_{\infty\parallel})\Omega_{\parallel}^{\text{sh}}}{\epsilon_{\infty\parallel}} \right]^2 \mu_{\text{m}\parallel}^2 + \frac{1}{2}(S+2) \left[\frac{\epsilon_{\infty\perp} + (1 - \epsilon_{\infty\perp})\Omega_{\perp}^{\text{sh}}}{\epsilon_{\infty\perp}} \right]^2 \mu_{\text{m}\perp}^2 \right\} \quad (2.44)$$

where the cavity field factor was calculated taking into account the following shape factors ($\Omega_{\lambda}^{\text{sh}}$) of ellipsoidal molecules or prolate spheroid molecules with semi-long axis a and semi-short axis b .

$$\Omega_{\parallel}^{\text{sh}} = 1 - \omega^2 + \frac{1}{2}\omega(\omega^2 - 1) \ln \frac{\omega+1}{\omega-1} \quad (2.45)$$

and

$$\Omega_{\perp}^{\text{sh}} = \frac{1}{2}\omega^2 - \frac{1}{4}\omega(\omega^2 - 1) \ln \frac{\omega+1}{\omega-1} \quad (2.46)$$

So,

$$\Omega_{\perp}^{\text{sh}} = \frac{1}{2}(1 - \Omega_{\parallel}^{\text{sh}})$$

where

$$\omega^2 = \frac{a^2}{a^2 - b^2} \quad (2.47)$$

Taking apparent molecular length (l_{ap}) obtained from X-ray study as the value of $2a$, b is calculated using the relation

$$b = \frac{1}{2} \left[\frac{6M}{\pi N_A l_{ap} \rho} \right]^{\frac{1}{2}} \quad (2.48)$$

on the assumption that the volume occupied by a molecule in the liquid crystalline phase is equal to the geometrical volume of the molecule [69]. They also used $\epsilon_{||\infty} = 1.05 n_{||}^2$ to take into account the atomic polarization factor. Since, according to Kirkwood and Fröhlich theory, the effective value of molecular dipole moment is given by:

$$\mu_{\text{eff},||}^2 = \frac{9kT}{4\pi N} \frac{(\epsilon_{||} - \epsilon_{\infty||})(2\epsilon_{||} + \epsilon_{\infty||})}{\epsilon_{||}(\epsilon_{\infty||} + 2)^2} \quad (2.49)$$

So, with the help of equation (2.37) we can rewrite equation (2.49) as

$$\mu_{\text{eff},||}^2 = f_{||}(\epsilon, \Omega_{||}) g_{||}(\epsilon, T_{||}) \langle \mu_{||}^2 \rangle \quad (2.50)$$

So that

$$g_{||} = \frac{\mu_{\text{eff},||}^2}{f_{||} \langle \mu_{||}^2 \rangle} \quad (2.51)$$

Similarly for the perpendicular component we have:

$$\mu_{\text{eff},\perp}^2 = \frac{9kT}{4\pi N} \frac{(\epsilon_{\perp} - \epsilon_{\infty\perp})(2\epsilon_{\perp} + \epsilon_{\infty\perp})}{\epsilon_{\perp}(\epsilon_{\infty\perp} + 2)^2} \quad (2.52)$$

and

$$g_{\perp} = \frac{\mu_{\text{eff},\perp}^2}{f_{\perp} \frac{\langle \mu_{\perp}^2 \rangle}{2}} \quad (2.53)$$

where the factor 2 arises due to rotational symmetry. Equations 2.51 and 2.53 were used to calculate $g_{||}$ and g_{\perp} . Further for a uniaxial liquid crystals de Jeu et al. [70,71] obtained the following equation for short range order parameter (T_{λ})

$$T_{\lambda} = (1 - g_{\lambda}) \frac{kT}{4\pi N \langle \mu_{\lambda}^2 \rangle} \quad (2.54)$$

2.2.6 Frequency Domain Dielectric Spectroscopy

Dielectric spectroscopy occupies an important role among numerous modern methods used for physical and chemical analysis of materials. By studying dielectric spectroscopy one can investigate the relaxation processes of complex systems over an extremely wide range of characteristic times. I have already discussed about the dielectric permittivity in static fields. When the field is removed the orientational polarization decays exponentially with a characteristic time τ called relaxation time. On reversing the field a definite time interval is required for reorientation of the permanent dipoles. In alternating fields this leads to a time lag between the average orientation of the dipole moments and fields. At much higher frequencies the orientation polarization can no longer follow the variation of the field and response of materials to alternating fields is characterized by a complex dielectric permittivity and is expressed as

$$\varepsilon^*(\omega) = \varepsilon'(\omega) - i\varepsilon''(\omega) \quad (2.55)$$

where $\varepsilon'(\omega)$ is the real part of dielectric permittivity, which is related to the stored energy within the medium, and $\varepsilon''(\omega)$ is the imaginary part of the permittivity and is related to the dissipation (or loss) of energy within the medium.

Debye and Cole-Cole Model

According to Debye, complex dielectric permittivity can be described in terms of a single relaxation time τ as follows:

$$\varepsilon^* = \varepsilon'(\omega) - i\varepsilon''(\omega) = \varepsilon_\infty + \frac{\varepsilon_0 - \varepsilon_\infty}{1 + i\omega\tau} \quad (2.56)$$

This is known as Debye equation [72]. ε_0 and ε_∞ are the low and high frequency permittivities, ω is the angular frequency of the applied field and τ is the dielectric relaxation time related to the critical frequency (f_c) by the formula

$$\tau = \frac{1}{2\pi f_c} \quad (2.57)$$

Debye equation (2.56) can be separated into real and imaginary parts:

$$\epsilon' = \epsilon_{\infty} + \frac{\epsilon_0 - \epsilon_{\infty}}{1 + (\omega\tau)^2} \quad (2.58)$$

$$\epsilon'' = \frac{\epsilon_0 - \epsilon_{\infty}}{1 + (\omega\tau)^2} \omega\tau \quad (2.59)$$

where the first equation (2.58) describes the dispersion process and the second equation (2.59) describes the absorption process. ϵ'' reaches its maximum at critical frequency:

$$\epsilon''(f) = \epsilon''_{\max} = \frac{\epsilon_0 - \epsilon_{\infty}}{2} \quad (2.60)$$

$\Delta\epsilon = \epsilon_0 - \epsilon_{\infty}$, is called the dielectric increment or strength. If one plots both the components of the dielectric permittivity versus frequency on the logarithmic scale one obtains typical dielectric spectrum as shown in the Figure 2.9. The curve which relates the frequency dependence of ϵ' is known as the dispersion curve whereas that of frequency dependence of ϵ'' is called the absorption curve. The frequency at which ϵ'' reaches its maximum is known as critical frequency (or relaxation frequency). Plot of ϵ'' against ϵ' is known as Cole-Cole plot which for a Debye type liquid is a semi-circle.

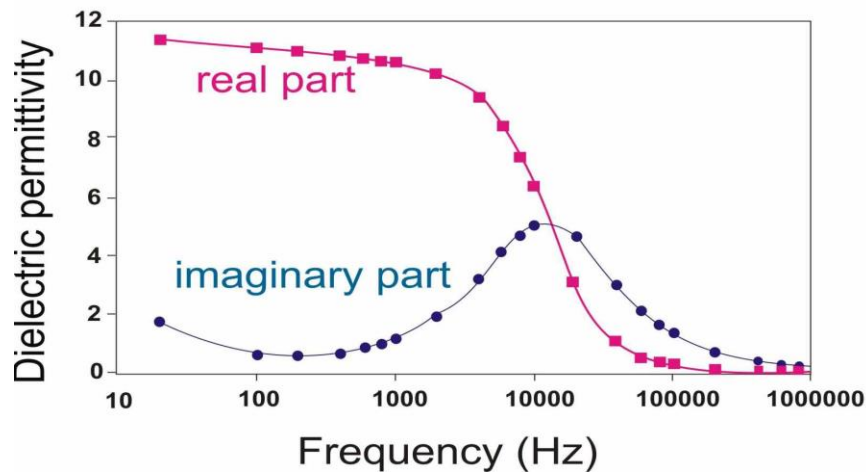


Figure 2.9: A typical dielectric spectra for a Debye type liquid crystal

In case of paraelectric, ferroelectric, ferrielectric and antiferroelectric liquid crystals, dielectric spectroscopy detects stochastic reorientation of molecular dipole moments and

collective fluctuations of spontaneous polarization [72]. The dielectric spectrum for liquids and solid rotator phases of organic polar compounds [73-75] usually shows Debye-type behaviour. However, some systems composed of flexible molecules [74,76-78], some disordered solid phases [79-81] and achiral and chiral liquid crystals [72,82] that exhibit broad dielectric spectra cannot be described by Debye equation. In order to describe those systems, which do not relax with a single relaxation time, Cole and Cole [83] have extended the Debye equation by introducing the relaxation distribution parameter α as follows:

$$\varepsilon^* = \varepsilon' - i\varepsilon'' = \varepsilon_\infty + \frac{\varepsilon_0 - \varepsilon_\infty}{1 + (i\omega\tau_0)^{1-\alpha}} - i \frac{\sigma}{\omega\varepsilon_0} \quad (2.61)$$

which can be separated into two components:

$$\varepsilon'(\omega) = \varepsilon_\infty + \Delta\varepsilon \frac{1 + (\omega\tau_0)^{1-\alpha} \sin\left(\frac{1}{2}\pi\alpha\right)}{1 + 2(\omega\tau_0)^{1-\alpha} \sin\left(\frac{1}{2}\pi\alpha\right) + (\omega\tau_0)^{2(1-\alpha)}} \quad (2.62)$$

$$\varepsilon''(\omega) = \Delta\varepsilon \frac{1 + (\omega\tau_0)^{1-\alpha} \cos\left(\frac{1}{2}\pi\alpha\right)}{1 + 2(\omega\tau_0)^{1-\alpha} \sin\left(\frac{1}{2}\pi\alpha\right) + (\omega\tau_0)^{2(1-\alpha)}} + \frac{\sigma}{\omega\varepsilon_0} \quad (2.63)$$

Distribution parameter α varies from 0 to 1 which is responsible for symmetric distribution of the relaxation times. $\Delta\varepsilon = \varepsilon_0 - \varepsilon_\infty$ is the dielectric strength, τ_0 is in this case the most probable relaxation time related to the critical frequency ($\omega_0\tau_0=1$). $\varepsilon_0 = 8.85 \text{ pFm}^{-1}$ is the dielectric permittivity of the free space and σ is the conductivity. Here conductivity is related to the motion of charge carriers and is added to classical Cole-Cole function. The maximum value of $\varepsilon''(\omega)$ depends on the parameter α according to the formula:

$$\varepsilon''(\omega_c) = \varepsilon''_{\max} = \frac{\varepsilon_0 - \varepsilon_\infty}{2} \frac{\cos\frac{\pi\alpha}{2}}{1 + \sin\frac{\pi\alpha}{2}} \quad (2.64)$$

For small values of the α parameter ($\alpha < 0.1$) above equation takes the form:

$$\epsilon''_{\max} \cong \frac{\epsilon_0 - \epsilon_\infty}{2 + \alpha\pi} \quad (2.65)$$

From the above relation it is clear that for the non-Debye dielectric relaxation processes the absorption peak is lower and broader as shown in the Figure 2.10. A more general function was proposed by Havriliak and Negami [74] which is more convenient to describe the relaxation of some disordered solids and also FLCs as well as AFLCs [84-90].

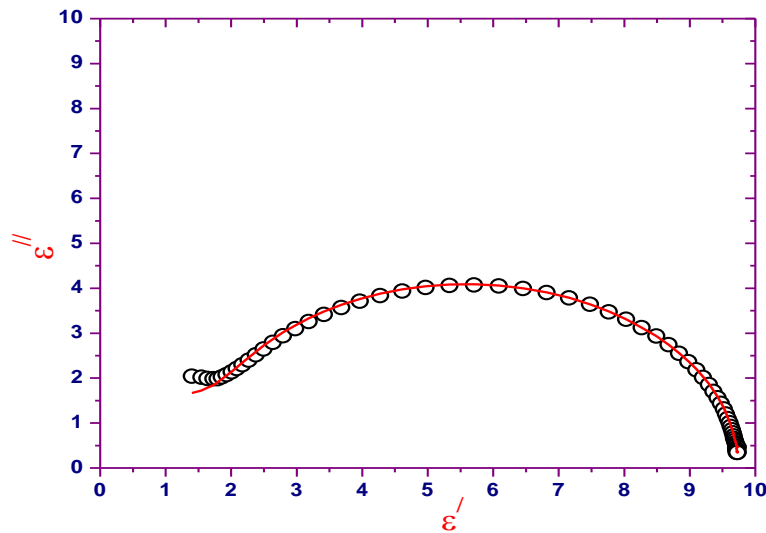


Figure 2.10: Cole-Cole plot for a Debye-type spectrum

Different Relaxation Processes in Chiral and Achiral Liquid Crystal Phases

There are basically two different types of relaxation processes in both chiral and achiral liquid crystalline phase; viz. non-collective (molecular) and collective process. However, detection of the collective processes in the achiral phases is beyond the scope of dielectric relaxation measurement technique.

Non-Collective Processes

Non-collective processes can be observed in achiral and chiral systems i.e, molecules possessing nematic and smectic phases or possessing chiral smectic phases. There are four non-collective relaxation modes viz.

- I] Molecular rotation around short axis.
- II] Molecular rotation around long axis.
- III] Intramolecular rotation around single bond.
- IV] Motions of electrons relative to their nuclei.

In order to discuss the first two processes in nematic phase let us consider a molecule with a permanent dipole moment μ which makes an angle β with the long axis of a molecule shown in Figure 2.11. For nematic liquid crystal the order parameter always less than one, therefore each of the components of dipole moment, longitudinal and transverse to the long axis (μ_l and μ_t), should have a non zero projection both parallel and perpendicular to the director \mathbf{n} , resulting in four relaxations, two in each measurement geometry, $\mathbf{E} \parallel \mathbf{n}$ and $\mathbf{E} \perp \mathbf{n}$. But because of weak intensities of two absorptions related to μ_l and μ_t , we are left with two fundamental and characteristic absorptions of non-collective types in the chiral and achiral liquid crystal phases. The first one is observed in the homeotropic orientation and this molecular rotation is hindered by the nematic potential. The characteristic frequency is observed in the kHz and low MHz regime. The second process is observed in planar orientation and is not affected by the nematic potential and its characteristic frequency is observed in the high MHz and GHz regime as in normal liquids.

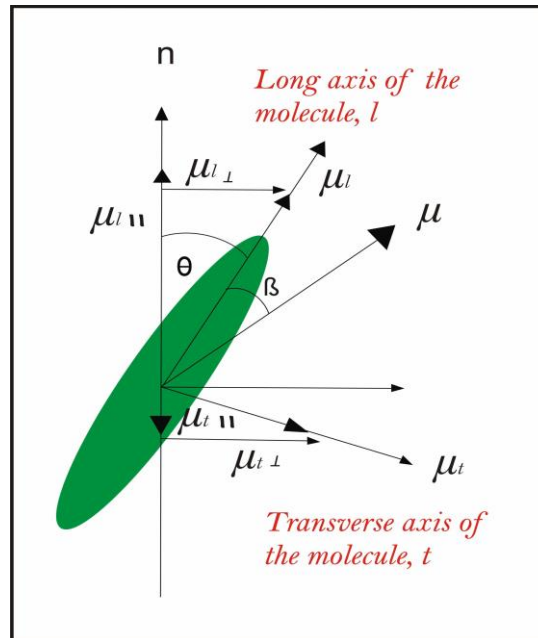


Figure 2.11: The molecular aspect of different dielectric absorption peaks

Collective Processes

In case of chiral smectic phases there are two additional collective absorption processes connected with the director fluctuation. These are

- I] Soft mode (observed in SmA^* phase and near $\text{SmC}^* - \text{SmA}^*$ transition)
- II] Goldstone mode (observed in SmC^* phase)

The Goldstone mode (GM) and the soft mode (SM), has been examined by dielectric relaxation spectroscopy [91-94].

The Soft Mode

Soft mode relaxation arises due to the tilt angle fluctuation of the director. In SmA phase the molecules are aligned in the direction parallel to the layer normal and the stability of the structure is maintained by elastic constant. However due to thermal energy there may be some local instantaneous fluctuation of the tilt angle. Now if SmA phase is cooled down to $\text{SmA}^* - \text{SmC}^*$ transition, the elastic constant controlling the tilt fluctuation gets soft. Thus the fluctuation amplitude increases drastically and consequently the phase will lose its stability and the

molecules fluctuate collectively like a group of drunken people. When a weak electric field is applied in a direction perpendicular to the director it can easily perturb the tilt fluctuation depending on how near the system is to the transition temperature. Thus the permittivity diverges and the frequency of tilt fluctuation falls to zero when the temperature approaches the transition temperature. In case of non-chiral SmA phase the amount of induced dipole moment due to the applied electric field is too small to be detected but for chiral SmA*, the chirality enhances the value of induced dipole moment due to the electroclinic effect which permits the soft mode study by dielectric measurement. In case of SmC* phase there exist a spontaneous tilt angle which grows from zero at transition and increases with decreasing temperature. Here also the molecules fluctuate collectively around the equilibrium tilt angle. Thus soft mode is present both in SmC and SmA phase. The characteristic frequency corresponding to soft mode is observed usually in the kHz regime.

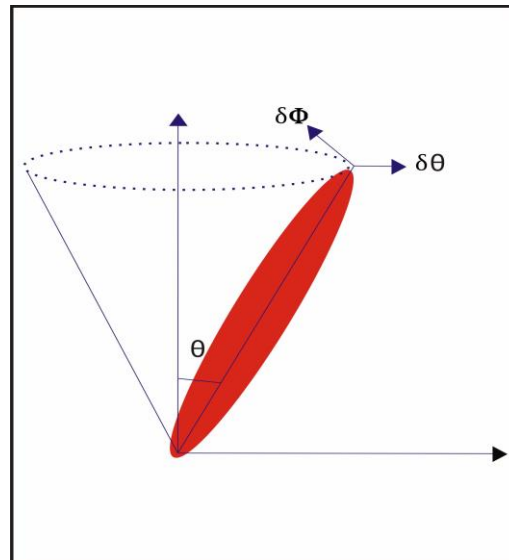


Figure 2.12: Molecular arrangement of tilt angle fluctuation and phase fluctuation

The Goldstone Mode

Beside tilt fluctuation, chiral SmC* phase possess phase fluctuation i.e, the molecules collectively oscillate around the smectic cone which gives rise to another collective relaxation, called the goldstone mode or phasor mode. The smectic C* phase has helical structure and molecular tilt. The director of smectic C* phase makes azimuthal angle φ with the smectic layer which changes from layer to layer resulting in a helical structure with helix axis parallel to the

smectic layer normal. Now if by thermal excitation the director in a certain layer fluctuate then that fluctuation will propagate along the helix axis which actually generates the phase fluctuation. The characteristic frequency corresponding to goldstone mode relaxation is observed normally in the frequency range between 10 Hz to 1 kHz. The GM dielectric increment ($\Delta\epsilon_G$) is usually large compared to the SM increment ($\Delta\epsilon_S$), so it is difficult to study the SM mode properties in the SmC* phase. Yet, this problem can be overcome by applying a DC bias field to the SmC* phase, the field should be strong enough to unwind the helical arrangement of the polarization vector. The SM can be studied almost separately by suppressing GM in this situation.

Dielectric Measurement Technique

To measure dielectric constant of a liquid crystalline sample, the ratio of capacitances of the filled and empty cell is to be found. For measuring the capacitances we employed an impedance analyzer (HP 4192A / HIOKI 3532-50) equipped with data acquisition system through RS232 interface. The temperature was controlled with a mettler hot stage (Mettler Toledo FP90) with an accuracy of $\pm 0.1^\circ\text{C}$. The dielectric spectra were measured over the frequency range from 40 Hz to 5 MHz. Commercial cells (EHC/AWAT), of thickness few μm , were used in the form of a parallel plate capacitors made of indium tin oxide (ITO) coated glass plates which were pre-rubbed by polymer for achieving homogeneous (HG) alignment of the molecules. Cells were filled by capillary action with samples in isotropic state and cooled down to desired temperature very slowly to get homogeneously aligned sample. By applying sufficient DC bias field homeotropic (HT) alignment of the molecules were achieved in the same cell. HG cell gives the ϵ_{\perp} component when the measuring electric field was perpendicular to the nematic director and HT cell gives the ϵ_{\parallel} component, measuring field being parallel to the director. On the other hand, custom built gold cells of thickness few μm and effective area 1.3×0.7 sq. cm were used for frequency dependent complex dielectric permittivity measurements. By AC capacitance bridge technique [95,96], the real and imaginary parts of the complex dielectric permittivity are obtained as a function of frequency at temperatures of interest. The experimental setup for dielectric permittivity measurement is shown in Figure 2.13.

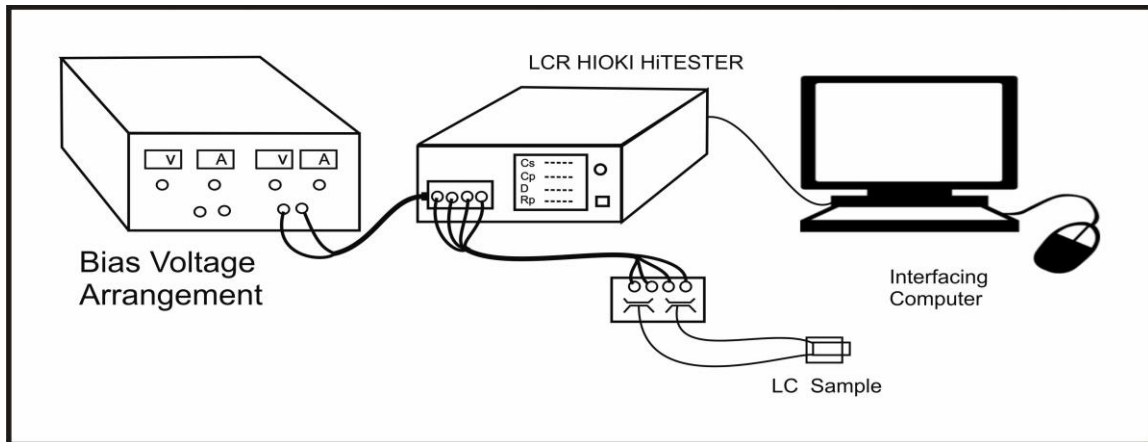


Figure 2.13: Schematic arrangement for the measurement of dielectric permittivity

2.2.7 Elastic Constants

The performances of liquid crystal display devices depend on the elastic properties of the liquid crystal. Liquid crystal molecules exhibit an elastic restoring force due to which if a system experiences an external force that perturbs it from an equilibrium position a restoring torque returns the system to its initial state. If the liquid crystal is deformed by electrical or magnetic forces so as to result in a splay deformation, a reactive elastic force will tend to restore the initial configuration and the reactive forces is described by splay elastic constant (K_{11}). The same phenomenon will occur for a twist deformation as well as for a bend deformation and the respective constants are called twist elastic constant (K_{22}) and bend elastic constant (K_{33}). The three types of director deformations are shown in Figure 2.14. As a liquid crystal medium prefers a uniform director distribution, a variation of the director in space induces an increase of the free energy. According to the elastic theory for liquid crystals, the distortion energy can be expressed as

$$f_d = \frac{1}{2} \left[k_{11} (\nabla \cdot \bar{n})^2 + k_{22} (\bar{n} \cdot \nabla \times \bar{n})^2 + k_{33} (\bar{n} \times \nabla \times \bar{n})^2 \right] \quad (2.66)$$

This equation is known as the Oseen-Frank distortion energy [97]. For most liquid crystal compounds, the three elastic constants have the following relationship: $K_{33} > K_{11} > K_{22}$.

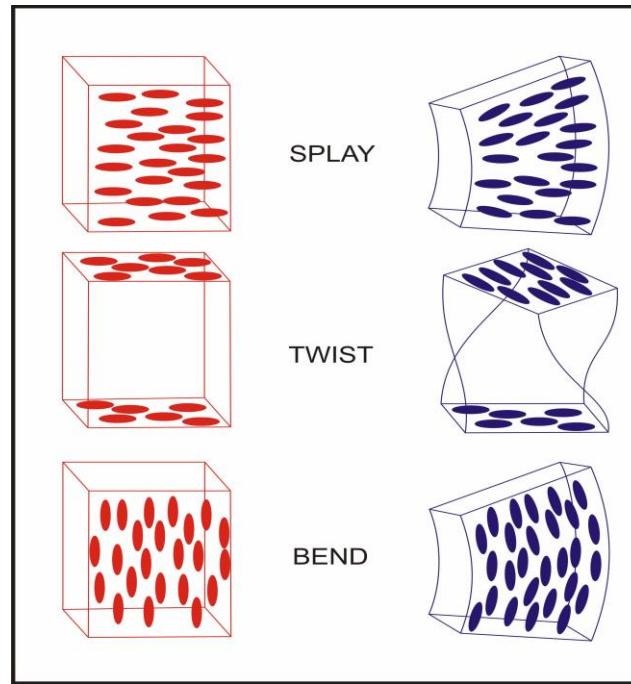


Figure 2.14: Molecular configuration of Splay, Twist and Bend elastic constants

Determination of Elastic Constants: Freedericksz Transition

The elastic constants are measured by the Freédericksz transition technique [98] where, an external electric or magnetic field is applied to deform the thin layer of surface aligned nematic liquid crystal having a uniform director (\mathbf{n}) pattern. For a nematic liquid crystal with positive dielectric anisotropy ($\Delta\epsilon > 0$), the determination of the elastic constants by threshold measurements requires a liquid-crystal cell made of two conducting glass plates with the director oriented parallel to the surface before the application of the field. Below the critical field the molecules remains surface aligned and above it the molecules align along the direction of the field. This phenomenon is known as Freedericksz transition. From the geometry of arrangement, the splay, twist and bend elastic constants can be determined from Freedericksz transition in a magnetic field. After application of an external electric field the dielectric energy is decreased by a tilting of the director and the total bulk free energy per unit area of the cell is given by [99]

$$G = \frac{1}{2} \int_0^L \left\{ (K_{11} \cos^2 \phi + K_{33} \sin^2 \phi) \left(\frac{d\phi}{dz} \right)^2 - E \cdot D \right\} dz \quad (2.67)$$

where $\Phi(z)$ is the tilt angle which is a function of the coordinate z along the cell thickness L . The first and second terms in the integrand are the elastic and dielectric energy densities and \mathbf{E} and \mathbf{D} are the electric and displacement fields respectively. The tilt angle is related to applied voltage V by [99]

$$\frac{V}{V_{th}} = \frac{2}{\pi} \sqrt{1 + \gamma \sin^2 \phi_m} \int_0^{\pi/2} \left[\frac{(1 + k \sin^2 \phi_m \sin^2 \psi)}{F(\psi)} \right]^{\frac{1}{2}} d\psi \quad (2.68)$$

where

$$F(\psi) = (1 + \gamma \sin^2 \phi_m \sin^2 \psi)(1 - \sin^2 \phi_m \sin^2 \psi),$$

$$k = (K_{33} - K_{11}) / K_{11}, \quad \gamma = (\varepsilon_{\parallel} - \varepsilon_{\perp}) / \varepsilon_{\perp}$$

and

$$V_{th} = \pi \sqrt{\frac{K_{11}}{\varepsilon_0 \Delta \varepsilon}} \quad (2.69)$$

is the Freédericksz threshold voltage, ε_0 is the dielectric constant of vacuum. The maximum distorted angle at the centre is $\Phi(L/2) = \Phi_m$, where $d\Phi/dz = 0$. For the twisted planar geometry

$$V_{th} = \pi \sqrt{\frac{1}{\varepsilon_0 \Delta \varepsilon} \left[K_{11} + \frac{K_{33} - 2K_{22}}{4} \right]} \quad (2.70)$$

Thus by measuring Freédericksz threshold voltage and dielectric anisotropy, it is possible to find splay elastic constant K_{11} using equation 2.69. As switching time is inversely related to the elastic constant, a smaller value would result in a system that takes a longer amount of time to return to its equilibrium state which suggests the proper balance between response time and driving voltage is necessary for a better display application.

2.2.8 Measurement of Tilt Angle

Tilt angle is considered as the primary order parameter of ferroelectric SmC* phase which reflects the angle between the direction of molecular long axis and the layer normal. There are two ways to measure the tilt, one is optical method and another one is x-ray method. In a ferroelectric liquid crystal sample, on application of an external field, molecular director is switched by an angle 2θ (θ being the tilt angle of the material) in the plane of the substrates in SSFLC geometry as discussed in chapter 1. To get the tilt angle θ , first a homogeneously aligned FLC cell is mounted on the polarizing microscope. The polarizer and analyzer of the microscope are set in a crossed position. An electric field in the form of a square wave of very low frequency 0.1 Hz is applied to the sample so that molecules in the whole sample are aligned uniformly with a tilt θ away from the layer normal. The sample is rotated on a microscope table to get minima in optical transmission. When the field is reversed the molecules rotate along the tilt cone so that the final tilt becomes $-\theta$ from the layer normal. One has to rotate the sample stage until the previous minima (normally black) is obtained. The angle by which the microscope table was rotated from one minimum position to other minimum will be twice the tilt angle (2θ). One can measure it as a function of temperature.

Tilt angle can also be determined from X-ray study. To get the tilt angle one has to measure the layer spacing (d) by analyzing x-ray photographs and then by using the relation $\theta = \cos^{-1}(d/L)$, tilt angle can be evaluated, where L is the most extended length of the molecule found by geometry optimization. Often layer spacing in smectic A (d_A) phase is used instead of L .

2.2.9 Spontaneous Polarization

Ferroelectric liquid crystals possess non-enantiomorphic polar symmetry in their structures giving rise to a polarization that exists within a material in the absence of the application of an external field which called spontaneous polarization (P_s). In ferroelectric liquid crystals spontaneous polarization is treated as the secondary order parameter, since it is a result of the tilt of the molecules which is called the primary order parameter. The response time or

switching time (τ) of an FLC device is the most significant parameter and it is related to the spontaneous polarization as given by [100]

$$\tau = \frac{\gamma \sin \theta}{P_s E} \quad (2.71)$$

where γ is rotational viscosity, θ is tilt angle and E is the applied electric field. Thus to achieve faster switching speed, τ should be as low as possible. For a portable device of low power consumption applied field E as well as viscosity γ and tilt angle θ should be low and P_s should be high. But a high value of P_s causes a current flow through the cell, which is undesirable. So a moderate level of P_s is required for a short switching time.

Measurements of Spontaneous Polarization by Triangular Wave Method

There are number of methods to measure the magnitude of P_s . One of the standard methods to know the ferroelectric behaviour is the Tower-Sawyer technique [101]. Other useful methods are reverse current method [102,103], reverse field method [104], electric-field dependent dielectric constant and pyroelectric method [105]. We have used the reverse current method using a triangular wave to calculate the spontaneous polarization (P_s). The experimental set up for this purpose is shown in Figure 2.15. As depicted in the figure a high resistance R (10, 100 or 1000 k Ω) is connected in series with the cell and output voltage across the standered resistance R is fed to the oscilloscope (Tektronix TDS 2012B). A 10 Hz, 20Vpp triangular signal was used from HP 34401A function generator, amplified by F20A Voltage amplifier for the purpose.

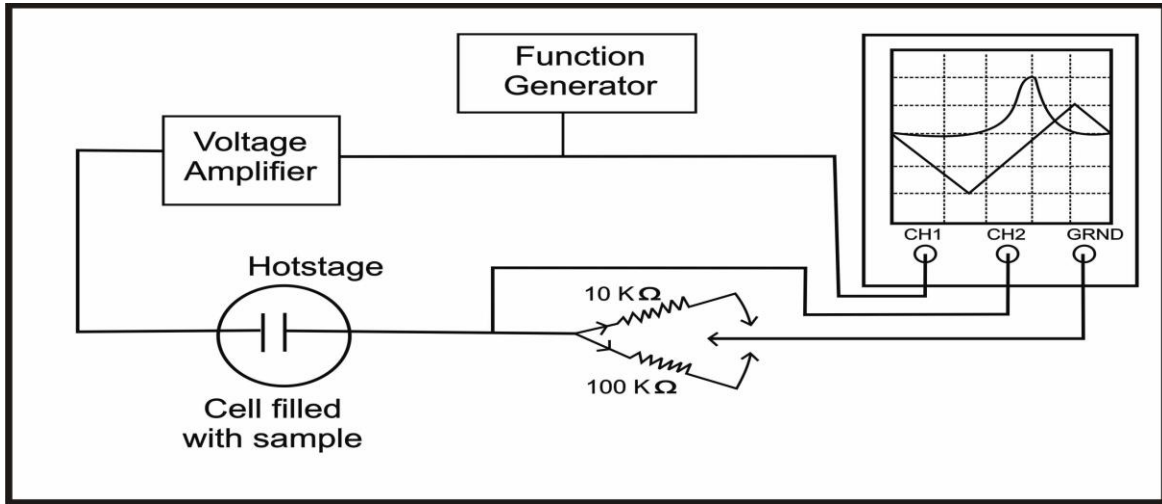


Figure 2.15: Experimental set up to measure the value of P_s

Current $I(t)$ induced in the ferroelectric LC cell by applying a voltage $V(t)$ can be written as a sum of the following three contributions:

$$I = I_c + I_p + I_i = C \left(\frac{dV}{dt} \right) + \frac{dP}{dt} + \frac{V}{R'} \quad (2.72)$$

where I_c is charge accumulation in the capacitor (displacement current), I_p is the polarization realignment current and I_i is the ionic current R' is the effective resistance of the circuit. By selecting a suitable value of resistance R one can get suitable overall current profile to subtract the ionic and capacitive currents by drawing a baseline. The polarization current peaks appear on the oscilloscope due to polarization reversal and the area under the peaks gives direct estimate of P_s [106].

$$P_s = \frac{\int V dt}{2AR} \quad (2.73)$$

where R is the resistance used to record the V - t curve and A is the effective area of the cell used. Area under the curve was determined from the stored image after creating appropriate base line using Origin 7 software.

2.2.10 Measurement of Response Time: Electrical method

Response time is one of the most critical issues for nearly all liquid crystal (LC) devices involving dynamic switching. Response time in SSFLC depends on cell thickness, field strength, surface anchoring etc. as well as on material parameters like polarization, tilt angle and rotational viscosity [107]. Response time contains rise time and decay time. To quantify a display device, rise time and decay time is usually defined as intensity change between 10% and 90%. Response time can be measured either by monitoring electrical response to an applied square wave [108,109] or by using optical method [110].

The response time was studied in a setup similar to that used for spontaneous polarization measurement. In this case, instead of a triangular wave, a square wave signal is applied to FLC sample in SSFLC geometry and the current response associated with switching process is monitored as voltage across a series resistance in storage oscilloscope [109]. Polarization bump occurs away on the time scale from square pulse edge of the applied voltage, delay in time is caused by the response time of the FLC sample. Thus the time delay on the occurrence of the polarization bump from the applied square pulse edge directly gives response time of FLC sample.

2.2.11 Rotational Viscosity

Rotational viscosity (γ_ϕ), which is related to rotations of the molecular directors about the smectic C* cone, is another important parameters of the SmC* phase and strongly influences the switching time between the field-induced states of FLCs. So, rotational viscosity plays a critical role to LC dynamics. Both the rise time and decay time are linearly proportional to γ_ϕ . Thus, for most LC devices, low rotational viscosity material is favorable as evident from equation 2.71.

Measurement of Coefficient of Rotational Viscosity

The rotational viscosity in Goldstone mode was determined using the following relation derived from generalized Landau model [111]:

$$\gamma_{\phi} = \frac{1}{4\pi\epsilon_0} \cdot \frac{1}{\Delta\epsilon f_c} \left(\frac{P_s}{\theta} \right)^2 \quad (2.74)$$

where Goldstone mode dielectric strength ($\Delta\epsilon$) and relaxation frequency (f_c) were obtained from dielectric relaxation study and tilt angle (θ) was obtained from optical or X-ray techniques. From the molecular standpoint, the rotational viscosity depends on the molecular constituents, dimensions, molecular interactions and moment of inertia.

2.2.12 Theory of Crystal Structure Determination

Since molecular order in liquid crystals is intermediate between that in liquid and crystalline state, molecular conformation and arrangement in the crystalline state often found to predetermine the molecular organization in the mesomorphic state. Bernal and Crowfoot [112] in the early 1930's, made the first attempt to correlate the molecular arrangement in the mesomorphic state with the crystal structure of the mesogenic material. However, after that a very few studies had been made for many years in the crystal structure determination. In the late 70's, due to the introduction of computer programs for solving structures a large number of structures of liquid crystal forming compounds have been determined which are mostly nematogens [113-127]. A detailed review on mesophase structure-property relationship was first given by Bryan [128] in early eighties and later by Haase and Athanassopoulou [129] in 1999. Crystal structures of a number of mesogenic compounds had also been reported from our laboratory in order to investigate the structure-property relationship [113-121, 130-133].

In a crystal the constituent atoms or molecules are arranged in a regular and periodic manner and they possess long range positional as well as orientational order. A unit cell of such arrangement can be constructed by three non coplanar vectors **a**, **b**, **c** along the three edges where α , β , and γ are the angles between the edges. When X-rays are scattered by the electrons of the

atoms the 2-D diffraction photographs so obtained contains features where intensity varies as a function of position. To locate the positions of the individual atoms in the unit cell, the intensity of the diffracted pattern must be measured and analyzed. If f_j be the amplitude scattered by the j -th atom at point \mathbf{r}_j and if there are N such atoms within the cell, then the amplitude of the radiation scattered from the array of planes represented by the Miller indices (hkl) is given by [134],

$$F_{hkl} = \sum_{j=1}^N f_j \exp 2\pi i (hx_j + ky_j + lz_j) \quad (2.75)$$

where, f_j is called atomic scattering factor or form factor, F_{hkl} is known as the structure factor for the reflection hkl . $|F_{hkl}|$ is called the structure amplitude, a pure number- number of electrons. The above equation may also be written as

$$\mathbf{F}_{\mathbf{H}} = \sum_{j=1}^N f_j \exp(2\pi \mathbf{H} \cdot \mathbf{r}_j) \quad (2.76)$$

where the reciprocal lattice vector has been replaced by \mathbf{H} . As the atoms in the unit cell are at the positions of high electron density $\rho(\mathbf{r})$, so $\mathbf{F}_{\mathbf{H}}$ can be expressed as

$$\mathbf{F}_{\mathbf{H}} = \int_V \rho(r) \exp(2\pi \mathbf{H} \cdot \mathbf{r}) dV \quad (2.77)$$

where V is the volume of the unit cell. The electron density $\rho(\mathbf{r})$ can be represented as a Fourier series in three dimensions with structure factors as the Fourier coefficients

$$\rho(\mathbf{r}) = \frac{1}{V} \sum_h \sum_k \sum_l F_{\mathbf{H}} \exp(-2\pi \mathbf{H} \cdot \mathbf{r}) \quad (2.78)$$

Now by Fourier summation with a large number of $\mathbf{F}_{\mathbf{H}}$ obtained from diffraction experiment, one can derive the crystal structure directly. However, from diffraction experiments one gets a set of diffraction intensities ($I_{\mathbf{H}}$) from different hkl planes which helps to get the magnitude of the structure factors $|F_{\mathbf{H}}|$, but not their phases $\phi_{\mathbf{H}}$ and this is the well-known *Phase Problem* in crystallography. To overcome this problem, we generally take help of four main methods viz., Patterson method, Direct methods, Isomorphous replacement technique and Anomalous scattering method. Only the direct methods [135] have been discussed briefly, since the structure of a liquid crystalline compound has been determined by this method.

Direct Methods

Direct methods try to evaluate the phases $\phi_{\mathbf{H}}$ directly from the observed intensities (I_{obs}) through probabilistic calculations. The direct methods are very efficient in solving crystal structures especially of low molecular weight organic compounds following the pioneering work of Herbert Hauptman and Jerome Karle for which they were awarded Nobel prize in chemistry in 1985. Different computer programs are now available for solving crystal structures by direct methods viz., MULTAN [136], SIMPEL [137], SHELX[138], XTAL [139], SIR 92 [140], NRCVAX [141], SAPI [142], MITHRIL [143] etc.

A systematic account of the detail theory of direct methods is beyond the scope of this thesis. Only the basic principles and working formulae will be discussed here.

Structure Invariant and Seminvariants

A structure invariant is defined as a quantity that is independent of the shift of the origin of the unit cell. A simple example is that the intensities $I_{\mathbf{H}}$ of reflections i.e. $|F_{\mathbf{H}}|^2$ are structure invariants. However the structure factor itself is not structure invariant, otherwise the phase problem would not have occurred. This is because, for any shift in the origin by, say, $\Delta\mathbf{r}$ the phase of $F_{\mathbf{H}}$ changes by $-2\pi\mathbf{H}\cdot\Delta\mathbf{r}$ radians while the amplitude remains invariant. However, although individual phases depend on the structure and choice of origin, some combinations of them is structure invariant. For example, if $\mathbf{H}_1+\mathbf{H}_2+\mathbf{H}_3=0$ then $\phi_{\mathbf{H}_1}+\phi_{\mathbf{H}_2}+\phi_{\mathbf{H}_3}$ is structure invariant for every space group. It follows directly from the fact that the product $F_{-\mathbf{H}}F_{\mathbf{K}}F_{\mathbf{H}-\mathbf{K}}$ is an invariant. Since the moduli of the structure factors are invariant themselves, the angular part of $F_{-\mathbf{H}}F_{\mathbf{K}}F_{\mathbf{H}-\mathbf{K}}$ is also invariant i.e. $\phi_{-\mathbf{H}} + \phi_{\mathbf{K}} + \phi_{\mathbf{H}-\mathbf{K}} = \phi(\mathbf{H},\mathbf{K}) = \phi_3$ is invariant. The value of a structure invariant is not, however, always known, even though it can only be a function of other structure invariants, e.g., intensities.

The structure seminvariants are those linear combinations of the phases whose values are uniquely determined by the crystal structure i.e., they do not change value on transfer from one special origin to another. It originates from space group symmetry. For example in space group $P\bar{1}$, the linear combination $2\phi_{-\mathbf{H}} + \phi_{2\mathbf{H}}$ is a structure invariant for any reciprocal vector \mathbf{H} . For each space group they have to be derived separately. In any space group any structure invariant is

also a structure seminvariant, but reverse is always not true. A complete theory is given in a series of papers by Hauptman and Karle [144-146] and by Schenk [147].

Structure Determination Procedures

In order to solve the crystal structure a set of intensity data is required which is collected from the single crystal by computer-controlled CAD4 X-ray diffractometer using usually $\text{CuK}\alpha/\text{MoK}\alpha$ radiation. The intensity data are corrected for Lorentz polarization factors [148]. The intensities are converted into the structure factors on an absolute scale by determining the scale factor by the method introduced by A. J. C Wilson [149]. A temperature factor is also obtained during the process that takes into account the thermal vibrations of the real atoms. After that the following steps are taken:

- I] Estimation of normalised structure factors $|E|$'s from $|F_{\text{obs}}|$ values
- II] Set up of phase relationships via structure invariants and seminvariants, starting phase determination, phase extension and refinement
- III] Calculation of figure of merit of different phase sets
- IV] Production of E-map by Fourier method and their interpretation
- V] Refinement of structures through Fourier synthesis, Difference Fourier synthesis and Least-squares refinement techniques.

I] Estimation of $|E|$'s from $|F_{\text{obs}}|$ values

In direct methods, since the phases of the structure factors are estimated directly from the structure amplitudes so it becomes necessary that the structure amplitudes be judged on their intrinsic merit where the decrease of the atomic scattering factor with increasing scattering angle has to be eliminated. As the amplitudes of the different structure factors, $F_{\mathbf{H}}$, cannot be compared directly, since the scattering factor decreases with increasing reflection angle θ , the observed $|F_{\mathbf{H}}|$ is therefore modified so that they correspond to the hypothetical diffracted waves which would be obtained if atoms were stationary point atoms. The modified structure factor, called 'Normalised structure factor' ($E_{\mathbf{H}}$), is defined as,

$$|E_{\mathbf{H}}|^2 = \frac{I_h}{\langle I \rangle} = \frac{|F_{\mathbf{H}}|^2}{\varepsilon \sum_{j=1}^N f_j^2}$$

where ε is an integer characteristic of the space group symmetry.

II] Setting up of phase relationships, starting phase determination, phase extension and refinement

At the beginning, phases of strong reflections are determined. In practice 10 reflections per atom in the asymmetric unit seem quite satisfactory and in some cases as few as three to five per atom have served. If the crystal is triclinic or non-centrosymmetric; more reflections may be required.

The most commonly used phase relation is a three phase structure invariants based on the positivity of electron density criterion, as proposed by Karle and Karle [146]:

$$\phi_{\mathbf{H}} \approx \phi_{\mathbf{K}} + \phi_{\mathbf{H}-\mathbf{K}} \quad (2.79)$$

which for centrosymmetric structure is expressed by signs as

$$S(\mathbf{H}) \approx S(\mathbf{K}) S(\mathbf{H}-\mathbf{K}) \quad (2.80)$$

Relation (2.79) is used to generate phases $\phi_{\mathbf{H}}$ when the values of the phases on the right-hand side are known and it is used in a cyclic manner to propagate the phases to all the selected reflections. These relations are probability relations and the probability is high when the reflections have large $|E|$ values in addition to satisfying the criterion $\mathbf{H} + \mathbf{K} + \mathbf{L} = 0$. These are called Σ_2 phase relations. Probability of the phase of \mathbf{H} being equal to the sum of the phases of $-\mathbf{H}$ and $\mathbf{H}-\mathbf{K}$ is given by the following relations. In centrosymmetric case [150]:

$$P_+(\mathbf{H}, \mathbf{K}) = \frac{1}{2} + \frac{1}{2} \tanh \left[\frac{1}{2} k(\mathbf{H}, \mathbf{K}) \right] \quad (2.81)$$

In non-centrosymmetric case [151]:

$$P[\phi(\mathbf{H}, \mathbf{K})] = \frac{\exp\{k(\mathbf{H}, \mathbf{K})\cos[\phi(\mathbf{H}, \mathbf{K})]\}}{2\pi I_0\{k(\mathbf{H}, \mathbf{K})\}} \quad (2.82)$$

where I_0 is a zero-order modified Bessel function of the first kind.

Now the question arises about deciding the phase of a particular reflection when there are several pairs of known phases, the estimate from each of which might be well different. The answer to this important problem was given by Karle and Hauptman [152] in 1956. They introduced the tangent formula

$$\tan \phi_{\mathbf{H}} \approx \frac{\sum_{\mathbf{K}} k(\mathbf{H}, \mathbf{K}) \sin(\phi_{\mathbf{K}} + \phi_{\mathbf{H}-\mathbf{K}})}{\sum_{\mathbf{K}} k(\mathbf{H}, \mathbf{K}) \cos(\phi_{\mathbf{K}} + \phi_{\mathbf{H}-\mathbf{K}})} = \frac{B(\mathbf{H})}{A(\mathbf{H})} \quad (2.83)$$

where

$$k(\mathbf{H}, \mathbf{K}) = 2\sigma_3\sigma_2^{-\frac{3}{2}} |E_{\mathbf{H}}| |E_{\mathbf{K}}| |E_{\mathbf{H}-\mathbf{K}}|$$

$$\sigma_n = \sum_{j=1}^N Z_j^n$$

Z_j being the atomic number of the j^{th} atom in a unit cell containing a total of N atoms. For identical atoms $\sigma_3\sigma_2^{-\frac{3}{2}} = N^{-\frac{1}{2}}$.

In order to use the tangent formula to obtain a new phase, the values of some phases have to be known and put into the right-hand side of the tangent formula. The set of the known phases is called a starting set from which the tangent formula derives more and more new phases and refines them in a self-consistent manner. But in this way all phases cannot be determined with acceptable reliability. It is therefore useful at this stage to eliminate about 10% of these reflections whose phases are most poorly defined by the tangent formula (2.83). An estimate of the reliability of each phase is obtained from $\alpha(\mathbf{H})$:

$$\alpha(\mathbf{H}) = \left\{ A(\mathbf{H})^2 + B(\mathbf{H})^2 \right\}^{\frac{1}{2}} \quad (2.84)$$

When the relation (2.84) contains only one term, as it may in the initial stages of the phase determination, then $\alpha(\mathbf{H}) = k(\mathbf{H}, \mathbf{K})$.

The larger the value of $\alpha(\mathbf{H})$, the more reliable is the phase estimate. The relation between $\alpha(\mathbf{H})$ and the variance is given by Karle and Karle [146], in 1966, as

$$\sigma^2(\mathbf{H}) = \frac{\pi^2}{3} + 4 \sum_{t=1}^{\infty} \frac{(-1)^t}{t^2} \frac{I_t\{\alpha(\mathbf{H})\}}{I_0\{\alpha(\mathbf{H})\}}$$

From (2.88) it can be seen that $\alpha(\mathbf{H})$ can only be calculated when the phases are known. However, an estimate of $\alpha(\mathbf{H})$ can be obtained from the known distribution of three phase structure invariants [151]. The estimated $\alpha(\mathbf{H})$ at the initial stage is given approximately by

$$\alpha_{\text{est}}(\mathbf{H}) = \sum_{\mathbf{K}} k(\mathbf{H}, \mathbf{K}) \frac{I_1\{k(\mathbf{H}, \mathbf{K})\}}{I_0\{k(\mathbf{H}, \mathbf{K})\}} \quad (2.85)$$

The first step in phase extension is to fix the origin and enantiomorphs as the tangent phasing process is usually initiated with a few ‘known’ phases. This is done by imposing the condition in terms of structure factor seminvariant phases. The selection of starting phases is critical to the success of the multisolution methods. To maximize the connection between starting phases, the generator reflections are sorted by a convergence-type process by Germain, Main and Woolfson [136]. At the end of the convergence procedure a number of reflections, sufficient to fix the origin and the enantiomorphs whose phases are known, are obtained. A few other reflections are also chosen to which different phase values are assigned (either numerically or symbolically) to create different starting points for phase extension through Σ_2 relations. The strength of convergence procedure is that it ensures, as far as possible, that the initial phases will develop through strong and reliable phase relationships. For each starting phase set, phases of all the selected strong reflections are generated and refined as explained in earlier section. Thus we get a multiple phase sets.

III] Calculation of figure of merit of the generated phase sets

When a number of sets of phases have been developed, it is necessary to rank them according to some Figure-of-Merit (FOM), prior to computing a Fourier map (in this case E-map). Combining all weights from various FOM viz., Absolute Figure-of-Merit (ABSFOM), Relative Figure-of-Merit (RFOM), R-factor Figure-of-Merit (RFAC), Psi (zero) Figure-of-Merit (PSIO) etc. Combined Figure-of-Merit (CFOM) is calculated for each set. The most likely correct sets of phases are those with the highest value of CFOMs.

IV] E-map calculation and interpretation

Using the best phase set, E-maps are calculated using equation 2.78 at a large number of grid points covering the entire unit cell. The complete interpretation of the maps is done in three stages: peak search, separation of peaks into potentially bonded clusters and application of simple stereochemical criteria to identify possible molecular fragments. The molecular fragments thus obtained can be compared with the expected molecular structure. The computer can thus present the user with a list of peaks and their interpretation in terms of the expected molecular structure quite automatically. It is also common practice to have an output of the picture of the molecule as an easy check on the structure the computer has found.

V] Refinement of structures

Generally we use following three methods, viz., 1) Fourier synthesis, 2) Difference Fourier synthesis and 3) Least squares refinement [153,154] for refinement of a model structure (partial or complete) obtained from E-map. The Fourier synthesis gives the refined co-ordinates of the atoms and also tends to reveal the position of any atom that is not included in computing the structure factors using equation (2.75). The Difference Fourier map is very useful for correcting the position of an atom used in structure factor calculation. This is also very useful in locating H-atoms towards the final stages of refinement procedure.

An analytical method of refinement of great power and generality is that based on the principle of least squares. In brief, least-squares refinement consists in using the squares of the differences between observed and calculated structure factors as a measure of their disagreement and adjusting the parameters so that the total disagreement is a minimum.

The degree of refinement is indicated by an agreement between the calculated structures factors F_c and those observed, F_o . The most common method of assessing the agreement is calculating the residual or reliability index of the form

$$R = \frac{\sum (|F_o| - |F_c|)}{\sum |F_o|} \quad (2.86)$$

the summation being over all the reflections. Evidently, the lower the value of R, the better is the agreement. Another form of the residual of common use is

$$R_w = \left[\frac{\sum w (|F_o - F_c|^2)}{\sum w |F_o|^2} \right]^{\frac{1}{2}} \quad (2.87)$$

where the frequently used weight is,

$$w = \frac{1}{\sigma^2(F_o)}$$

$\sigma(F_o)$ being the standard deviation of F_o . Using standard techniques, various parameters like bond lengths, bond angles, torsion angles, non bonded distance etc., are determined by determining the structure with a reasonably low R-value.

2.3 REFERENCES

- [1] M. Born; Sitzb. kgl. preub. Akad. Wiss., 614 (1916), Theorie der flussigen Kristalle und des electrischen Kerr Effects in Flussigkeiten.
- [2] P. G. de Gennes; The Physics of Liquid Crystals, Clarendon Press, Oxford (1974); P. G. de Gennes and J. Prost, 2nd ed. Clarendon Press, Oxford (1993).
- [3] A. L. Tsykalo; Thermophysical properties of liquid crystals, Gordon and Breach Science Publishers, (1991).
- [4] S. Chandrasekhar, Liquid Crystals, 2nd Edn., Cambridge University Press, Cambridge, (1992).
- [5] I. Musevic, R. Blinc and B. Zeks's, The Phases of Ferroelectric and Antiferroelectric Liquid Crystals, World Scientific, Singapore (2000).
- [6] W. Maier and A. Saupe, Z. Naturforsch 13a, 564 (1958), Eine einfach molekularstatische theorie der nematischen kristallinflussign phase, Dispersionswechselwirkung; W. Maier, and A. Saupe, Z. Naturforsch, 14a, 882 (1959), Eine einfach molekularstatische theorie der nematischen kristallinflussign phase. Teil I; W. Maier, and A. Saupe, Z. Naturforsch, 15a, 287 (1960), Eine einfach molekularstatische theorie der nematischen kristallinflussign phase. Teil II; A. Saupe and W. Maier, Z. Naturforsch, 16a, 816 (1961), Methoden zur Bestimmung des Ordnungsgrades nematischer Schichten; W Maier, Angew. Chem. 73, 660 (1961), Struktur und Eigenschaften nematisscher Phasen.
- [7] A. L. Tsykalo, Thermophysical Properties of Liquid Crystals, Gordon and Breach Science Publishers, p27 (1991).
- [8] K. K. Kobayashi; Phys. Lett. A, 31, 125-126 (1970); On the theory of translational and orientational melting with application to liquid crystals.
- [9] W. L. McMillan; Phys. Rev. A 4, 1238-1246 (1971), Simple molecular model for the smectic A phase of liquid crystals.
- [10] W. L. McMillan; Phys. Rev.A 6, 936 (1972), X-Ray Scattering from Liquid Crystals. I. Cholesteryl Nonanoate and Myristate.
- [11] A. L. Tsykalo, Thermophysical Properties of Liquid Crystals. Gordon and Breach Science Publishers, p 164 (1991).

- [12] R. J. Meyer and W. L. McMillan; *Phys. Rev. A*, 9, 899 (1974), Simple molecular theory of the smectic C, B, and H phases.
- [13] S. Chandrashekar; *Liquid crystals*, Cambridge University Press (1977).
- [14] G. Vertogen and W. H. de Jeu; *Thermotropic Liquid crystals, Fundamentals*. Springer-Verlag, Berlin (1988).
- [15] P. J. Collings and Michael Hird; *Introduction to Liquid Crystals Chemistry and Physics*. Taylor and Francis (1998).
- [16] G. R. Luckhurst; *Molecular Physics of Liquid Crystals*, Academic Press (1979).
- [17] R. L. Humphries, P. G. James and G. R. Luckhurst; *J. Chem. Soc., Faraday Trans. 2*, 68, 1031 – 1044 (1972), Molecular field treatment in nematics.
- [18] K. K. Kobayashi; *J. Phys. Soc. (Japan)*, 29, 101 (1970), Theory of Translational and Orientational Melting with Application to Liquid Crystals I.
- [19] K. K. Kobayashi; *Mol. Cryst. Liq. Cryst.*, 13, 137 (1971), Theory of Translational and Orientational Melting with Application to Liquid Crystals.
- [20] B. K. Vainstein; *Diffraction of X-rays by Chain Molecules*, Elsevier, Amsterdam (1966).
- [21] H. Kelkar and R. Hatz; *Handbook of Liquid Crystals*, Verlag Chemie, Ch. 5 (1980).
- [22] P. S. Pershan; *Structure of Liquid Crystalline Phases*, World Scientific, Singapore (1988).
- [23] G. Ungar in *Physical properties of liquid crystals*, D. A. Dunmur, A. Fukuda and G. R. Luckhurst (Eds.), INSPEC, London, Ch. 4.1 (2001).
- [24] G. Vertogen and W. H. de Jeu (Eds.), *Thermotropic Liquid Crystals Fundamentals*., Springer-Verlag, p-207 (1988).
- [25] G. R. Luckhurst in *Liquid Crystals & Plastic Crystals* (Eds. G. W. Gray and P. A. Winsor), Ellis Horwood Limited, Vol 2, p-144 (1974).
- [26] C. L. Khetrapal and A. C. Kunwar in *Advances in Liquid Crystals*, Vol. 1-6, Ed. Glenn H. Brown, p-173, AP (1983).
- [27] V. D. Neff in *Liquid Crystals & Plastic Crystals* (Ed. G. W. Gray and P. A. Winsor), Ellis Horwood Limited, Vol 2, p-231 (1974).
- [28] S. J. Gupta, R. A. Gharde and A. R. Tripathi; *Mol. Cryst. Liq. Cryst.*, 364, 461- 468 (2001), Phase Transition Temperatures of LCs using Fabry-Perot Etalon.
- [29] D. Demus, *Textures of liquid crystals*, Verlag Chemie Weinheim, New York (1978).

- [30] I. Dierking, Textures of liquid crystals WILEY-VCH, GmbH & Co. KGaA p-16 (2003).
- [31] A. J. Slaney, K. Takatohi and J. W. Goodby in The Optics of Thermotropic Liquid Crystals, Ed. S. Elston and R. Sambles, Taylor & Francis (1998), Defect textures in liquid crystals.
- [32] Y. Bouligand in Handbook of Liquid Crystals. Vol. 1 (Fundamentals), Ed. D. Demus, J. Goodby, G. W. Gray, H.-W. Spiess and V. Vill, WILEY-VCH, Verlag GmbH, Weinheim, FRG (1998), Defects and textures.
- [33] B. Jha and R. Paul; Proc. Nucl. Phys. and Solid State Phys. Symp., India . 19C, 491 (1976) A Design for High Temperature X-ray Camera for the Study of Liquid Crystals in a Magnetic Field.
- [34] B. Jha, S. Paul, R. Paul and P. Mandal; Phase Transitions, 15, 39-48 (1989), Order parameters of some homologue cybotactic nematics from X-ray diffraction measurements.
- [35] S. Diele. P. Brand and H. Sackmann; Mol. Cryst. Liq. Cryst., 16, 105-116 (1972), X-ray Diffraction and Polymorphism of Smectic Liquid Crystals 1. A-, B- and C-modifications.
- [36] A. de Vries; Pramana, Suppl. No. 1, 93 (1975), X-Ray Studies of Liquid Crystals: V, Classification of Thermotropic Liquid Crystals and Discussion of Intermolecular Distances.
- [37] A. de Vries, A. Ekachi and N. Sielberg; J. de Phys., 40, C3-147 (1979), X-Ray Studies of Liquid Crystals VI. The Structure of the Smectic A, C, B_n and B_t Phases of Trans-1, 4-Cyclohexane-DI-NOctyloxybenzoate.
- [38] A. J. Leadbetter, J. Prost, J. P. Gaughan and M. A. Mazid; J. de Phys., 40, C3-185 – C3-193 (1979), The structure of the crystal, SmE and SmB forms of IBPBAC.
- [39] A. J. Leadbetter and P. G. Wrighton; J. de Phys., 40, C3-234 – C3-242 (1979), Order parameters in S_A, S_C, and N phases by X-ray diffraction.
- [40] V. M. Sethna, A. de Vries and N. Spielberg; Mol. Cryst. Liq. Cryst., 62, 141-153 (1980), X-Ray Studies of Liquid Crystals VIII: A Study of the Temperature Dependence of the Directly Observed Parameters of the Skewed Cybotactic Nematic Phase of Some Bis-(4'-n-Alkoxybenzal)-2-Chloro-1,4-Phenylenediamines.

- [41] L.V. Azaroff and C. A. Schuman; *Mol. Cryst. Liq. Cryst.*, 122, 309-319 (1985), X-Ray Diffraction by Cybotactic Nematics.
- [42] A. de Vries; *Mol. Cryst. Liq. Cryst.*, 131, 125-145 (1985), The Use of X-Ray Diffraction in the Study of Thermotropic Liquid Crystals with Rod-Like Molecules.
- [43] P. Mandal, M. Mitra, S. Paul and R. Paul; *Liq. Cryst.*, 2, 183-193 (1987), X-Ray Diffraction and Optical Studies of an Oriented Schiff's Base Liquid Crystal.
- [44] A. de Vries; *Mol. Cryst. Liq. Cryst.*, 10, 219-236 (1970), X-ray photographic studies of liquid crystals I. A cybotactic nematic phase.
- [45] A. de Vries; *Mol. Cryst. Liq. Cryst.*, 11, 361-383 (1970), X-Ray Photographic Studies of Liquid Crystals II. Apparent Molecular Length and Thickness in Three Phases of Ethyl-p-Ethoxybenzal-p-Aminobenzoate.
- [46] C. Kittel; *Intro to Solid State Physics*, Wiley Eastern, Chapter 2 (1976).
- [47] G. Pelzl in *Handbook of Liquid Crystals. Vol. 1 (Fundamentals)*, Ed. D. Demus, J. Goodby, G. W. Gray, H.-W. Spiess and V. Vill, WILEY-VCH, Verlag GmbH, Weinheim, FRG (1998).
- [48] D. A. Dunmur in *The Optics of the Thermotropic Liquid Crystals*. Ed. S. Elston and R. Sambles, Taylor & Francis (1998).
- [49] S. M. Kelly, M. O'Neill; Chapter 1, *Liquid Crystals For Electro-optic Applications*.
- [50] A. K. Zeminder, S. Paul and R. Paul; *Mol. Cryst. Liq. Cryst.* 61, 191-206 (1980), Refractive Indices and Orientational Order Parameter of Five Liquid Crystals in Nematic Phase.
- [51] M. F. Vuks; *Optics and Spectroscopy*, 20, 361-368, (1966), Determination of optical anisotropy of aromatic molecules from the double refraction of crystals.
- [52] H. E. J. Neugebauer, *J. Canad. Phys.*, 32, 1-8 (1954), Clarius-Mossoti equation for certain types of anisotropic crystals.
- [53] S. Chandrasekhar; *Liquid Crystals*, second edn., Cambridge University Press, Cambridge, p39, (1992).

- [54] W. H. de Jeu, *Physical Properties of Liquid Crystalline Materials*, Ed G. Gray, Gordon and Breach, Vol. 1, p 41 (1980).
- [55] P. G. de Gennes; *Mol. Cryst. Liq. Cryst.* 12, 193-214 (1971), Short Range Order Effects in the Isotropic Phase of Nematics and Cholesterics.
- [56] I. Haller, H. A. Huggins, H. R. Lilienthal and T. R. McGuire; *J. Phys. Chem.*, 77, 950 (1973), Order-Related Properties of Some Nematics; I. Haller; *Jappl. Phys. Lett.*, 24, 349 (1974), Alignment and wetting properties of Nematics.
- [57] K. Toriyama, K. Suzuki, T. Nakagomi, T. Ishibashi and K. Odawara; *J. de Phys*, 40, C3-317 (1979), A design of liquid crystal material for multiplexed liquid crystal display.
- [58] D. A. Dunmur and W. H. Miller; *Mol. Cryst. Liq. Cryst.*, 60, 281-283 (1980), Dipole-Dipole Correlation in Nematic Liquid Crystals.
- [59] R. E. Michel and G. W. Smith; *J. Appl. Phys.* 45, 3234 (1974), Dependence of birefringence threshold voltage on dielectric anisotropy in a nematic liquid crystals.
- [60] C. J. F. Böttcher, *Theory of Electric Polarization*, 2nd edition, Vol I (1973) and C. J. F. Böttcher and P. Bordewijk, 2nd edition, Elsevier Scientific Publishing Co., Vol II (1978).
- [61] W. H. de Jeu and T. W. Lathouwers; *Z. Naturforsch* 29a, 905 (1974), Dielectric constants and molecular structure of nematics. I. Terminally substituted azobenzene and azoxybenzenes.
- [62] W. Maier and G. Meier, *Z. Naturforsch*; 16a, 262 (1961), Einfache Theorie der dielektrischen Eigenschaften von homogen orientierten nematischen Phasen.
- [63] L. Onsager; *J. Am. Chem. Soc.*, 58, 1486-1493 (1936), Electric Moments of Molecules in Liquids.
- [64] L. Bata and A. Buka; *Mol. Cryst. Liq. Cryst.* 63, 307 (1981), Dielectric Permittivity and Relaxation Phenomena in smectic Phases.
- [65] H. Frohlich, *Theory of Dielectrics*. Clarendon Press, Oxford (1949); H. Frohlich, *J. Chem. Phys.*, 22, 1804 (1954).

- [66] P. Bordewijk; *Physica*, 69, 422-432 (1973), On the derivation of the Kirkwood-Fröhlich equation.
- [67] P. Bordewijk; *Physica*, 75, 146-156 (1974), Extension of the Kirkwood-Fröhlich theory of the static dielectric permittivity to anisotropic liquids.
- [68] P. Bordewijk and W. H. de Jeu; *J. Chem. Phys.* 68 (1), 116 (1978), Calculation of dipole correlation factors in liquid crystals with use of a semiempirical expression for the internal field.
- [69] W. H. de Jeu and P. Bordewijk; *J. Chem. Phys.* 68 (1), 109 (1978), Physical studies of nematic azoxybenzenes. II. Refractive indices and the internal field.
- [70] W. H. de Jeu, T. W. Lathouwers and P. Bordewijk; *Phys. Rev. Lett.* 32, 40 (1974), Dielectric properties of n and S_A p,p'-di-n-heptylazoxybenzene.
- [71] W. H. de Jeu, J. W. A. Goosens and P. Bordewijk; *J. Chem. Phys.* 61, 1985(1974), Influence of smectic order on the static dielectric permittivity of liquid crystals.
- [72] P. Debye, *Polar molecules*, Dover Pub. Inc., NX (1929).
- [73] C. J. F. Böttcher and P. Bordewijk, Ed., *Theory of Electric Polarization, Vol II, Dielectric in time-dependent fields*, Elsevier, Scientific Publishing Co. (1973).
- [74] S. Havriliak and S. Negami; *J. Polime*, 8, 161-210 (1967), A complex plane representation of dielectric and mechanical relaxation processes in some polymers.
- [75] A. Wurflinger; *Int. Rev. Phys. Chem.*, 12, 89 (1993), Dielectric studies under pressure on plastic and liquid crystals.
- [76] W. Haase, H. Pranoto, F. J. Bormuth, *Ber. Bunsenges. Phys. Chem.*, 89, 1229-1234 (1985), Dielectric Properties of Some Side Chain Liquid Crystalline Polymers.
- [77] F. J. Bormuth, Ph.D. Thesis, Technische Hochschule, Darmstadt (1998).
- [78] V. I. Minkin, O. A. Osipov, Y. A. Zhdanov, *Dipole Moments in Organic Chemistry*, New York- London, (1970).

- [79] A. K. Jonscher, Dielectric Relaxation In Solids, Chelsea Dielectric Press, London (1983).
- [80] S. Wrobel, B. T. Gowda, W. Haase, J.Chem. Phys., 106 (10), 5904 (1997), Dielectric study of phase transitions in 3-nitro-4-chloro-aniline.
- [81] V. K. Agarwal and A. H. Price; Mol. Cryst. Liq. Cryst., 98, 193-200 (1983), Dielectric Relaxation and Order Parameters in Mixtures of 4-cyanobiphenyl and MBBA.
- [82] V. V. Daniel, Dielectric Relaxation, Academic Press, London and N.Y. (1967).
- [83] K. S. Cole and R. H. Cole; J. Chem. Phys. 9, 341-351 (1941), Dispersion and Absorption in Dielectrics I. Alternating Current Characteristics.
- [84] J. Hatano, Y. Hakanai, H. Furue, H. Uehara, S. Saito, and K. Murashiro, Jpn. J. Appl. Phys., 33, 5498-5502 (1994), Phase Sequence in Smectic Liquid Crystals Having Fluorophenyl Group in the Core.
- [85] S. Merino, M. R. de la Fuente, Y. Gonzalez, M. A. Perez Jubindo, M. B. Ros, J. A. Puertolas; Phys. Rev., E 54, 5169-5177 (1996), Broadband dielectric measurements on the (R)-1-methylheptyl-6-(4'-decyloxybenzoyloxy)-2-naphthalene carboxylate antiferroelectric liquid crystal.
- [86] A. Fafara, B. Gestblom, S. Wrobel, R. Dabrowski, W. Drzewinski, D. Kilian, W. Haase; Ferroelectrics, 212, 79-90 (1998), Dielectric spectroscopy and electrooptic studies of new MHPOBC analogues.
- [87] M. Marzec, R. Dabrowski, A. Fafara, W. Haase, S. Hiller and S. Wrobel; Ferroelectrics, 180,127-135(1996), Gold-stone mode and Domain mode relaxation in ferroelectric phases of 4'-[(S,S) - 2,3 - epoxyhexyloxy] Phenyl 4 (Decyloxy) Benzoate (EHPDB).
- [88] H. Uehara, Y. Hakanai, J. Hatano, S. Saito and K. Murashiro; Jpn. J. Appl. Phys., 34, 5424-5428 (1995), Dielectric Relaxation Modes in the Phases of Antiferroelectric Liquid Crystals.
- [89] M. Buivydas, S. T. Lagerwall, F. Gouda, R. Dubal, A. Takeichi; Ferroelectrics, 212, 55-65 (1998), The dependence of polarization and dielectric biaxiality on the enantiomeric excess in chiral dopant added to a smectic C host mixture.

- [90] H. Kresse, H. Schmalfluss, W. Weissflog, C. Tschierske, A. Hauser; *Mol. Cryst. Liq. Cryst.*, 366, 505-517 (2001), Dielectric Characterization of Bn Phases.
- [91] W. Kuczynski, Electrooptical studies of relaxation processes in ferroelectric liquid crystals, in: W. Haase, S. Wrobel (Eds), *Relaxation phenomena* –Springer-Verlag, Berlin-Heidelberg, pp 422-444 (2003), Liquid crystals, magnetic systems, polymers, high-TC superconductors, metallic glasses.
- [92] A. M. Biradar, S. Wrobel and W. Haase; *Phys. Rev. A*, 39 2693-2702 (1989), Dielectric relaxation in the smectic-A* and smectic-C* phases of a ferroelectric liquid crystal.
- [93] J. K. Ahuja and K. K. Raina; *Jpn. J. Appl. Phys.*, 39, 4076-4081 (2000), Polarization Switching and Dielectric Relaxations in Ferroelectric Liquid Crystals.
- [94] Y. P. Panarin, O. Kalinovskaya, J. K. Vij and J. W. Goodby; *Phys. Rev. E*, 55, 4345-4353 (1997), Observation and investigation of the ferrielectric subphase with high qT parameter.
- [95] I.-S. Baik, S. Y. Jeon, S. H. Lee, K. A. Park, S. H. Jeong, K. H. An, and Y. H. Lee; *Appl. Phys. Lett.* 87, 263110 (2005), Electrical-field effect on carbon nanotubes in a twisted nematic liquid crystal cell.
- [96] F. Haraguchi, K.-I Inoue, N. Toshima, S. Kobayashi, and K. Takatoh; *Jpn. J. Appl. Phys.* 46, L796 (2007), Reduction of the Threshold Voltages of Nematic Liquid Crystal Electrooptical Devices by Doping Inorganic Nanoparticles.
- [97] F. C. Frank; *Disc. Faraday Soc.*, 25, 19-28 (1958), On the theory of liquid crystals.
- [98] I. W. Stewart, *The Static and Dynamic Continuum Theory of Liquid Crystals*, Taylor and Francis, London (2004).
- [99] B. Kundu, S. K. Pal, S. Kumar, R. Pratibha, N.V. Madhusudana; *Phys. Rev. E: Stat. Nonlinear Soft Matter Phys.* 82, 061703 (2010), Splay and bend elastic constants in the nematic phase of some disulfide bridged dimeric compounds.
- [100] M. Hird; *Liq. Cryst.*, 38, 1467–1493 (2011), Invited topical review (Ferroelectricity in liquid crystals -materials, properties and applications).

- [101] C. B. Sawyer and C. H. Tower; *Phys. Rev.* 35, 269-273 (1930), Rochelle Salt as a Dielectric.
- [102] W. J. Merz; *Phy. Rev.* 95(3), 690-698 (1954), Domain Formation and Domain Wall Motions in Ferroelectric BaTiO₃ Single Crystals; Y. Ouchi, T. Uemura, H. Takezoe and A. Fukuda; *Jpn. J. Appl. Phys.*, 24 (4), L235- L238 (1985), Correspondence between Stroboscopic Micrographs and Spontaneous Polarization Measurements in Surface Stabilized Ferroelectric Liquid Crystal Cells.
- [103] W. J. Merz; *J. Appl. Phys.* 27(8), 938-943 (1956), Switching Time in Ferroelectric BaTiO₃ and Its Dependence on Crystal Thickness.
- [104] H. D. Megaw; *Acta Cryst.*, 7,187-194 (1954), Ferroelectricity and crystal structure II.
- [105] M. E. Lines and A. M. Glan; Oxford, Clarendon 128 (1977), Principles and Applications of Ferroelectric and Related Materials.
- [106] K. Miyasato, S. Abe, H. Takezoe, A. Fukuda and E. Kuze; *Jpn. J. Appl. Phys.* 22 (10), L661-L663 (1983), Direct Method with Triangular Waves for Measuring Spontaneous Polarization in Ferroelectric Liquid Crystals.
- [107] S. Kaur, A. K. Thakur, R. Chauhan, S. S. Bawa and A. M. Biradar; *Physica B*, 352, 337-341 (2004), The effect of rotational viscosity on the memory effect in ferroelectric liquid crystal.
- [108] S. S. Bawa, A. M. Biradar and S. Chandra; *Jpn. J. Appl. Phys.* 25(6), L446 (1986), Frequency Dependent Polarization Reversal and the Response Time of Ferroelectric Liquid Crystal by Triangular Wave Method.
- [109] J-Z. Zue, M. A. Handschy and N. A. Clark; *Ferroelectrics*, 73, 305-314 (1987), Electrooptic response during switching of a ferroelectric liquid crystal cell with uniform director orientation.
- [110] K. Skarp, I. Dahl, S. T. Lagerwall and B. Stebler; *Mol. Cryst. Liq. Cryst.*, 114, 283-297 (1984), Polarization and Viscosity Measurements in a Ferroelectric Liquid Crystal by the Field Reversal Method.

- [111] T. Carlsson, B. Zeks, C. Filipic, A. Levstik; *Physical Review A*, 42, 877–889 (1990), Theoretical model of the frequency and temperature dependence of the complex dielectric constant of ferroelectric liquid crystals near the smectic C* - smectic A phase transition.
- [112] J. D. Bernal and D. Crowfoot; *Trans. Farad. Soc.*, 29, 1032-1049 (1933), Crystalline phases of some substances studied as liquid crystals.
- [113] P. Mandal and S. Paul; *Mol. Cryst. Liq. Cryst.*, 131, 223-235 (1985), X-Ray Studies on the Mesogen 4'-n-Pentyloxy-4-Biphenylcarbonitrile (5OCB) in the Solid Crystalline State.
- [114] P. Mandal, S. Paul, H. Schenk and K. Goubitz; *Mol. Cryst. Liq. Cryst.*, 135, 35-48 (1986), Crystal and Molecular Structure of the Nematogenic Compound 4-Cyanophenyl-4'-n-Heptylbenzoate (CPHB).
- [115] P. Mandal, B. Majumdar, S. Paul, H. Schenk and K. Goubitz; *Mol. Cryst. Liq. Cryst.*, 168, 135-146 (1989), An X-ray Study of Cyanophenyl Pyrimidines, Part I - Crystal Structure of PCCPP.
- [116] P. Mandal, S. Paul, C. H. Stam and H. Schenk; *Mol. Cryst. Liq. Cryst.*, 180, 369-378 (1990), X-Ray Studies of Cyanophenyl Pyrimidines Part II The Crystal and Molecular Structure of 5-(4-Ethylcyclohexyl)-2-(4-Cyanophenyl) Pyrimidine.
- [117] S. Gupta, P. Mandal, S. Paul, M. de Wit, K. Goubitz and H. Schenk; *Mol. Cryst. Liq. Cryst.*, 195, 149-159 (1991), An X-Ray Study of Cyanophenylpyrimidines Part III. Crystal Structure of 5-(trans-4-Heptylcyclohexyl)-2-(4-Cyanophenyl) Pyrimidine.
- [118] P. Mandal, S. Paul, H. Schenk and K. Goubitz; *Mol. Cryst. Liq. Cryst.*, 210, 21-30 (1992), Crystal and Molecular Structure of a Cybotactic Nematic Compound bis-(4'-n-Butoxybenzal)-2-Chloro-1,4-Phenylenediamine.
- [119] P. Mandal, S. Paul, K. Goubitz and H. Schenk; *Mol. Cryst. Liq. Cryst.*, 258, 209-216 (1995), X-ray Structural Analysis of a Mesogenic Compound N,N'-Bis-(p Butoxybenzylidene)- α, α' -bi - p-Toluidine.
- [120] A. Nath, S. Gupta, P. Mandal, S. Paul and H. Schenk; *Liq. Cryst.*, 20, 765-770 (1996), Structural analysis by X-ray diffraction of a non-polar alkenyl liquid crystalline compound.

- [121] B. R. Jaishi, P. K. Mandal, K. Goubitz, H. Schenk, R. Dabrowski and K. Czuprynski; *Liq. Cryst.*, 30, 1327-1333 (2003), The molecular and crystal structure of a polar mesogen 4-cyanobiphenyl-4'-hexylbiphenyl carboxylate.
- [122] P. A. C. Gane and A. J. Leadbetter; *Mol. Cryst. Liq. Cryst.*, 78, 183-200 (1981), The Crystal and Molecular Structure of N-(4-n octyloxy benzylidene) -4'-butylaniline (80.4) and the Crystal-Smectic G Transition.
- [123] L. Malpezzi, S. Bruckner, D. R. Ferro and G. R. Luckhurst; *Liq. Cryst.*, 28, 357-363 (2001), Crystal structure and packing analysis of the liquid crystal dimer α,ω -bis(4-cyanobiphenyl-4'-yloxy)octane.
- [124] M. A. Sridhar, N. K. Lokanath, J. Shashidhara Prasad, C. V. Yelammagad and Varshney, *Liq. Cryst.*, 28, 45-49 (2001), Crystal structure of a cholesterol-based dimesogen.
- [125] V. K. Gupta, P. Bhandhoria, M. Kalyan, M. Mathews and C. V. Yelamagad; *Liq. Cryst.*, 32, 741-747 (2005), Crystal structure of a liquid crystal non - symmetric dimer: cholesteryl 4 - [4 - (4 - n - butylphenylethynyl) phenoxy]butanoate.
- [126] L. Walz, F. Nepveu and W. Haase; *Mol. Cryst. Liq. Cryst.*, 148, 111-121 (1987), Structural Arrangements of the Mesogenic Compounds 4-Ethyl-4'-(4''-pentylcyclohexyl) biphenyl and 4-Ethyl-2'-fluoro-4'-(4''-pentylcyclohexyl) biphenyl (BCH's) in the Crystalline State.
- [127] P. S. Patil, V. Shettigar, S. M. Dharmaprakash, S. Naveen, M. A. Sridhar and J. Shashidhara Prasad, *Mol. Cryst. Liq. Cryst.*, 461, 123-130 (2007), Synthesis and Crystal Structure of 1-(4-fluorophenyl)-3-(3,4,5-trimethoxyphenyl)-2-propen-1-one.
- [128] R. F. Bryan, *Proceedings of the Pre-Congress Symposium on Organic Crystal Chemistry*, Poznan, Poland, 105 (1979); *J. Structural Chem.*, 23, 128 (1982).
- [129] W. Haase and M. A. Athanassopoulou; *Liquid Crystals*, D.M.P. Mingos (Ed.), Springer-Verlag, Vol. I, pp. 139-197 (1999).
- [130] S. Biswas, S. Haldar, P. K. Mandal, K. Goubitz, H. Schenk, and R. Dabrowski; *Cryst. Res. Technol.* 42, 10, 1029-1035 (2007), Crystal structure of a polar nematogen 4-(trans-4-undecylcyclohexyl) isothiocyanatobenzene.

- [131] S. Haldar, S. Biswas, P. K. Mandal, K. Goubitz, H. Schenk and W. Haase; *Mol. Cryst. Liq. Cryst.*, 490, 80–87 (2008), X-Ray Structural Analysis in the Crystalline Phase of a Nematogenic Fluoro-Phenyl Compound.
- [132] S. Haldar, P. K. Mandal, S. J. Prathap, T. N. Guru Row and W. Haase; *Liq. Cryst.*, 35, 11, 1307–1312 (2008), X-ray studies of the crystalline and nematic phases of 49-(3,4,5-trifluorophenyl)-4-propylbicyclohexyl.
- [133] P. Das, A. N. Biswas, S. Acharya, A. Choudhury, P. Bandyopadhyay, P. K. Mandal and S. Upreti; *Mol. Cryst. Liq. Cryst.*, 501, 53–61 (2009), Structure of Liquid Crystalline 1-Phenyl-3-{4-[4-(4-octyloxybenzoyloxy)phenyloxycarbonyl]phenyl}triazene-1-oxide at Low Temperature.
- [134] B. K. Vainshtein, *Diffraction of X-rays by Chain Molecules*, Elsevier, Amsterdam, p12 (1966).
- [135] M. F. C. Ladd and R. A. Palmer, *Theory and practice of Direct methods in Crystallography*, Plenum Pub. Co., N. Y., (1980).
- [136] G. Germain, P. Main and M. M. Woolfson; *Acta Cryst.*, B26, 274-285 (1970), On the application of phase relationships to complex structures.
- [137] H. Schenk and C. T. Kiers, *Simpel 83*, an automatic direct method program package, University of Amsterdam (1983); H. Schenk; *Recl. Trav. Chim. Pays-bas*, 102, 1(1983).
- [138] G. M. Sheldrick, *Direct method package program*, University of Gottingen, Germany (1993).
- [139] S. R. Hall and J. M. Stewart, *XTAL*, University of Western Australia and Maryland (1989).
- [140] A. Altomere, G. Cascarano, C. Giacovazzo, A. Guagliardi, M. C. Burla, G. Polidori and M. Camalli, *The SIR 92 Programme* (1992).
- [141] P. S. White, *PC Version of NRCVAX (88)*, University of New Brunswick, Canada (1988).

- [142] Yao Jia-Xing, Zheng Chao-de, Quian Jin-Zi, Han Fu-Son, Gu Yuan-Zin and Fan Hai-Fu, SAPI: A Computer Program for Automatic Solution of Crystal Structures from X-ray Data, Institute of Physics, Academia Sinica, Beijing (1985).
- [143] C. J. Gilmore, *J. App. Cryst.*, 17, 42-46 (1984), MITHRIL-an integrated direct-methods computer program.
- [144] H. Hauptman and J. Karle, *Acta Cryst.*, 9, 45-55 (1956), Structure invariants and seminvariants for noncentrosymmetric space groups; *ibid.*, 12, 93-97 (1959); Seminvariants for centrosymmetric space group with conventional centered cells.
- [145] J. Karle and H. Hauptman, *Acta Cryst.*, 14, 217-223 (1961), Seminvariants for non-centrosymmetric space groups with conventional centered cells.
- [146] J. Karle and I. L. Karle, *Acta Cryst.*, 21, 849-859 (1966), The symbolic addition procedure for phase determination for centrosymmetric and non-centrosymmetric crystals.
- [147] H. Schenk (Ed), *Direct Methods in Solving Crystal Structures*, NATO ASI Series, Plenum Press, New York (1991).
- [148] G. H. Stout and L. H. Jensen, *X-ray Structure Determination*, Macmillan, New York p195 (1968).
- [149] A. J. C. Wilson, *Nature*, 150, 152 (1942), Determination of Absolute from Relative X-Ray Intensity Data.
- [150] W. Cochran and M. M. Woolfson, *Acta Cryst.*, 8, 1-12 (1955), "The theory of sign relations between structure factors".
- [151] W. Cochran, *Acta Cryst.*, 8, 473-478 (1955), Relations between the phases of structure factors.
- [152] J. Karle and H. Hauptman, *Acta Cryst.*, 9, 635-651 (1956), A theory of phase determination for the four types of non-centrosymmetric space groups.

[153] M. J. Buerger, *Crystal Structure Analysis*, Wiley, New York (1960).

[154] G. H. Stout and L. H. Jensen, *X-ray Structure Determination*, Macmillan, New York, p353 (1968).

CHAPTER 3

HIGH BIREFRINGENCE LATERALLY FLUORINATED TERPHENYL ISOTHIOCYANATES: STRUCTURAL, OPTICAL AND DYNAMICAL PROPERTIES

Part of the work has been published in Mol. Cryst. Liq. Cryst., Vol. 562: pp. 156–165, 2012; Physica B Vol. 441: pp. 100–106, 2014 and Phase Transitions, Vol. 88, No. 2, pp. 153-168, 2015.

3.1 INTRODUCTION

Performance of a liquid crystal (LC) display device depends on the nature of the liquid crystalline material and the construction of the device. Fluoro substituted LC materials are found to be useful in large information content display devices. These are also promising materials for photonic applications because of their high birefringence [1–6]. Response time of a nematic liquid crystal (LC) based display device is proportional to rotational viscosity and square of the display cell thickness [7]. But reduced cell thickness (d) necessitates high birefringence material to attain the appropriate optical path given by Gooch–Tarry first minima condition ($d \cdot \Delta n = \sqrt{3}\lambda/2$) in a twisted nematic cell [8]. Fast response time is especially important for color-sequential liquid crystal displays (LCDs) using blinking backlight [9] or primary-color (RGB) light emitting diodes (LEDs) [10]. In the RGB LED-backlit color-sequential LCDs, the pigment color filters can be eliminated, which not only reduces the LCD cost but also triples the device resolution. High Δn materials ($0.3 < \Delta n < 0.5$) are also useful in non-display applications like laser beam steering [11], tunable colour filters [12], focus tunable lens [13], electrically controlled phase shifter in GHz and THz region [14]. High birefringence also enhances the display brightness and contrast ratio of polymer-dispersed liquid crystals (PDLC), holographic PDLC, cholesteric LCD and LC gels [15–17]. In order to meet the demand for fast electro-optic response in nematic liquid crystal based display devices, new high birefringence (Δn) materials are, therefore, synthesized and their properties are studied in both pure and mixture state. The most effective method of increasing birefringence is to elongate the π -electron conjugation of the LC compounds by introducing multiple bonds or unsaturated (phenyl) rings in the rigid core structure. But highly conjugated liquid crystal compounds have the following problems viz; high melting temperature, increased viscosity, reduced UV stability and relatively low resistivity. The high melting temperature effect can be reduced through the lateral fluorination of the rigid core, which also hinders formation of smectic phases because of increased lateral force due to increased volume effect and lateral dipole moment (dipole moment of fluorobenzene is 1.50D) [18]. Although increased viscosity is inherent to all highly conjugated compounds, it can be mitigated by the proper choice of polar groups. UV stability can be improved by forming the rigid core of unsaturated rings instead of multiple bonds. The common rigid cores are phenyl, tolane and terphenyl structures and common polar groups are cyano (CN)

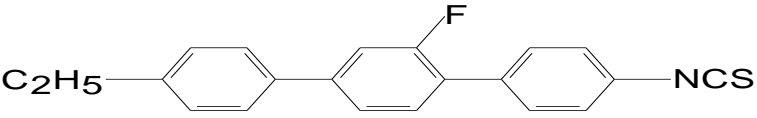
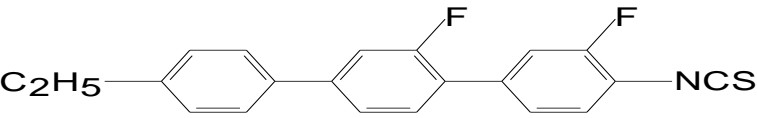
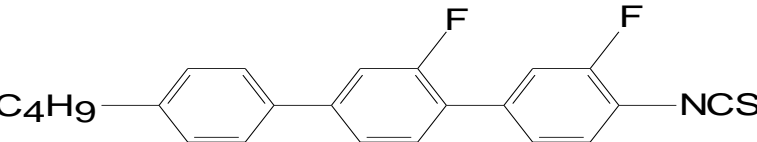
and isothiocyanato (NCS) which can serve the purpose. Moreover, due to lower dipole moment of NCS group ($\mu = 3.7$ D) compared to CN group ($\mu = 3.9$ D), viscosity of the NCS compounds is observed to be lower than the nitrile based systems [19]. This is thought to be due to formation of dimmers as a result of strong intermolecular interactions between the nitrile groups which is less probable in isothionato systems. However, a major concern of the CN- and NCS- based LC materials is their relatively low resistivity because of ion trapping near the polyimide alignment interfaces in device structure. Low resistivity leads to a low voltage holding ratio resulting in increased image flickering in thin film transistor (TFT) addressed liquid crystal displays. However, by fluorinating NCS compounds resistivity can be increased retaining high birefringence. Moreover, as mentioned, lateral fluorine substitution in the core also reduces the melting point substantially and hinders the formation of the smectic phases because of increased lateral force due to increased volume effect and lateral dipole moment.

In view of the above discussion three isothiocyanate terphenyl compounds with different lateral fluorine substitutions were selected for detailed investigation. In this chapter structural, optical and dynamical properties of those fluorinated compounds are reported and compared to see the effect of fluorination and chain flexibility. Eutectic mixtures of high birefringence nematogenic compounds are usually developed in order to satisfy various other physical properties including wide phase range, smectic compounds are also used in such mixture formulation [7,20,21]. In this respect the compounds under investigation are expected to be very useful in such mixture formulation. Other than positional ordering, reorientations of entire molecules around their short and long axes are one of the features that distinguish the liquid crystalline state from crystalline phase where these reorientations as well as intra-molecular reorientations are usually frozen, vibration of atoms about their equilibrium positions still persist. Therefore, information about the nature of molecular dynamics is possible to obtain from frequency and temperature dependent dielectric spectroscopic study. Although static dielectric data is available in the literature on some fluoro-substituted nematics, the authors are not aware of any report on their dielectric relaxation behavior.

3.2 COMPOUNDS STUDIED

Molecular structures of the investigated fluorinated terphenyl isothiocyanato compounds along with their abbreviated names and transition temperatures are given in the Table 3.1.

Table 3.1: Molecular structures and transition temperatures of 2TP-3'F-4NCS, 2TP-3',3F-4NCS and 4TP-3',3F-4NCS

Name	Molecular structure with transition temperature
2TP-3'F-4NCS	 <p style="text-align: center;">Cr 102.5°C SmA 120.5°C N 188.2°C I</p>
2TP-3',3F-4NCS	 <p style="text-align: center;">Cr 80.2°C N 188°C I</p>
4TP-3',3F-4NCS	 <p style="text-align: center;">Cr 58.1°C SmA 96.9°C N 181.8°C I</p>

3.3 EXPERIMENTAL METHODS

The fluorinated terphenyl isothiocyanato compounds used in this investigation were supplied by Prof. R. Dabrowski, Military University of Technology, Warsaw, Poland. The phase behavior of the compounds was studied under an Olympus BX41 polarizing microscope regulating the temperature within $\pm 0.1^\circ\text{C}$ using Mettler FP 82 central processor and FP84 hot stage. Small and wide angle X-ray scattering measurements on randomly oriented samples were made using Ni filtered $\text{CuK}\alpha$ radiation and a custom built high temperature camera from ENRAF NONIUS FR590 X-Ray generator. X-ray photographs were scanned in 24 bit RGB colour format using HP2400C scanner. Optical densities of the pixels were calculated from the colour values and subsequently converted to X-ray intensities with the help of a calibration strip prepared by exposing the film for several known time intervals. Intensity distribution, obtained from the linear scan of X-ray photographs along the equatorial and meridional diffraction peaks, was used to determine average intermolecular distance (D) and apparent molecular length (l) in nematic phase or smectic layer spacing (d) with an accuracy of 0.02 \AA and 0.1 \AA respectively. The detailed procedures have been discussed in chapter 2 [22-25].

Static and frequency dependent dielectric properties have been studied using impedance analyzers HIOKI 3532-50 (50 Hz – 5 MHz) and HP 4192A (100 Hz – 13 MHz), interfaced to a computer by RS-232 cable. Low resistivity (about $20 \Omega/\square$) polyimide-coated homogeneous (HG) cells in the form of parallel plate capacitors with indium tin oxide (ITO) electrodes of $\sim 3\text{-}5 \mu\text{m}$ cell gaps were used for static dielectric measurements. By applying sufficient DC bias field ($\sim 5\text{V } \mu\text{m}^{-1}$) homeotropic (HT) alignment of the molecules was achieved in the same cell. Perpendicular and parallel components of the dielectric constants were obtained from capacitive measurements in HG and HT cells respectively as described in chapter 2. On the other hand, custom-built gold cells of thickness $\sim 19 \mu\text{m}$ were used for frequency dependent complex dielectric permittivity measurements. In both cases, the cells were filled by capillary action with samples in isotropic state and cell temperature was maintained within $\pm 0.1^\circ\text{C}$ using Eurotherm 2216e temperature controller. Very slow regulated cooling of the sample was made to get proper alignment.

Temperature dependent refractive indices were measured with He-Ne laser source ($\lambda=633 \text{ nm}$) using Chatelain-Wedge principle. Thin prisms, with angles $\sim 1^\circ$, were constructed using

optically flat glass slides rubbed with polyvinyl alcohol solution (1%) in such a way that the molecules are aligned with nematic director lying parallel to the edge of the wedge. Prisms were filled with samples in isotropic phase and cooled down very slowly. Further details of the measurement of refractive indices (n_o and n_e) have been described in chapter 2. The densities were measured at different temperatures using a dilatometer of capillary type which also has been described in chapter 2.

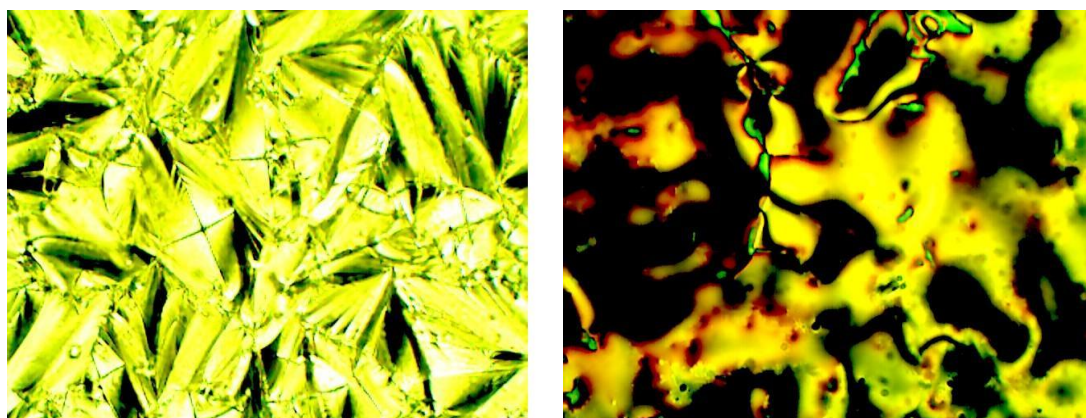
Molecules in the nematic phase have no positional correlation but they do have long-range orientational ordering. The extent of ordering is usually qualified by orientational order parameters (OOPs), which are uniaxial and are expressed by a traceless symmetric tensor of rank 2. Many physical properties like optical birefringence, dielectric anisotropy, threshold voltage for switching, etc., which are important device parameters, depend upon the OOPs. Orientational order parameter $\langle P_2 \rangle$ was calculated using the principal molecular polarizabilities α_o and α_e , perpendicular and parallel to the direction of optic axis, following de Gennes relation [26] as described in chapter 2. From the measured refractive indices and density values, the principal polarizabilities were calculated following the method of Neugebauer [27] as detailed in chapter 2.

3.4 RESULTS AND DISCUSSIONS

This chapter basically deals with fluorinated terphenyl compounds with a polar isothiocyanate (NCS) terminal group. With the goal of achieving the highest possible birefringence (Δn) value while retaining a relatively low viscosity and suitable mesomorphic properties, two types of lateral fluorine substitutions were studied. The first two compounds (2TP-3'F-4NCS and 2TP-3',3F-4NCS) have the same chain length with a single difference of one extra laterally fluorine substitution in the core and the third one (4TP-3',3F-4NCS) differs from the first two in respect of the chain length having two more carbon atoms. In this section, different characteristics of the compounds will be examined and comparisons will be made based on their structures and effect of fluorination.

3.4.1 Optical Polarization Microscopy

Observed textures, which are topological defect structures seen under optical microscope in crossed polarizers, confirmed the presence of different liquid crystalline phases and the transition temperatures for the above compounds. Typical textures have been obtained for all the phases of the three compounds. Observed focal conic texture in SmA phase and schlieren texture in nematic phase of 2TP-3'F-4NCS are shown in the Figure 3.1 as representative example. It is observed that the singly fluorinated compound 2TP-3'F-4NCS exhibits both smectic and nematic phase. Introduction of another lateral fluorine atom in the core (2TP-3',3F-4NCS) results in sharp decrease of melting point and complete suppression of smectic phase although clearing point remains same. In 4TP-3',3F-4NCS, where the terminal chain length is increased from 2 to 4 carbon atoms, the melting point is further reduced but SmA phase reappears. The smectic phase stability also increases in doubly fluorinated compound 4TP-3',3F-4NCS than the singly fluorinated compound 2TP-3'F-4NCS, being 38.8° and 18° respectively. All the three compounds possess nematic phase over a considerable temperature range – 68°C, 108°C and 85°C.



(SmA Phase 108°C)

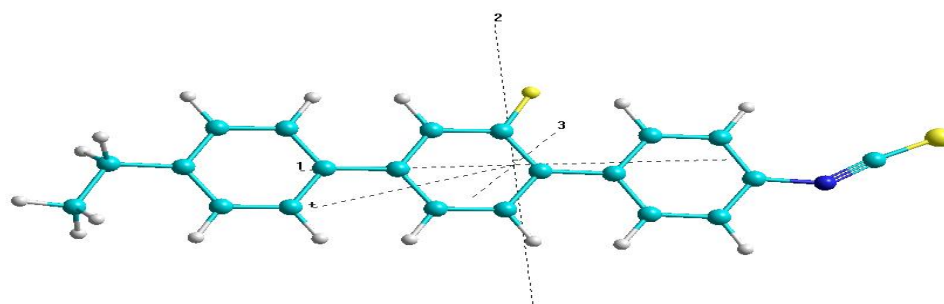
(Nematic Phase 180°C)

Figure 3.1: Selected textures observed in 2TP-3'F-4NCS

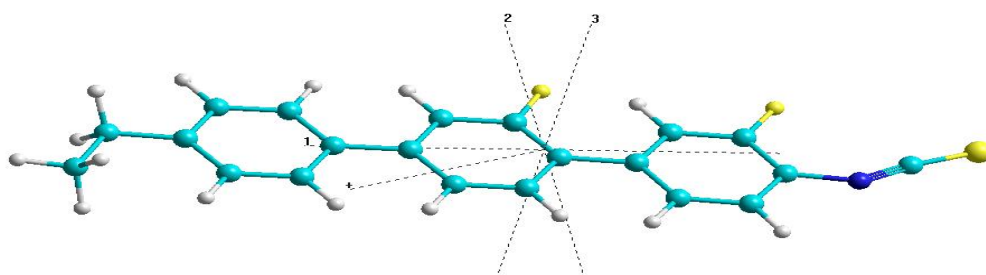
3.4.2 Optimized Geometry Using Molecular Mechanics

To elucidate the structure of the investigated compounds, optimized geometry of the molecules were determined by molecular mechanics calculation using PM3 method in Hyperchem software package [28]. The optimized structures of the molecules, directions of the principal moments of inertia axes along with the direction of their electric dipole moments are shown in Figure 3.2. Values of optimized lengths of the molecules, dipole moments with the components along the three principal moments of inertia axes and the corresponding moments of inertia are shown in the Table 3.2.

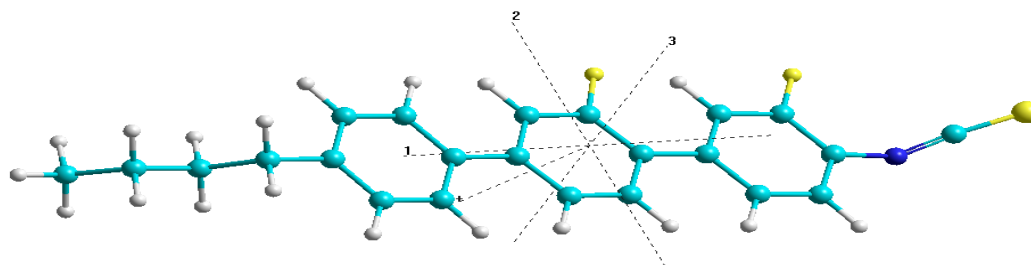
Terphenyl core is found to be planar and the – NCS group is almost in the same plane but not along the para axis of the core in all cases. At this point geometrical features of these molecules may be compared with those of an isothiocyanato compound 11CHBT for which crystal structural data are available [29]. Length of CN bond, by which the isothiocyanato group is connected to the phenyl ring, is found to be 1.41Å in all cases which is similar to that in 11CHBT (1.398Å). Observed NC and CS bond lengths are, in all cases, 1.24Å and 1.49Å. N-C-S bond angles are 172.9° (2TP-3'F-4NCS), 171.9° (2TP-3',3F-4NCS) and 172.8° (4TP-3',3F-4NCS) which was 176.1° in 11CHBT. The values of C-N-C bond by which the NCS group is connected to the phenyl ring are respectively 140.9°, 142.1° and 140.3° which was 168.4° in 11CHBT. Also C-N-N-S torsion angle is found to be almost 180° in all cases whereas that in 11CHBT was 167.3°. Thus the conformation of the isothiocyanato phenyl group differs not only from that of 11CHBT molecule in the crystalline state but it is different in the three present molecules. As a result, dipole moment of 2TP-3'F-4NCS is found to be 5.57D, much larger than the dipole moment of the – NCS group. This further increases to 6.68D in 2TP-3',3F-4NCS. However increase of chain length in 4TP-3',3F-4NCS does not increase the dipole moment rather it decreases slightly to 6.29D. Change of molecular conformation may be responsible for this.



(a)



(b)



(c)

Figure 3.2: Optimized structure of the compounds (a) 2TP-3'F-4NCS, (b) 2TP-3',3F-4NCS and (c) 4TP-3',3F-4NCS

Molecular dipole moment is found to increase from 1.93D to 3.21D when in an axially fluorinated phenyl bicyclohexyl compound an additional lateral fluorine atom is added, but no change is observed when chain length is increased by two C-atoms (discussed in chapter 4). No change in dipole moment was reported in 1CB to 12CB molecules when measured by solution technique [30]. Such behavior was also observed in nCHBT series [31].

Table 3.2: Optimized length, dipole moment and moment of inertia

Compound	Optimized Length (Å)	Dipole Moment with components (Debye)	Moment of Inertia ($\times 10^{-46}$ kg m ²)		
			I _{xx}	I _{yy}	I _{zz}
2TP-3'F-4NCS	18.56	5.57 [5.48, 1.02, 0]	68.27	1471.02	1538.24
2TP-3',3F-4NCS	18.05	6.68 [6.39, 1.95, 0]	76.7	1550.0	1626.6
4TP-3',3F-4NCS	20.82	6.29 [5.83, 2.33, 0.41]	102.86	2048.83	2146.04

3.4.3 X-Ray Diffraction Study

X-ray diffraction photographs shows smectic and nematic phases clearly. The diffraction photographs contain two major diffraction maxima. Typical X ray diffraction photographs in SmA and nematic phases of the compounds are shown in Figures 3.3 – 3.5. Layer structure in SmA phase was clearly visible in the form of sharp inner ring compared to the nematic pattern. As discussed in chapter 2, the inner ring is related to the layer spacing (d) in the smectic phase and the apparent length of the molecule (l) in the nematic phase. The diffused outer ring arises

due to interaction of the neighboring molecules in a plane perpendicular to the molecular axis providing average intermolecular distance (**D**) [32].

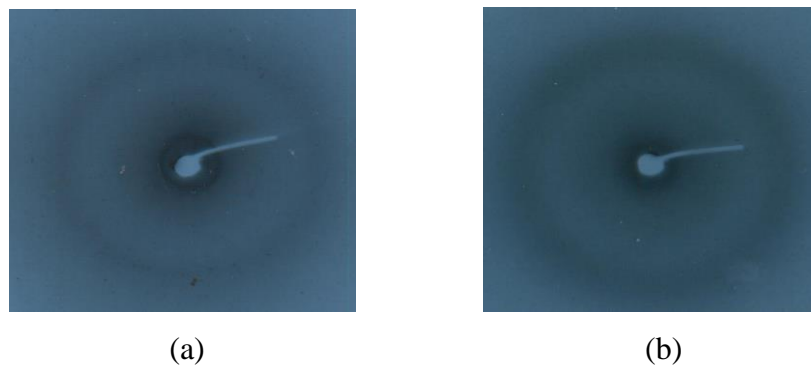


Figure 3.3: X-ray diffraction photographs in (a) SmA phase (110°C) and (b) nematic phase (125°C) of 2TP-3'F-4NCS



Figure 3.4: X-ray diffraction photographs in nematic phase (95°C) of 2TP-3',3F-4NCS

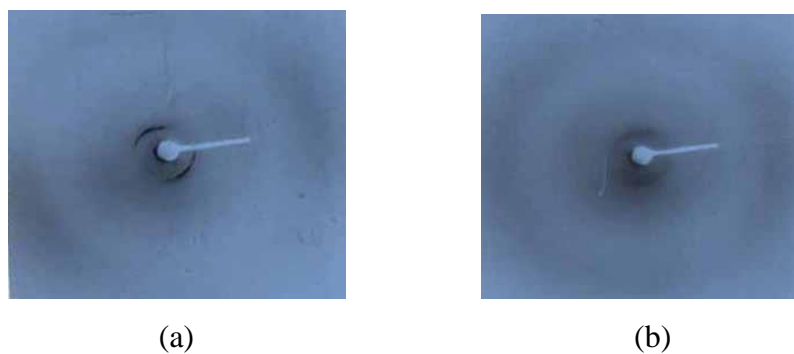


Figure 3.5: X-ray diffraction photographs in (a) SmA phase (60°C) and (b) nematic phase (100°C) of 4TP-3',3F-4NCS

Temperature dependence of the average intermolecular distance, apparent molecular length and smectic layer spacing are depicted in Figures 3.6 – 3.8 for the three compounds. It is evident that

D increases with temperature indicating a slight decrease in molecular packing. Average value of the intermolecular distances (D) in SmA phase is 5.03 Å which increases to 5.30 Å in nematic phase in 4TP-3',3F-4NCS. These values are considerably less than in singly fluorinated 2TP-3'F-4NCS; observed average values are 5.38 Å and 5.76 Å respectively. In doubly fluorinated 2TP-3',3F-4NCS also the average value is found to be 5.66 Å. It appears that increased flexibility in the chain results in more efficient packing of molecules in compound 4TP-3',3F-4NCS than the other two compounds. While comparing the compounds 2TP-3'F-4NCS and 2TP-3',3F-4NCS having the same chain length, D values are found to be slightly less in the singly fluorinated 2TP-3'F-4NCS compared to those observed in the doubly fluorinated 2TP-3',3F-4NCS. This is expected since introduction of additional F-atom in the core benzene ring increases lateral volume. This is further supported by the fact that in several homologues of non-fluorinated phenyl cyclohexyl based isothiocyanates D-values in nematic phase were found to vary from 5.06 to 5.12 Å [33], much less compared to the fluorinated molecules. D was observed as 5.48 Å when one lateral fluorine atom was present in the benzene ring of a terminally fluorinated nematogenic bicyclohexyl phenyl compound, whereas it increased to 5.60 Å when two lateral fluorine atoms were connected on opposite sides of the benzene ring [34]. Therefore, present observation on D is consistent with previous reported data of structurally similar compounds.

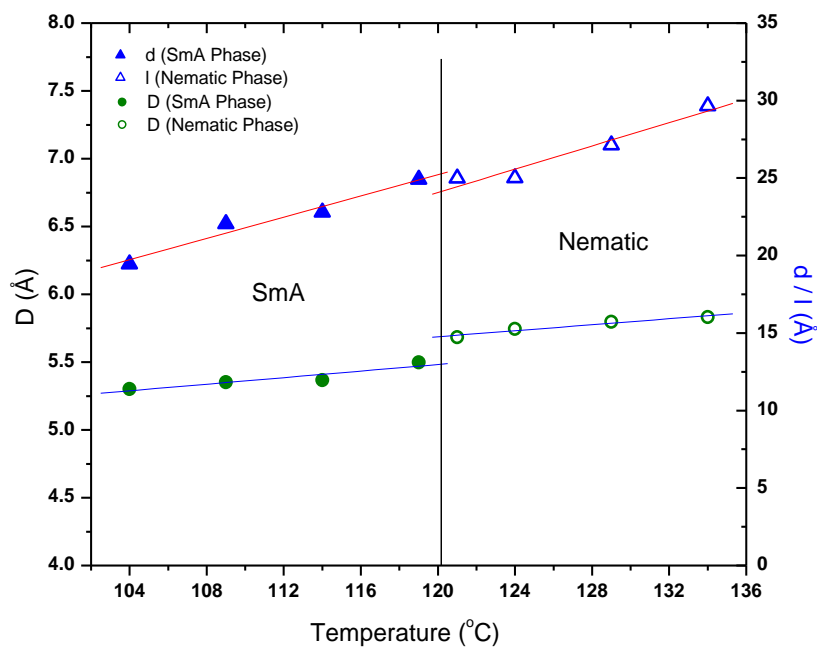


Figure 3.6: Temperature dependence of average intermolecular distance (D), smectic layer spacing (d) and apparent molecular length (l) of 2TP-3'F-4NCS

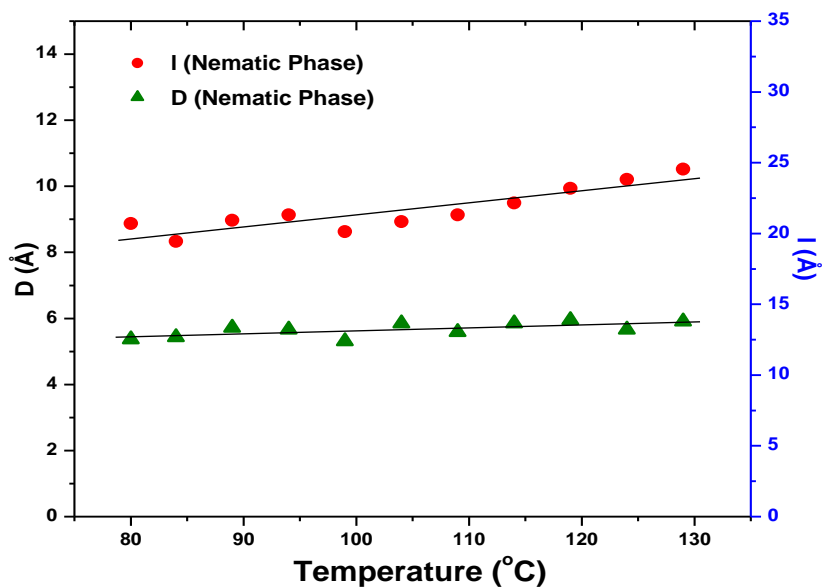


Figure 3.7: Temperature dependence of average intermolecular distance (D) and apparent molecular length (l) of 2TP-3',3F-4NCS

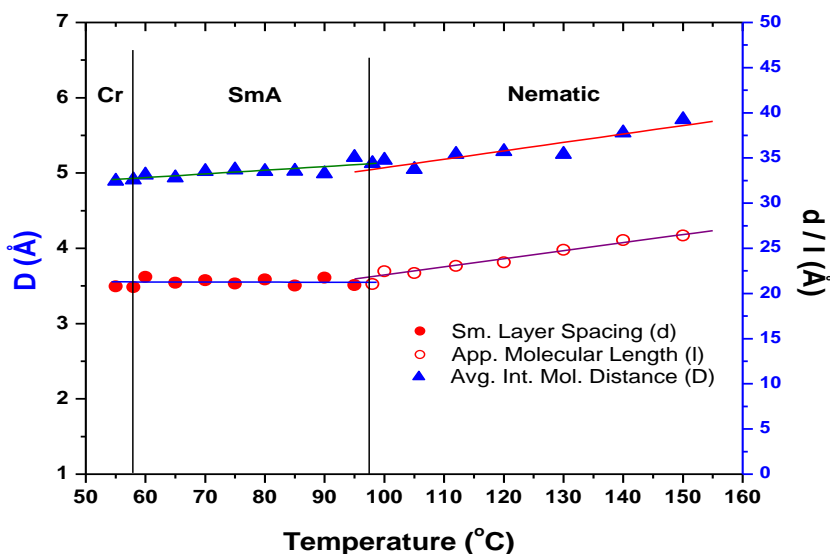


Figure 3.8: Temperature dependence of average intermolecular distance (D), smectic layer spacing (d) and apparent molecular length (l) of 4TP-3',3F-4NCS

In 2TP-3'F-4NCS and 4TP-3',3F-4NCS, the smectic layer spacing (d) is found to increase respectively from 19.45 Å to 22.78 Å and 20.7 Å to 21.0 Å, while effective length of the molecules (l) increases from 24.9 Å to 27.12 Å and 22.5 Å to 26.4 Å in the nematic phase as shown in Figure 3.6 and 3.8 respectively. However in 2TP-3',3F-4NCS which possess only nematic phase, the effective length of the molecules (l) is found to increase from 20.7 Å to 24.5 Å. Linearly fitted data show clear discontinuities at SmA-N transition in both the parameters D and l , more in 2TP-3'F-4NCS than in 4TP-3',3F-4NCS, signifying first order phase transition; although according to Mc Millan theory it should be second order in nature since observed T_{NA}/T_{NI} in both the cases is less than 0.87 [35,36]. Moreover, observed effective length of the molecules in N phase and layer spacing in smectic phase are slightly higher (more in less chained system) than the molecular length obtained from geometry optimization for all the three compounds. Similar behavior was also observed in non-fluorinated isothiocyanatobenzenes [37]. To explain this observation, some sort of molecular association among the neighboring molecules are considered, usually antiparallel molecular associations are suggested in molecules having terminal polar groups [38], no such association is observed in systems having no terminal polar groups from either X-ray study or dielectric study [39,40]. Crystal structure analysis on structurally similar terminally and laterally fluorinated phenyl bicyclohexyl compounds also

revealed such type of associations [41,42]. Molecular mechanics calculations yielded the parallel and perpendicular component of dipole moments as 5.48D and 1.02D for the compound 2TP-3' F-4NCS which were 6.39D and 1.95D respectively in 2TP-3',3F-4NCS whereas in 4TP-3',3F-4NCS the values are 5.83D and 2.33D respectively. Thus, although the molecules are not strictly axially polar but axial dipole moments are much stronger than the transverse components resulting in antiparallel associations. In the homologues of non-fluorinated alkylcyclohexyl isothiocyanatobenzenes we observed l to vary from 1.04 to 1.16 at $T=0.98T_{NI}$ [33]. Although dipole moments of the present compounds are much larger than that of alkylcyclohexyl isothiocyanatobenzenes, slightly less molecular overlap in the antiparallel dimeric association is observed in the present case compared to the non-fluorinated isothiocyanatobenzenes. This may be the result of increased steric interaction due to the presence of lateral fluorine atoms and shorter terminal chain. With increasing temperature thermal energy probably helps to overcome the dipolar interaction partially, thereby increasing the layer spacing and the apparent molecular length. Antiparallel molecular associations in NCS compounds were also confirmed from crystal structure analysis of the 11CHBBT, the 11th member of phenyl cyclohexyl isothiocyanates [43].

3.4.4 Static Dielectric Study

Dielectric Permittivities

Dielectric permittivity measurements were made at 10 kHz in planar (HG) cell. In order to determine switching voltage required to switch molecular alignment from planar (HG) to homeotropic (HT) configuration, dielectric permittivity was measured as a function of DC bias voltage across the cell. The switching characteristic in nematic phase is shown in Figure 3.9 for all the three compounds. Voltage at which the real part of dielectric permittivity increases by 10% from its minimum value is called threshold voltage (V_{th}) and at which it reaches 90% of the maximum value is termed as driving voltage (V_d). In 4TP-3',3F-4NCS threshold and driving voltages are found to be respectively 4.78V and 10.12V where as in 2TP-3' F-4NCS these are found to be 4.52 V and 9.6 V and for 2TP-3',3F-4NCS the corresponding values are 3.8V and 7.0V. Threshold and driving voltage increase slightly with chain length but decreases considerably with addition of another lateral fluorine atom. Thus increasing chain length has

more effect on switching of the molecules compared to increased lateral fluorination. However the combined effect of increased chain length and lateral fluorination is less than the effect of individual changes. However, driving field for all the compounds is suitable for thin ($< 2\mu\text{m}$) TFT based LC display cells. Nevertheless, $5\text{V}\mu\text{m}^{-1}$ field was used for switching from HG to HT configuration while measuring ϵ_{\parallel} .

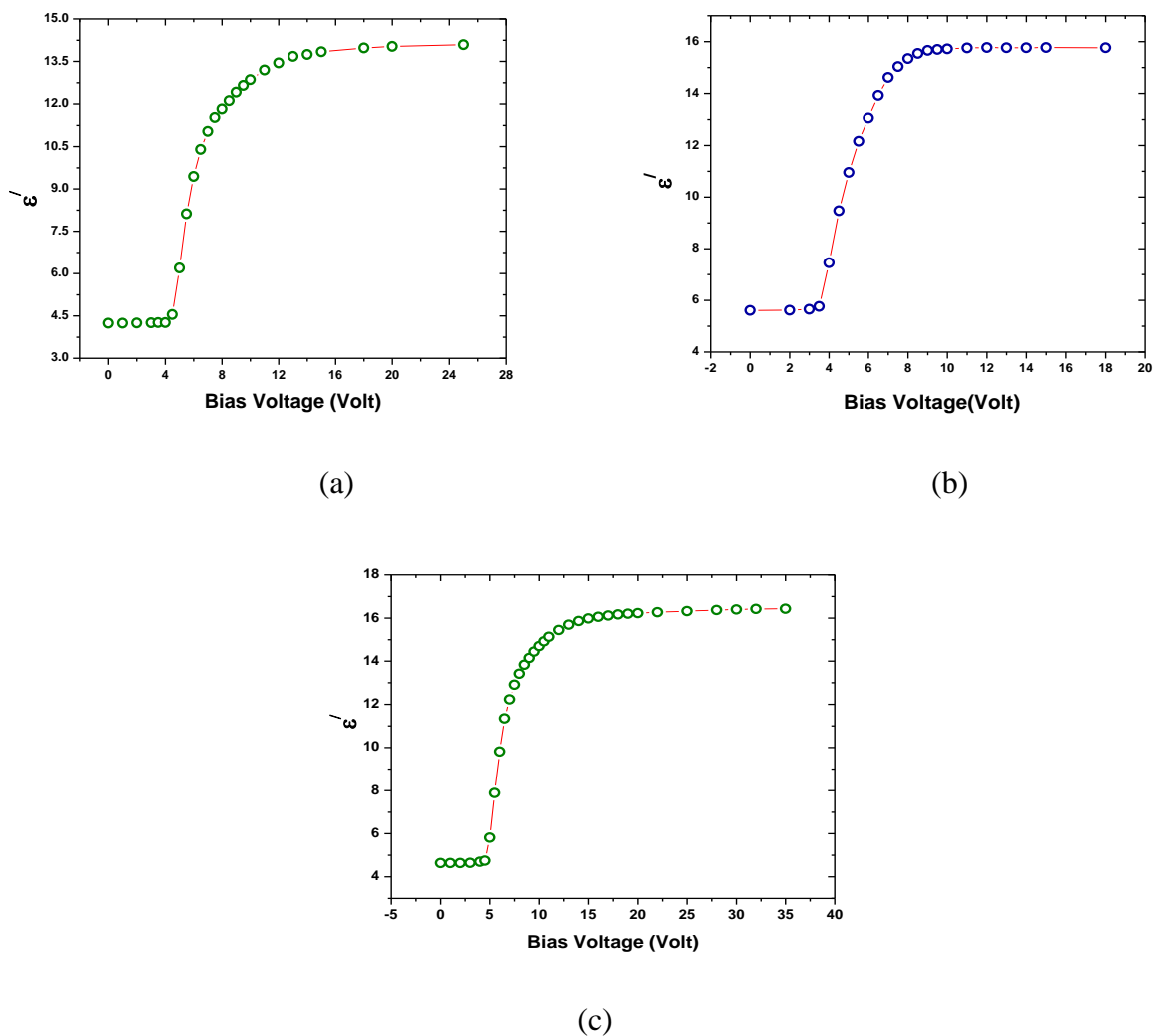


Figure 3.9: Real part of dielectric constant (ϵ') in nematic phase as a function of bias voltage at 10 kHz in ITO cell for (a) 2TP-3' F-4NCS, (b) 2TP-3',3F-4NCS and (c) 4TP-3',3F-4NCS.

Temperature variations of principal dielectric constants along and perpendicular to the molecular axis have been depicted in Figures 3.10 – 3.12. It is observed that in SmA phase ϵ_{\parallel}

decreases slowly with increasing temperature whereas ϵ_{\perp} remains almost constant for the compounds 2TP-3', F-4NCS and 4TP-3',3F-4NCS. Slight discontinuity is observed in the dielectric parameters at SmA-N transition although not as prominent as observed in X-ray study. Average value of the dielectric constant ϵ_{av} , defined as $(\epsilon_{\parallel} + 2 \epsilon_{\perp})/3$, also remain almost independent of temperature. In nematic phase stronger temperature dependence of both the components are observed. Selected values are shown in the Table 3.3. Since the molecules possess quite strong axial dipole moment, ϵ_{\parallel} is found to be large (about 17.4 near Cr-SmA transition) compared to ϵ_{\perp} (about 4.3) whereas corresponding values are 17 and 6, and 14.9 and 3.9, respectively in the doubly and singly fluorinated homologues. Comparatively larger values in the former two compounds compared to the later is due to the fact that the dipole moments along and perpendicular to molecular axes are large in the former two compounds than in the latter as noted earlier.

Temperature variations of dielectric anisotropy ($\Delta\epsilon = \epsilon_{\parallel} - \epsilon_{\perp}$) for all the compounds are shown in Figure 3.13 for comparison. Dielectric anisotropy is found to decrease with temperature; decrement rate is, however, less in smectic than in nematic phase. $\Delta\epsilon$ near Cr-N transition in 2TP-3',3F-4NCS is found to be 10.64 whereas in 2TP-3' F-4NCS observed $\Delta\epsilon$ near Cr-SmA transition is 10.97 and near SmA-N transition it is 9.7. In 4TP-3',3F-4NCS the corresponding values are 13.02 and 12.2 respectively which is considerably higher than in the ethyl compounds. From the figure it is evident that with increased lateral fluorination $\Delta\epsilon$ slightly decreases, but it increases when chain length is also increased by two carbon atoms. In a 4-propylphenylbicyclohexyl-3,4-difluorobenzene compound with two fluorine substituents at terminal position of the benzene ring (abbreviated as 3PBC^{3,4}F₂) maximum value of $\Delta\epsilon$ was found to be about 6 [44], whereas in a 4,4'-propylterphenyl compound having the same alkyl chain at both ends but with two fluorine substituents at vicinal position of the central benzene ring it was about -1.2 [45]. Thus present observation on $\Delta\epsilon$ is consistent with previous reports on structurally similar compounds.

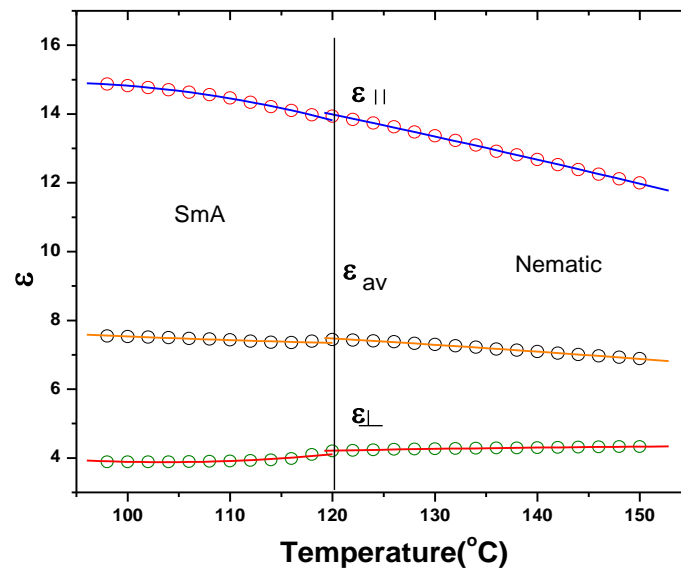


Figure 3.10: Variation of static dielectric constants as a function temperature at 10 KHz in ITO cell in 2TP-3'F-4NCS

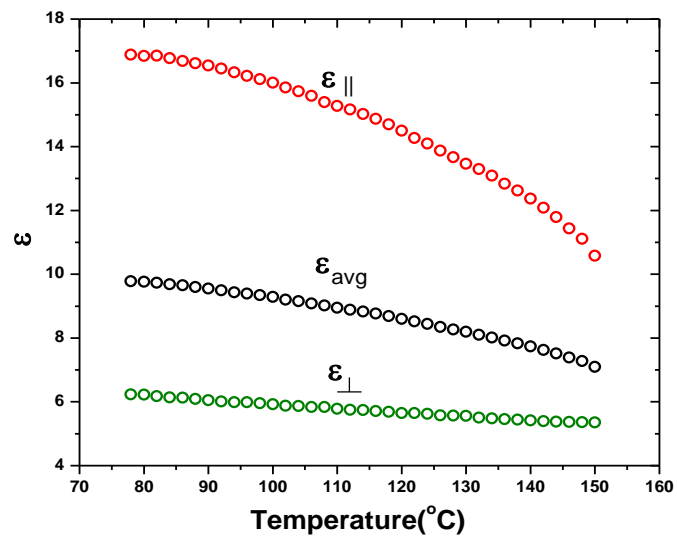


Figure 3.11: Variation of static dielectric constants as a function temperature at 10 KHz in ITO cell in 2TP-3',3F-4NCS

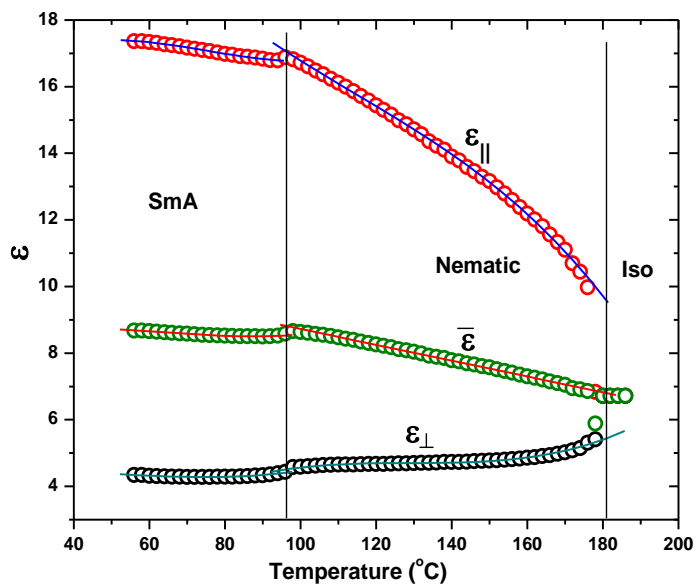


Figure 3.12: Variation of static dielectric constants as a function of temperature at 10 KHz in ITO cell in 4TP-3',3F-4NCS

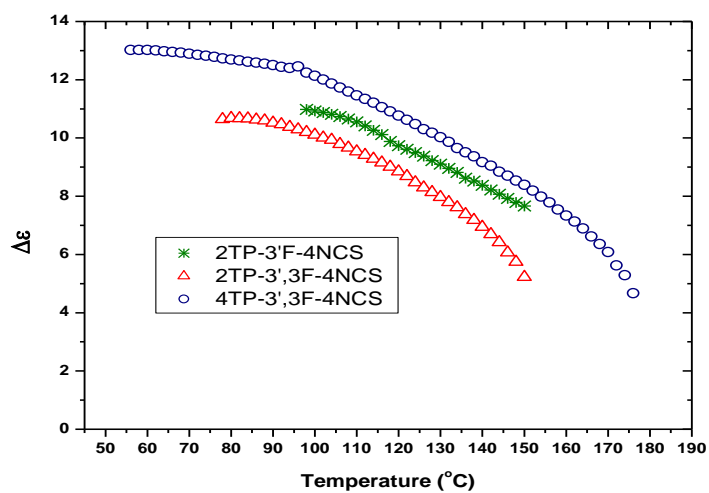


Figure 3.13: Temperature dependence of dielectric anisotropy of the compounds

Table 3.3: Selected static dielectric parameters of compounds

Compound	Threshold voltage (V_{th}) (V)	Driving voltage (V_d) (V)	$\epsilon_{ }$ (Near melting point)	ϵ_{\perp} (Near melting point)	$\Delta\epsilon$ (Near melting point)
2TP-3'F-4NCS	4.52	9.6	14.86	3.88	10.97
2TP-3',3F-4NCS	3.8	7.0	16.88	6.23	10.64
4TP-3',3F-4NCS	4.78	10.12	17.36	4.34	13.02

Dipole Correlation Factors

Effective values of dipole moments (μ_{eff}) were calculated following Bordewijk [46] theory of anisotropic dielectrics, as described in chapter 2. μ_{eff} was found to be less in both smectic and nematic phases compared to free molecular dipole moments in all the compounds again suggesting antiparallel correlation of the neighbouring molecules. To obtain a quantitative measure of this correlation, dipole-dipole correlation factor g_{λ} , was calculated, as described in chapter 2. It is noted that $g_{\lambda} = 1$ signifies no correlation at all (monomeric system), $g_{\lambda} = 0$ means perfect antiparallel correlation and $g_{\lambda} = 2$ means perfect parallel correlation. Calculated values are shown in Table 3.4. In 2TP-3'F-4NCS, $g_{||}$ is found to be 0.35 in smectic phase and 0.39 in nematic phase signifying weak antiparallel correlation of the components of dipole moments along the molecular axes in nematic phase, correlation slightly improves in smectic phase.

Table 3.4: Effective value of dipole moments (μ_{eff}) and dipole correlation factors (g_{λ})

Compound	Temp (°C)	μ_{eff} (D)	g_{\parallel}	g_{\perp}
2TP-3'F-4NCS	105	5.37 (SmA)	0.35	0.88
	110		0.37	0.85
	120		0.38	0.95
	125	5.40 (N)	0.39	0.96
	130		0.39	0.97
	140		0.40	0.95
	150		0.41	0.92
2TP-3',3F-4NCS	85	6.0 (N)	0.37	0.91
	90		0.37	0.92
	100		0.38	0.90
	110		0.37	0.88
	120		0.37	0.85
	130		0.36	0.80
	140		0.35	0.75
	150		0.31	0.70
4TP-3',3F-4NCS	60	6.05 (SmA)	0.38	0.52
	80		0.40	0.54
	100	6.36 (N)	0.44	0.62
	120		0.45	0.66
	140		0.48	0.66
	160		0.52	0.64
	180		0.55	0.67

Corresponding values of g_{\perp} were 0.88 and 0.96 suggesting almost no antiparallel correlation of the perpendicular components of the dipole moments. Antiparallel correlations in both directions decrease further with temperature. In 2TP-3',3F-4NCS antiparallel correlation along the

molecular axis is slightly less ($g_{\parallel} = 0.37$) in nematic phase than in the singly fluorinated compound. g_{λ} values in 4TP-3',3F-4NCS suggests that slight increase of chain flexibility results in further decrease of antiparallel correlation along the molecular axis slightly but correlation increases substantially in the perpendicular direction. Although it was thought before that NCS compounds do not form dimers [21] like the CN compounds but X-ray study in the crystalline and liquid crystal phases as well as dielectric study in liquid crystal phases confirm antiparallel correlation of neighboring molecules. X-ray and dielectric study in the crystalline and mesomorphic phase in other NCS compounds also supports this observation [29,31].

Dielectric Relaxation Study

To see the dynamic response of the molecules to an ac field, frequency dependent dielectric study was performed as a function of temperature in a gold coated cell. The frequency dependences of dielectric permittivities (real and imaginary part) of the three compounds are shown in Figures 3.14 – 3.16. It is clear from the figures that the real part of dielectric permittivity remains almost constant in the low frequency region and decreases sharply at higher frequencies. As temperature increases real part of dielectric permittivity is found to decrease continuously in singly fluorinated 2TP-3'F-4NCS and doubly fluorinated 4TP-3',3F-4NCS. On the other hand, in the doubly fluorinated 2TP-3',3F-4NCS, initially it is found to increase slightly, then decreases although it contains only nematic phase. Different temperature dependence may be due to different phase behaviour. Considerable supercooling effect is observed and dielectric behaviour is slightly different in the supercooled state in the ethyl compounds.

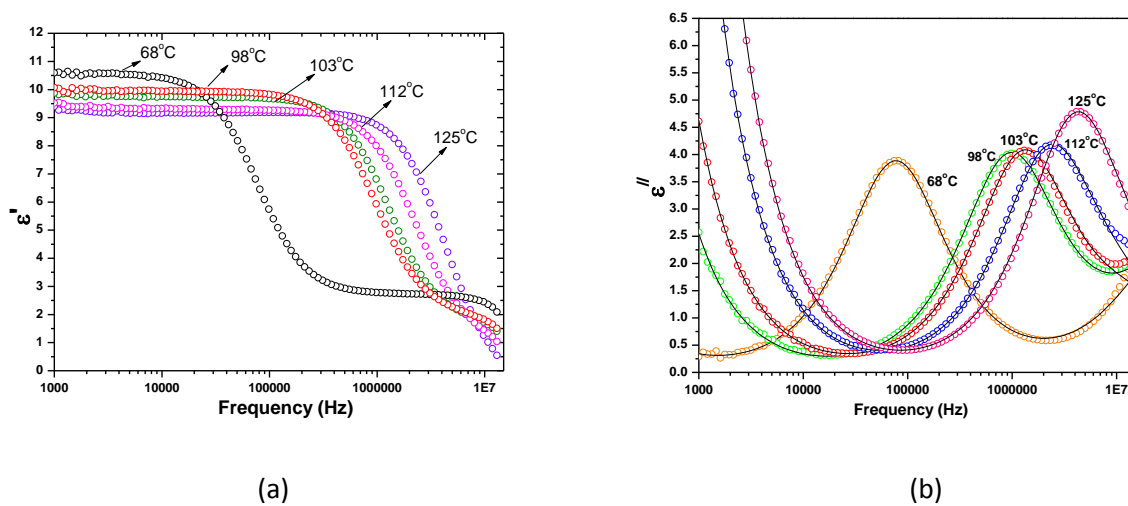


Figure 3.14: Dispersion (a) and absorption (b) spectra at some selected temperatures in 2TP-3'F-4NCS. Solid curves in (b) represent curves fitted to modified Cole-Cole function as described in text

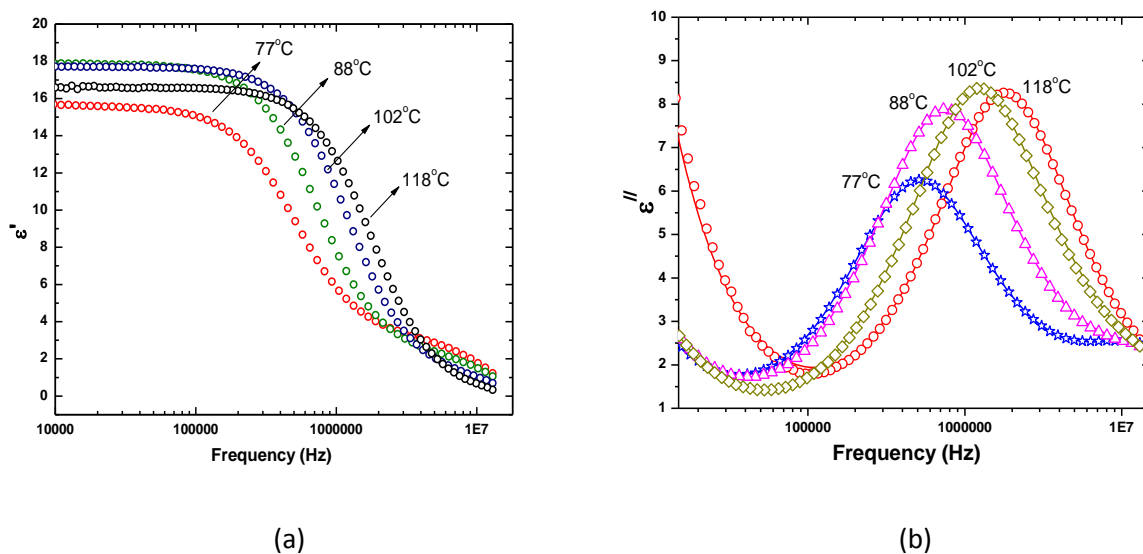


Figure 3.15: Dispersion (a) and absorption (b) spectra at some selected temperatures in 2TP-3',3F-4NCS. Solid curves in (b) represent curves fitted to modified Cole-Cole function as described in text

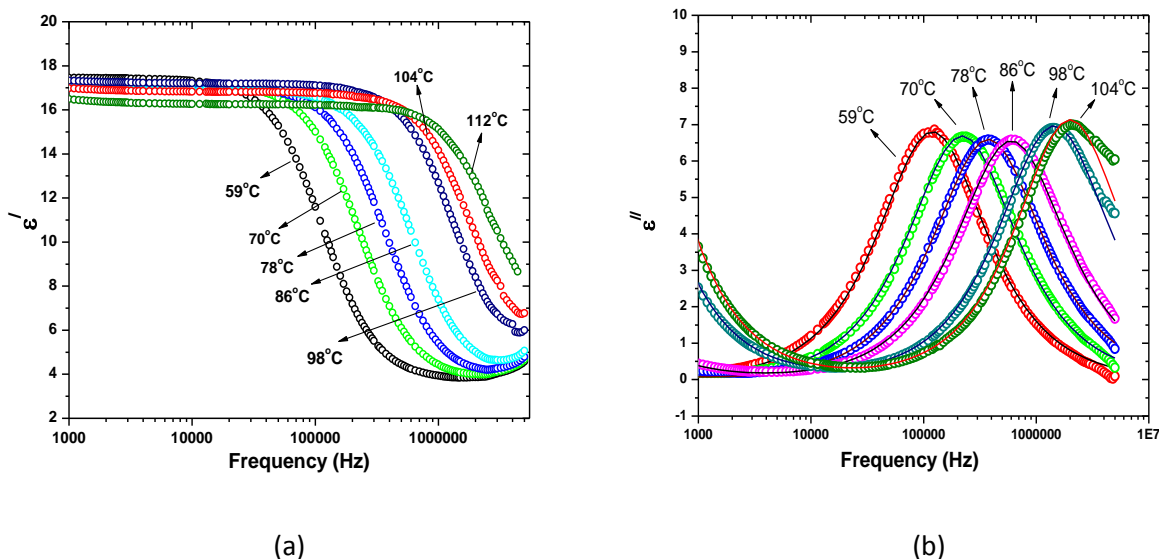


Figure 3.16: Dispersion (a) and absorption (b) spectra at some selected temperatures in 4TP-3',3F-4NCS. Solid curves in (b) represent curves fitted to modified Cole-Cole function as described in text

Only one strong absorption process is observed in dielectric spectra as evident from Figures 3.14(b), 3.15(b) and 3.16(b), for clarity spectra only at some selected temperatures are presented. The ϵ'' peak height increases slightly with temperature in the smectic A as well as in the nematic phase in 2TP-3',3F-4NCS and considerably in 2TP-3',3F-4NCS and thus there are a larger number of free molecules (monomers) with a corresponding enhancement of the effective dipole moment at higher temperature [47]. But in case of 4TP-3',3F-4NCS, there is no effective change in the ϵ'' peak height with temperature implying no appreciable change in dipolar correlation at higher frequencies in this compound. However, in all the compounds relaxation frequencies are found to increase with temperature. Assuming the relaxation behavior is a result of Cole–Cole type process, the complex dielectric permittivity was fitted with the modified Cole–Cole equation [48] to get the actual values of relaxation frequency (f_c) and symmetric distribution parameter (α), details have been described in chapter 2. As real and imaginary parts of dielectric constants are related through Kramers-Kronig relations, the Cole-Cole plot of the fitted spectra at a particular temperature for all the compounds are presented in Figure 3.17 –

3.19, which shows that the fitting was quite good. Nature of the absorption process is found to be almost Debye type since in no case fitted α is more than 0.05.

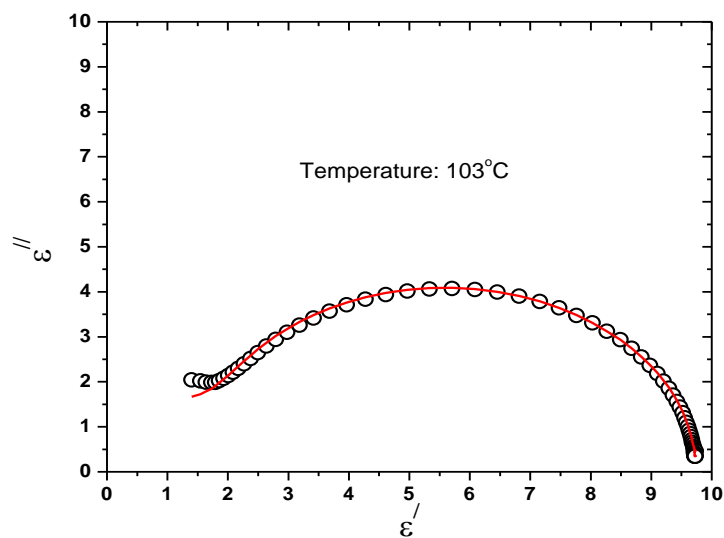


Figure 3.17: Cole-Cole plot of 2TP-3'F-4NCS

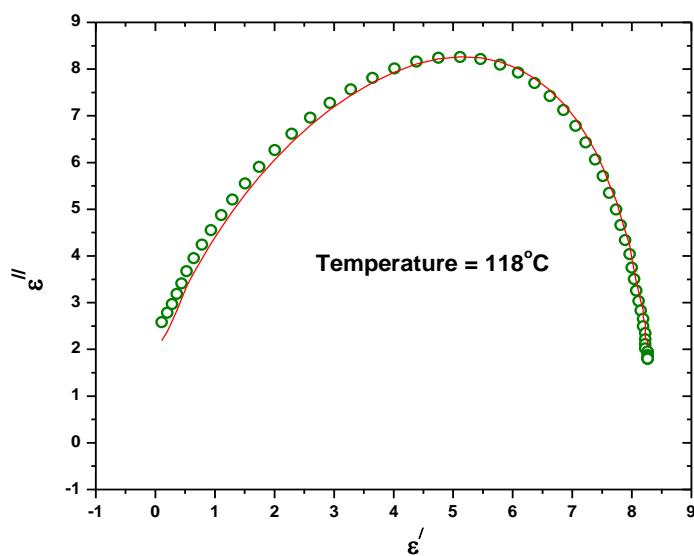


Figure 3.18: Cole-Cole of 2TP-3',3F-4NCS

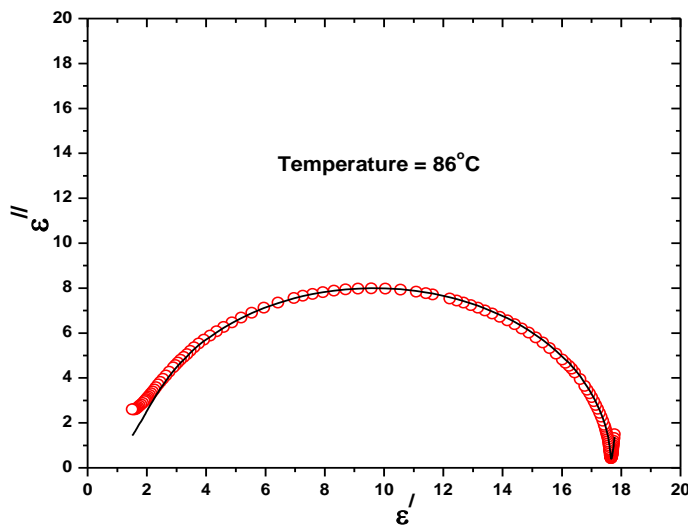


Figure 3.19: Cole-Cole plot of 4TP-3',3F-4NCS

Relaxation frequency, assumed to be associated with rotation around short molecular axis (flip-flop mode), increases systematically with temperature, shown in Table 3.5 and Figures 3.20 – 3.22. Critical frequency in nematic phase is found to decrease with increased fluorination and chain length, effect is more in the former case. In SmA phase opposite behavior is observed in low temperature region. In various smectic phases, however, critical frequencies were found to increase as the homologous series is ascended and was explained by introducing the idea of their dependence on anisotropic free volume [49,50].

Critical frequencies of the present compounds are lower than in cyanobiphenyls e.g. in 5CB it was 15.6 MHz [51]. This is expected since for rigid molecules critical frequency varies inversely with square root of moment of inertia [52] and the present molecules have larger moments of inertia (listed in Table 3.2) mainly because of large increase in their molecular mass compared to 5CB in which the moment of inertia was calculated from optimized geometry and found to be $42.9 \times 10^{-46} \text{ kg m}^2$, $844.1 \times 10^{-46} \text{ kg m}^2$, $884.3 \times 10^{-46} \text{ kg m}^2$. In a structurally more closely related compound, propyl terphenyl isothiocyanatobenzene with fluorine atoms at 3,5 positions of isothiocyanato benzene group (which may be abbreviated as 3TP-3,5-4NCS), relaxation frequency was found to vary from 900 kHz to 4 MHz [53], closer to present observation.

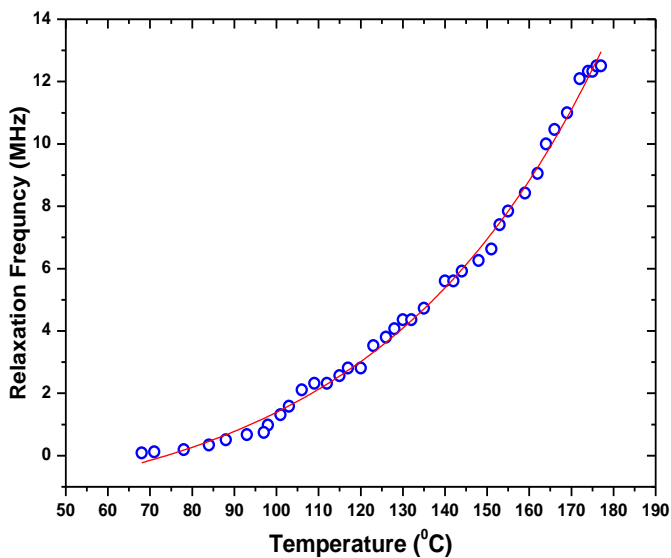


Figure 3.20: Temperature variation of relaxation frequency of compound 2TP-3'F-4NCS

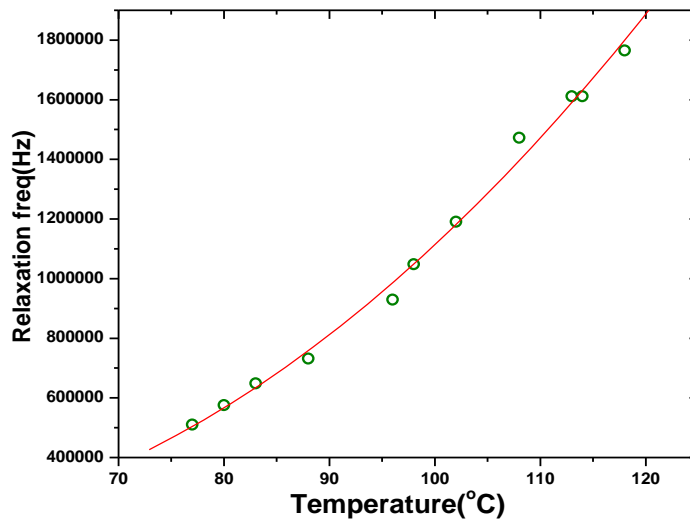


Figure 3.21: Temperature variation of relaxation frequency of compound 2TP-3',3F-4NCS

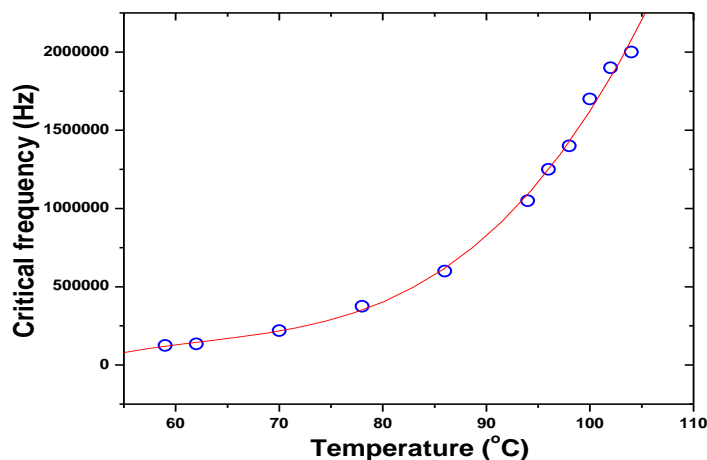


Figure 3.22: Temperature variation of relaxation frequency of compound 4TP-3',3F-4NCS

Reorientations of the entire molecules around their short axis are influenced by smectic and nematic potential barrier which increases with increasing molecular length and decreasing temperature. Relaxation frequency thus increases with temperature and is found to obey Arrhenius law [48,54,55]. From least squares straight line fitting of a plot of $\ln(\tau)$ versus inverse temperature (Figures 3.23 – 3.25), height of the activation energy barrier of the thermally activated relaxation process was calculated and are listed in Table 3.5. A close look in the values suggests that effect of fluorination and chain length is similar to that of critical frequency.

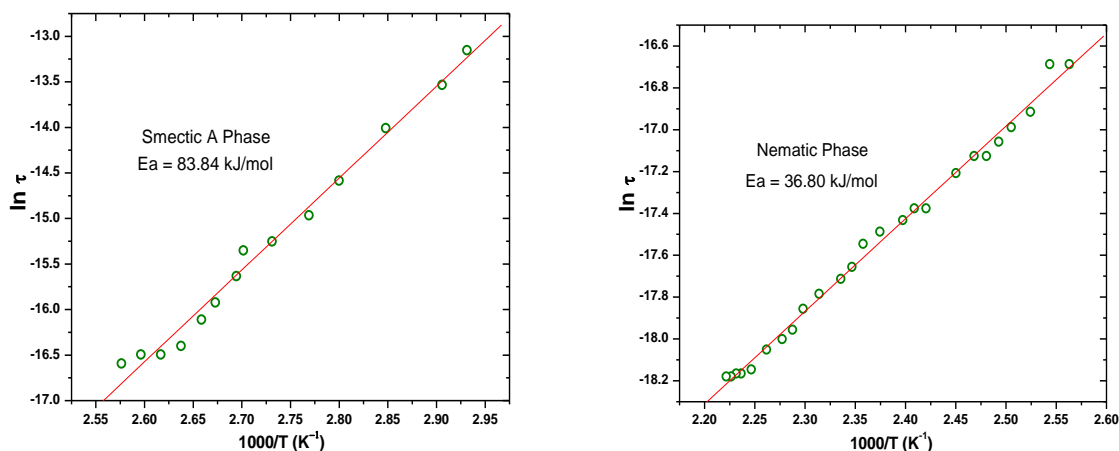


Figure 3.23: Variation of $\ln \tau$ against $1000/T$ showing Arrhenius behavior in 2TP-3'F-4NCS.

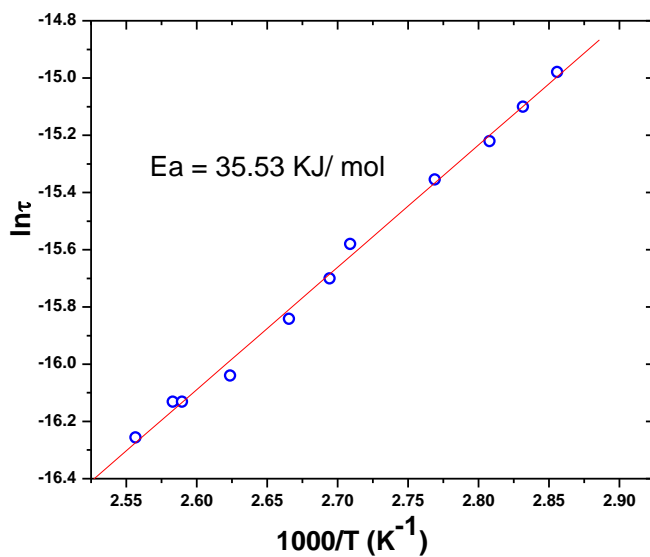


Figure 3.24: Variation of $\ln \tau$ against $1000/T$ showing Arrhenius behavior in 2TP-3',3F-4NCS.

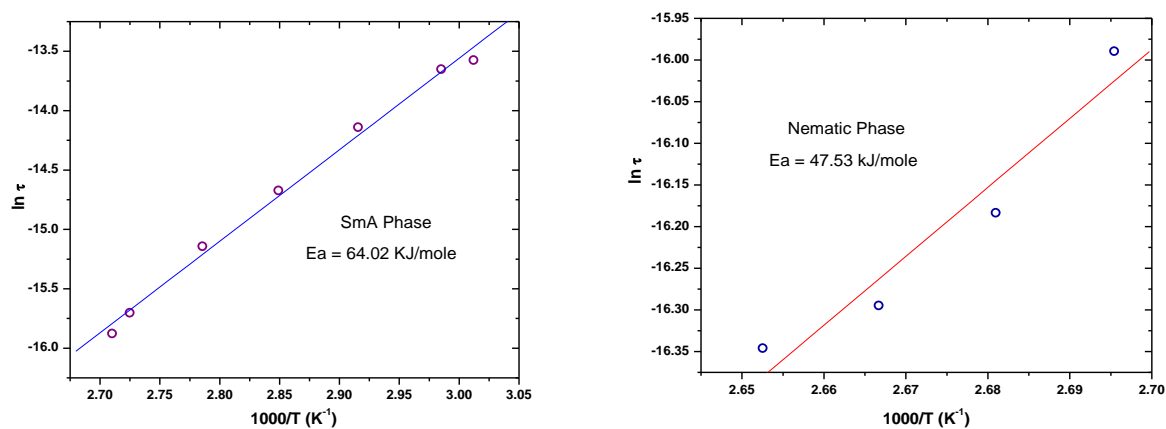


Figure 3.25: Variation of $\ln \tau$ against $1000/T$ showing Arrhenius behavior in 4TP-3',3F-4NCS.

Table 3.5: Selected dynamic dielectric parameters of the compounds

Compound	Relaxation Frequency (f_c)	Activation Energy (kJ/mole)
2TP-3'F-4NCS	82 kHz – 2.5 MHz (SmA)	83.8 (SmA)
	2.81 MHz – 12.5 MHz (N)	36.8 (N)
2TP-3',3F-4NCS	510 kHz – 1.77 MHz (N)	35.2 (N)
4TP-3',3F-4NCS	110 kHz to 1.4 MHz (SmA)	64.02 (SmA)
	1.45 MHz to 2 MHz (N)	47.53 (N)

3.4.6 Elastic Constants

The splay elastic constant (K_{11}), another important parameter for switching in nematic display devices, were measured using Freédericksz transition method [56]. And their dependence on temperature is shown in Figure 3.26. As K_{11} is proportional to dielectric anisotropy ($\Delta\epsilon$), it is, as expected, found to exhibit similar decreasing trend with temperature. Near melting point K_{11} in 2TP-3',3F-4NCS is 1.4×10^{-10} N which is almost 1.5 times in 2TP-3'F-4NCS (2.05×10^{-10} N), and almost double (2.67×10^{-10} N) in 4TP-3',3F-4NCS. Thus with increased fluorination splay elastic constant decreases but with increasing chain length it increases. Observed value of K_{11} in 2TP-3',3F-4NCS near Cr-N transition is found to be similar to that observed in non-fluorinated hexylcyclohexyl isothiocyanatobenzene [57] and in singly fluorinated 4-propylphenylbicyclohexyl-3-fluorocyanobenzene but more than that observed in doubly

fluorinated 3PBC^{3,4}F₂ [44]. Since switching time is inversely proportional to K_{11} , faster response is expected in 4TP-3',3F-4NCS than the ethyl chain based compounds.

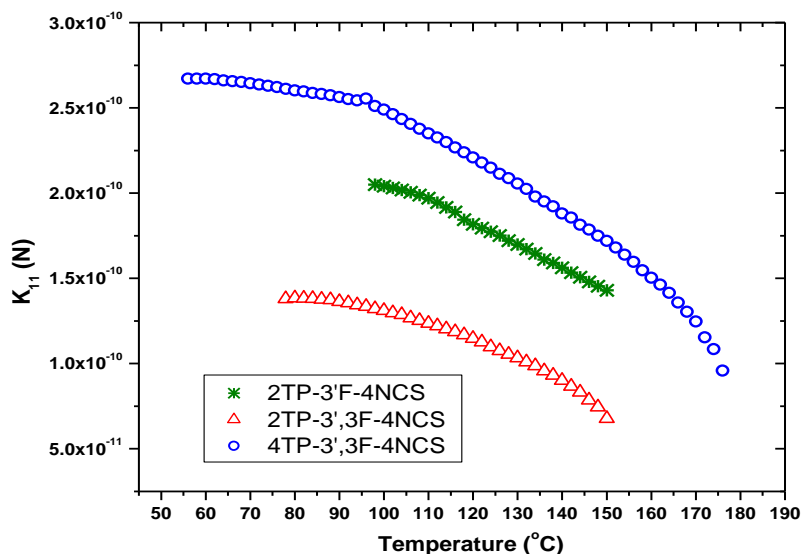


Figure 3.26: Temperature variation of splay elastic constant (K_{11}) of the three compounds.

3.4.7 Optical Birefringence Study

High birefringence (Δn) values are expected for the compounds in question, as the unsaturated rings of the terphenyl structure elongate the π -electron conjugation through the entire rigid core of the molecules and the compounds indeed are found to show high Δn . Selected values of ordinary, extraordinary and average refractive indices (n_o , n_e , n_{av}) and that of optical birefringence (Δn) at some selected temperatures within nematic phase are presented in Table 3.6. Temperature variations of these parameters are shown in Figure 3.27 and Figure 3.28. No measurement was possible in the smectic phase of 2TP-3'F-4NCS and 4TP-3',3F-4NCS. From the figures one can conclude that, although ordinary refractive index is almost the same in 2TP-3'F-4NCS and 2TP-3',3F-4NCS, extraordinary refractive index in 2TP-3',3F-4NCS is found to be less than in 2TP-3'F-4NCS. In 4TP-3',3F-4NCS both n_o and n_e is found to be less compared to the ethyl compounds. Value of n_{av} also found to decrease with fluorination and increasing chain length. This may be due to less π -electron conjugation along the molecular axis because of

the introduction of additional lateral fluorine atom (laterally substituted fluorine atoms trap π -electrons and pull them away from the conjugation along the main molecular axis) and increased chain flexibility; less order parameter values (discussed below) may also contribute. As expected all the compounds exhibit high birefringence, highest values near melting point being 0.373, 0.357 and 0.333 in 2TP-3'F-4NCS, 2TP-3',3F-4NCS and 4TP-3',3F-4NCS respectively. These values are comparable to reported values in nematic mixtures formulated using isothiocyanato terphenyls or isothiocyanato tolanes [7,21,58]. Although Δn decreases with temperature, it is found to be greater than 0.3 till 164°C in 2TP-3'F-4NCS, 136°C in 2TP-3',3F-4NCS and 130 °C in 4TP-3',3F-4NCS. Commercially available high- Δn TFT-grade LC mixtures usually have $\Delta n \sim 0.2$ at ambient temperature [59]. Present compounds are therefore expected to be very suitable for formulating high birefringence nematic mixtures, the most suitable will be the singly fluorinated ethyl compound.

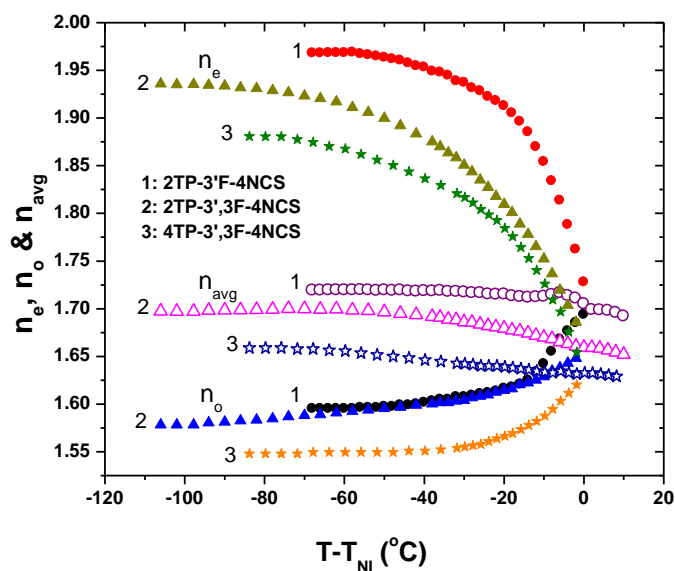


Figure 3.27: Temperature dependence of refractive indices (n_e , n_o , n_{av}) of the three compounds.

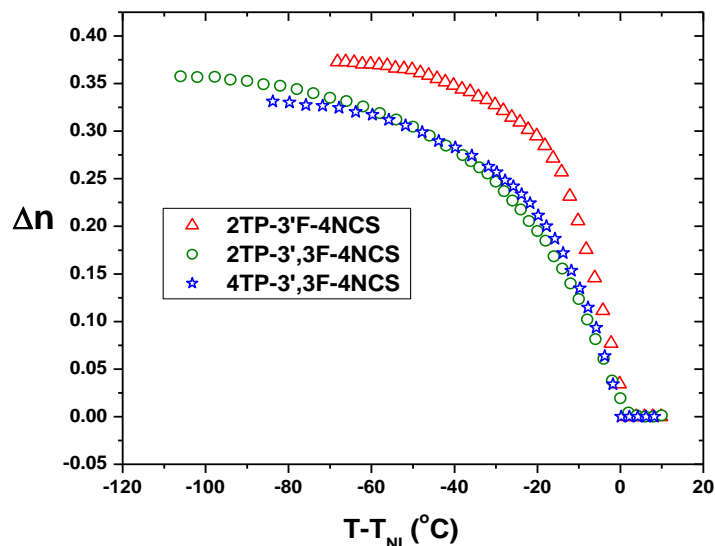


Figure 3.28: Temperature variation of Δn of 2TP-3'F-4NCS, 2TP-3',3F-4NCS and 4TP-3',3F-4NCS.

3.4.8 Density Study

Density values at some selected temperatures are listed in Table 3.6. Variation of density of the compounds with temperature is shown graphically in Figure 3.29. Density is found to decrease strongly with temperature in the ethyl systems. Compared to butyl system singly fluorinated ethyl compound shows stronger temperature dependence than the doubly fluorinated compounds. Because of the second lateral fluorine atom, 2TP-3',3F-4NCS is found to be less densely packed. It is further evident that density increases with chain length (2TP-3',3F-4NCS to 4TP-3',3F-4NCS) but it remains lower than that of 2TP-3'F-4NCS, this may be due to different phase behavior of the molecules.

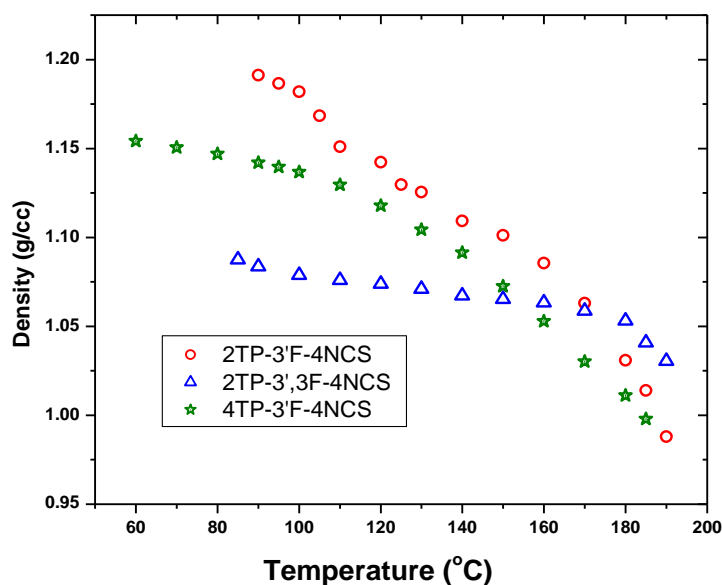


Figure 3.29: Temperature variation of density of 2TP-3'F-4NCS, 2TP-3',3F-4NCS and 4TP-3'F-4NCS.

Molecular Polarizabilities and Order Parameter

Dependence of calculated principal molecular polarizabilities (α_o , α_e and α_{av}) with temperature is found to be similar to that of the refractive indices. Average value of α is found to be $28.73 \times 10^{-24} \text{ cm}^3$ and $31.04 \times 10^{-24} \text{ cm}^3$ respectively in the singly and doubly fluorinated ethyl compounds. Compound 4TP-3',3F-4NCS possess slightly higher value, α_{av} being $31.25 \times 10^{-24} \text{ cm}^3$. So increased chain length increases α_{av} only marginally but increased fluorination has pronounced effect on α_{av} . Polarizability anisotropy ($\Delta\alpha$) is found to exhibit similar decreasing trend with temperature as observed in Δn . From the polarizability values orientational order parameters $\langle P_2 \rangle$ were calculated as described in chapter 2.

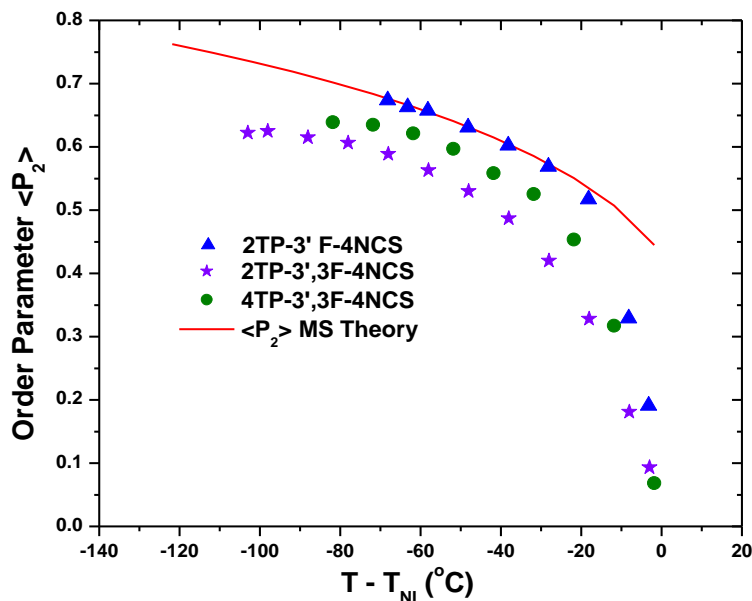


Figure 3.30: Temperature variation of order parameters of 2TP-3'F-4NCS, 2TP-3',3F-4NCS and 4TP-3',3F-4NCS.

The values of polarizability anisotropy ($\Delta\alpha$) and order parameters $\langle P_2 \rangle$ at some selected temperatures for the three compounds are listed in Table 3.6. Temperature variation of $\langle P_2 \rangle$ is depicted graphically in Figure 3.30. Order parameters computed on the basis of Maier-Saupe (MS) mean field theory for calamitic nematogens have also been depicted in the same figure. As expected, order parameter is more in smectic phase than in nematic phase in 2TP-3'F-4NCS and 4TP-3',3F-4NCS. Order parameter of the singly fluorinated ethyl compound is substantially more than the doubly fluorinated ones. Thus the doubly fluorinated ethyl compound is not only less densely packed but orientationally less ordered as well. Order parameter of 4TP-3',3F-4NCS lies between the two ethyl compounds. Thus combined effect of increased chain flexibility and lateral fluorination on order parameter is less than only lateral fluorination. Moreover, only in the singly fluorinated ethyl compound $\langle P_2 \rangle$ values match nicely with MS theoretical values, while in the other two compounds these are considerably less. Such behavior has been reported earlier [60-62]. However, no discontinuity is observed at transitions in refractive indices, densities and order parameters as seen in dielectric and structural parameters.

Table 3.6: Selected refractive indices (n_e & n_o), optical birefringence (Δn), density (ρ), polarizability anisotropy ($\Delta\alpha$) and order parameter $\langle P_2 \rangle$

Compound	Temp (°C)	n_e	n_o	Δn	ρ (g/cc)	$\Delta\alpha$	$\langle P_2 \rangle$
2TP-3'F-4NCS	120	1.969	1.596	0.373	1.142	20.500	0.674
	125	1.969	1.596	0.373	1.129	20.165	0.663
	130	1.969	1.596	0.373	1.126	20.009	0.658
	140	1.963	1.598	0.365	1.109	19.197	0.631
	150	1.949	1.604	0.345	1.101	18.328	0.602
2TP-3',3F-4NCS	85	1.935	1.578	0.357	1.087	20.388	0.622
	90	1.935	1.578	0.357	1.084	20.473	0.625
	100	1.932	1.582	0.350	1.079	20.138	0.615
	110	1.929	1.585	0.344	1.076	19.860	0.606
	120	1.922	1.588	0.334	1.074	19.279	0.589
	130	1.911	1.592	0.319	1.071	18.445	0.563
	140	1.895	1.596	0.299	1.067	17.361	0.530
	150	1.875	1.600	0.275	1.065	15.949	0.487
4TP-3',3F-4NCS	100	1.881	1.548	0.333	1.137	20.228	0.639
	110	1.877	1.548	0.329	1.129	20.161	0.635
	120	1.870	1.549	0.321	1.118	19.833	0.621
	140	1.836	1.551	0.285	1.091	18.053	0.558
	160	1.793	1.564	0.229	1.053	14.956	0.454
	170	1.740	1.582	0.158	1.030	10.507	0.317

3.5 CONCLUSION

Effect of lateral fluorination and increased chain length on several physical parameters, important from application consideration, of three compounds 2TP-3'F-4NCS, 2TP-3',3F-4NCS and 4TP-3',3F-4NCS having terphenyl rigid core structures with terminal isothiocyanate (NCS) polar groups has been investigated. The first and the third compound possess smectic phase as well as nematic phase while the second compound possess only nematic phase. All the three compounds exhibit very broad range nematic phase viz., 68°C, 108°C and 85°C respectively. Molecular mechanics calculation revealed that the molecules possess a strong axial dipole moment of 5.57D, 6.68D and 6.29D respectively. From optimized geometry the calculated length of the molecules are found to be 18.56 Å, 18.05 Å and 20.82 Å respectively which are slightly less than that obtained from X-Ray diffraction study. This suggests, contrary to common perception that NCS molecules do not form dimers, presence of weak antiparallel correlation of molecules in all the three compounds. Calculated effective values of dipole moments in mesophases and dipole-dipole correlation factors support this observation. Observed dielectric anisotropy is positive in all the three compounds and strong enough to ensure a driving voltage suitable for thin TFT based LC display cell. Calculated splay elastic constants suggest that the singly fluorinated compound (2TP-3'F-4NCS) will exhibit faster response than the other two doubly fluorinated compounds. Only one relaxation process with strong absorption, related with rotation around short molecular axis, is observed, critical frequency of which is found to decrease with increased fluorination and chain length. The singly fluorinated compound is found to exclude the possibility of undesirable energy absorption below MHz range applications. Nature of the absorption process is found to be almost Debye type in all the systems. Above all the compounds exhibit high birefringence, highest values being 0.373, 0.357 and 0.333 respectively. Thus with increasing fluorination and increasing chain length the birefringence gradually decreases. Combined effect of increased chain flexibility and lateral fluorination on order parameter is less than only lateral fluorination. These compounds are, therefore, expected to be very suitable for formulating high birefringence nematic mixtures for fast switching displays.

3.6 REFERENCES

- [1] S. Gauza, H. Wang, C. H. Wen, S. T. Wu, A. Seed and R. Dabrowski; *Jpn. J. Appl. Phys.*, 42, 3463 (2003), High Birefringence Isothiocyanato Tolane Liquid Crystals.
- [2] J. S. Gasowska, S. J. Cowling, M. C. R. Cockett, M. Hird, R. A. Lewis, E. P. Raynes and J. W. Goodby; *J. Mater. Chem.*, 20, 299 (2010), The influence of an alkenyl terminal group on the mesomorphic behaviour and electro-optic properties of fluorinated terphenyl liquid crystals.
- [3] A. Mori, M. Hashimoto and S. Ujiie; *Liq. Cryst.*, 38, 263 (2011), Effects of a semi-fluorinated side chain and a lateral polar group on mesomorphic properties of 5-cyanotroponoids and benzonitriles.
- [4] D. Demus, Y. Goto, S. Swada, E. Nakagawa, H. Saito and R. Tarao; *Mol. Cryst. Liq. Cryst.*, 260, 1 (1995), Trifluorinated Liquid Crystals for TFT Displays.
- [5] T. Nishi, A. Matsubara, H. Okada, H. Onnagawa, S. Sugimori, and K. Miyashita; *Jpn. J. Appl. Phys.*, 34, 236 (1995), Relationship between Molecular Structure and Temperature Dependence of Threshold Voltage in Fluorinated Liquid Crystals.
- [6] V. F. Petrov; *Liq. Cryst.*, 19, 729 (1995), Liquid crystals for AMLCD and TFT-PDLC applications.
- [7] S. Gauza, X. Zhu, W. Piecek, R. Dabrowski, S. T. Wu; *J. Disp. Technol.* 3 (3), 250-252 (2007), Fast Switching Liquid Crystals for Color-Sequential LCDs.
- [8] M. Schadt, W. Helfrich; *Appl. Phys. Lett.*, 18, 127 (1971), Voltage-dependent optical activity of a twisted nematic liquid crystal.
- [9] K. Nishiyama, M. Okita, S. Kawaguchi, K. Teranishi, R. Takamatsu; *SID Tech. Dig.* 36, 132 (2005), 32" WXGA LCD TV using OCB Mode, Low Temperature p-Si TFT and Blinking Backlight Technology.
- [10] G. Harbers, C. Hoelen, *SID Tech. Dig.* 32, 702 (2001), High Performance LCD Backlighting using High Intensity Red, Green and Blue Light Emitting Diodes.

- [11] D. P. Resler, D. S. Hobbs, R. C. Sharp, L. J. Friedman, T.A. Dorschner; *Opt. Lett.* 21 (9), 689 (1996), High-efficiency liquid-crystal optical phased-array beam steering.
- [12] J. Y. Hardeberg, F. Schmitt, H. Brettel; *Opt. Eng.* 41 (10), 2532 (2002), Multispectral color image capture using a liquid crystal tunable filter.
- [13] H. C. Lin, Y. H. Lin; *Opt. Express*, 20 (3), 2045 (2012), An electrically tunable-focusing liquid crystal lens with a low voltage and simple electrodes.
- [14] T.T. Ru, C.C. Yuan, R.P. Pan, C.L. Pan, X.C. Zhang; *IEEE Microwave Wireless Compon. Lett.* 14 (2) (2004), Electrically controlled room temperature terahertz phase shifter with liquid crystal.
- [15] R. L. Sutherland, V. P. Tondiglia, L.V. Natarajan; *Appl. Phys. Lett.* 64, 1074 (1994), Electrically switchable volume gratings in polymer-dispersed liquid crystals.
- [16] N. Mizoshita, K. Hanabusa, T. Kato; *Adv. Funct. Mater.* 13, 313 (2003), Fast and High-Contrast Electro-optical Switching of Liquid-Crystalline Physical Gels: Formation of Oriented Microphase-Separated Structures.
- [17] Y. H. Fan, H. W. Ren, S. T. Wu; *Appl. Phys. Lett.* 82, 2945 (2003), Normal-mode anisotropic liquid-crystal gels.
- [18] M. Hird; *Chem. Soc. Rev.*, 2007; 36, 2070, Fluorinated liquid crystals – properties and applications.
- [19] J. A. Malecki and J. Nowak; *J. Molecular Liquids*, vol. 81, 245-252 (1999), Intermolecular interactions in benzene solutions of 4-heptyl-3'-cyano-biphenyl studied with non-linear dielectric effects.
- [20] S. Gauza, J. Li, S. T. Wu, A. Spadlo, R. Dabrowski, Y. N. Tzeng, K. L. Cheng, *Liq. Cryst.* 32(8), 1077 (2005), High birefringence and high resistivity isothiocyanate-based nematic liquid crystal mixtures.

- [21] S. Gauza, S. T. Wu, A. Spadło, R. Dabrowski, *J. Disp. Technol.* 2(3), 247 (2006), High performance room temperature nematic liquid crystals based on laterally fluorinated isothiocyanto-tolanes.
- [22] D. Sinha, D. Goswami, P. K. Mandal, Ł. Szczucinski, R. Dabrowski; *Mol Cryst Liq Cryst.*, 562,156 (2012), On the nature of molecular associations, static permittivity and dielectric relaxation in a uniaxial nematic liquid crystal.
- [23] B. Jha, S. Paul, R. Paul, P. Mandal; *Phase Transitions*, 15, 39 (1989), Order parameters of some homologue cybotactic nematics from X-ray diffraction measurements.
- [24] A. de Vries; *Mol Cryst Liq Cryst.*, 10, 31 (1970), Evidence for the existence of more than one type of nematic phase.
- [25] B. R. Jaishi, P. K. Mandal; *Liq Cryst.*, 33, 753 (2006), Optical microscopy, DSC and X-ray diffraction studies in binary mixtures of 4-pentyloxy-4'-cyanobiphenyl with three 4,4'-di(alkoxy) azoxybenzenes.
- [26] P.G. de Gennes; *Mol. Cryst. Liq. Cryst.*, 12, 193 (1971), Short range order effects in the isotropic phase of nematics and cholesterics.
- [27] H. E. J. Neugebauer; *Canad. J. Phys.*, 32, 1-8 (1954), Clarius-Mossoti equation for certain types of anisotropic crystals.
- [28] Hyperchem 6.03, Hypercube Inc., Gainesville, FL, USA.
- [29] S. Biswas, S. Haldar, P. K. Mandal, K. Goubitz, H. Schenk and R. Dabrowski, *Crystal Research and Technology*, Vol. 42, No.10, P. 1029 – 1035 (2007), Crystal structure of a polar nematogen 4-(trans-4-undecylcyclohexyl) isothiocyantobenzene.
- [30] E. Megnassan and A. Proutierre; *Mol. Cryst. Liq. Cryst.*, 108, 245-254 (1984), Dipole Moments and Kerr Constants of 4-n-Alkyl-4'-Cyanobiphenyl Molecules (From 1CB to 12CB) Measured in Cyclohexane Solutions.

- [31] P. Sarkar, P. Mandal, S. Paul, R. Paul; *Liq. Cryst.*, Vol. 30, No. 4, 507–527 (2003), X-ray diffraction, optical birefringence, dielectric and phase transition properties of the long homologous series of nematogens 4-(trans-4'-n-alkylcyclohexyl) isothiocyanatobenzenes.
- [32] A de Vries; *Mol Cryst Liq Cryst.*, 10, 219 (1970), X-ray photographic studies of liquid crystals I. A cybotactic nematic phase.
- [33] P. Sarkar, P. Mandal, S. Paul, R. Dabrowski, K. Czuprynski; *Liq.Cryst.* 30 (4), 507 (2003), X-ray diffraction, optical birefringence, dielectric and phase transition properties of the long homologous series of nematogens 4-(trans -4'- n -alkylcyclohexyl) isothiocyanatobenzenes.
- [34] S. Haldar, S. Barman, P. K. Mandal, W. Haase, R. Dabrowski; *Mol. Cryst. Liq.Cryst.*, 528, 81-95 (2010), Influence of Molecular Core Structure and Chain Length on the Physical Properties of Nematogenic Fluorobenzene Derivatives.
- [35] W. L. McMillan; *Phys. Rev A*, 4, 1238-1246 (1971), Simple molecular model for the smectic A phase of liquid crystals.
- [36] W. L. McMillan; *Phys. Rev A*, 6, 936 (1972), X-Ray Scattering from Liquid Crystals. I. Cholesteryl Nonanoate and Myristate.
- [37] P. Sarkar, P. Mandal, S. Paul, R. Dabrowski, K. Czuprynski; *Liq Cryst.* 30 (4), 507 (2003), X-ray diffraction, optical birefringence, dielectric and phase transition properties of the long homologous series of nematogens 4-(trans-4'-n-alkylcyclohexyl) isothiocyanatobenzenes.
- [38] A. J. Leadbetter, R. M. Richardson, C. N. Cooling; *J Phys (Paris)*, 36 (C1), 37 (1975), The structure of a number of nematogens.
- [39] P. K. Sarkar, S. Paul, P. Mandal; *Mol Cryst Liq Cryst.*, 265, 249 (1995), Small angle X-ray scattering studies on smectic and nematic phases of a toluidine compound.
- [40] N. V. Madhusudana, S. Chandrasekhar; *Pramana Suppl.*, 1, 57 (1975), The role of permanent dipoles in nematic order.

- [41] S. Haldar, S. Biswas, P. K. Mandal, K. Goubitz, H. Schenk and W. Haase; *Mol. Cryst. Liq. Cryst.*, 490, 80-87 (2008), X-Ray Structural Analysis in the Crystalline Phase of a Nematogenic Fluoro-Phenyl Compound.
- [42] S. Haldar, P. K. Mandal, S.J. Prathap, T. N. Guru Row and W. Haase; *Liq. Cryst.*, 35, 1307-1312 (2008), X-ray studies of the crystalline and nematic phases of 49-(3,4,5-trifluorophenyl)-4-propylbicyclohexyl.
- [43] S. Biswas, S. Haldar, P. K. Mandal, K. Goubitz, H. Schenk, R. Dabrowski; *Crystal Res Technol.*, 42(10), 1029-1035 (2007), Crystal structure of a polar nematogen 4-(trans-4-undecylcyclohexyl) isothiocyanatobenzene.
- [44] H. Ishikawa, A. Toda, H. Okada, H. Onnagawa, S. Sugimori; *Liq. Cryst.*, 22, 743 (1997), Relationship between order parameter and physical constants in fluorinated liquid crystals.
- [45] S. Urban, P. Kula, A. Spadlo, M. Geppi, A. Marini; *Liq. Cryst.*, 37, 1321 (2010), Dielectric properties of selected laterally fluoro-substituted 4,4''-dialkyl, dialkoxy and alkyl-alkoxy [1:1';4':1''] terphenyls.
- [46] P. Bordewijk, *Physica*, 75, 146 (1974), Extension of the Kirkwood-Frölich Theory of the Static dielectric Permittivity to anisotropic Liquids.
- [47] N. V. Madhusudana, B. S. Srikanta, R. Subramanya, M. Urs, *Mol. Cryst. Liq. Cryst.* 108, 19 (1984), Comparative X-ray and dielectric studies on some structurally related smectogenic compounds.
- [48] J. Schacht, P. Zugenmaier, M. Buivydas, L. Komitov, B. Stebler, S. T. Lagerwall, F. Gouda, F. Horii; *Phys Rev E.*, 61, 3926 (2000), Intermolecular and intramolecular reorientations in nonchiral smectic liquid-crystalline phases studied by broadband dielectric spectroscopy.
- [49] S. Urban, R. Dabrowski, J. Dziaduszek, J. Janik, J. K. Moscicki; *Liq. Cryst.* 26, 1817 (1999), Mesomorphic and dielectric properties of fluorosubstituted isothiocyanates with different bridging groups.
- [50] L. Benguigui; *Phys. Rev. A*, 28, 1852 (1983), Dielectric relaxation in the crystalline smectic-B phase.

- [51] M. Gu, Y. Yin, S. V. Shiyankovskii, O. D. Lavrentovich; *Phys Rev E.*, 76, 061702 (2007), Effects of dielectric relaxation on the director dynamics of uniaxial nematic liquid crystals.
- [52] H. Baessler, R. B. Beard, M. M. Labes; *J Chem Phys.*, 52, 2292 (1970), Dipole Relaxation in a Liquid Crystal.
- [53] J. Czub, R. Dabrowski, J. Dziaduszek, S. Urban; *Phase Transition*, 82, 485-495 (2009), Dielectric properties of ten three-ring LC fluorosubstituted isothiocyanates with different mesogenic cores.
- [54] A. C. Diogo, A. F. Martins; *J Phys (Paris).*, 43, 779 (1982), Order parameter and temperature dependence of the hydrodynamic viscosities of nematic liquid crystals.
- [55] S. Arrhenius; *Z Phys Chem.*, 4, 226 (1889), On the reaction rate of the inversion of non-refined sugar upon souring.
- [56] B. Kundu, S. K. Pal, S. Kumar, R. Pratibha, N. V. Madhusudana; *Physical Review E.*, 82, 061703 (2010), Splay and bend elastic constants in the nematic phase of some disulfide bridged dimeric compounds.
- [57] R. Dhar, A. S. Pandey, M. B. Pandey, S. Kumar and R. Dabrowski; *Applied Physics Express* 1, 121501 (2008), Optimization of the display parameters of a room temperature twisted nematic display material by doping single-wall carbon nanotubes.
- [58] M. D. Gupta, A. Mukhopadhyay, S. K. Roy, R. Dabrowski; *J Appl Phys.*, 113, 053516 (2013), High birefringence liquid crystal mixtures: Optical properties and order parameter.
- [59] E. Nowinowski-Kruszelnicki, J. Kedzierski, Z. Raszewski, L. Jaroszewicz, R. Dabrowski, M. Kojdecki, W. Piecek, P. Perkowski, K. Garbat, M. Olifierczuk, M. Sutkowski, Karolina Ogrodnik, P. Morawiak, E. Miszczyk; *Optica Applicata*, Vol. XLII, No. 1, oa120116 (2012), High birefringence liquid crystal mixtures for electro-optical devices.
- [60] H. S. Subramanyam, C. S. Prabha and D. Krishnamurti; *Mol. Cryst. Liq. Cryst.*, 28, 201 (1974), Optical Anisotropy of Nematic Compounds.

[61] M. Mitra, S. Paul and R. Paul; *Pramāna J. Phys.*, 29, 409 (1987), Optical Birefringence and Order Parameter of Three Nematogens.

[62] N. V. Madhusudana, *Mol. Cryst. Liq. Cryst.*, 59, 117 (1980), Polarization Field and Orientational Order in Liquid Crystals.

CHAPTER 4

INFLUENCE OF MOLECULAR STRUCTURE, FLUORINATION AND CHAIN LENGTH ON THE DIELECTRIC PROPERTIES OF NEMATOGENIC BI-CYCLOHEXYL PHENYL DERIVATIVES

*Part of the work has been published in *Liquid Crystals*, Vol. 40: No. 5: pp. 689–698, 2013.*

4.1 INTRODUCTION

Liquid crystal materials have many unique physical, optical and electro-optical properties and have received much attention in case of display applications and nematic liquid crystals are the most valuable in this regard. Nematic liquid crystals (NLCs) consist of anisotropic molecules that tend to align in a common local direction called the director which results in possessing several anisotropic properties like viscosity, elasticity, birefringence, dielectric permittivity, etc. In addition to this, NLCs have long-range orientational order, which gives rise to many properties important for LC displays [1–5]. Partially fluorinated phenyl-bicyclohexyl and biphenyl-cyclohexyl compounds are wide-range nematic materials characterised by low viscosity and high chemical stability, large dielectric anisotropy, low optical anisotropy and very good voltage holding ratio and they exhibit mesomorphism at ambient temperatures and have high bulk resistivity and low current consumption. These materials are, therefore, expected to be useful in making active matrix displays (AMDs) such as TFT (thin-film transistor) and MIM (metal–insulator–metal) systems [6-9]. These materials are also found to be useful in large information content display technology as well as for photonic applications [7-17]. Various physical properties of the compounds of this series have been investigated by many authors employing different experimental techniques like phase transitions and thermal properties [6, 18], optical birefringence [19], order parameter [12], viscosity [20], spectroscopic [21], dielectric, and elastic properties [14,22,23].

In this chapter dielectric behavior of six fluorinated bicyclohexyl compounds have been described which were studied in our laboratory by X-ray diffraction and optical birefringence methods [24,25].

Dielectric studies of liquid crystals have proven to be very useful as a source of information about specific intermolecular interactions, molecular associations, molecular dynamics and relaxation mechanisms, also important in the development of electro-optic devices [26-28]. The study of temperature dependence of the permittivity is also of considerable practical importance. The threshold voltage (V_{th}) and other operational parameters of liquid crystal display devices depend on the anisotropy of the permittivity ($\Delta\epsilon$) [29] and the multiplexity of matrix displays may be limited by the temperature dependence of the permittivity. Due to frequency dependence of $\Delta\epsilon$, V_{th} varies with frequency and causes the unfavorable problems on the display quality like lowered contrast, cross talk, etc. Understanding the factors that determine the

dielectric behaviour of liquid crystals will supplement the development of new materials with better display properties. So, the dielectric permittivities of liquid crystals have extensively been studied. Moreover, subject to an ac field, two non-collective molecular mode dielectric relaxations are observed in non-chiral low-molecular mass nematic liquid crystals. One is associated with rotation of the molecules around its short axis and the other occurs when the molecule rotates around its long axis. Other than positional ordering, reorientations of entire molecules around their short and long axes are one of the features that distinguish the liquid crystalline state from crystalline phase where these reorientations as well as intramolecular reorientations are usually frozen, and vibration of atoms about their equilibrium positions still persist. Therefore, information about the nature of molecular dynamics is possible to obtain from frequency and temperature dependent dielectric spectroscopic study [30–34].

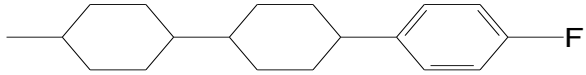
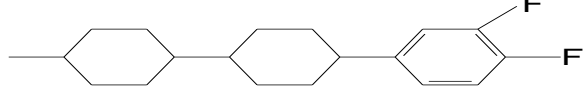
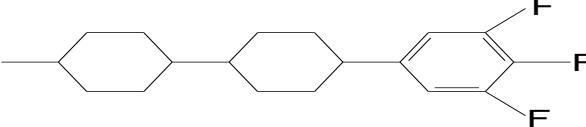
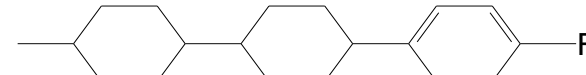
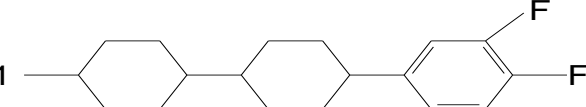
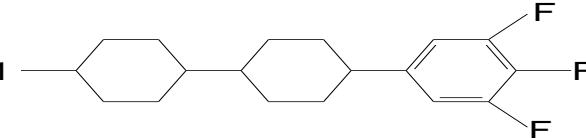
Results of crystal structure analysis of one of the compounds (5ccp-fff) have also been reported and an attempt has been made to find the effect of the molecular geometry and packing in the crystalline state on its phase behavior and different physical properties [35]. Crystal and molecular structures of related compounds 3ccp-ff and 3ccp-fff were reported from our laboratory before [36,37].

The compound 5ccp-fff is obtained by the introduction of one ethyl group to the chain of the compound 3ccp-fff and one ethyl group to the chain and one fluorine atom to the phenyl ring of 3ccp-ff. It is observed that transformation of 3ccp-fff to 5ccp-fff leads to the substantial increase of melting point and decrease of the nematogenic range [3ccp-fff: **Cr** 66.0 **N** 94.1 **I** and 5ccp-fff: **Cr** 88.0 **N** 102.4 **I**], and in case of transformation of 3ccp-ff to 5ccp-fff, change in the above thermal behaviour is more drastic [3ccp-ff: **Cr** 46.0 **N** 123.8 **I**]. In order to investigate how the molecular structure and packing of the three compounds differ in the crystalline state and their effect on observed phase behaviour, we have determined the crystal structure of 5ccp-fff. An excellent review on crystal structures of many liquid crystal compounds and their effect on mesogenic behaviour can be found in [38].

4.2 COMPOUNDS STUDIED

Molecular structures of the investigated fluorinated bicyclohexyl compounds along with their abbreviated names and transition temperatures (in °C) are given in the Table 4.1. In the

Table 4.1: Molecular structures and transition temperatures of the studied compounds

Name	Molecular structure with transition temperature
4-propyl-4'-(4-fluorophenyl) bicyclohexane (3ccp-f)	C_3H_7 —  Cr 90.0 (71.0) N 158.0 I
4-propyl-4'-(3,4-difluorophenyl) bicyclohexane (3ccp-ff)	C_3H_7 —  Cr 45.6 N 123.8 I
4-propyl-4'-(3,4,5-trifluorophenyl) bicyclohexane (3ccp-fff)	C_3H_7 —  Cr 64.7 N 93.7 I
4-pentyl-4'-(4-fluorophenyl) bicyclohexane (5ccp-f)	C_5H_{11} —  Cr 68.0 SmB 75.0 N 157.0 I
4-pentyl-4'-(3,4-difluorophenyl) bicyclohexane (5ccp-ff)	C_5H_{11} —  Cr 47.0 (26.8) N 125.2 I
4-pentyl-4'-(3,4,5-trifluorophenyl) bicyclohexane (5ccp-fff)	C_5H_{11} —  Cr 87.3 N 101.2 I

abbreviated names the number at the beginning denotes the number of carbon atoms present in the alkyl chain, 'c' and 'p' represent respectively the cyclohexyl and phenyl ring in the core, f(s) denote the number of fluorine atoms in the terminal phenyl ring. All the investigated compounds exhibit nematic phase over a considerable temperature range, although the compound 5ccp-f shows, in addition, SmB phase within small temperature range, however, no studies have been made in that phase.

Table 4.2: Phase transition temperatures ($^{\circ}\text{C}$) of 3ccp-ff, 3ccp-fff and related compounds

Compound	Phase sequence
3ccp	Cr 76 SmB 97 N 103 I
3ccp-F	Cr 88.6 N 158.5 I
3ccp-Cl	Cr 75.1 Sm 79 N 192 I
3ccp-I	Cr 119 Sm 139.2 N 189.2 I
3ccp-CN	Cr 73.1 Sm 81.1 N 238.9 I
3ccp-ff	Cr 45.6 N 123.8 I
3ccp-fff	Cr 64.7 N 93.7 I
3ccp - OCF ₃	Cr 38.0 Sm 69.0 N 154 I
5ccp - C ₃ H ₇	Cr 48.6 Sm 181 I
5cpp - C ₃ H ₇	Cr 29 Sm 160 N 170 I

It is observed from the literature [9,39,40] that unsubstituted 4-phenyl-4-propyl-bicyclohexyl (3ccp) and para-substituted 3ccp, i.e. 3ccp-Cl, 3ccp-I and 3ccp-CN or para-substituted 5ccp-C₃H₇ and 5cpp-C₃H₇ exhibit both smectic and nematic phases, whereas mono-, di- and tri-substituted 3ccp exhibit only a nematic phase (Table 4.2). However, 3ccp-ff does not show mesogeneity at all [39].

4.3 EXPERIMENTAL DETAILS

The phase behavior of the fluorinated bicyclohexyl compounds was studied using an optical polarizing microscope. Crystal and molecular structure was determined by direct methods. Static and frequency dependent dielectric properties was studied using computer controlled impedance analyzers HIOKI 3532-50 (50 Hz – 5 MHz) and HP 4192A (100 Hz –13 MHz). The elastic constants were measured by the Fréedericksz transition technique [29]. The dipole-dipole correlation factor (g_λ) was determined following Bata and Buka [41]. Details of all the procedures have been described in chapter 2.

4.3.1 Structure Determination and Refinement

Crystal structure of only 5ccp-fff was determined as mentioned in the introduction. Crystals suitable for structure determination by X-rays were obtained from a mixture of dichloromethane and methyl alcohol by slow evaporation technique at room temperature. Transparent plate-shaped crystal (approximately 0.40 x 0.25 x 0.20 mm³) was used for data collection on an CAD-4 diffractometer (Enraf-Nonius B.V., Rotterdam, The Netherlands) with graphite-monochromated CuK α radiation and ω -2 θ scan. A total of 4112 unique reflections were measured within the range $-6 \leq h \leq 6$, $0 \leq k \leq 53$, $0 \leq l \leq 11$. Of these, 2528 were above the significance level of $2.5 \sigma(I_{\text{obs}})$ and were treated as observed. The range of $(\sin \theta)/\lambda$ was 0.044–0.626 Å⁻¹ ($3.9 \leq \theta \leq 74.7^\circ$). Two reference reflections [(0 8 1), (1 2 1)] were measured hourly and showed no decrease during the 60-h collection time. Unit-cell parameters were refined by a least-squares fitting procedure using 23 reflections with $40.05 \leq \theta \leq 42.49^\circ$. Corrections for Lorentz and polarisation effects were applied. The structure was solved by the direct method program package CRUNCH [42]. Positions of the hydrogen atoms were calculated. Full-matrix least-squares refinement on F, anisotropic for the non-hydrogen atoms and isotropic for the hydrogen atoms, keeping the latter fixed at their calculated positions with an atomic displacement parameter (ADP) of $U=0.15 \text{ \AA}^2$, converged to $R=0.095$, $R_w = 0.093$, $(\Delta/\sigma)_{\text{max}}=0.01$, $S=1.0$. A weighting scheme $W = [2.5 + 0.01 \cdot \{\sigma(\text{Fobs})\}^2 + 0.001/\{\sigma(\text{Fobs})\}]^{-1}$ was used. A final difference Fourier map revealed a residual electron density between -0.38 and 0.37 e \AA^{-3} . Scattering factors were taken from Cromer and Mann and International Tables for X-ray Crystallography [43,44]. The anomalous scattering of F was taken into account [45]. All

calculations were performed with XTAL [46], unless stated otherwise. Supplementary tables and molecular picture were made with PLATON [47]. Important crystallographic data and refinement parameters are given in Table 4.3. The crystal structure has been deposited at the Cambridge Crystallographic Data Centre and allocated the deposition number CCDC 836063.

4.4 RESULTS AND DISCUSSIONS

4.4.1 Optimized Geometry Using Molecular Mechanics

To elucidate the structure of the investigated compounds, their optimized geometry was calculated using PM3 molecular mechanics method in Hyperchem software package [48]. Optimized lengths of the molecules, dipole moments and the corresponding moments of inertia values (along the three principal moments of inertia axes) are shown in the Table 4.4. It is observed that the dipole moment of the molecules increases as one move from f to ff to fff systems of a particular series, however increment is more in f to ff derivatives than in ff to fff derivatives. However no change in dipole moment is observed when the number of carbon atom in the chain increases. Such behavior has been reported before in nCHBT and nCB series [49-51], as discussed in chapter 3. Previously reported theoretical values for 3ccp-ff are 3.32D [7] and 3.2D [14]. Thus the value obtained from our calculation (3.21 D) agrees with that reported by Klasen et al. [14]. Molecular conformation in optimized geometry has been compared with that obtained from crystal structure analysis in the next section.

Table 4.3: Important Crystallographic data

Formula	C ₂₃ H ₃₃ F ₃
Formula Weight	366.49g/mol
T (K)	293(2)
Radiation, λ (CuK α)	1.54180 Å
Crystal System	monoclinic
Space group	P21/n
a	4.9860(9)Å
b	42.875(5) Å
c	9.623(3) Å
β	92.08(2)°
V	2055.8(8)Å ³
Z	4
D _{cal}	1.184g/cc
F(000)	792
Crystal Size	0.4 0x 0.25x 0.20 mm ³
Independent reflections	4112
No. of observed reflections	2528 [I>2.5 σ (I)]
Refinement method	full-matrix least-squares on F
R (Observed reflection)	0.095
R _w (Observed reflection)	0.093

Table 4.4: Optimized length, dipole moment and moment of inertia of the investigated compounds

Compound	Optimized Length (Å)	Dipole Moment (Debye)	Moment of Inertia ($\times 10^{-46}$ Kg m ²)		
			I _{xx}	I _{yy}	I _{zz}
3ccp-f	17.01	1.93	383.40	7024.29	7106.98
3ccp-ff	17.02	3.21	440.27	7298.36	7954.52
3ccp-fff	17.02	3.72	580.69	8457.54	8573.88
5ccp-f	19.38	1.93	426.42	9503.92	9568.43
5ccp-ff	19.38	3.12	519.99	10342.2	10477.9
5ccp-fff	19.46	3.77	675.42	11574.4	11678.6

4.4.2 Three-Dimensional Crystal Structure Determination

Figure 4.1 represents the molecular structure and the atom numbering schemes of non-hydrogen atoms. Final positional coordinates with equivalent isotropic thermal parameters, anisotropic thermal parameters, bond lengths and bond angles of the non-hydrogen atoms are listed in Tables 4.5 – 4.9. The average aromatic bond length and bond angle of the phenyl ring are found to be 1.368 (9) Å and 120.0 (6)⁰, consistent with corresponding values in 3ccp-ff and 3ccp-fff which are 1.377 (6) Å and 120.0 (4)⁰ and 1.368(6) Å and 120.0 (4)⁰ respectively. These values are also in agreement with the geometry of the other phenyl moieties reported in literature [52–54]. The cyclohexyl groups are in chair conformation as was observed in 3ccpff, 3ccp-fff and other mesogenic molecules [55–57]. The alkyl chain is in all-*trans* conformation with mean bond distance of 1.509(9) Å and bond angle 114.7(6)⁰ as found in other mesogenic compounds [58–60]. These values are in good agreement with the corresponding values in 3ccp-ff and 3ccp-fff 1.519(8) Å and 113.7(5)⁰, and 1.520(6) Å and 111.6 (4)⁰. Bond lengths of C1–F1, C2–F2 and C6–F3 are found to be 1.378(7)Å, 1.361(8) Å and 1.352(8) Å close to the values observed in 3ccp-ff [1.351(4) Å, 1.353(5) Å] and in 3ccp-fff [1.344(5) Å, 1.354(4) Å and 1.354(5) Å] and in other fluorophenyl compounds 1.347(3) Å in reference [61] and 1.363(4) Å in reference [62]. Thus it may be inferred that the bond lengths and angles of 5ccp-fff is similar to 3ccp-ff and 3ccp-fff and to other mesogenic molecules.

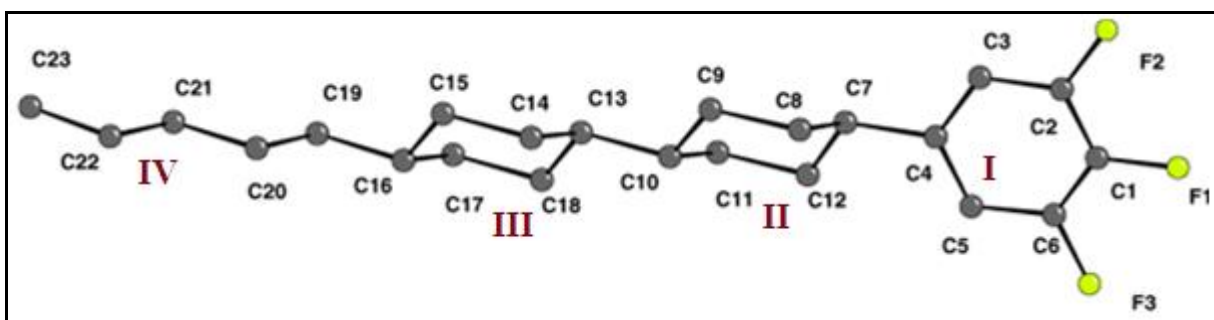


Figure 4.1: A perspective view of 5ccp-fff molecule with atom numbering scheme. Meaning of figures I-IV has been discussed in the text

Geometry of the 5ccp-fff molecule may be described in terms of four planes of the phenyl ring (**I**), the two cyclohexyl rings (**II** and **III**) and the plane of the alkyl chain (**IV**), as shown in Figure 4.1. The phenyl ring is highly planar and the three fluorine atoms are almost in the same

plane. Almost similar phenyl ring geometry was observed in 3ccp-ff and 3ccp-fff. The dihedral angles between the planes (**I** and **II**), (**I** and **III**), (**I** and **IV**), (**II** and **III**), (**II** and **IV**) and (**III** and **IV**) are 47.2° , 68.7° , 91.7° , 22.5° , 44.7° and 23.0° respectively. The corresponding angles are 83.2° , 83.4° , 51.3° , 0.8° , 35.9° and 36.4° in 3ccp-fff and, 122.1° , 123.5° , 8.8° , 3.4° , 127.8° and 128.7° in 3ccp-ff respectively. Thus, in 3ccp-fff and 3ccp-ff, the dihedral angles between the two cyclohexyl groups were found to be 0.8° and 3.4° respectively compared to 22.5° in this case. The phenyl ring and the pentyl chain are at right angle (dihedral angle 91.7°) in 5ccp-fff whereas they were at an angle 51.3° in 3ccp-fff and 8.8° in 3ccp-ff respectively. Dihedral angles between the phenyl and nearby cyclohexyl ring is found to be 47.2° in 5ccp-fff, where the values were 83.2° in 3ccp-fff and 122.1° in 3ccp-ff respectively. Thus it is observed that molecular conformation of 5ccp-fff is quite different from those of 3ccp-fff and 3ccp-ff systems, although their bond lengths and angles are quite similar.

Table 4.5: Fractional co-ordinates and equivalent isotropic thermal parameters of the non-Hydrogen atoms with e.s.d's in parentheses of 5ccp-fff

Atom	X	Y	Z	U_{eq} (\AA^2)
F1	-0.0988(8)	0.44143(8)	0.3107(5)	0.0917(16)
F2	0.3085(9)	0.47200(10)	0.4424(5)	0.108(2)
F3	-0.4128(9)	0.47212(9)	0.1217(5)	0.0979(19)
C1	-0.0554(13)	0.47246(13)	0.2820(7)	0.058(2)
C2	0.1475(13)	0.48755(15)	0.3485(7)	0.066(2)
C3	0.1955(13)	0.51910(14)	0.3225(7)	0.068(3)
C4	0.0358(12)	0.53428(13)	0.2252(6)	0.0530(19)
C5	-0.1678(13)	0.51900(14)	0.1557(7)	0.062(2)
C6	-0.2083(13)	0.48733(14)	0.1883(7)	0.061(2)
C7	0.0938(12)	0.56910(13)	0.1967(7)	0.061(2)
C8	-0.0011(16)	0.58942(14)	0.3135(7)	0.078(3)
C9	0.0758(17)	0.62408(15)	0.2917(7)	0.080(3)
C10	-0.0190(12)	0.63688(13)	0.1530(6)	0.056(2)
C11	0.0647(16)	0.61570(15)	0.0364(7)	0.080(3)
C12	-0.0191(16)	0.58102(14)	0.0611(7)	0.078(3)
C13	0.0721(12)	0.67115(13)	0.1291(6)	0.054(2)
C14	-0.0137(15)	0.69319(14)	0.2438(7)	0.073(2)
C15	0.0760(14)	0.72708(13)	0.2182(7)	0.069(2)
C16	-0.0153(12)	0.73956(13)	0.0790(6)	0.057(2)
C17	0.0718(15)	0.71773(14)	-0.0341(7)	0.071(2)
C18	-0.0219(14)	0.68352(14)	-0.0109(7)	0.067(3)
C19	0.0869(13)	0.77282(13)	0.0511(7)	0.063(2)
C20	-0.0196(13)	0.79844(15)	0.1410(7)	0.071(3)
C21	0.0856(14)	0.83021(14)	0.1047(8)	0.072(3)
C22	-0.0195(15)	0.85694(16)	0.1927(9)	0.087(3)
C23	0.0952(19)	0.88741(17)	0.1604(11)	0.114(4)

Table 4.6: Anisotropic thermal parameters of the non-Hydrogen atoms with the e.s.d's in parentheses

The temperature factor is of the form

$$\exp [2\pi^2 (U_{11}h^2a^{*2}+U_{22}k^2b^{*2}+U_{33}l^2c^{*2}+2U_{12}hka^*b^*+2U_{13}hla^*c^*+2U_{23}klb^*c^*)]$$

Atom	U ₁₁	U ₂₂	U ₃₃	U ₂₃	U ₁₃	U ₁₂
F1	0.101(3)	0.051(2)	0.123(3)	0.015(2)	0.003(3)	-0.002(2)
F2	0.118(4)	0.070(3)	0.133(4)	0.026(3)	-0.043(3)	0.003(3)
F3	0.098(3)	0.064(3)	0.129(4)	-0.010(2)	-0.033(3)	-0.012(2)
C1	0.063(4)	0.040(3)	0.072(4)	-0.002(3)	0.003(3)	-0.001(3)
C2	0.066(4)	0.057(4)	0.075(4)	0.011(3)	-0.014(4)	0.010(3)
C3	0.072(4)	0.050(4)	0.080(5)	0.004(3)	-0.003(4)	-0.001(3)
C4	0.052(3)	0.047(3)	0.060(4)	0.001(3)	0.001(3)	0.008(3)
C5	0.065(4)	0.051(4)	0.070(4)	-0.003(3)	-0.006(3)	0.007(3)
C6	0.062(4)	0.049(3)	0.071(4)	-0.010(3)	-0.011(3)	0.001(3)
C7	0.059(4)	0.051(3)	0.072(4)	-0.002(3)	0.007(3)	0.004(3)
C8	0.122(6)	0.048(4)	0.063(4)	0.003(3)	0.006(4)	-0.006(4)
C9	0.124(6)	0.052(4)	0.064(4)	0.001(3)	-0.001(4)	-0.009(4)
C10	0.062(4)	0.045(3)	0.061(4)	0.001(3)	0.007(3)	0.005(3)
C11	0.122(6)	0.049(4)	0.071(5)	-0.003(3)	0.021(4)	0.008(4)
C12	0.127(6)	0.045(4)	0.063(4)	-0.004(3)	-0.001(4)	0.010(4)
C13	0.062(4)	0.044(3)	0.056(4)	-0.002(3)	0.007(3)	0.001(3)
C14	0.103(5)	0.049(3)	0.068(4)	-0.004(3)	0.020(4)	-0.003(4)
C15	0.096(5)	0.042(3)	0.069(4)	-0.004(3)	0.014(4)	-0.003(3)
C16	0.061(4)	0.049(3)	0.062(4)	0.003(3)	0.012(3)	0.002(3)
C17	0.100(5)	0.048(3)	0.065(4)	0.004(3)	0.013(4)	0.005(3)
C18	0.090(5)	0.049(4)	0.062(4)	0.002(3)	0.004(4)	0.002(3)
C19	0.075(4)	0.038(3)	0.078(4)	0.000(3)	0.016(4)	-0.001(3)
C20	0.069(4)	0.059(4)	0.086(5)	-0.005(3)	0.022(4)	-0.003(3)
C21	0.082(5)	0.041(3)	0.095(5)	0.001(3)	0.016(4)	-0.002(3)
C22	0.087(5)	0.055(4)	0.119(6)	-0.002(4)	0.024(5)	0.003(4)
C23	0.125(7)	0.049(4)	0.168(9)	-0.007(5)	0.012(7)	0.002(5)

**Table 4.7: Bond lengths (Å) of the non-Hydrogen atoms
with standard deviations in parentheses**

Atom	Atom	Bond Length	Atom	Atom	Bond Length
F1	C1	1.378(7)	C10	C11	1.514(9)
F2	C2	1.361(8)	C10	C13	1.558(8)
F3	C6	1.352(8)	C11	C12	1.565(9)
C1	C2	1.343(9)	C13	C14	1.526(9)
C1	C6	1.323(9)	C13	C18	1.507(9)
C2	C3	1.398(9)	C14	C15	1.543(8)
C3	C4	1.371(9)	C15	C16	1.498(9)
C4	C5	1.363(9)	C16	C17	1.511(9)
C4	C7	1.547(8)	C16	C19	1.541(8)
C5	C6	1.410(9)	C17	C18	1.558(9)
C7	C8	1.512(9)	C19	C20	1.507(9)
C7	C12	1.493(9)	C20	C21	1.505(9)
C8	C9	1.551(9)	C21	C22	1.529(10)
C9	C10	1.503(9)	C22	C23	1.464(11)

**Table 4.8: Bond angles (°) involving non-Hydrogen atoms
with standard deviations in parentheses**

Atom	Atom	Atom	Angle	Atom	Atom	Atom	Angle
F1	C1	C2	119.4(6)	C9	C10	C11	117.7(5)
F1	C1	C6	120.7(6)	C9	C10	C13	113.1(5)
C2	C1	C6	119.9(6)	C11	C10	C13	111.5(5)
F2	C2	C1	119.7(6)	C10	C11	C12	112.0(5)
F2	C2	C3	119.5(6)	C7	C12	C11	111.3(5)
C1	C2	C3	120.8(6)	C10	C13	C14	112.7(5)
C2	C3	C4	118.9(6)	C10	C13	C18	112.4(5)
C3	C4	C5	120.7(5)	C14	C13	C18	110.0(5)
C3	C4	C7	118.1(5)	C13	C14	C15	112.2(5)
C5	C4	C7	121.2(5)	C14	C15	C16	113.5(5)
C4	C5	C6	117.6(6)	C15	C16	C17	109.7(5)
F3	C6	C1	119.8(5)	C15	C16	C19	113.2(5)
F3	C6	C5	118.1(6)	C17	C16	C19	110.0(5)
C1	C6	C5	122.2(6)	C16	C17	C18	112.6(5)
C4	C7	C8	111.0(5)	C13	C18	C17	112.0(5)
C4	C7	C12	114.7(5)	C16	C19	C20	116.7(5)
C8	C7	C12	109.5(5)	C19	C20	C21	113.2(6)
C7	C8	C9	111.5(6)	C20	C21	C22	114.9(6)
C8	C9	C10	113.5(6)	C21	C22	C23	114.0(7)

Length of the 5ccp-fff molecule in the crystalline state is found to be 19.85 Å [F1-H233], whereas the model length in the most extended conformation is 20.14 Å. Thus, the molecules are almost in the most extended conformation as was observed in 3ccp-fff and 3ccp-ff.

Packing of the molecules in the unit cell is shown in Figure 4.2, which shows that the molecules run almost parallel to each other but not parallel to any crystallographic axis as was seen in 3ccp-fff and 3ccp-ff systems. To describe the nature of packing, the direction cosines of the molecular long axis, defined as the best fitted line through all the non-H atoms, have been calculated and are found to be 0.4197, 0.8928 and 0.1637. In other words, the molecules are inclined to the orthogonal X, Y and Z axes at angles 65.2° , 26.8° and 80.6° respectively. The corresponding angles are 67.5° , 121.5° and 40.4° in case of 3ccp-fff and 75.95° , 99.0° and 16.8° in 3ccp-ff.

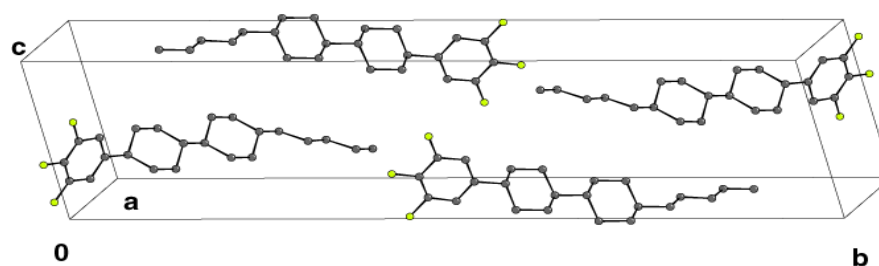


Figure 4.2: Partial packing of 5ccp-fff molecule in the crystallographic unit cell

Projections of the crystal structure along the crystallographic axes **a** and **c** are shown in Figure 4.3 and Figure 4.4, respectively. It is evident that the molecules are packed with various degrees of overlapping with the neighbouring ones. Orientation of the molecules in adjacent layers is opposite to each other. Overlaps of the molecules in the neighbouring layers are in the phenyl-phenyl groups in one side and in the cyclohexyl-alkyl chain part on the other side. Similar type of overlapping has been found for the compounds 3ccp-fff and 3ccp-ff. This type of imbricated mode of packing is usually observed in crystalline phase as a precursor to nematic phase [15,58].

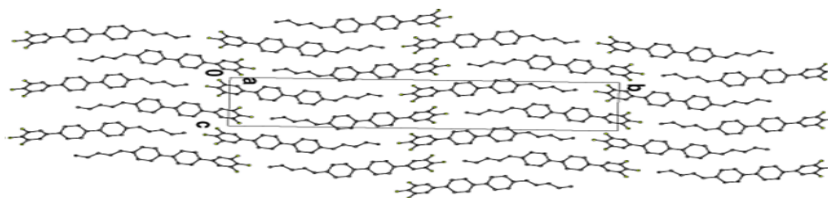


Figure 4.3: Crystal structure of 5ccp-fff projected along *a*-axis.

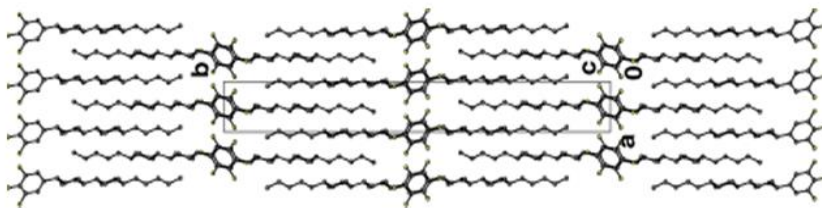


Figure 4.4: Crystal structure of 5ccp-fff projected along c -axis.

Intermolecular distances between the neighbouring molecules were calculated and several van der Waals interactions were observed. Selected intermolecular distances, less than 4.0 \AA , are shown in Table 4.9.

Table 4.9: Selected intermolecular short contact distances less than 4.0 \AA of 5ccp-fff

Atom	Atom	Distance	Atom	Atom	Distance
F1	F2(a)	3.511	F3	C6(b)	3.884
F3	F2(a)	3.429	F3	C12(b)	3.993
F3	C1(a)	3.606	C5	F3(b)	3.352
F3	C2(a)	3.218	C6	F3(b)	3.884
F3	C3(a)	3.446	C12	F3(b)	3.993
F3	C4(a)	3.981	F1	C23(c)	3.549
C1	F2(a)	3.577	F2	C23(c)	3.821
C5	C3(a)	3.609	C8	C23(d)	3.997
C6	F2(a)	3.555	C14	C19(d)	3.818
C6	C2(a)	3.613	C15	C19(d)	3.992
F3	F3(b)	3.436	C20	C17(d)	3.764
F3	C5(b)	3.352			

Subscripted atoms are at (a) $x-1, y, z$ (b) $-x-1, -y+1, -z$

(c) $-x-1/2, -y-1/2, -z+1/2$ (d) $-x-1/2, -y+3/2, z+1/2$

Four different types of molecular overlaps are observed between neighbouring molecules as shown in Figure 4.5: (i) pair of parallel molecules in head-to-head configuration overlaps completely (related by symmetry operation 'a' having pair length 20.31 Å), (ii) pair of antiparallel molecules in head-to-tail configuration overlaps partially (related by symmetry operation 'b' having associated length 35.23 Å), (iii) pair of parallel molecules in head-to-head configuration with no overlap (related by symmetry operation 'c' having associated length 41.36 Å and (iv) pair of antiparallel molecules in head-to-tail configuration overlaps partially in the alkyl cyclohexyl group (related by symmetry operation 'd' having associated length 27.03 Å).

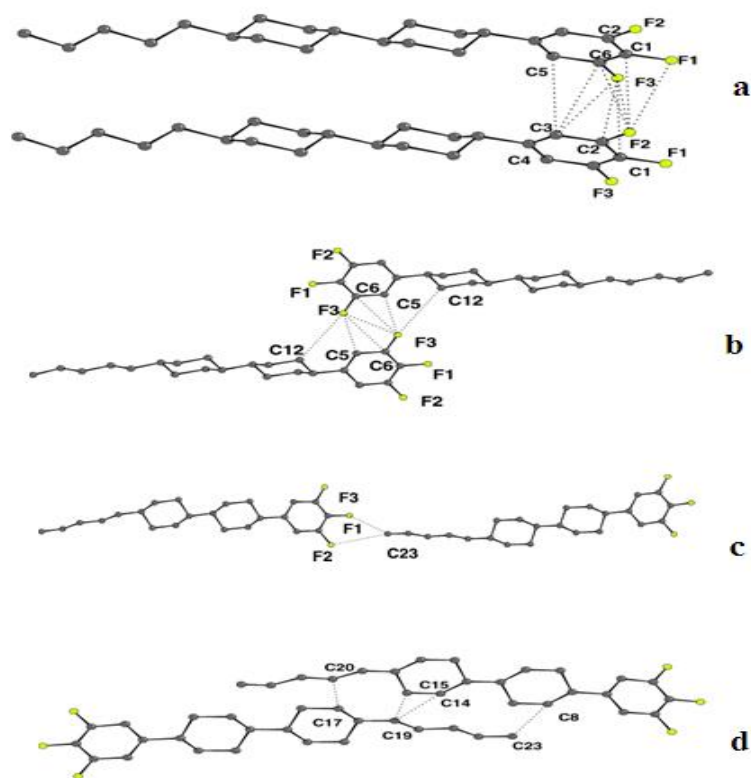


Figure 4.5: Different types of molecular associations observed in the crystal structure of 5ccp-fff. Values of the relevant inter atomic distances and meaning of the symmetry relations (a), (b), (c) and (d) are given in Table 4.9

As noted before, a preliminary molecular modelling calculation was made using the semi-empirical PM3 method and almost similar molecular conformation with molecular length of 19.46 Å was obtained when the geometry of the molecule was optimised assuming it as if in

vacuo. A single point energy calculation on an isolated molecule, as extracted from the crystal data, yields a dipole moment (μ) of 3.77 D with direction cosines 0.26, 0.95 and -0.17 . Optimised geometry also results in same dipole moment with same direction cosines. But in case of 3ccp-ff and 3ccp-fff, the values are not same. In 3ccp-ff, single point energy calculation on crystal data and optimised geometry revealed slightly different dipole moments (3.54 D and 3.21 D) and in 3ccp-fff the values are 3.61 D and 3.72 D, respectively. Moreover, dipole moments, estimated from optimised geometry, are inclined at angles 18° , 17° and 43° with the molecular long axes in 5ccp-fff, 3ccp-fff and 3ccp-ff, respectively. Thus, conformation of 5ccp-fff in vacuo and in crystalline state appears to be same whereas they differ in two states in both 3ccp-ff and 3ccp-fff.

Calculated density in the crystalline state of 5ccp-fff is found to be slightly less (1.184 g/cc) than in 3ccp-fff (1.19 g/cc). Measured density in the nematic state was also less in 5ccp-fff (0.98 g/cc) than in 3ccpfff (1.08 g/cc) (near **Cr-N** transition point) [24]. Thus, 5ccp-fff molecules are more efficiently packed in both crystalline and nematic phases compared to 3ccp-fff. This explains that 5ccp-fff has higher melting point than that of 3ccp-fff. From small-angle X-ray diffraction study on magnetically aligned samples, average intermolecular distance (D) and apparent molecular length (l) were also measured in our laboratory [63]. Observed D values were found to be slightly more in 5ccp-fff (5.64 Å) than in 3ccp-fff (5.55 Å) and 3ccp-ff (5.35 Å) near **Cr-N** transition temperature. Apparent lengths of the molecules were found to be 27.1 Å, 24.9 Å and 22.8 Å, respectively, in 5ccp-fff, 3ccp-fff and 3ccp-ff systems. It is observed that in each case the apparent molecular length (l) is more than the model length obtained from most extended conformation. Thus, there exist some sort of bimolecular associations in all three molecular systems. This type of molecular association was observed in the isothiocyanato systems described in chapter 3 and was also reported in nematogenic 5CB and 7CB [64] and later found in other systems [60,65].

4.4.3 Static Dielectric Study

Principal dielectric constants (ϵ_{\parallel} and ϵ_{\perp}) of all the six compounds were measured at 10 kHz in planar (HG) cell. In order to determine switching voltage required to switch molecular alignment from planar (HG) to homeotropic (HT) configuration, dielectric permittivity was

measured as a function of DC bias voltage across the cell and results are shown in the Figure 4.6 – 4.11. Values of threshold voltage (V_{th}), driving voltage (V_d) and driving field for the six compounds are listed in Table 4.10.

Table 4.10: Threshold voltage, driving voltage and driving field of the compounds

Compounds	Threshold Voltage (V_{th}) (Volt)	Driving Voltage (V_d) (Volt)	Driving Field ($V\mu m^{-1}$)
3ccp-f	2.57	9.07	1.71
3ccp-ff	1.61	8.08	1.52
3ccp-fff	1.02	6.12	1.20
5ccp-f	2.73	10.0	1.96
5ccp-ff	2.27	8.48	2.22
5ccp-fff	1.1	5.0	1.05

It is clear from the above table that, as number of fluorine increases threshold voltage as well as driving voltage decrease considerably in both the series (3ccp series & 5ccp series) while with increasing chain length V_{th} and V_d increases slightly except in triply fluorinated compound. In other words, increase of chain length by two carbon atoms has less effect on switching property compared to increased lateral fluorination. Similar behavior was also observed in isothiocyanato compounds as described in chapter 3. It is further observed, comparing data in Tables 3.3 and 4.10, that threshold voltage in these compounds are considerably less than that observed in the laterally fluoro-substituted terphenyl-based isothiocyanato compounds (2TP-3'F-4NCS, 2TP-3',3F-4NCS and 4TP-3',3F-4NCS). This is may be due to the replacement of two phenyl groups by more flexible cyclohexyl groups and the bulky isothiocyanato group by small fluoro group. However, driving field for all the compounds is suitable for thin ($< 2\mu m$) TFT based LC display

cells. Nevertheless, $5\text{V}\mu\text{m}^{-1}$ field was used for switching from HG to HT configuration while measuring ϵ_{\parallel} and ϵ_{\perp} .

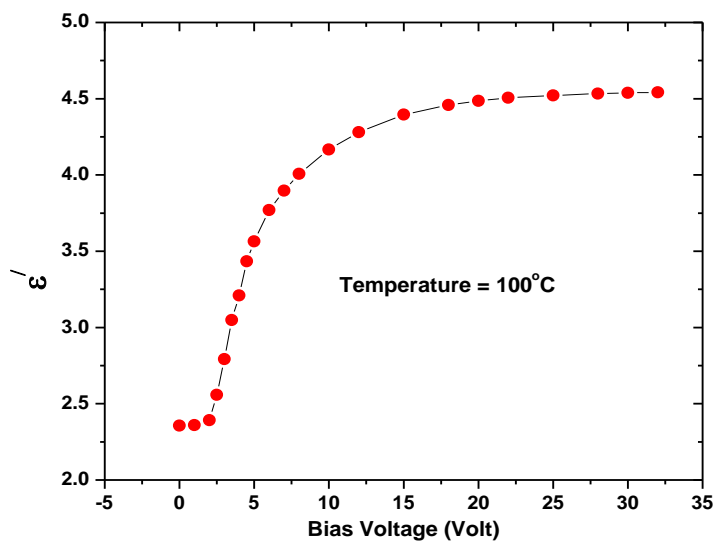


Figure 4.6: Real part of dielectric constant (ϵ') as a function of bias voltage at 10 kHz in 3ccp-f

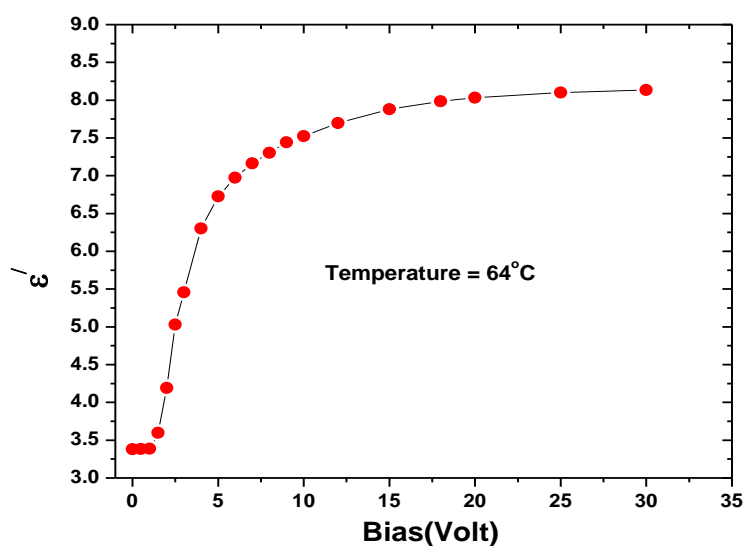


Figure 4.7: Real part of dielectric constant (ϵ') as a function of bias voltage at 10 kHz in 3ccp-ff

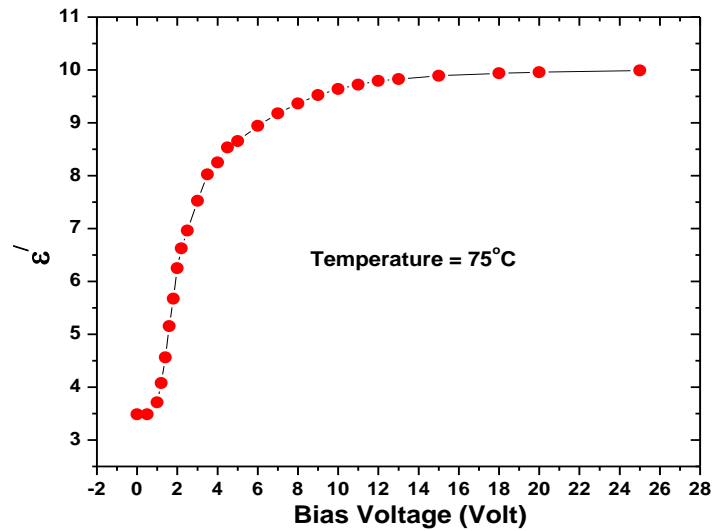


Figure 4.8: Real part of dielectric constant (ϵ') as a function of bias voltage at 10 kHz in 3ccp-fff

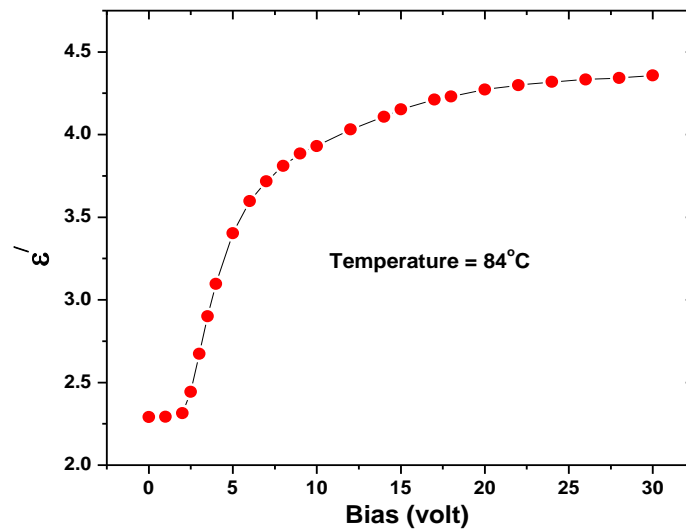


Figure 4.9: Real part of dielectric constant (ϵ') as a function of bias voltage at 10 kHz in 5ccp-f

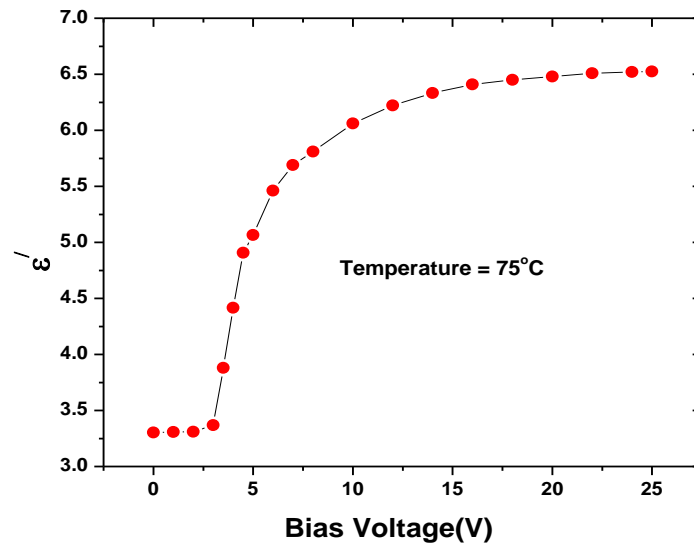


Figure 4.10: Real part of dielectric constant (ϵ') as a function of bias voltage at 10 kHz in 5ccp-ff

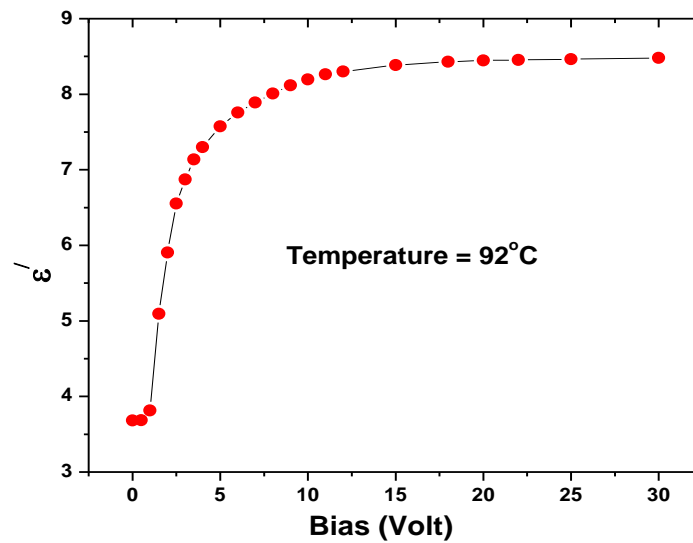


Figure 4.11: Real part of dielectric constant (ϵ') as a function of bias voltage at 10 kHz in 5ccp-fff

Dielectric constants parallel (ϵ_{\parallel}) and perpendicular (ϵ_{\perp}) to molecular axis, their average value ϵ_{av} , in nematic phase and value in isotropic phase (ϵ_{iso}) have been determined as a function of temperature. Variations of principal dielectric constants with temperature are shown in Figures 4.12 – 4.17. Since the molecules possess quite strong axial dipole moment, value of dielectric constants parallel to molecular axis is found to be large compared to component perpendicular to the molecular axis. It is not clear why in 5ccp-f and 5ccp-ff systems ϵ_{\parallel} approaches quite fast to ϵ_{\perp} far away from T_{NI} . Average value of the dielectric constant is found to be slightly less than the extrapolated values of ϵ_{iso} in all cases [labeled as $(\epsilon_{iso})_{ext}$ in the figures]. Similar difference has been observed in systems having strong axial moments [66-68]. In contrary, nonpolar molecules like di-alkyl azobenzenes do not show such discontinuity [32]. This has been explained assuming the presence of short-range antiparallel order in the nematic state [36,69].

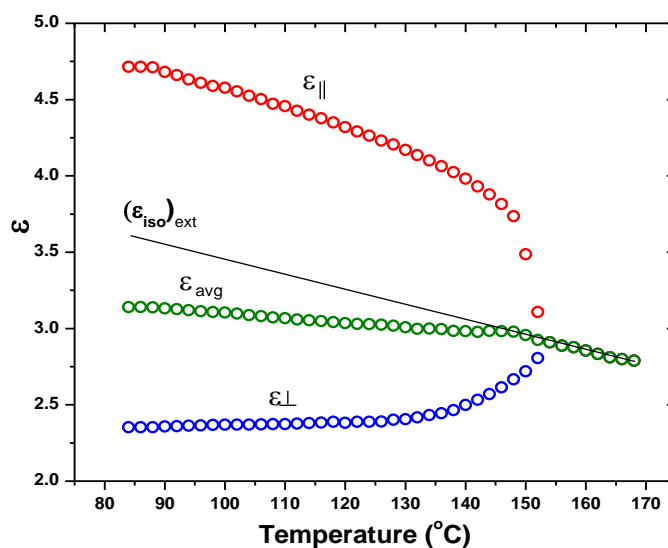


Figure 4.12: Temperature dependence of dielectric permittivity of compound 3ccp-f

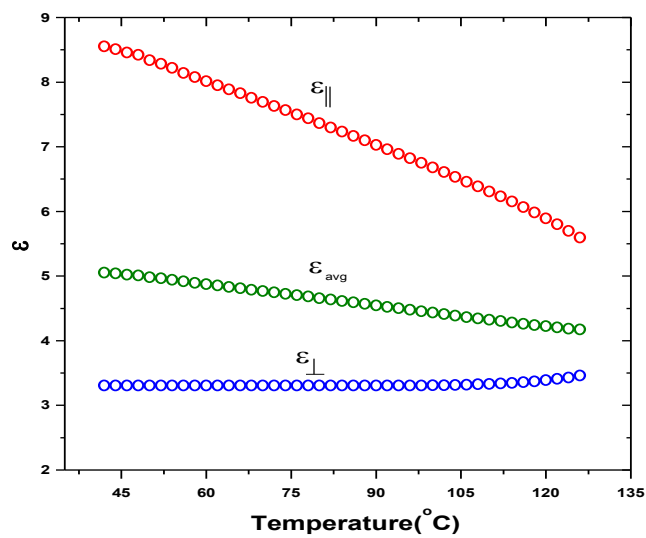


Figure 4.13: Temperature dependence of dielectric permittivity of compound 3ccp-ff

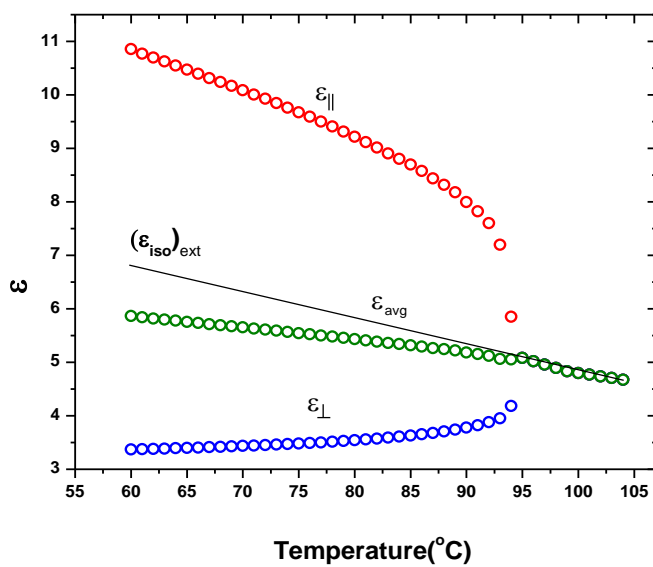


Figure 4.14: Temperature dependence of dielectric permittivity of compound 3ccp-fff

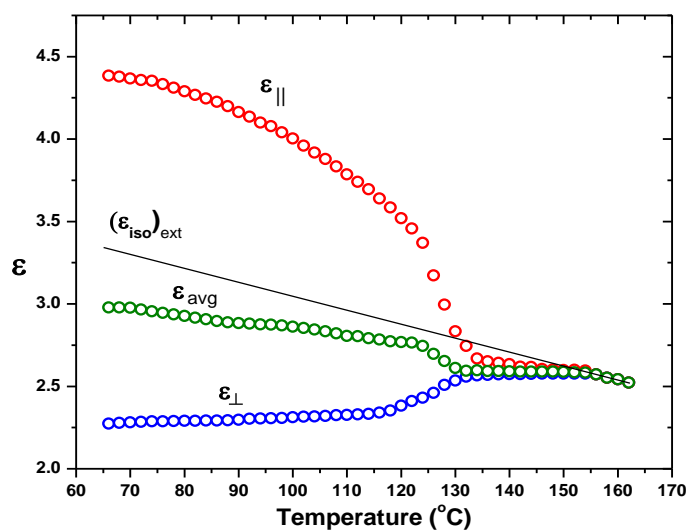


Figure 4.15: Temperature dependence of dielectric permittivity of compound 5ccp-f

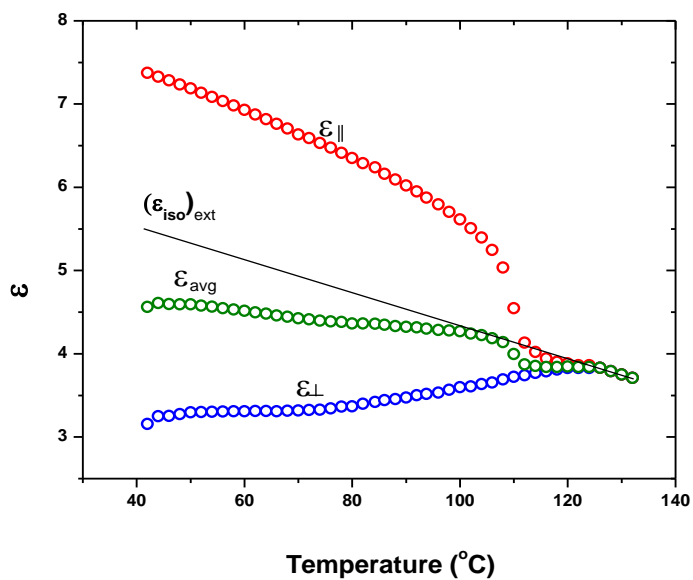


Figure 4.16: Temperature dependence of dielectric permittivity of compound 5ccp-ff

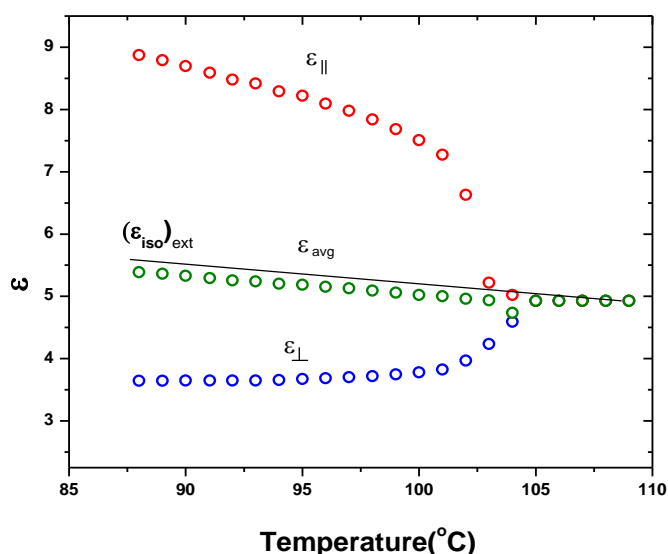


Figure 4.17: Temperature dependence of dielectric permittivity of compound 5ccp-fff

Temperature dependence of dielectric anisotropy ($\Delta\epsilon = \epsilon_{||} - \epsilon_{\perp}$) for all the compounds is shown in Figure 4.18. It is found to be positive in all and also decreases with temperature. The highest $\Delta\epsilon$ values near crystal to nematic transition are found to be 2.36, 5.25, 7.48 in 3ccp-f, 3ccp-ff and 3ccp-fff respectively and that in 5ccp series are 2.12, 4.22 and 6.46 respectively. It is clear that increased fluoro substitution causes increased dielectric anisotropy as observed in terphenyl compounds in chapter 3. However, unlike in terphenyl compounds, increased chain length causes slightly decreased $\Delta\epsilon$ in these compounds. Moreover, $\Delta\epsilon$ in this case is very less than that observed in terphenyl-based isothiocyanato nematic compounds, described in chapter 3. This is expected since dipole moment of fluorobenzene is 1.50 D while that of isothiocyanato group is 3.7 D.

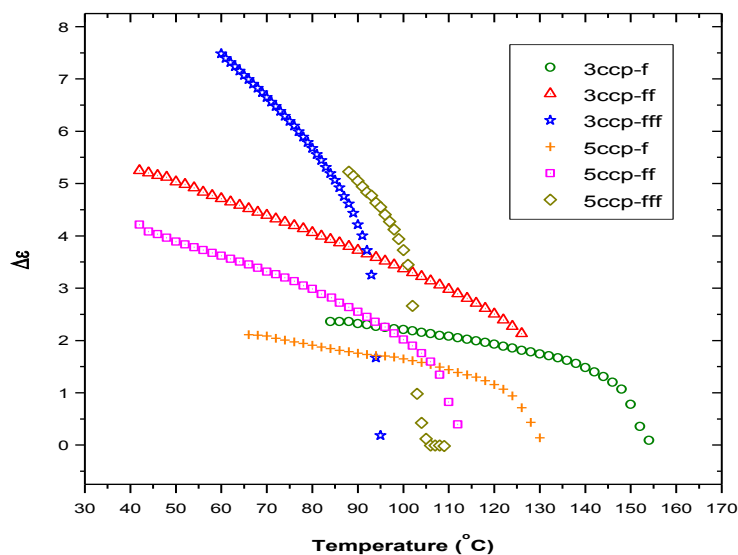


Figure 4.18: Temperature dependence of dielectric anisotropy ($\Delta\epsilon$) of the compounds

The splay elastic constant (K_{11}), is found to exhibit similar decreasing trend with temperature as observed in dielectric anisotropy and is shown in Figure 4.19. It is noted that K_{11} near melting point for the compounds 3ccp-f and 5ccp-f are 13.9×10^{-12} N, 14.1×10^{-12} N; for 3ccp-ff and 5ccp-ff are 0.122×10^{-10} N, 11.2×10^{-12} N and for 3ccp-fff and 5ccp-fff are 6.9×10^{-12} N, 5.6×10^{-12} N. Thus with increased fluorination K_{11} decreases, becomes almost half in case of single to triple fluoro substitution, but with chain length very small unsystematic change is observed. Thus fluorination and chain length dependence of K_{11} is different from terphenyl based compounds as discussed in chapter 3. K_{11} of the present compounds are also much less than that observed in terphenyl-based isothiocyanato nematic compounds. This is probably due to the replacement of two phenyl groups by more flexible cyclohexyl groups and the bulky isothiocyanato group by small fluoro group. Since switching time is inversely proportional to K_{11} , faster response is expected in triply fluorinated compounds than the singly and doubly fluorinated compounds.

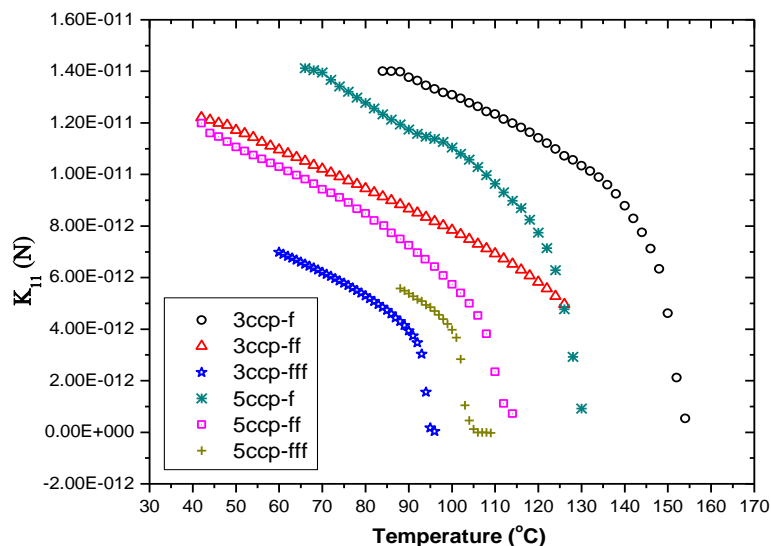


Figure 4.19: Temperature variation of splay elastic constant (K_{11}) of the compounds

Effective value of the dipole moment in nematic phase for all the six compounds were calculated following Bordewijk theory [70] of anisotropic dielectrics as detailed in chapter 2 and found to be 1.82D, 2.96D, 3.50D, 1.83D, 2.95D and 3.56D for 3ccp-f, 3ccp-ff, 3ccp-fff, 5ccp-f, 5ccp-ff and 5ccp-fff respectively whereas free molecule dipole moments were 1.93D, 3.21D, 3.72D, 1.93D, 3.12D and 3.77D respectively (Table 4.4 and 4.11). Smaller values of dipole moments within nematic phase suggest anti-parallel association of molecules. From X-ray diffraction study [24,25], it has observed that the apparent length of the molecules in nematic phase was more than the single molecular length which also suggests the presence of molecular associations. To obtain a quantitative measure of this anti-parallel correlation, dipole-dipole correlation factor g_λ has also been calculated. It is noted that $g_\lambda = 1$ signifies no correlation at all (monomeric system), $g_\lambda = 0$ means perfect antiparallel correlation and $g_\lambda = 2$ means perfect parallel correlation. The ensemble averages of the \parallel and \perp components of the dipole-dipole correlation factor are listed in Table 4.11.

Table 4.11: Effective values of dipole moments and dipole correlation factors

Compounds	g_{\parallel} (near melting point)	g_{\perp} (near melting point)	μ_{eff} (D)
3ccp-f	0.575	1.024	1.82
3ccp-ff	0.386	0.923	2.96
3ccp-fff	0.523	0.891	3.50
5ccp-f	0.479 *	0.976 *	1.83
5ccp-ff	0.488	1.028	2.95
5ccp-fff	0.473	1.119	3.56

*near SmB – N transition

Observed values of parallel correlation factor g_{\parallel} signify weak anti-parallel correlation of the components of dipole moments along the molecular axes in nematic phase for all the compounds. Corresponding values of g_{\perp} suggests almost no anti-parallel correlation of the perpendicular components of the dipole moments. It is further observed that, anti-parallel correlation along the molecular axis slightly improves in mono and tri fluorinated derivatives of pentyl compounds compared to propyl compounds, however in bi fluorinated derivative more correlation is observed in propyl compound.

4.4.4 Dielectric Relaxation Study

To see the dynamic response of the compounds to ac field, frequency dependent dielectric study was performed as a function of temperature. The frequency dependences of real and imaginary parts of dielectric permittivities of the six compounds are shown in Figures 4.20 – 4.25. It is clear from the figures that the real part of dielectric permittivity remains almost constant in the low temperature region (upto ~100 kHz) and decreases sharply at higher frequencies and it decreases with temperature for all the compounds. Only one strong absorption process is observed in the absorption spectra; for clarity spectra only at some selected

temperatures are presented. In each case relaxation frequencies are found to increase with temperature. Assuming the relaxation behavior is a result of Cole–Cole type process, the complex dielectric permittivity was fitted with the modified Cole-Cole equation [33] to get the actual values of relaxation frequency (f_c) and symmetric distribution parameter (α) as detailed in chapter 2. As real and imaginary parts of dielectric constants are related through Kramers-Kronig relations, the Cole-Cole plot of the fitted spectra only at one temperature for all the six compounds are presented in Figures 4.26 – 4.31, which shows that the fitting was quite good. Nature of the absorption process is found to be almost Debye type since in no case fitted α is more than 0.05.

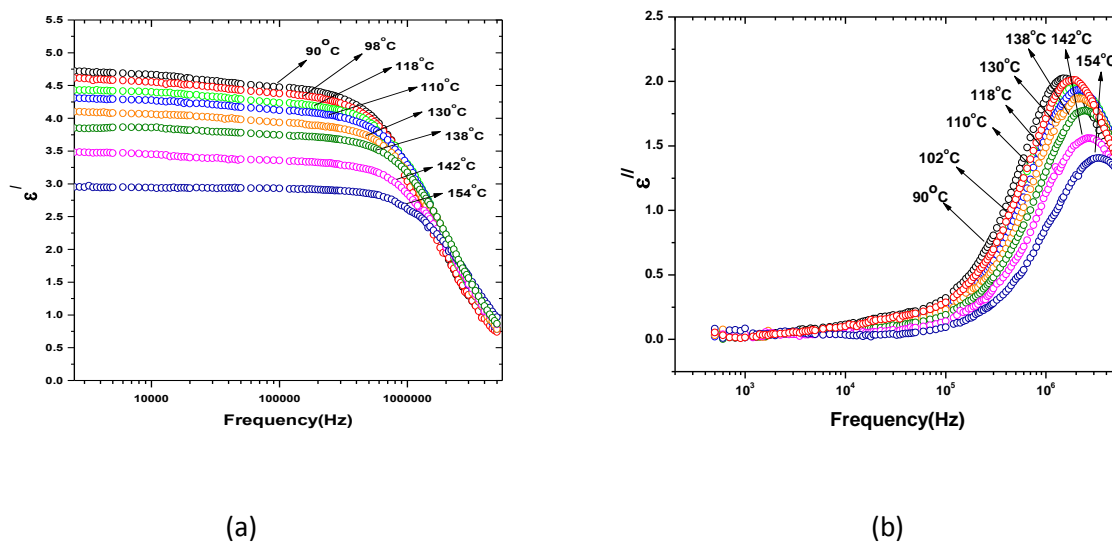
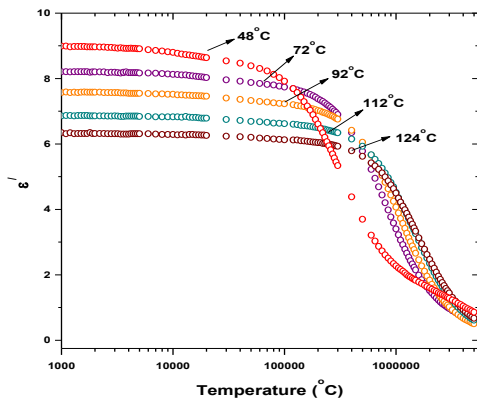
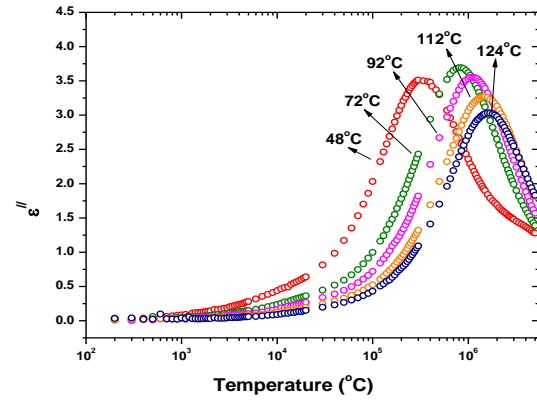


Figure 4.20: Temperature variation of (a) real and (b) imaginary part of dielectric permittivity of 3ccp-f

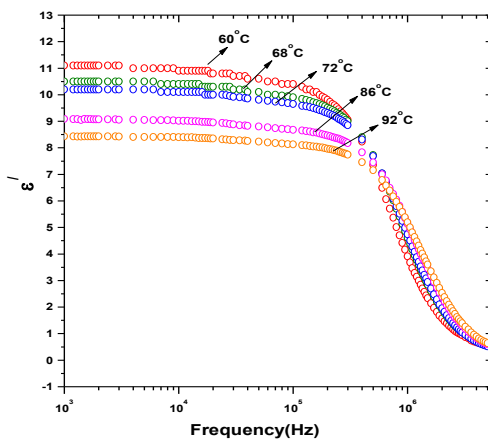


(a)

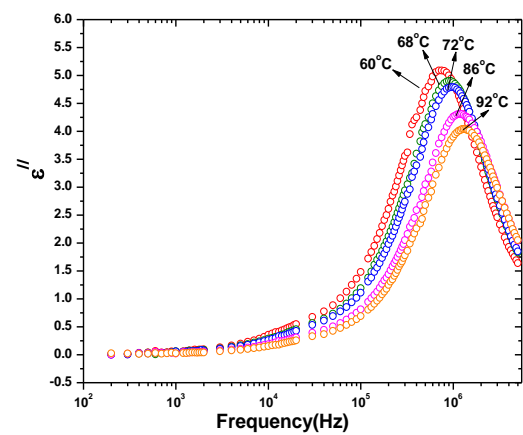


(b)

Figure 4.21: Temperature variation of (a) real and (b) imaginary part of dielectric permittivity of 3ccp-ff

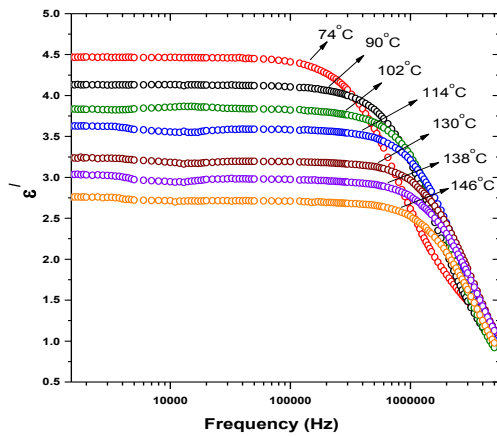


(a)

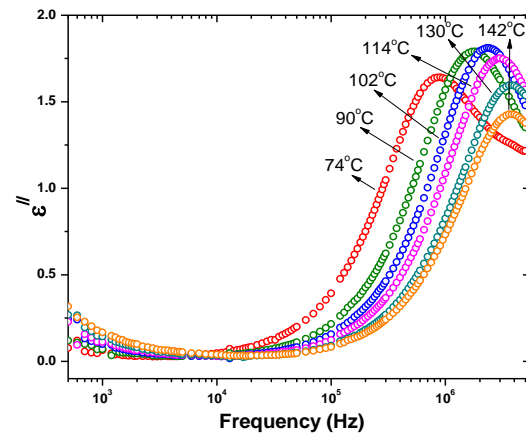


(b)

Figure 4.22: Temperature variation of (a) real and (b) imaginary part of dielectric permittivity of 3ccp-fff

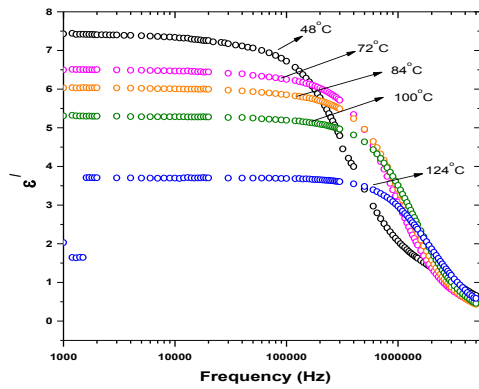


(a)

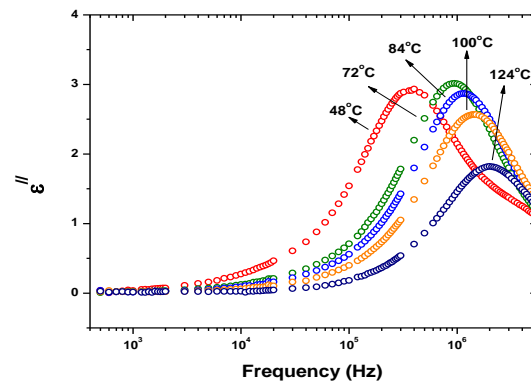


(b)

Figure 4.23: Temperature variation of (a) real and (b) imaginary part of dielectric permittivity of 5ccp-f



(a)



(b)

Figure 4.24: Temperature variation of (a) real and (b) imaginary part of dielectric permittivity of 5ccp-ff

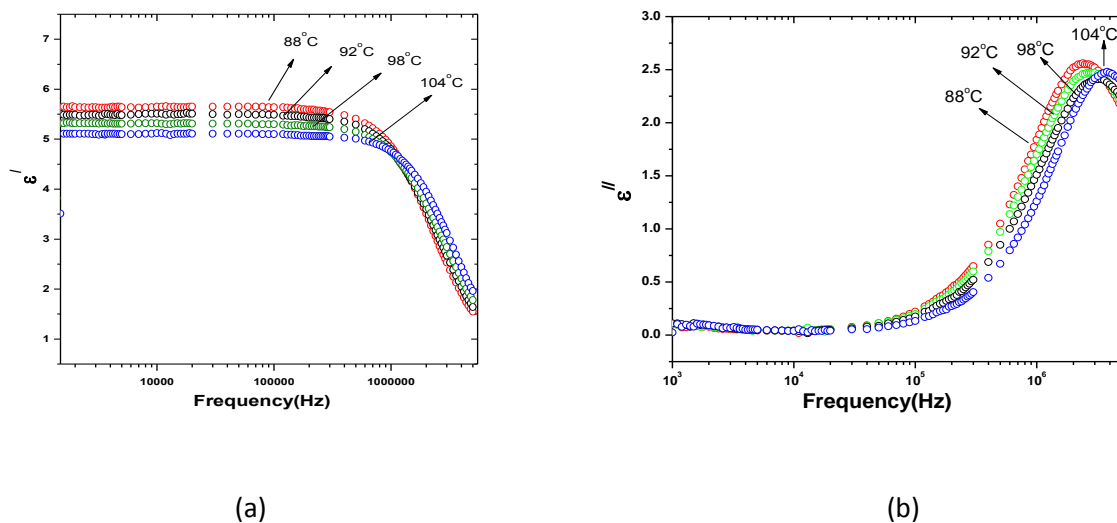


Figure 4.25: Temperature variation of (a) real and (b) imaginary part of dielectric permittivity of 5ccp-fff

Since reorientation around the long axis is usually found in GHz, observed relaxation frequencies are assumed to be associated with rotation around short molecular axis (flip-flop mode) and found to increase systematically with temperature. Observed range of relaxation frequencies of all the compounds are listed in Table 4.12.

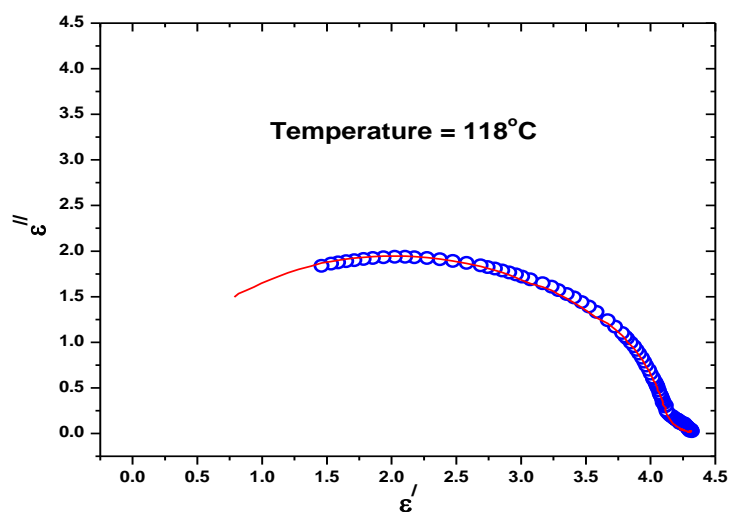


Figure 4.26: Cole-cole plot of 3ccp-f

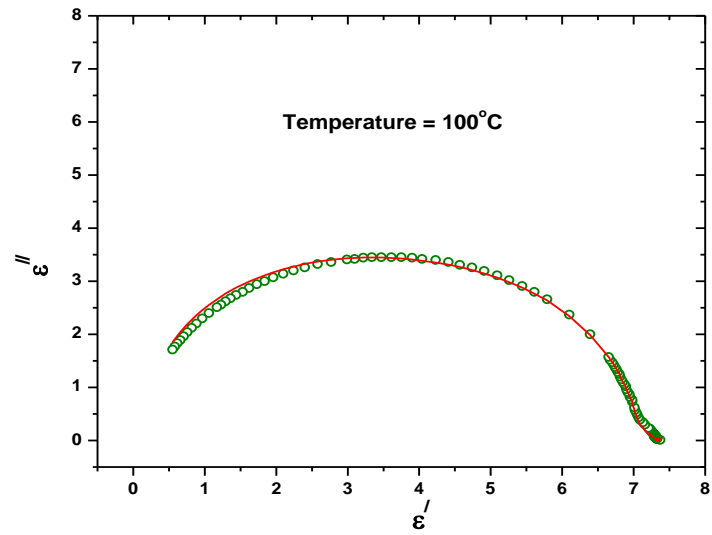


Figure 4.27: Cole-cole plot of 3ccp-ff

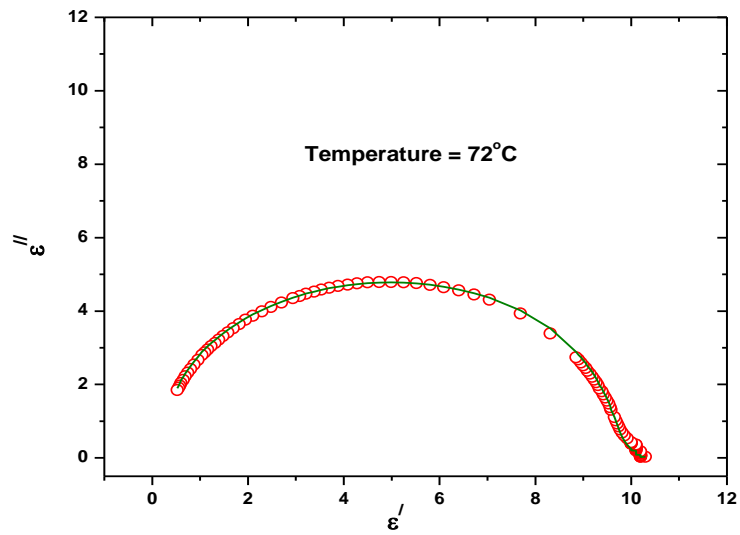


Figure 4.28: Cole-cole plot of 3ccp-fff

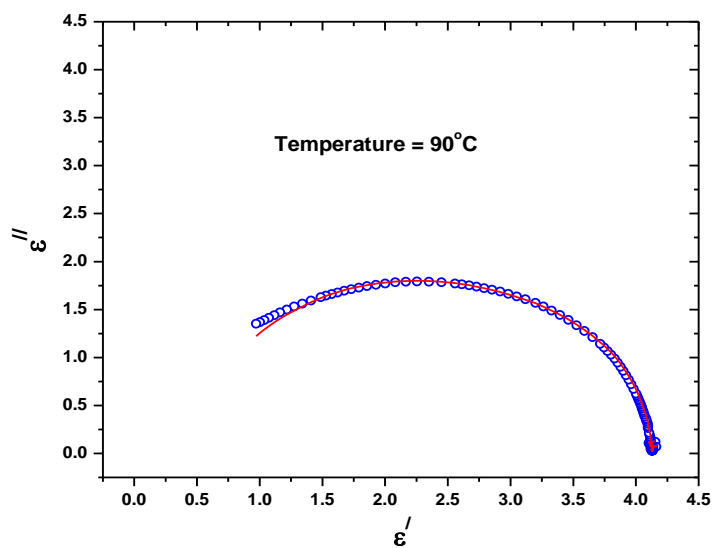


Figure 4.29: Cole-cole plot of 5ccp-f

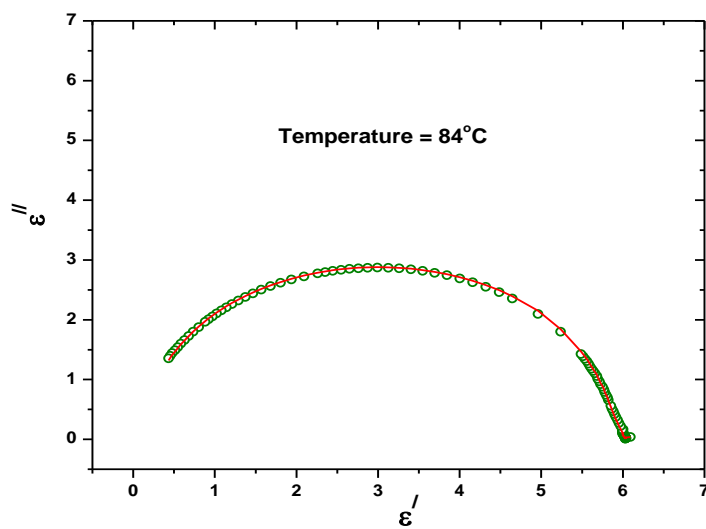


Figure 4.30: Cole-cole plot of 5ccp-ff

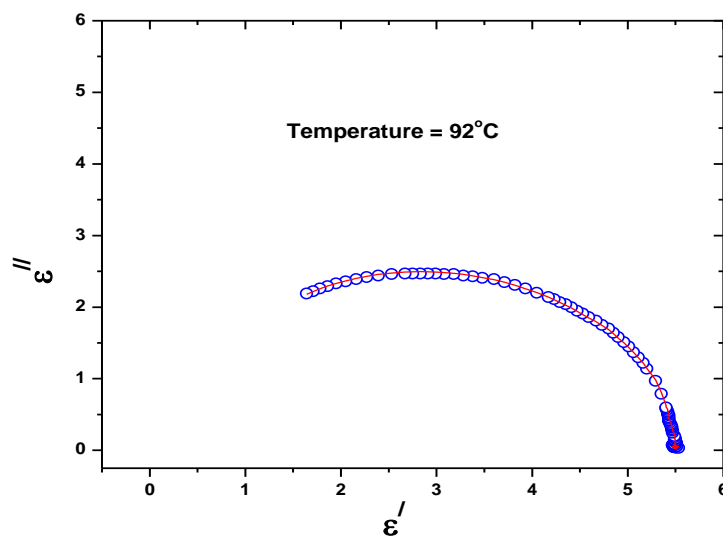


Figure 4.31: Cole-cole plot of 5ccp-fff

It is observed that for 3ccp-ff, 3ccp-fff, 5ccp-f and 5ccp-ff relaxation frequency varies from kHz regime to few MHz regimes, but for 3ccp-f and 5ccp-fff, it varies within MHz regime. In low temperature regime, relaxation frequency (f_c) decreases sharply from f to ff derivatives but increases from ff to fff derivatives in both the series. Increased chain length however, caused increased relaxation frequency except in the mono fluorinated derivatives. In terphenyl series also f_c was found to decrease with increased fluorination as noted in chapter 3. Observed values are lower than in cyanobiphenyls e.g. in 5CB it was 15.6 MHz [71]. This is expected since for rigid molecules f_c varies inversely with square root of moment of inertia [72] and present molecules have larger moments of inertia (listed in Table 4.4) mainly because of large increase in their molecular mass compared to 5CB.

Table 4.12: Relaxation frequency and activation energy of the studied compounds

Compounds	Relaxation Frequency (f_c) within nematic range	Activation Energy (kJ/mole)
3ccp-f	1.5 MHz (90°C) – 3.46 MHz (158°C)	16.14
3ccp-ff	270 kHz (45°C) – 1.78 MHz (124°C)	22.58
3ccp-fff	800 kHz (64°C) – 1.4 MHz (94°C)	20.56
5ccp-f	900 kHz (73°C) – 4.7 MHz (146°C)	29.45
5ccp-ff	400 kHz (48°C) – 2.25 MHz (128°C)	22.77
5ccp-fff	2.4 MHz (88°C) – 3.6 MHz (102°C)	32.63

Exponential increase of relaxation frequency with temperature suggests that it should obey Arrhenius law [33,73,74], following this height of the activation energy barrier of the thermally activated relaxation process was calculated and the values are listed in the Table 4.12. Activation energies of the present compounds are substantially less than the terphenyl compounds described in last chapter. These are also less than in 5CB which was reported to be 66 kJ/mole [33]. Above table also suggests that increased chain length substantially increases the activation energy in nematic phase, however, increment is marginal in ff derivatives.

It is worth of mention that the present compounds, unlike the terphenyl compounds show very low optical birefringence (Δn) in the range 0.067 to 0.034 [24,25].

4.5 CONCLUSION

Effect of fluorination and chain length on the physical properties of six phenyl bicyclohexyl compounds (3ccp-f, 3ccp-ff, 3ccp-fff, 5ccp-f, 5ccp-ff, 5ccp-fff) have been investigated, all of which exhibit nematic phase over a wide range of temperatures. Molecular mechanics calculation reveals that dipole moments of the molecules increases (1.93D to 3.37D)

with fluorination in both propyl and pentyl based systems; increment in f to ff derivatives is more than in ff to fff derivatives. However no change in dipole moment is observed with increased chain length. Molecular geometry and conformation, packing in the crystalline state and density, magnitude of molecular dipole moments and its orientation with molecular long axes of the compound 5ccp-fff is found to be different from those in closely related compounds 3ccp-f and 3ccp-fff. These differences are probably the cause of the substantial increase of melting point and decrease of nematic range in 5ccp-fff compared to compounds 3ccp-f and 3ccp-fff. The fact that in the nematic phase apparent length of the molecules is more than the most extended molecular lengths, average value of dielectric constant (ϵ_{avg}) is less than the extrapolated values of ϵ_{iso} in isotropic phase, effective values of the dipole moments are less than the free molecular dipole moments as well as calculated values of dipole-dipole correlation factors (g_{\parallel} and g_{\perp}) give conclusive evidence of existence of short range antiparallel order in all the compounds. Antiparallel correlation (g_{\parallel}) along the molecular axis is found to improve slightly with increased chain length in mono and trifluorinated compounds. Increased fluoro substitution caused increased dielectric anisotropy however; increased chain length resulted in opposite behavior but in lower degree. As a result, improved switching characteristics (V_{th} and V_{d}) is observed in 3ccp series compared to 5ccp series and increased lateral fluorination resulted in further improvement. Increased fluorination also decreases splay elastic constant, thus faster response expected in triply fluorinated compounds. Only one Debye type relaxation process, connected with reorientations around the short axis, is observed. In low temperature regime, relaxation frequency (f_c) decreases sharply from f to ff derivatives but increases from ff to fff derivatives in both the series. Increased chain length however caused increased relaxation frequency.

4.6 REFERENCES

- [1] B. Bahadur, (1991). *Liquid Crystals Applications and Uses*, World Sci.: Singapore.
- [2] G. H. Heilmeyer and L. A. Zanoni; *Appl. Phys. Lett.* 13, 91 (1968), Guest-host interactions in nematic liquid crystals: a new electro-optic effect.
- [3] S. Marino, M. Castriota, V. Bruno, E. Cazzanelli, G. Strangi, C. Versace and N. Scaramuzza; *J. Appl. Phys.*, 97, 013523 (2005), Changes of the electro-optic response of nematic liquid crystal cells due to inserted titania-vanadia films.
- [4] M. Oh-e and K. Kondo; *Appl. Phys. Lett.*, 69, 623 (1996), Response mechanism of nematic liquid crystals using the in-plane switching mode.
- [5] R. Muenster, M. Jarasch, X. Zhuang and Y. R. Shen; *Phys. Rev. Lett.*, 78, 42 (1997), Dye-Induced Enhancement of Optical Nonlinearity in Liquids and Liquid Crystals.
- [6] Y. Goto, T. Ogawa, S. Swada and S. Sugimori; *Mol. Cryst. Liq. Cryst.*, 209, 1–7 (1991), Fluorinated Liquid Crystals for Active Matrix Displays.
- [7] D. Demus, Y. Goto, S. Sawada, E. Nakagawa, H. Saito, R. Tarao; *Mol Cryst Liq Cryst.*, 260, 1–21(1995), Trifluorinated liquid crystals for TFT displays.
- [8] T. Nishi, A. Matsubara, H. Okada, H. Onnagawa, S. Sugimori, K. Miyashita; *Jpn J Appl Phys.*, 34, 236–239 (1995), Relationship between molecular structure and temperature dependence of threshold voltage in fluorinated liquid crystals.
- [9] V. F. Petrov; *Liq Cryst.*, 19, 729–741 (1995), Liquid crystals for AMLCD and TFTPDLCD applications; V. F. Petrov, Sofia I. Torgova ; Ludmila A. Karamysheva ; Shunsuke Takenaka; *Liq. Cryst.*, 26, 1141-1162 (1999), The trans-1,4-cyclohexylene group as a structural fragment in liquid crystals.
- [10] S. Gauza, H. Wang, C. H. Wen, S. T. Wu, A. Seed, R. Dabrowski; *Jpn J Appl Phys.*, 42, 3463–3466 (2003), High birefringence isothiocyanato tolane liquid crystals.

- [11] J. S. Gasowska, S. J. Cowling, M. C. R. Cockett, M. Hird, R. A. Lewis, E. P. Raynes, J. W. Goodby; *Mater Chem.*, 20, 299–307 (2010), The influence of an alkenyl terminal group on the mesomorphic behavior and electro-optic properties of fluorinated terphenyl liquid crystals.
- [12] H. Ishikawa, A. Toda, H. Okada, H. Onnagawa, S. Sugimori; *Liq Cryst.*, 22, 743–747 (1997), Relationship between order parameter and physical constants in fluorinated liquid crystals.
- [13] M. Hird; *Chem Soc Rev.*, 36, 2070–2095 (2007), Fluorinated liquid crystals – properties and applications.
- [14] M. Klasen, M. Bremer, A. Gotz, A. Manabe, S. Naemura, K. Tarumi; *Jpn J Appl Phys.*, 37, L945–L948 (1998), Calculation of optical and dielectric anisotropy of nematic liquid crystals.
- [15] K. Hori, M. Maeda, M. Yano, M. Kunugi; *Liq Cryst.*, 38, 287–293 (2011), The effect of fluorination (2): dependence of alkyl chain length on the crystal structures of mesogenic alkyl 4-[2-(perfluorohexyl) ethoxy] benzoates.
- [16] M. R. Cargill, G. Sandford, A. J. Tadeusiak, G. D. Love, N. Hollfelder, F. Pleis, G. Nelles, P. Kilickiran; *Liq Cryst.*, 38, 1069–1078 (2011), Highly fluorinated biphenyl ether systems as dopants for fastresponse liquid crystal display applications.
- [17] S. Haldar, K. C. Dey, D. Sinha, P. K. Mandal, W. Haase, P. Kula; *Liq Cryst.*, 39, 1196–1203 (2012), X-ray diffraction and dielectric spectroscopy studies on a partially fluorinated ferroelectric liquid crystal from the family of terphenyl esters.
- [18] E. Bartmann, D. Dorsch, U. Finkenzeller, H. A. Kurmeier and E. Poetsch; *Freiburger Arbeitstagung Flüssigkristalle*, 19, P8 (1990).
- [19] U. Finkenzeller, A. Kurmeier and E. Poetsch; *Freiburger Arbeitstagung Flüssigkristalle*, 18, P17 (1989).
- [20] P. Kirsch, S. Naemura and K. Tarumi; *Freiburger Arbeitstagung Flüssigkristalle*, 27, P45 (1998).

- [21] K. Tabayashi and K. Akasaka; *Liq. Cryst.*, 26, 127-129 (1999), Preliminary communication Natural abundance ^2H NMR for liquid crystal studies: deuterium isotope effect on microscopic order.
- [22] H. Ishikawa, A. Toda, A. Matsubara, T. Nishi, H. Okada, H. Onnagawa, S. Sugimori and K. Miyashita; 20th Jpn. Symp. *Liq. Cryst.*, Nagoya 1G505 (1994).
- [23] D. A. Dunmur, R. Hanson, H. Okada, H. Onnagawa, S. Sugimori and K. Toriyama; *Asia Display' 95 Proceeding*, S22-2, 563 (1995), Effect of Intermolecular Interactions on Threshold Voltages for TN and TFT LC-Displays: Dipole Association in F-Substituted Cyclohexyl cyclohexyl benzenes.
- [24] S. Biswas, S. Haldar, P. K. Mandal, W. Haase; *Liq Cryst.*, 34, 365–372 (2007), X-ray diffraction and optical birefringence studies on four nematogenic difluorobenzene derivatives.
- [25] S. Haldar, S. Barman, P. K. Mandal, W. Haase, R. Dabrowski; *Mol Cryst Liq Cryst.*, 528, 81–95 (2010), Influence of molecular core structure and chain length on the physical properties of nematogenic fluorobenzene derivatives.
- [26] I. C. Khoo and S. T. Wu; *Optics and Nonlinear Optics of Liquid Crystals*, World Scientific: Singapore, (1993).
- [27] L. M. Blinov, V. G. Chigrinov; *Electro-Optic Effects in Liquid Crystal Materials*, Springer: New York, (1996).
- [28] M. Schadt; *Annu. Rev. Mater. Sci.*, 27, 305–379 (1997), Liquid crystal materials and liquid crystal displays.
- [29] B. Kundu, S. K. Pal, S. Kumar, R. Pratibha, N. V. Madhusudana; *Phys Rev E.*, 82, 061703-1–061703-9 (2010), Splay and bend elastic constants in the nematic phase of some disulfide bridged dimeric compounds.
- [30] H. Kresse; Dynamic dielectric properties of nematics. In: Dunmur, DA. Fukuda, A. Luckhurst, GR, editors. *Physical properties of liquid crystals: nematics*. London: INSPEC; 2001. p. 277–287.

- [31] H. Kresse; Dielectric properties of nematic liquid crystals. In: Demus, D. Goodby, J. Gray, GW. Spiess HW. Vill, V, editors. Handbook of liquid crystals. Vol. 2A. Weinheim, FRG: Wiley-VCH, Verlag GmbH, p. 91–112 (1998).
- [32] W. H. de Jeu, T. W. Lathouwers, D. Constants; ZNaturforsch, 29a, 905–911 (1974), Molecules structure of nematic liquid crystals. I. Terminally substituted azobenzene and azoxybenzenes.
- [33] J. Schacht, P. Zugenmaier, M. Buivydas, L. Komitov, B. Stebler, S. T. Lagerwall, F. Gouda, F. Horii; Phys Rev E., 61, 3926–3935 (2000), Intermolecular and intramolecular reorientations in nonchiral smectic liquid-crystalline phases studied by broadband dielectric spectroscopy.
- [34] D. A. Dunmur, W. H. Miller; Mol Cryst Liq Cryst., 60, 281–292 (1980), Dipole–Dipole correlation in nematic liquid crystals.
- [35] S. Haldar, D. Sinha, P. K. Mandal, K. Goubitz and R. Peschar; Liquid Crystals, Vol. 40, No. 5, 689–698 (2013), Effect of molecular conformation on the mesogenic properties of a partially fluorinated nematogenic compound investigated by X-ray diffraction and dielectric measurements.
- [36] S. Haldar, P. K. Mandal, K. Goubitz, H. Schenk, W. Haase; Mol Cryst Liq Cryst., 490, 80–87 (2008), X-ray structural analysis in the crystalline phase of a nematogenic fluoro-phenyl compound.
- [37] S. Haldar, P. K. Mandal, S. J. Prathap, T. N. Guru Row, W. Haase; Liq Cryst., 35, 1307–1312 (2008), X-ray studies of the crystalline and nematic phases of 4-(3,4,5-trifluorophenyl)-4-propylbicyclohexyl.
- [38] W. Haase, M. A. Athanassopoulou; Vol. I. Berlin: Springer, p. 139–197 (1999), Crystal structures of LC mesogens. In: Mingos, M, editor. Structure and bonding.
- [39] M. Hird and K. J. Toyne; Mol. Cryst. Liq. Cryst., 323, 1-67 (1998), Fluoro Substitution in Thermotropic Liquid Crystals.
- [40] V. Vill; Liq. Cryst. Database, Version 4.4 , LCI Publisher, GmbH, Hamburg (2003) and references therein.

- [41] L. Bata and A. Buka; *Mol. Cryst. Liq. Cryst.*, 63, 307-320 (1981), Dielectric Permittivity and Relaxation Phenomena in smectic Phases.
- [42] R. deGelder, R. A. G. de Graaff, H. Schenk; *Acta Cryst.*, A49, 287-293 (1993), Automatic determination of crystal structures using Karle-Hauptman matrices.
- [43] D. T. Cromer, J. B. Mann; *Acta Cryst.*, 24A, 321-324 (1968), X-ray scattering factors computed from numerical Hartree-Fock wave functions.
- [44] International Union of Crystallography. *International tables for X-ray crystallography*. Vol. IV, Birmingham: Kynoch Press, pp. 55 (1974).
- [45] D. T. Cromer, D. Liberman; *J Chem Phys.*, 53, 1891-1898 (1970), Relativistic calculation of anomalous scattering factors for X-rays.
- [46] S. R. Hall, D. J. du Boulay, R. Olthof-Hazekamp, editors. *XTAL3.7 system*. Lamb: University of Western Australia (2000).
- [47] Spek AL. PLATON, An integrated tool for the analysis of the results of a single crystal structure determination. *Acta Cryst.*, A46, C-34 (1990).
- [48] Hyperchem 6.03, Hypercube Inc., Gainesville, FL, USA.
- [49] P. Sarkar, P. K. Mandal, S. Paul, R. Paul; *liq. Cryst.*, Vol. 30, No. 4, 507-527 (2003), X-ray diffraction, optical birefringence, dielectric and phase transition properties of the long homologous series of nematogens 4-(trans-4'-n-alkylcyclohexyl) isothiocyanatobenzenes.
- [50] E. Megnassan and A. Proutierre; *Mol. Cryst. liq. Cryst.*, 108, 245 (1984), Dipole Moments and Kerr Constants of 4-n Alkyl-4'-Cyanobiphenyl Molecules (From 1CB to 12CB) Measured in Cyclohexane Solutions.
- [51] K. P. Gueu, E. Megnassan and A. Proutierre; *Mol. Cryst. liq. Cryst.*, 132, 303 (1986), Dipole Moments of 4-n Alkyl-4'-Cyanobiphenyl Molecules (from OCB to 12CB) Measurement in Four Solvents and Theoretical Calculations.

- [52] W. Haase, H. Paulus, R. Pendzialek; *Mol. Cryst. Liq. Cryst.*, 100: 211-221 (1983), Solid State Polymorphism in 4-Cyano-4'-n-Propyl biphenyl and X-Ray Structure Determination of the Higher Melting Modification.
- [53] B. R. Jaishi, P. K. Mandal, K. Goubitz, H. Schenk, R. Dabrowski, K. Czuprynski; *Liq.Cryst.*, 30, 1327-1333 (2003), The molecular and crystal structure of a polar mesogen 4-cyanobiphenyl-4'-hexylbiphenyl carboxylate.
- [54] S. Biswas, S. Haldar, P. K. Mandal, K. Goubitz, H. Schenk, R. Dabrowski; *Cryst. Res. Technol.*, 42, 1029-1035 (2007), Crystal structure of a polar nematogen 4-(trans-4-undecylcyclohexyl) isothiocyanatobenzene.
- [55] L. Walz, W. Haase, R. Eidenschink; *Mol. Cryst. Liq. Cryst.*, 168, 169-182 (1989), The Crystal and Molecular Structures of Four Homologous, Mesogenic trans,trans-4,4'-dialkyl-(1 α ,1'-bicyclohexyl)-4 β -carbonitril (CCN's).
- [56] S. Gupta, P. Mandal, S. Paul, K. Goubitz, M. de Wit, H. Schenk; *Mol. Cryst. Liq.Cryst.*, 195, 149-159 (1991), An X-Ray Study of Cyanophenylpyrimidines Part III. Crystal Structure of 5-(trans-4-Heptylcyclohexyl)-2-(4-Cyanophenyl) Pyrimidine.
- [57] A. Nath, S. Gupta, P. Mandal, S. Paul, H. Schenk; *Liq. Cryst.*, 20, 765-770 (1996), Structural analysis by X-ray diffraction of a non-polar alkenyl liquid crystalline compound.
- [58] P. Mandal, S. Paul, H. Schenk, K. Goubitz; *Mol. Cryst. Liq. Cryst.*, 210: 21-30 (1992), Crystal and Molecular Structure of a Cybotactic Nematic Compound bis-(4'-n-Butoxybenzal)-2-Chloro-1,4-Phenylenediamine.
- [59] P. Mandal, S. Paul, H. Schenk, K. Goubitz; *Mol. Cryst. Liq. Cryst.*, 135, 35-48 (1986), Crystal and Molecular Structure of the Nematogenic Compound 4-Cyanophenyl-4'-n-Heptylbenzoate (CPHB).
- [60] P. Mandal, S. Paul; *Mol. Cryst. Liq. Cryst.*, 131, 223-235 (1985), X-Ray Studies on the Mesogen 4'-n-Pentyloxy-4-Biphenylcarbonitrile (5OCB) in the Solid Crystalline State.

- [61] L. Walz, F. Nepveu, W. Haase; *Mol. Cryst. Liq. Cryst.*, 148, 111-121 (1987), Structural Arrangements of the Mesogenic Compounds 4-Ethyl-4'-(4''-pentylcyclohexyl)biphenyl and 4-Ethyl-2'-fluoro-4'-(4''-pentylcyclohexyl)biphenyl (BCH's) in the Crystalline State.
- [62] P. S. Patil, V. Shettigar, S. M. Dharmaprakash, S. Naveen, M. A. Sridhar, J. S. Prasad; *Mol. Cryst. Liq. Cryst.*, 461, 123-130 (2007), Synthesis and Crystal Structure of 1-(4-fluorophenyl)-3-(3,4,5-trimethoxyphenyl)-2-propen-1-one.
- [63] S. Haldar; S. Barman; P. K. Mandal; W. Haase; R. Dabrowski; *Mol. Cryst. Liq. Cryst.*, Vol. 528, 81–95 (2010), Influence of Molecular Core Structure and Chain Length on the Physical Properties of Nematogenic Fluorobenzene Derivatives.
- [64] A. J. Leadbetter, R. M. Richardson, C. N. Colling; 36, C1-37–C1-43 (1975), The structure of a number of nematogens. *J Phys (Paris)*.
- [65] S. Gupta, G-P Chang-Chien, W-S Lee, R. Centore, S. P. Sen Gupta; *Liq Cryst.*, 29, 657–661 (2002), Crystal structure of the mesogenic alkene monomer, 3-[4-(4_-ethylbiphenyl)]-1-propene.
- [66] B. R. Ratna, R. Shashidhar; *Mol Cryst Liq Cryst.*, 42, 113–125 (1977), Dielectric studies on liquid crystals of strongly positive dielectric anisotropy.
- [67] B. R. Ratna, R. Shashidhar; *Mol Cryst Liq Cryst.*, 45, 103–116 (1978), Dielectric properties of some nematics of positive dielectric anisotropy.
- [68] M. Schadt; *J Chem Phys.*, 56, 1494–1497 (1972), Dielectric properties of some nematic liquid crystals with strong positive dielectric anisotropy.
- [69] N. V. Madhusudana, S. Chandrasekhar; *Pramana.*, 1, 57–68 (1975), The role of permanent dipoles in nematic order.
- [70] P. Bordewijk; *Physica.*, 75, 146 (1974), Extension of the Kirkwood-Fröhlich theory of the static dielectric permittivity to anisotropic liquids.
- [71] M. Gu, Y. Yin, S. V. Shiyankovskii, O. D. Lavrentovich; *Phys Rev E.*, 76, 061702 (2007), Effects of dielectric relaxation on the director dynamics of uniaxial nematic liquid crystals.

[72] H. Baessler, R. B. Beard, M. M. Labes; *J Chem Phys.*, 52, 2292 (1970), Dipole Relaxation in a Liquid Crystal.

[73] A. C. Diogo, A. F. Martins; *J Phys (Paris)*, 43, 779 (1982), Order parameter and temperature dependence of the hydrodynamic viscosities of nematic liquid crystals.

[74] S. Arrhenius; *Z Phys Chem.*, 4, 226 (1889), On the reaction rate of the inversion of non-refined sugar upon souring.

CHAPTER 5

**MOLECULAR AND DYNAMICAL PROPERTIES OF TWO
PERFLUORINATED LIQUID CRYSTALS WITH DIRECT TRANSITION
FROM FERROELECTRIC S_mC^* PHASE TO ISOTROPIC PHASE**

Part of the work has been published in Journal of Molecular Liquids., Vol. 182: pp. 95–101, 2013.

5.1 INTRODUCTION

In 1974, Meyer [1] concluded from symmetry argument that chiral molecules in smectic C phase should exhibit ferroelectricity and such phenomenon was indeed discovered soon in a Schiff's base compound DOBAMBC, thus started a new branch of material science, ferroelectric liquid crystals. These materials are only known intrinsic polar fluid materials that possess the ferroelectric, electro-optic, piezoelectric and pyroelectric properties of solid polar dielectrics with the physical flow characteristics of liquids. After the discovery of antiferroelectricity by Fukuda group [2] in MHPOBC it has been shown that between antiferroelectric and para-electric phases three different sub phases (SmC_α^* , SmC_β^* and SmC_γ^*) also exist [2-5] and their stability depends strongly on the optical purity of the compounds [6]. Different types of chiral liquid crystal compounds are found to possess one or more of the phases like antiferroelectric SmC_A^* , ferroelectric SmC^* (including its sub-phases) and paraelectric SmA^* phases making them attractive from both theoretical and application points of view. Ferroelectric liquid crystals (FLCs) have been studied extensively due to their various interesting basic properties, FLCs are also promising materials for fast switching electro-optical displays with wide viewing angle [7]. However, they are not used much commercially because of difficulties at various levels. Therefore effort is made to design new materials and study various physical properties so as to overcome these difficulties. Because of the small size of a fluoro substituent and high strength of the C-F bond, liquid crystals with fluoro substituents show low birefringence, viscosity, conductivity and high chemical and thermal stability. As a result many liquid crystal compounds with fluoro substituents both in the cores and alkoxy chains were designed and synthesized in both achiral and chiral systems [8-14]. Liquid crystals with fluorinated chains are also very promising as antiferroelectric materials especially as thresholdless ones [14-17]. Phase behavior, physical and electrooptical properties of fluorinated derivatives in many respects are quite different from their hydrogenous analogues which create new possibilities for their applications [16]. For example, protonated organosyloxane compounds exhibit both SmC^* and de Vries SmA^* phases [18, 19], but Naciri et al [20, 21] reported that analogous fluorinated compound exhibit only de Vries SmA^* phase. A terphenyl based ester compound with CH_3COO group at the achiral end exhibits SmC^* and SmA^* phases while analogous compound with CF_3COO group shows SmC_A^* phase in addition, but stronger polar

end group (CNCOO) shows only SmA^* phase [22]. Antiferroelectric phase was reported in an achiral bent-core molecule containing 2,3-difluorotolane unit when its protonated analogue did not show liquid crystalline phase at all [23]. Formation of cholesteric and blue phase is reported in molecules containing 1,4-tetrafluorophenylene units [24]. A fluorosubstituent at the chiral centre [25] or partially fluorinated chain [15,26] results in enhancement in spontaneous polarization (P_s). Effect of fluorination on the relaxation and switching behavior of para, ferro and antiferroelectric liquid crystals has been discussed by many authors [16, 17, 27-30]. Rigidity of the core structure, nature of chirality and extent of fluorination of the constituent molecules are found to have pronounced effect on the collective mode relaxation behavior of room temperature FLC mixtures [29]. A fairly recent review by Michael Hird [8] ‘introduces the phenomenon of ferroelectric liquid crystals and charts the development of the technology to commercially viable devices, with a specific focus on the development of suitable materials in terms of design, synthesis and properties’ wherein effect of fluorination has also been discussed in detail for both the achiral and chiral systems. Keeping this in view two recently synthesized ferroelectric liquid crystal compounds viz., (S) – (+)-4'-[3-(nonafluoropentanoyloxy) prop-1-oxy]biphenyl-4-yl 4-(1-methylheptyloxy) benzoate and (S)–(+)- 4'-[6-(nonafluoropentanoyloxy) hexyl-1-oxy]biphenyl-4-yl 4-(1-methylheptyloxy) benzoate (code 4F3R and 4F6R, first and second numbers respectively being the number of C atoms in the perfluorinated chain and oligomethylene spacer) [14] has been investigated in detail by X-ray diffraction, dielectric spectroscopy and electro-optic methods.

From small and wide angle X-ray diffraction study the nature of temperature dependence of layer thickness and tilt angle in different phases have been determined. Tilt angle has also been measured by optical methods. It has been discussed in chapter 2 that dielectric spectroscopy studies on ferroelectric liquid crystals are important since one can get information about the relaxation modes directly associated with ferroelectricity [31]. Since the two compounds possess ferroelectric SmC^* phase, one also having SmC_A^* phase, two types of collective relaxation modes may be associated with them, viz., Goldstone mode and Soft mode which can be examined by dielectric relaxation spectroscopy. The Goldstone mode appears in the SmC^* phase because of the phase fluctuations in the azimuthal orientation of the molecular director and its characteristic frequency is usually less than 10 kHz. The soft mode, on the other hand, appears in the neighbourhood of $\text{SmA}^* - \text{SmC}^*$ transition due to fluctuations in the tilt angles of the molecules.

Both these modes are called collective mode since they represent collective behaviour of the molecules under the influence of an ac field. As the Goldstone mode dielectric increment is usually large compared to the soft mode increment, sometimes it is difficult to study the soft mode properties in the SmC^* phase. Yet, this problem can be overcome by applying a DC electric field in the SmC^* phase, so-called the bias field, being strong enough to unwind the helical arrangement of the polarization vector. In such situation the Goldstone mode is suppressed and the soft mode can be studied almost separately. Although Goldstone mode dielectric increment is usually large compared to the soft mode increment but soft mode critical frequency is at least two orders higher than that of GM. Moreover, according to the generalized Landau model [32] GM critical frequency remains almost independent of temperature whereas that of SM is strongly temperature dependent being associated with the tilt fluctuation of the directors.

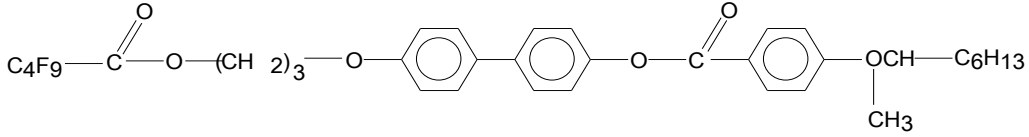
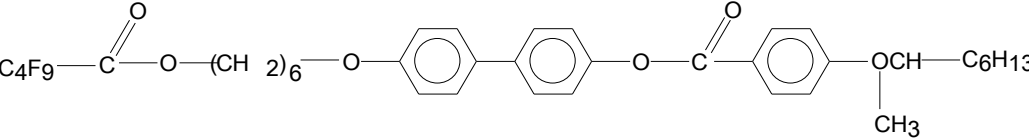
In antiferroelectric liquid crystalline (AFLC) materials double relaxation processes with critical frequencies in the kHz and MHz range are usually observed. The low frequency mode (P_L), known as the antiferroelectric mode, is the result of collective reorientation of the molecules in the same direction. The high frequency mode (P_H), known as the antiphase antiferroelectric mode, arises due to collective reorientation of the molecules in the opposite direction [33,34].

Along with frequency-dependent dielectric study spontaneous polarisation (P_S), which is a measure of order parameter and on which the switching time of ferroelectric liquid crystalline (FLC) display devices depends, has also been measured. The rotational viscosity and switching time were also determined to probe the suitability of the materials in display applications.

5.2 COMPOUNDS STUDIED

Molecular structures of the investigated fluorinated ferroelectric compounds and their abbreviated names and transition temperatures (in $^{\circ}\text{C}$) are given in the Table 5.1.

Table 5.1: Molecular structures and transition temperatures of the compounds 4F3R and 4F6R

Name	Molecular structure with transition temperature
4F3R	 <p style="text-align: center;">Cr 79.8°C SmC* 134.1°C I</p>
4F6R	 <p style="text-align: center;">Cr₁ 46.7°C Cr₂ 60.0°C SmC_A* 86.5°C SmC* 128.3°C I</p>

5.3 EXPERIMENTAL METHODS

The Phase behaviour of the compounds was investigated by polarizing microscope equipped with the heating stage. The heating and cooling rate was 1°C / min and the measurement accuracy was $\pm 0.1^\circ\text{C}$. Small and wide angle X-ray scattering measurements (SAXS and WAXS) on randomly oriented samples were made using Ni filtered $\text{CuK}\alpha$ radiation and a custom built high temperature camera and photographs were analyzed to find average intermolecular distance and layer spacing. Tilt angles (θ) were calculated using the relation $\theta = \cos^{-1}(d/L)$, where L is the most extended length of the molecules found by geometry optimization.

To perform the dielectric and electrooptic measurements polyimide-coated planar glass cells with low resistivity (about $20\Omega/\square$) indium tin oxide (ITO) electrodes of $4.2\ \mu\text{m}$ cell gap and active electrode area $1.2 \times 0.7\ \text{cm}^2$ were used. Cells were filled by capillary action with samples in isotropic state. Very slow regulated cooling of the sample yielded proper alignment. Complex

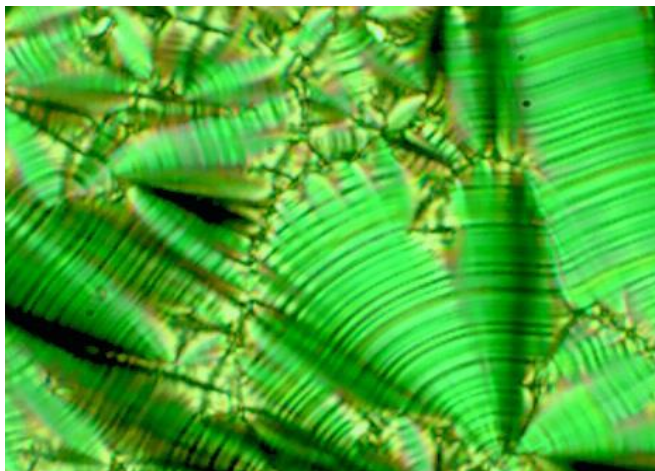
dielectric permittivity was measured using a Hewlett-Packard impedance analyzer HP 4192A in the frequency range from 100 Hz to 13 MHz. Automatic data acquisition arrangement was made using RS232 interfacing with a PC.

Spontaneous polarization (P_s) was measured as a function of temperature by the reversal current method [29] using a triangular wave at 10 Hz. The amplitude of the applied voltage was 20Vpp. An oscilloscope was used to record the voltage drop across a resistor in series with the cell as a function of time. The area under the curve was determined from the stored image after creating an appropriate base line following procedure described in chapter 2. Optical tilt of molecules in smectic layers was determined by measuring the angle of rotation of the analyzer between two extinction conditions while the sample was observed under a polarizing microscope in switching condition under a square wave of very low frequency (about 10 MHz). Response time of the sample was determined by measuring the time delay of occurrence of polarization bump from the applied square pulse edge (20Vpp, 10 Hz) while monitoring, in storage oscilloscope, the voltage across a resistor in series with the cell. Sample temperature was regulated by a Eurotherm controller 2216e within $\pm 0.1^\circ\text{C}$ in all measurements. Details of experimental procedure have already been discussed in chapter 2.

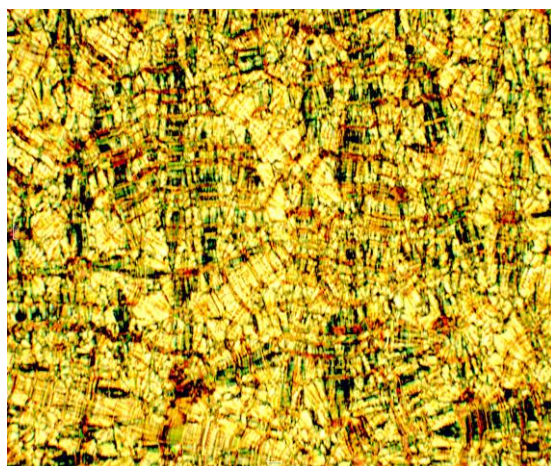
5.4 RESULTS AND DISCUSSION

The compound 4F3R exhibits only synclinic ferroelectric SmC^* phase over a considerable temperature range ($\Delta T = 54.3^\circ$) whereas the compound 4F6R exhibits both SmC_A^* phase ($\Delta T = 26.5^\circ$) and SmC^* phase ($\Delta T = 41.8^\circ$) at the cost of range of SmC^* phase compared to 4F3R. 4F6R also shows two crystalline modifications. Observed textures in different phases for the two compounds are shown in Figure 5.1. Beautiful broken fan shaped texture with clear sign of helicoidal structure in the form of equidistant parallel lines are observed in SmC^* phase of the first compound. In 4F3R measured enthalpies at the two transitions are 26.47 kJ/mol and 7.11 kJ/mol whereas in 4F6R these are 17kJ/mol, 15.78kJ/mol, 0.01kJ/mol and 7.75kJ/mol respectively [14]. Thus melting and clearing transitions in both the compounds are of first order; however anti-ferroelectric to ferroelectric transition is second order. Phase sequence similar to 4F3R was also observed in homologues with 3, 5 and 6 carbon atoms in the perfluorinated terminal chain [14]. Another important feature of these compounds is that they show direct

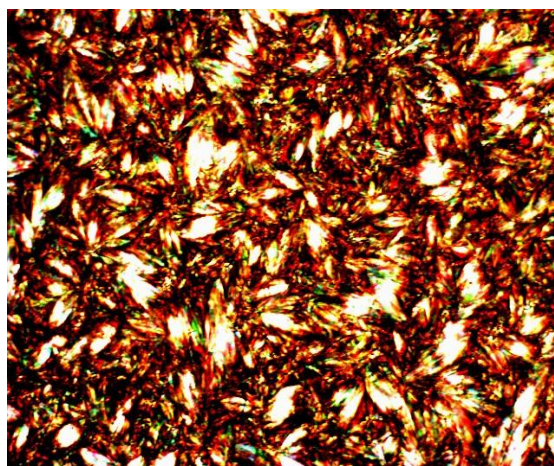
transition from the SmC* to isotropic phase, which is rare in FLC materials. It is also found that the compounds are useful for formulation of room temperature FLC mixture as discussed later.



SmC* phase of 4F3R (102°C)



SmC* phase of 4F6R (120°C)



SmC_A* phase of 4F6R (75°C)

Figure 5.1: Textures in different phases of compounds 4F3R and 4F6R

5.4.1 Optimized Geometry Using Molecular Mechanics

To elucidate the structure of the molecules, 4F3R and 4F6R, their geometry were optimized using PM3 molecular mechanics method in *Hyperchem* software package [35]. While optimizing the geometry the bond, angle and torsional interactions were considered in the force

field along with the van-der Waals and electrostatic interactions. The optimized structures of the molecules of the two compounds, direction of principal axes along with the direction of its electric dipole moment are shown in Figure 5.2. Optimized lengths of the molecules, dipole moments along with their components along the directions of the principal moments of inertia and the corresponding moments of inertia values along the three principal moments of inertia axes are shown in the Table 5.2. Moments of inertia values in 4F6R are significantly higher than those of 4F3R as expected. Dipole moment of 4F6R is also found to be substantially higher than that of 4F3R which is a result of change in molecular conformation due to the increased chain length. Major increase of dipole moment is in the y-component, which is transverse to the molecular long axis satisfying the criteria of presence of transverse dipole moment in the constituent chiral molecules in a tilted smectic phase for the occurrence of ferroelectric phase.

Table 5.2: Optimized length, dipole moment and moments of inertia of 4F3R and 4F6R

Compound	Optimized Length (Å)	Dipole Moment (Debye)	Moments of Inertia ($\times 10^{-46}$ kg m ²)		
			I _{xx}	I _{yy}	I _{zz}
4F3R	33.4	4.25 (-1.98, 3.67, -0.81)	680.3	11576.2	11924.4
4F6R	38.3	5.68 (-2.62, 4.99, 0.67)	3440.9	97612.7	99964.8

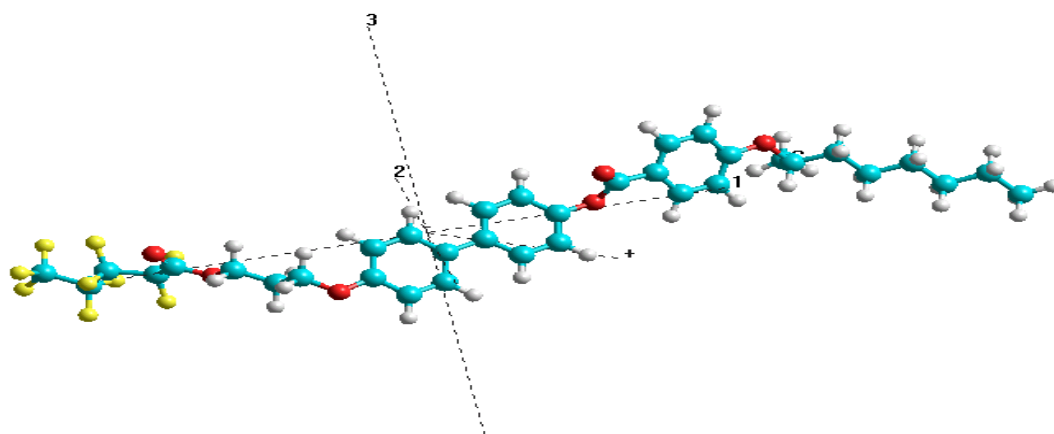


Figure 5.2(a): Optimized geometry of 4F3R

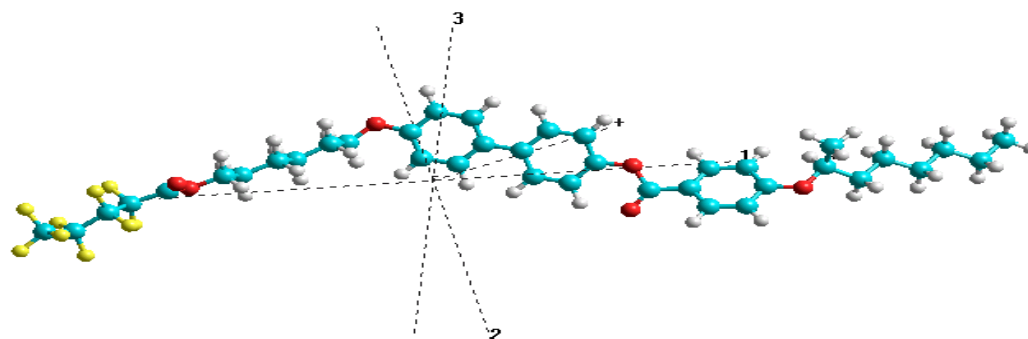


Figure 5.2(b): Optimized geometry of 4F6R

5.4.2 SAXS and WAXS Measurements

Two major diffraction features were observed in the X-ray photographs of randomly oriented sample. Diffused inner ring is related to the layer spacing (d) of the tilted smectic phase and diffused outer ring arises due to interaction of the neighboring molecules in a plane

perpendicular to the molecular axis providing average intermolecular distance (D). X-ray diffraction photographs observed in different phases of the compounds are shown in Figure 5.3.

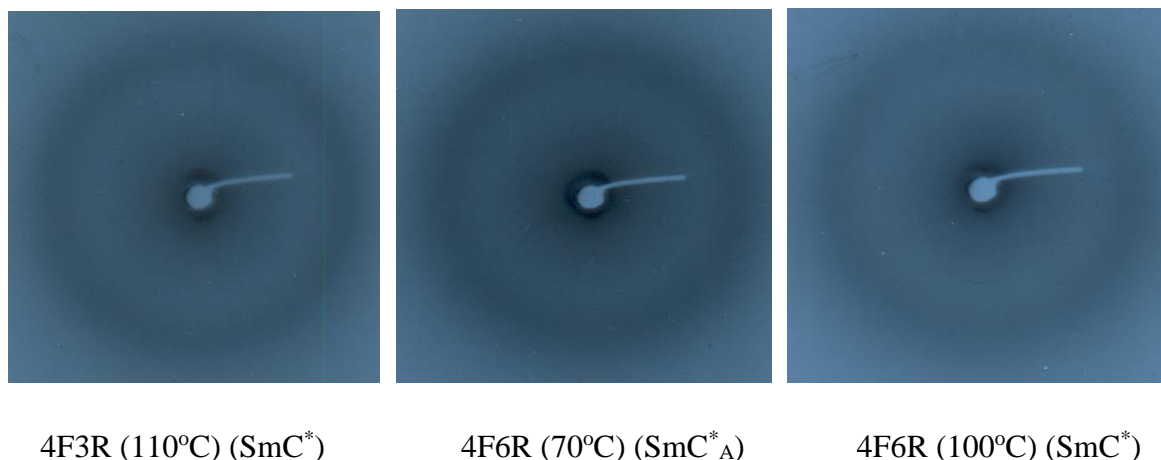


Figure 5.3: X-ray diffraction photographs in different chiral smectic phases of 4F3R and 4F6R

Temperature variations of average intermolecular distance and layer spacing are shown in Figure 5.4 and Figure 5.5. The figure shows that the average intermolecular distance remains almost constant and no discontinuity is observed at SmC_A^* to SmC^* transition in 4F6R. At 110°C in SmC^* phase, observed D in 4F3R is 5.87 Å while in 4F6R it is 6.89 Å. This considerable increase in D is a result of increased oligomethylene spacer group. The D values obtained in these compounds are also found to be larger than that observed (5.60 Å) in a nematogenic terphenyl compound having fluorine atom connected to the opposite side of a phenyl ring [36] and may be due to the presence of the bulky chiral $-\text{CH}_3$ group, the oligomethylene spacer and the ester bridge between the two phenyl rings. Present observation on D is consistent with other previous reported data [37,38]. Layer spacing (d) observed in 4F3R shows nonlinear increasing trend with temperature while in 4F6R it shows linear increasing trend in both ferroelectric and antiferroelectric smectic phases but observed d values are higher in SmC^* phase than in SmC_A^* phase. However, in this case clear discontinuities are observed at $\text{SmC}_A^* - \text{SmC}^*$ transition. In 4F3R, the layer spacing increases from 23 Å (79 °C) to 28.6 Å (129 °C) where as in 4F6R, d increases from 28.5 Å (64 °C) to 33 Å (84 °C) in SmC_A^* phase and further increases from 34.7 Å (89 °C) to 38.8 Å (124 °C) in SmC^* phase. Increased layer spacing is a result of decrease of tilt angle of the molecules with respect to the layer normal, if it is assumed that the molecules behave as rigid rods and molecular conformations do not change appreciably with temperature.

Similar variation of layer thickness with temperature is observed in related homologues of the series [14]. It is worth of mention that nonlinear increase of d with temperature had also been reported in both ferroelectric SmC^* and antiferroelectric SmC_A^* phases from synchrotron X-ray diffraction [39]. Continuous layer expansion on lowering of temperature or almost temperature independent layer spacing (hence free from chevron defects) had also been observed in pure or FLC mixtures [40].

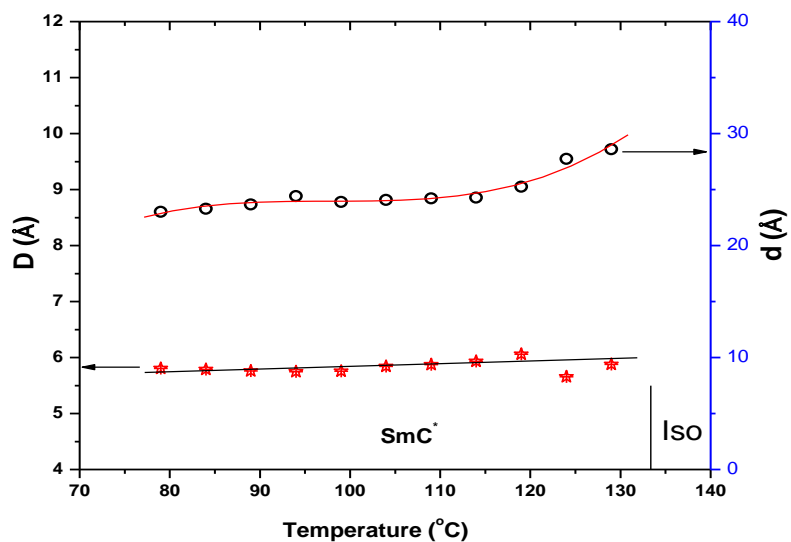


Figure 5.4: Variations of average intermolecular distance (D) and layer spacing (d) with temperature in 4F3R

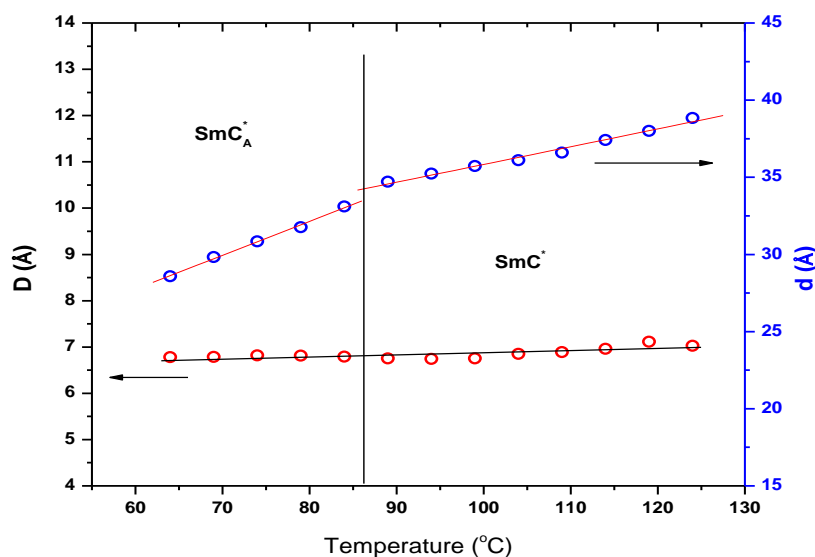


Figure 5.5: Variations of average intermolecular distance (D) and layer spacing (d) with temperature in 4F6R

The tilt angle (θ) of the molecular directors, often referred to as primary order parameter of FLC phase, was calculated under rigid rod approximation, estimated error in tilt angle being $\pm 0.5^\circ$. In both the compounds tilt angles were found to decrease with temperature as shown in Figure 5.6 and Figure 5.7. In 4F3R at 84°C tilt angle was found to be 45.5° which decreases to 30.9° at 129°C while in 4F6R at 64°C tilt angle was found to be 42.1° which decreases to 30.2° at 124°C . Thus both the compounds may behave as orthoconic antiferroelectric liquid crystals. Slight discontinuity in tilt is observed at SmC_A^* to SmC^* transition in 4F6R. Tilt angles were also determined optically and have also been depicted in Figure 5.6 and Figure 5.7 for comparison with X-ray tilt. Optical tilts reflect the angle between the direction of molecular core and the layer normal, since the principal axis of indicatrix coincides with the core direction. On the other hand, X-ray tilts determined by the ratio of the layer thickness in SmC^* phase to the most extended molecular length, are related to the average direction of total populations of electrons of the molecules. Moreover, it is difficult to ascertain the effect of change in molecular conformation in the FLC phase on the most extended molecular length in an isolated molecule. Thus X-ray tilt is usually found to be larger than optical tilt, which is found to be true in both the compounds. On the other hand, in a structurally similar compound with only an additional

carboxylate group in between the phenyl group and the chiral centre, the optical tilt was found to be near 45° and higher than that calculated from small-angle X-ray diffraction [41,42]. It might be mentioned here that high tilt materials are suitable for total internal reflection based microoptic switch for multimode fiber and for display devices with gray scale capability under proper surface anchoring condition [43-45].

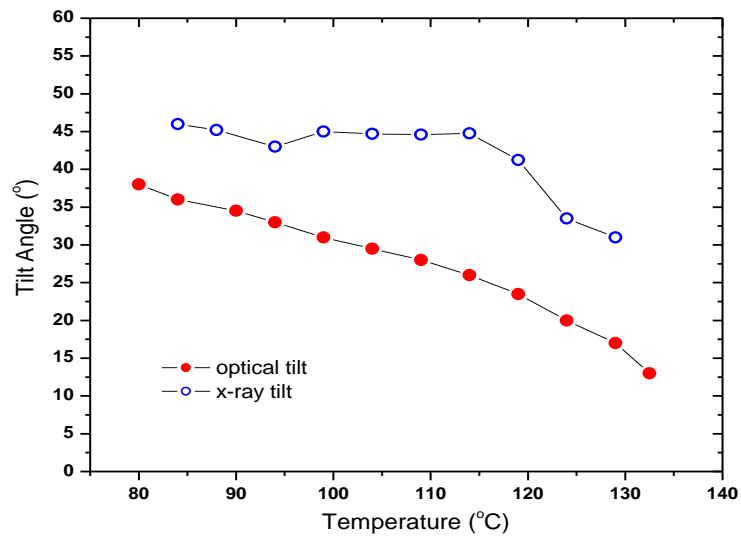


Figure 5.6: Temperature variation of X-ray and optical tilt of 4F3R

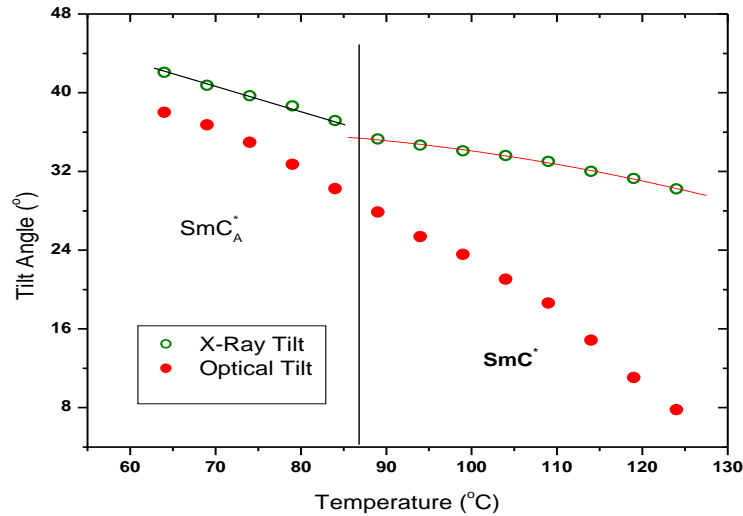


Figure 5.7: Temperature variation of X-ray and optical tilt of 4F6R

5.4.3 Frequency dependent dielectric relaxation study

Observed real (ϵ') and imaginary (ϵ'') parts of dielectric constants as function of frequency at different temperature for the two compounds are shown in Figure 5.8 and Figure 5.9. As a representative example, dielectric spectra in the SmC^* phase fitted to Cole-Cole function for 4F3R is shown in Figure 5.10. Separate contribution of each relaxation mode and conductivity are also shown in the figure along with the fitted parameters. Since real and imaginary parts of dielectric constants are related through Kramers-Kronig relations, Cole-Cole plot of the same data is shown in Figure 5.11, which shows that the fitting was good. Only one absorption peak (strong in 4F3R than in 4F6R) was observed in SmC^* phase which was found to be suppressed when a bias voltage of 15 Volt was applied. This absorption process is, therefore, definitely associated with GM relaxation mode. Absorption peak at around 600 kHz was observed at all temperatures which were presumed due to ITO. No SM process is observed, even when a dc bias field was applied in addition to the measuring field, due to non-existence of SmA^* phase in the two compounds. It is very unlikely that coincidence of SM critical frequency with ITO mode at all temperatures even with bias is the cause for non-observance of SM. It is clear from the figure that only GM relaxation was observed in the ferroelectric phase which persists in the antiferroelectric phase.

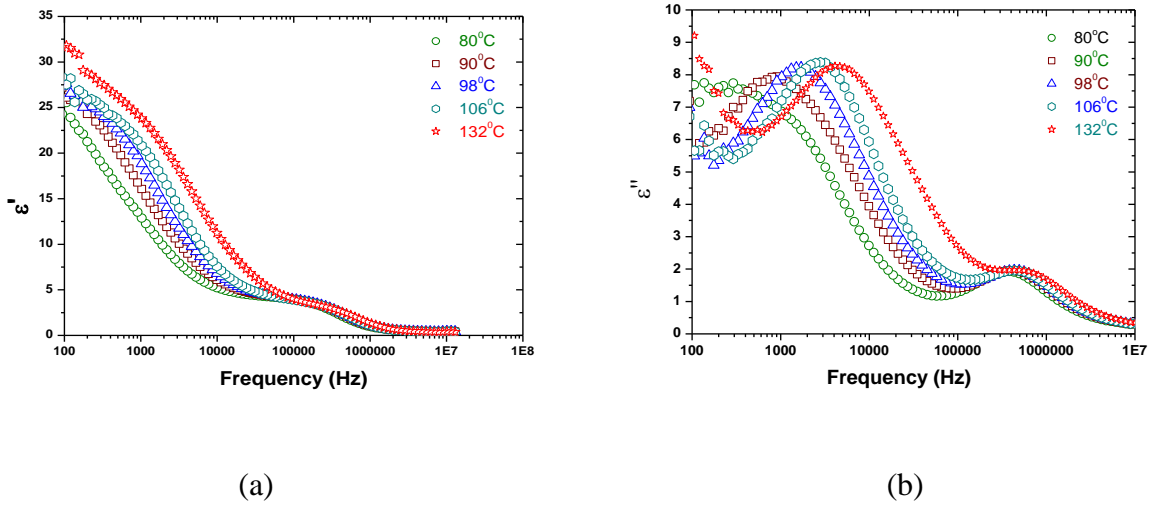


Figure 5.8: (a) Real (ϵ') and (b) imaginary part (ϵ'') of dielectric constant as function of frequency at selected temperatures of 4F3R

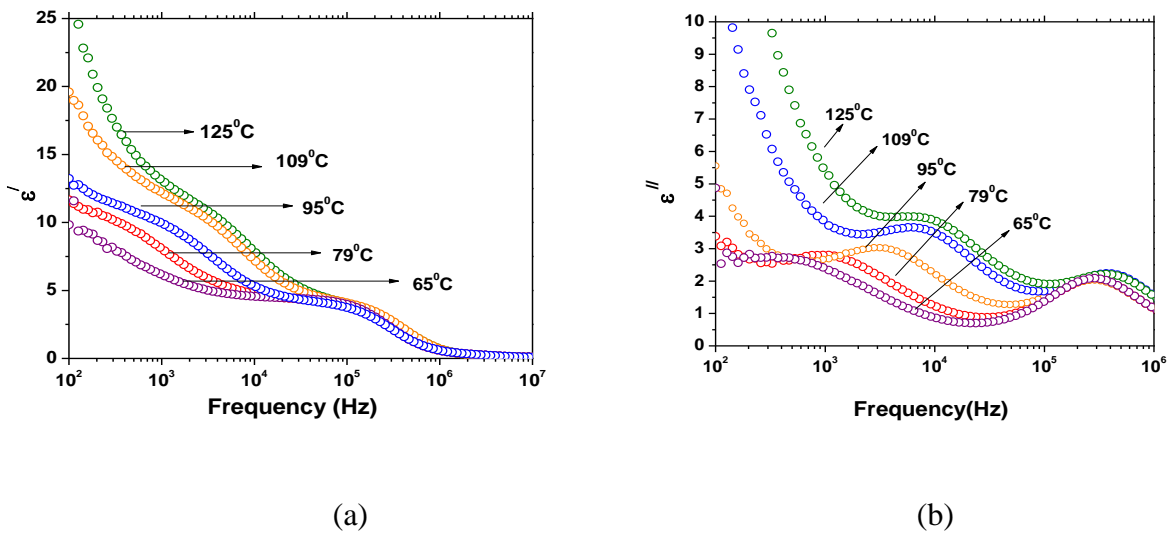


Figure 5.9: (a) Real (ϵ') and (b) imaginary part (ϵ'') of dielectric constant as function of frequency at selected temperatures of 4F6R

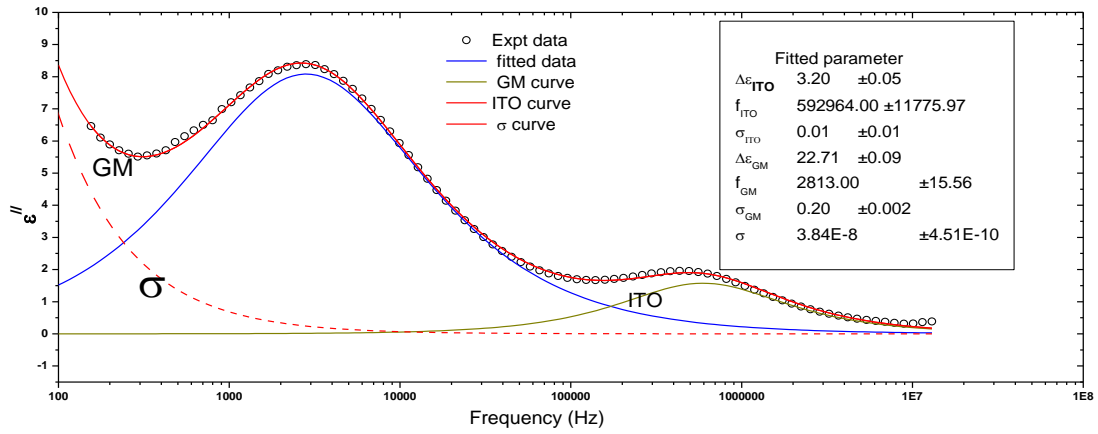


Figure 5.10: Fitted spectra in SmC* phase (106°C) of 4F3R along with observed data. GM, ITO and σ curves are also shown separately along with fitted parameters

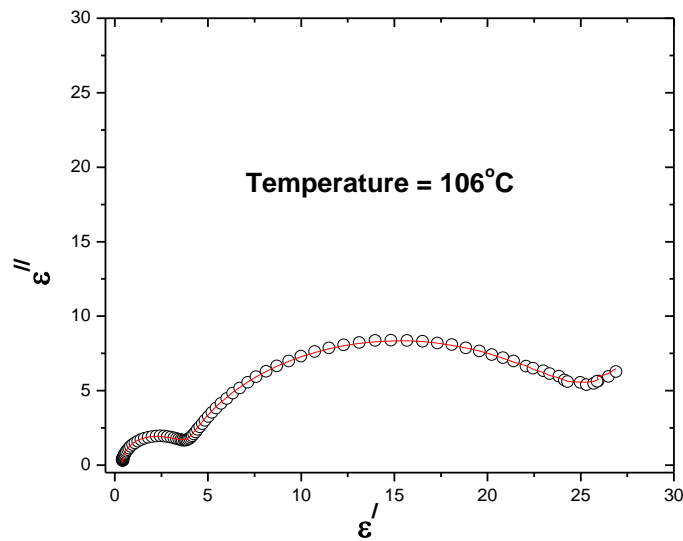


Figure 5.11: Cole-Cole plot of 4F3R

From the Landau model concept of soft mode was first introduced to the SmA*-SmC* phase transition by Blinc and Zeks [46] for the case of a modulated structure and later modified

by Carlsson *et al.* [47] where phase transition was described in terms of two order parameters – two-component tilt vector as primary order parameter and two-component in-plane polarization as the secondary order parameter. Two characteristic modes are observed in SmA*-SmC* second order phase transition where the continuous symmetry group of SmA* (D_∞) is spontaneously broken in SmC*(C_2). Whereas the soft mode is a symmetry breaking mode, which critically slows down (softens) on approaching the phase transition from above; the Goldstone mode is zero frequency mode that tries to restore the broken symmetry. Thus soft mode splits into the phase (GM) and amplitude (SM) modes in SmC* near the transition. According to Clark and Lagerwall [48], in majority of the reported cases, SmC* phase is formed by cooling from the SmA* phase through a second-order phase transition, whereas when SmC* phase is created directly from the nematic or from the isotropic liquid phase, layers of tilted molecules have to appear directly at the transition, which makes the transition first order. Since in the present compounds SmC* phase is created directly from isotropic phase, nature of phase transition is first order (as is revealed from the clearing point enthalpy and temperature dependence of both the primary and secondary order parameters), so theoretically no soft mode is expected which is confirmed by the present experiment. This is further supported by the fact that a higher homologue of the series viz., 7F3R which forms SmA* on heating the SmC* phase exhibits soft mode relaxation behaviour [49]. For two reasons it may not be proper to argue that the absence of SmA* phase is only because of the fluorinated ester unit in the achiral terminal chain of the molecules. First, from reference 15 it is observed that three other homologous members (1F3R, 2F3R AND 7F3R) of the present compounds also exhibit SmA* phase and second, another series of compounds having same rigid core but with achiral alkoxy chain exhibit N* phase above SmC* [50]. Rather the conformational change of the molecules especially with respect to the fluorinated ester unit having intervening oligomethylene spacer and consequence change in the dipole-dipole interaction between the molecules is probably the reason for the destabilization of SmA* phase and hence the absence of the soft mode in the dielectric relaxation behaviour.

Moreover, under a strong bias field, appearance of a residual mode usually at higher frequency, known in literature as domain mode [51–53] is also discussed for compounds having $P_s > 50 \text{ nC/cm}^2$, but no such mode is observed in the present case. This may be due to less P_s in the present compounds discussed below. It is also not clear whether presence of SM in SmC* and SmA* phases is a prerequisite for the detection of the domain mode, because in all the above

referred compounds SM was present in both the phases. As transitional effect, phase fluctuation is found to persist a few degrees above $\text{SmC}^*\text{-I}$ transition in the dielectric spectra. However, in the crystalline phase only ITO absorption peak is observed in the studied frequency window, signifying complete freezing of molecular motions.

Variations of dielectric increment and relaxation frequency as function of temperatures are shown in Figure 5.12 and Figure 5.13 for the compounds 4F3R and 4F6R respectively. A sharp discontinuity in $\Delta\epsilon$ is observed at $\text{SmC}_A^* - \text{SmC}^*$ transition as expected, but magnitude of $\Delta\epsilon$ in SmC_A^* phase is quite large (~ 6) which is usually of the order of one or at the most two as reported in literature for typical SmC_A^* [54-56] or for its variant like $\text{SmC}_A^*(1/3)$ and $\text{SmC}_A^*(1/2)$ phases [57]. Repetition of relaxation experiments with different cells confirmed the above observation. It is not possible to give any definite explanation for this, however, it may be thought that due to surface interactions under the confined geometry of thin dielectric cell (4.2 μm), the material is probably showing ferrielectric type behavior although in bulk it shows antiferroelectric phase. This is supported by the fact that in SmC_A^* phase only GM like absorption mode is observed instead of low frequency P_L and high frequency P_H modes which are usually observed in SmC_A^* phase. Dielectric increment ($\Delta\epsilon$) is found to increase considerably with temperature. In compound 4F3R it increases from 15.1 (80 $^\circ\text{C}$) to 25.8 (132 $^\circ\text{C}$), rate of increment is faster up to 110 $^\circ\text{C}$, where as in 4F6R it increases from 5.62 (61 $^\circ\text{C}$) to 6.51 (85 $^\circ\text{C}$) in SmC_A^* phase and further increases from 9.06 (87 $^\circ\text{C}$) to 12.93 (127 $^\circ\text{C}$) in SmC^* phase. Such increase has been reported in several FLC compounds [58-60]. Increase of dielectric strength with temperature in SmC^* may be explained if one assumes stronger biquadratic coupling between tilt and polarization compared to bilinear one in the expression for free energy density in generalized Landau model [32]. But in such situation, $\Delta\epsilon$ should decrease near transition temperature (T_c), which is not observed in the present study. Moreover, critical absorption frequency (f_c) is also found to increase considerably with temperature. Observed f_c for 4F3R increases from 331 Hz to 4751 Hz, where as for 4F6R it increases from 181Hz to 6738Hz. However, for both the compounds near $\text{SmC}^*\text{-I}$ transition f_c decreases slightly. In the literature both temperature independent f_c [53,58,59,61,62] and increase of f_c with temperature [60,63,64] are reported in pure and FLC mixtures. Although according to generalized Landau model critical frequency (f_c) of GM does not depend on temperature unlike that of SM which depends linearly

on $(T-T_C)$, GM critical frequency depends on modified elastic constant (K_Φ) and rotational viscosity (γ_G) of azimuthal motion and wave vector (q) of the helical pitch ($q=2\pi/p$, p =pitch of helix) in accordance with the relation $f_c = K_\Phi q^2 / (2\pi\gamma_G)$, it is expected that f_c will somehow depend on temperature as K_Φ , γ_G and q are functions of temperature.

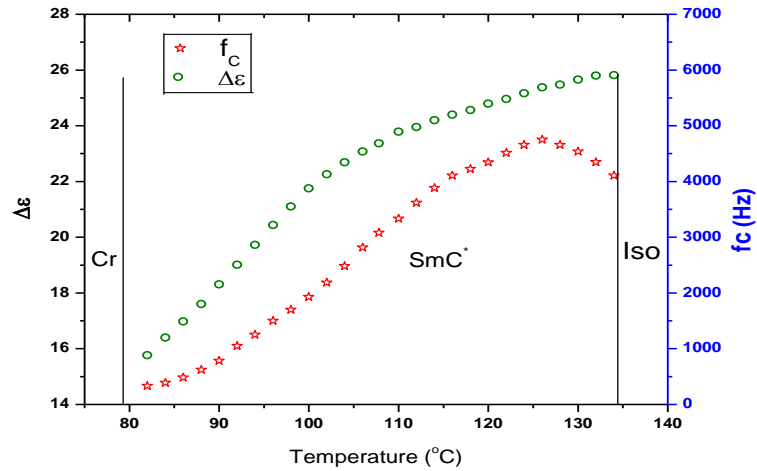


Figure 5.12: Variation of dielectric increment ($\Delta\epsilon$) and Goldstone mode relaxation frequency (f_c) as a function of temperature for 4F3R

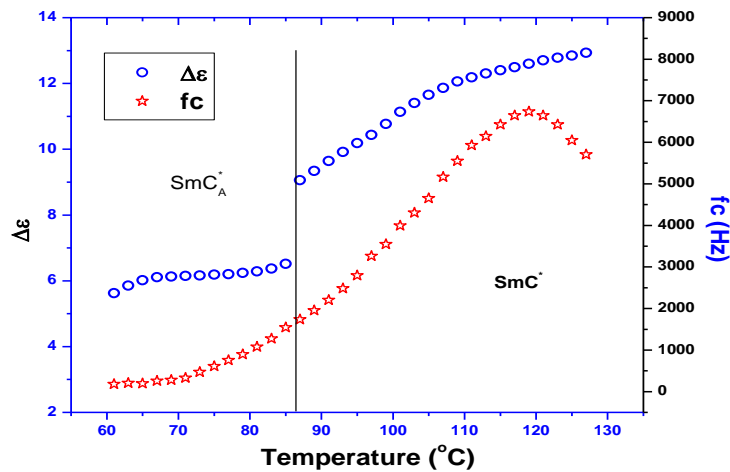


Figure 5.13: Variation of dielectric increment ($\Delta\epsilon$) and Goldstone mode relaxation frequency (f_c) as a function of temperature for 4F6R

Strength of the absorption is found to be nearly constant (around 8) throughout the ferroelectric phase of 4F3R whereas in 4F6R it varies in between 3-5. Much stronger absorption (about 35) was reported in $C_6F_{13}CH_2CH_2O-Ph-Ph-COO-Ph-COO-CH(CH_3)C_6H_{13}$ and $C_5H_{11}COO(CH_2)_6-O-Ph-Ph(2' 3' F)-Ph-COO-CH(CH_3)-C_6H_{13}$ [65,60]. Thus the investigated compounds will absorb, over a frequency range of a few hundred hertz to a few thousand hertz, far less energy from the input signal compared to the above two similar compounds.

5.4.4 Spontaneous Polarization

Spontaneous polarisation (P_S) was measured as a function of temperature. The input triangular pulse and output signal across a standard resistance in series with the liquid crystal cell captured in a digital oscilloscope are shown in Figure 5.14. From the polarization peak area P_S was calculated. P_S in the low temperature regime of SmC^* phase is about 8 nC/cm^2 higher in 4F6R compared to 4F3R. This is expected since 4F6R possess higher dipole moment. As depicted in Figure 5.15 and Figure 5.16, spontaneous polarization decreases slowly with temperature for both the compounds. In 4F3R it is found to decrease from 41.66 nC/cm^2 (75°C) to 16.66 nC/cm^2 (138°C) where as in 4F6R it decreases from 51.26 nC/cm^2 (61°C) to 17.28 nC/cm^2 (127°C). P_S values of this range is within acceptable limits for various applications especially from the point of switching time [29,66]. No discontinuity at the $SmC_A^*-SmC^*$ transition was observed, similar behaviour has been reported in other AFLCs [67].

For comparison it may be pointed out, compounds with similar backbone, only with different fluorinated carboxylate chain (Viz. $C_4F_9COO-(CH_2)_6$ and $C_5F_{11}COO-(CH_2)_6$) exhibit P_S of about 50 nC/cm^2 near $Cr-SmC^*$ transition but when longer fluorinated chain $C_8F_{17}COO-(CH_2)_2$ is introduced P_S increases to about 93 nC/cm^2 [14]. On the introduction of another carboxylate group in between the phenyl group and the chiral centre, P_S drastically increases to above 200 nC/cm^2 [12,65]. A partially fluorinated terphenyl based AFLC compound [$C_5F_{11}COO(CH_2)_6-O-Ph-Ph(2' 3' F)-Ph-COO-CH(CH_3)-C_6H_{13}$] showed P_S value 118.7 nC/cm^2 [60]. Thus both the core structure and chain length have pronounced effect on the magnitude of spontaneous polarization.



(a)



(b)

Figure 5.14: Input and output signals captured in a digital oscilloscope for (a) 4F3R and (b) 4F6R

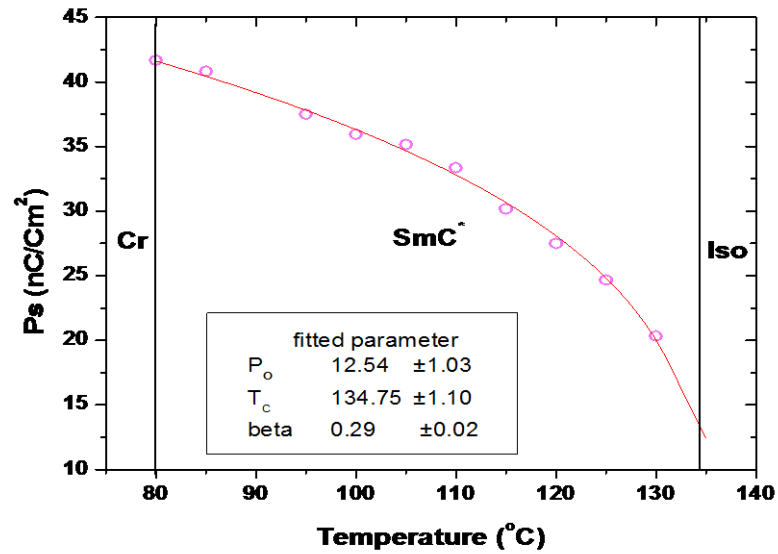


Figure 5.15: Temperature dependence of P_S of 4F3R. Mean field fitted curve is also shown

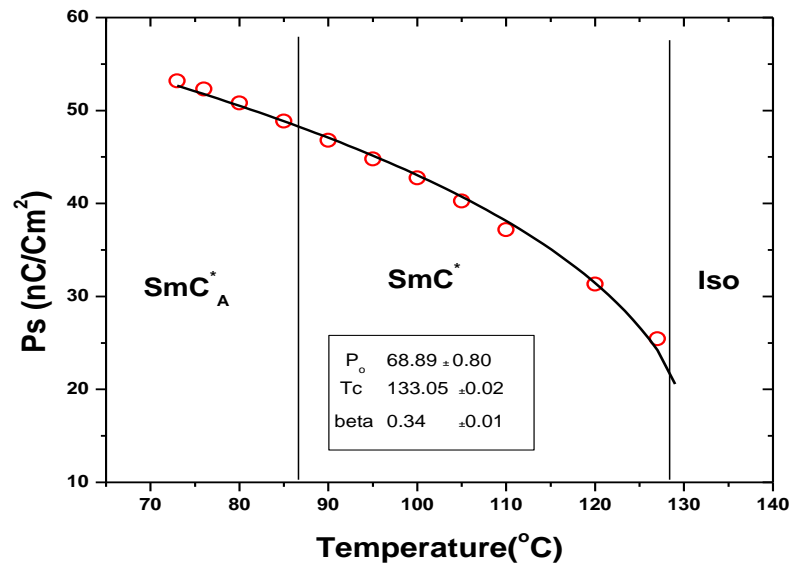


Figure 5.16: Temperature dependence of P_S of 4F6R. Mean field fitted curve is also shown

Moreover, measured P_S data were found to fit nicely to the mean-field model $P_S = P_0 (T_C - T)^\beta$ where T_C is the SmC^* to isotropic transition temperature and β is the critical exponent for the secondary order parameter P_S [68]. In 4F3R fitted T_C was found to be within 0.5 degree of the

observed critical temperature whereas it is within 5 degree in 4F6R. However, fitted β -value for the two cases are found to be 0.29 and 0.34 which deviate significantly from the mean field value (0.5), signifying the SmC^* to isotropic transition is not second order in nature according to Ehrenfest's classification, rather it is strongly first order. Observed change in enthalpy at SmC^* -I transition supports this view. Similar observation was reported before in ferroelectric phases of epoxy compounds [69]. As noted before this is also consistent with the general observation by Clark and Lagerwall [48] that when SmC^* phase is created directly from the nematic or from the isotropic phase, layers of tilted molecules have to appear directly at the transition, which makes the transition first order.

5.4.5 Rotational Viscosity and Activation Energy

Rotational viscosity (γ_ϕ), which is related to rotations of the molecular directors about the SmC^* cone, is one of the most important parameters of the SmC^* phase and strongly influences the switching time between the field-induced states of FLCs. Rotational viscosity (γ_ϕ) was determined using the following relationship derived from the generalized Landau model [32]:

$$\gamma_\phi = \frac{1}{4\pi\epsilon_0} \frac{1}{\Delta\epsilon f_c} \left(\frac{P_s}{\theta} \right)^2$$

where Goldstone mode dielectric strength ($\Delta\epsilon$) and relaxation frequency (f_c) were obtained from dielectric relaxation study and tilt angle (θ) was obtained from SAXS measurements. A similar expression was used to find its value in SmC_A^* for the compound 4F6R. γ_ϕ in SmC_A^* phase of 4F6R is about 5 times more than the highest value in SmC^* phase in 4F3R. Thus increased oligomethylene spacer group increases viscosity to a large extent. Variation of γ_ϕ with temperature is shown in Figure 5.17 and Figure 5.18 for the two compounds. It is observed that within a span of 10^0C , the rotational viscosity of 4F3R falls to about one fourth of its value near Cr- SmC^* transition, thereafter, it remains almost constant. In 4F6R also viscosity decreases quite fast with temperature in a non-linear manner, rate of decrement is different in antiferroelectric and ferroelectric phases. Moreover, rotational viscosity was found to obey following Arrhenius relationship:

$$\gamma_{\phi} \propto e^{\frac{E_a}{k_{\beta}T}}$$

where E_a is the activation energy for the molecular rotation on the cone when the AC field is applied to the FLC material and k_{β} is the Boltzmann constant. From a linear least squares fit of the plot of $\ln \gamma_{\phi}$ versus inverse temperature, activation energy was calculated. The activation energies are found to be $97.09 \text{ kJ mol}^{-1}$ and $105.04 \text{ kJ mol}^{-1}$ in 4F3R and 4F6R respectively. In a terphenyl based AFLC compound [60], the activation energy was found to be $48.14 \text{ kJ mol}^{-1}$, which is almost half of the activation energy of 4F3R. Optimizing the geometry of the above AFLC compound using Hyperchem it is found that its dipole moment is only 1.70 D, considerably less than the dipole moment of 4F3R (4.25D) and 4F6R (5.75D). Stronger dipole-dipole interaction between molecules of 4F3R and 4F6R may be responsible for higher activation energy.

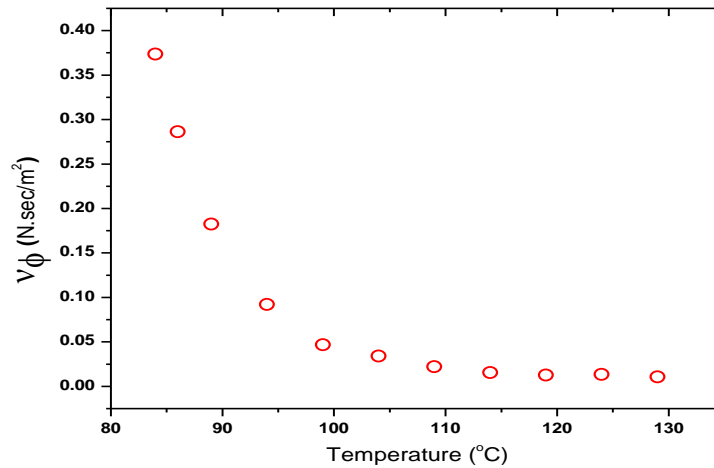


Figure 5.17: Variation of rotational viscosity (γ_{ϕ}) with temperature of 4F3R

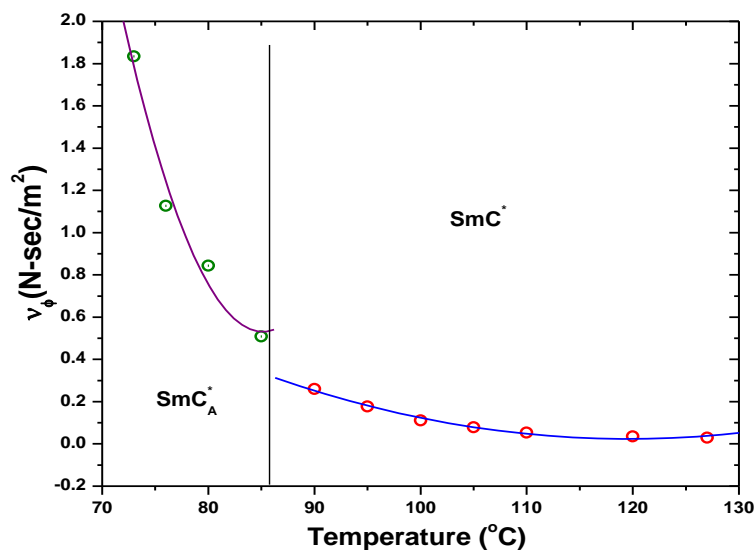


Figure 5.18: Variation of rotational viscosity (γ_ϕ) with temperature of 4F6R

5.4.6 Response Time

Electrical response time is a very important parameter for a display device. It is basically the time taken by the liquid crystalline samples to respond to an external electrical pulse. The compounds show very fast switching. The low value of electrical response time is basically due to the large Ps and low rotational viscosity possessed by the compounds. In 4F3R the response time varies from 24-88 μs in SmC^{*} phase, whereas in 4F6R it varies 235-595 μs in SmC_A^{*} and 117-223 μs in SmC^{*} phase. This is expected since the compound 4F6R possesses longer chain length than compound 4F3R which creates more hindrance in switching as well as responding to the external pulse. In other words slower response in 4F6R is due to higher viscosity. Temperature variations of electrical response time are shown in Figure 5.19 and Figure 5.20. It was found to decrease monotonically with increasing temperature, which is due to faster decrease of rotational viscosity (making the rotation of the molecules around the tilt cone easier) compared to spontaneous polarization. At this point it is worth to see how the response time changes with molecular cores and fluorination in chain or core. In a biphenyl based non-fluorinated FLC compound with ester group on both sides of core it was found to be of the order of a few millisecond [70], in a compound obtained with the addition of another mono-fluorinated

phenyl group in the above core structure response time was found to vary between 150-600 μs [62], in a terphenyl based non-fluorinated compound with similar core structure as of 4F3R reported response time is around 3 μs [71], in a terphenyl based fluorinated compound but with different core structure it is reported as 6-22 μs [72] and in a FLC mixture it was found to vary between 25-55 μs [64].

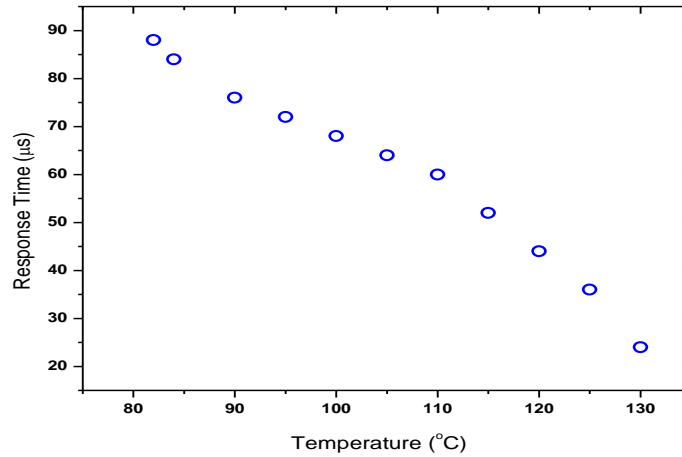


Figure 5.19: Variation of response time with temperature of 4F3R

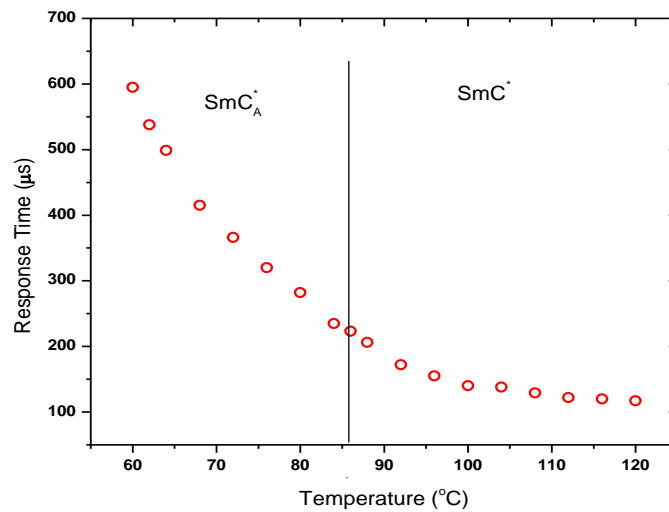
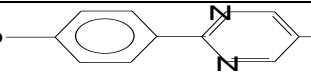
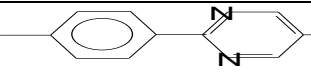
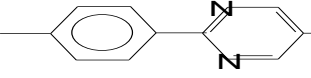
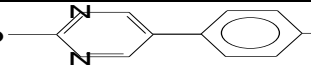


Figure 5.20: Variation of response time with temperature of 4F6R

5.5 ROOM TEMPERATURE MIXTURE FORMULATION

Although ferroelectric SmC^* phase in 4F3R is very broad but it is formed at quite high temperature (79.8°C), situation further deteriorates in 4F6R. In order to get SmC^* phase at low temperatures we first formulated a host mixture, having tilted SmC phase, by mixing four phenyl pyrimidine based compounds, of which two exhibit SmC and SmA phases and other two form nematic phase in addition. Phase sequence and transition temperatures of the host mixture was found to be 19°C SmC 69.4°C SmA 78.7°C N 81.2°C I . Compound 4F3R as dopant could induce ferroelectric SmC^* phase in the above host mixture at temperature even below ambient temperature, observed phase sequence being $\text{Cr} < 12.5^\circ\text{C}$ SmC^* 68.5°C SmA^* 88.6°C I . Alignment of the mixture in bookshelf geometry in a display cell will be easier because of the presence of SmA^* phase in the mixture above SmC^* phase, thus the mixture is expected to be a promising room temperature FLC mixture. The weight percentage of the host compounds along with their transition temperatures are given in the Table 5.3.

Table 5.3: Weight percentage and transition temperatures of host compounds

Name	Structure with Transition Temperature	Weight percentage
Host 1(9OCPO9)	$\text{C}_9\text{H}_{19}\text{O}$ —  $\text{Cr } 61.8^\circ\text{C}$ $\text{SmC } 95.6^\circ\text{C}$ $\text{SmA } 99.1^\circ\text{C}$ I	20%
Host 2 (7OCPO9)	$\text{C}_7\text{H}_{15}\text{O}$ —  $\text{Cr } 57.4^\circ\text{C}$ $\text{SmC } 95.1^\circ\text{C}$ $\text{SmA } 98.4^\circ\text{C}$ I	20%
Host 3 (9OCPO7)	$\text{C}_9\text{H}_{19}\text{O}$ —  $\text{Cr } 57.2^\circ\text{C}$ $\text{SmC } 79.1^\circ\text{C}$ $\text{SmA } 91.2^\circ\text{C}$ $\text{N } 94.7^\circ\text{C}$ I	20%
Host 4 (6OCPO8)	$\text{C}_8\text{H}_{17}\text{O}$ —  $\text{Cr } 27.5^\circ\text{C}$ $\text{SmC } 46.3^\circ\text{C}$ $\text{SmA } 57.5^\circ\text{C}$ $\text{N } 65.6^\circ\text{C}$ I	40%

Mixture Composition: Host (60%) + Dopant 4F3R (40%)

5.6 CONCLUSION

Optical polarizing microscopy, dielectric and electrooptic measurements confirm that the compound 4F3R possesses only ferroelectric SmC^* phase over a broad temperature range whereas compound 4F6R possesses both anti-ferroelectric SmC_A^* phase and ferroelectric SmC^* phase over a considerable temperature range. Both the compounds directly goes to isotropic phase from SmC^* phase which is not common in FLCs. Dipole moment of 4F6R is found to be substantially higher than that of 4F3R which might be the result of change of molecular conformation due increased oligomethylene spacer group. X-ray study reveals that the layer spacing in antiferroelectric and ferroelectric smectic phases show a slightly increasing trend where as average intermolecular distance remains almost constant. Clear discontinuities are observed at $\text{SmC}_A^*-\text{SmC}^*$ transition in 4F6R while studying the temperature variation of layer spacing, x-ray tilt, dielectric increment and rotational viscosity. Only Goldstone mode relaxation behavior is observed in both the compounds, increase of its dielectric strength and critical frequency with temperature has been explained in the light of generalized Landau model. Fitted data shows that the GM mode is of the Cole–Cole type. No soft mode is observed since the compound directly melts into isotropic phase. The fact that the compounds show quite strong dipole moments, about 45° tilt angle, moderately strong polarization, low viscosity, micro-second range switching and are capable of forming room temperature ferroelectric phase in appropriate host mixture make them suitable from application point of view.

5.7 REFERENCES

- [1] R. B. Meyer, Paper presented at the 5th Int. Liquid Crystal Conf., Stockholm, June, (1974); R. B. Meyer, L. Liebert, L. Strzelecki and P. Kelker, *J Phys (Paris) Lett.*, 36, L69 (1975), Ferroelectric liquid crystals.
- [2] A. D. L. Chandani, Y. Ouchi, H. Takezoe, A. Fukuda, K. Terashima, K. Furukawa and A. Kishi; *Jpn. J. Appl. Phys. Part 2*, 28, L1261 (1989), Novel Phases Exhibiting Tristable Switching.
- [3] Y. Iozaki, T. Fujikawa, H. Takezoe, A. Fukuda, T. Hagiwara, Y. Suzuki and I. Kawamura, *Phys. Rev. B*; 48, 13439 (1993), Devil's staircase formed by competing interactions stabilizing the ferroelectric smectic-C* phase and the antiferroelectric smectic-C_A* phase in liquid crystalline binary mixtures.
- [4] J. P. F. Lagerwall, D. D. Parghi, D. Krueker, F. Gouda, and P. Jagemalm, *Liq. Cryst.*, 29, 163 (2002), Phases, phase transitions and confinement effects in a series of antiferroelectric liquid crystals.
- [5] J. P. F. Lagerwall, P. Rudquist, and S.T. Lagerwall; *Liq. Cryst.*, 30, 399 (2003), On the phase sequence of antiferroelectric liquid crystals and its relation to orientational and translational order.
- [6] E. Gorecka, D. Pocięcha, M. Čepič, B. Žekš, R. Dabrowski; *Phys. Rev. E*, 65, 061703 (2002), Enantiomeric excess dependence of the phase diagram of antiferroelectric liquid crystals.
- [7] I. C. Sage, Applications, in: D. Demus, J. Goodby, G.W. Gray, H.W. Spiess, V. Vill (Eds.), *Handbook of Liquid Crystals Vol. I – Fundamentals*, Wiley-Vch., Weinheim, pp. 731-762 (1998).
- [8] M. Hird; *Liq. Cryst.*, 38, 1467–1493 (2011), Ferroelectricity in liquid crystals-materials, properties and applications.
- [9] P. J. Collings, Ferroelectric liquid crystals: The 2004 Benjamin Franklin Medal in Physics presented to Robert B. Meyer of Brandeis University, *J. Frankl. Inst.* 342, 599–608 (2005).
- [10] J. Wen, M. Tian, Q. Chen, *Liq. Cryst.* 16, 445-453 (1994), Novel fluorinated liquid crystals. II. The synthesis and phase transitions of a novel type of ferroelectric liquid crystals containing 1,4-tetrafluorophenylene moiety.

- [11] Y. Xu, W. Wang, Q. Chen, J. Wen; *Liq. Cryst.*, 21, 65-71 (1996), Synthesis and transition temperatures of novel fluorinated chiral liquid crystals containing 1,4-tetrafluorophenylene units.
- [12] R. Dąbrowski, J. Gąsowska, J. Otón, W. Piecek, J. Przedmojski, M. Tykarska; High tilted antiferroelectric liquid crystalline materials, *Disp.* 25, 9-19 (2004).
- [13] R. Dąbrowski, P. Kula, Z. Raszewski, W. Piecek, J. M. Otón, A. Spadło; *Ferroelectrics*, 395 116-132 (2010), New orthoconic antiferroelectrics useful for applications.
- [14] D. Ziobro, R. Dąbrowski, M. Tykarska, W. Drzewiński, M. Filipowicz, W. Rejmer, K. Kuśmierek, P. Morowiak, W. Piecek; *Liq. Cryst.* 39, 1011-1032 (2012), Synthesis and properties of new ferroelectric and antiferroelectric liquid crystals with a biphenyl benzoate rigid core.
- [15] H. T. Nguyen, J. C. Rouillon, A. Babeau, J. P. Marcerou, G. Sigaud; *Liq. Cryst.* 26, 1007-1019 (1999), Synthesis, properties and crystal structure of chiral semiperfluorinated liquid crystals with ferro and anticlinic smectic phases.
- [16] R. Dabrowski, *Ferroelectrics*, 243, 1-18 (2000), Liquid crystals with fluorinated terminal chains and antiferroelectric properties.
- [17] S. Seomun, T. Gouda, Y. Takanishi, K. Ishikawa, H. Takezoe; *Liq. Cryst.* 26, 151-161(1999), Bulk optical properties in binary mixtures of antiferroelectric liquid crystal compounds showing V-shaped switching.
- [18] J. V. Selinger, P. J. Collings, R. Shashidhar; *Phys. Rev. E* 64, 061705/1-9 (2001), Field-dependent tilt and birefringence of electroclinic liquid crystals: Theory and experiment.
- [19] W. M. Zoghaib, C. Carboni, A. K. George, S. AL-Manthari, A. Al-Hussaini, F. Al-Futaisi, , *Mol. Cryst. Liq. Cryst.* 542, 123–131 (2011), Novel fluorinated ferroelectric organosiloxane liquid crystals.
- [20] J. Naciri, C. Carboni, A. K. George; *Liq. Cryst.*, 30, 219-225 (2003), Low transition temperature organosiloxane liquid crystals displaying a de Vries smectic A phase.
- [21] J. Naciri, J. Ruth, G. Crawford, R. Shashidhar, B. R. Ratna; *Chem. Mater.*, 7, 1397-1402 (1995), Novel ferroelectric and electroclinic organosiloxane liquid crystals.

- [22] J. Dziaduszek, R. Dabrowski, K. Czuprynski, N. Bennis; *Ferroelectrics.*, 343, 3–9 (2006), Ferroelectric Compounds with Strong Polar Cyano Group in Terminal Position.
- [23] Z. Li, P. Salamon, A. Jakli, K. Wang, C. Qin, Q. Yang, C. Liu and J. Wen; *Liq. Cryst.*, 37 427–433 (2010), Synthesis and mesomorphic properties of resorcylic di[4-(4-alkoxy-2,3-difluorophenyl)ethynyl] benzoate liquid crystals.
- [24] Y. Yang, H. Li, J. Wen; *Liq. Cryst.*, 34, 975-979 (2007), Synthesis and mesomorphic properties of chiral fluorinated liquid crystals.
- [25] N. Shiratori, A. Yoshizawa, I. Nishiyama M. Fukumasa, A. Yokoyama, T. Hirai, M. Yamane; *Mol. Cryst. Liq. Cryst.* 199, 129-140 (1991), New Ferroelectric Liquid Crystals Having 2-Fluoro-2-Methyl Alkanoyloxy Group.
- [26] A. Fafara, B. Gestblom, S. Wróbel, R. Dabrowski, W. Drzewiński, D. Kilian, W. Haase; *Ferroelectrics*, 212, 79-90 (1998), Dielectric spectroscopy and electrooptic studies of new MHPOBC analogues.
- [27] D. M. Potukuchi, A. K. George, C. Carboni, S. H. Alharthi, J. Naciri; *Ferroelectrics*, 300, 79-93 (2004), Low Frequency Dielectric Relaxation, Spontaneous Polarization, Optical Tilt Angle and Response Time Investigations in a Fluorinated Ferroelectric Liquid Crystal, N125F2(R*).
- [28] D. M. Potukuchi, A. K. George; *Mol. Cryst. Liq. Cryst.*, 487, 92–109 (2008), Phase Transitions and Characterization in a Chiral Smectic- $A_{de\ Vries}$ Liquid Crystal by Low-Frequency Dielectric Spectroscopy.
- [29] P. K. Mandal, S. Haldar, A. Lapanik, W. Haase; *Jpn. J. Appl. Phys.*, 48, 011501-6 (2009), Induction and enhancement of ferroelectric smectic C* phase in multi-component room temperature mixtures.
- [30] K. Hiraoka, A. Taguchi, Y. Ouchi, H. Takezoe and A. Fukuda; *Jpn. J. Appl. Phys.*, 29, 1473-1476 (1990), Electric-Field-Induced Transitions among Antiferroelectric, Ferroelectric and Ferroelectric Phases in a Chiral Smectic MHPOBC.

- [31] A. M. Biradar, S. Wróbel, and W. Haase; *Phys. Rev. A*, 39, 2693-2702 (1989), Dielectric relaxation in the smectic-A* and smectic-C* phases of a ferroelectric liquid crystal.
- [32] T. Carlsson, B. Zeks, C. Filipic, A. Levstik; *Phys. Rev. A*, 42, 877-889 (1990), Theoretical model of the frequency and temperature dependence of the complex dielectric constant of ferroelectric liquid crystals near the smectic-C* - smectic-A phase transition.
- [33] B. Zeks, M. Cepic, in *Relaxation Phenomena: Liquid Crystals, Magnetic Systems, Polymers, High-TC Superconductors, Metallic Glasses*; W. Haase, S. Wrobel, Eds. Springer Verlag: Berlin-Heidelberg, p 477 (2003).
- [34] M. Buivydas, F. Gouda, S. T. Lagerwall, B. Stebler; *Liq. Cryst.*, 18, 879-886 (1995), The molecular aspect of the double absorption peak in the dielectric spectrum of the antiferroelectric liquid crystal phase.
- [35] Hyperchem 6.03, Hypercube Inc., Gainesville, FL, USA.
- [36] S. Haldar, S. Barman, P. K. Mandal, W. Haase, R. Dabrowski; *Mol. Cryst. Liq. Cryst.*, 528, 81-95 (2010), Influence of molecular core structure and chain length on the physical properties of nematogenic fluorobenzene derivatives.
- [37] P. Sarkar, P. Mandal, S. Paul, R. Paul, R. Dabrowski, K. Czuprynski; *Liq. Cryst.*, 30, 507-527 (2003), X-ray diffraction, optical birefringence, dielectric and phase transition properties of the long homologous series of nematogens 4-(trans-4'-n-alkylcyclohexyl) isothiocyanatobenzenes.
- [38] D. Sinha, D. Goswami, P. K. Mandal, Ł. Szczucinski, R. Dabrowski; *Mol. Cryst. Liq. Cryst.* 562, 156-165 (2012), On the nature of molecular associations, static permittivity and dielectric relaxation in a uniaxial nematic liquid crystal.
- [39] U. Manna, R. M. Richardson, A. Fukuda, J.K. Vij; *Phys. Rev. E*, 81, 050701-4 (2010), X-ray diffraction study of ferroelectric and antiferroelectric liquid crystal mixtures exhibiting de Vries SmA*-SmC* transitions.

- [40] S. T. Lagerwall, Ferroelectric liquid crystals in : D. Demus, J. Goodby, G.W. Gray, H. W. Spiess, V. Vill (Eds.), Handbook of Liquid Crystals Vol. 2B – Low molecular weight liquid crystals, Wiley-Vch., Weinheim, pp 515-664 (1998).
- [41] W. Piecek, Z. Raszewski, P. Perkowski, J. Przedmojski, J. Kedzierski, W. Drzewinski, R. Dabrowski, J. Zielinski; Ferroelectrics., 310, 125–129 (2004), Apparent tilt angle and structural investigations of the fluorinated antiferroelectric liquid crystal material for display application.
- [42] J. P. F. Lagerwall, A. Saipa, F. Giesselmann, R. Dabrowski; Liq. Cryst. 31, 1175–1184 (2004), On the origin of high optical director tilt in a partially fluorinated orthoconic antiferroelectric liquid crystal mixture.
- [43] K. D'havé, P. Rudquist, S.T. Lagerwall, H. Pauwels, W. Drzewinski, R. Dabrowski; Appl. Phys. Lett., 76, 3528-3530 (2000), Solution of the dark state problem in antiferroelectric liquid crystal displays.
- [44] W. K. Robinson, C. Carboni, P. Kloess, S. P. Perkins, H. J. Coles; Liq. Cryst., 25, 301–307 (1998), Ferroelectric and antiferroelectric low molar mass organosiloxane liquid crystals.
- [45] E. P. Haridas, S. S. Bawa, A. M. Biradar, S. Chandra, Jpn. J. Appl. Phys., 34, 3602-3606 (1995), Anisotropic surface anchoring conditions for gray-scale capability in high-tilt-angle ferroelectric liquid crystal.
- [46] R. Blinc, B. Zeks; Phys. Rev. A. 18, 740-745 (1978), Dynamics of helicoidal ferroelectric smectic-C* liquid crystals.
- [47] T. Carlsson, B. Zeks, C. Filipic, A. Levstik; Physical Review A, 42, 877–889 (1990), Theoretical model of the frequency and temperature dependence of the complex dielectric constant of ferroelectric liquid crystals near the smectic—smectic-A phase transition.
- [48] N. A. Clark, S. T. Lagerwall, Introduction to ferroelectric liquid crystals, in: J.W. Goodby, R. Blinc, N. A. Clark, S. T. Lagerwall, M.A. Osipov, S.A. Pikin, T. Sakurai, K. Yoshino, B. Zeks (Eds), Ferroelectric Liquid Crystals Principles, Properties and Applications, Gordon and Breach, Philadelphia, 1991, pp. 1-97.
- [49] D. Goswami, P. K. Mandal, R. Dabrowski; to be published.

- [50] S. Sato, J. Hatano, S. Tatemori, H. Uehara, S. Saito, E. Okabe; *Mol. Cryst. Liq. Cryst. A* 328, 411-418 (1999), Antiferroelectricity of a Chiral Smectic Liquid Crystal Having Three Isolated Phenyl Rings in the Core.
- [51] M. Marzec, W. Haase, E. Jakob, M. Pfeiffer, S. Wróbel; *Liquid Crystals*, 14, 1967- 1976 (1993), The existence of four dielectric modes in the planar oriented SmC* phase of a fluorinated substance.
- [52] S. Wróbel, G. Cohen, D. Davidov, W. Haase, M. Marzec, M. Pfeiffer; *Ferroelectrics*, 166, 211–222 (1995), Dielectric, electro optic and X-ray studies of a room temperature ferroelectric mixture.
- [53] J. M. Czerwiec, R. Dabrowski, K. Garbat, M. Marzec, M. Tykarska, A. Wawrzyniak, S. Wróbel; *Liquid Crystals*, 39, 1503–1511 (2012), Dielectric and electro-optic behaviour of two chiral compounds and their antiferroelectric mixtures.
- [54] Y. P. Panarin, O. Kalinovskaya, J. K. Vij, and J. W. Goodby; *Phys. Rev. E*, 55, 4345-4353 (1997), Observation and investigation of the ferrielectric subphase with high qT parameter.
- [55] Y. P. Panarin, O. Kalinovskaya, and J. K. Vij; *Liq. Cryst.*, 25, 241-252 (1998), The investigation of the relaxation processes in antiferroelectric liquid crystals by broad band dielectric and electro-optic spectroscopy.
- [56] J. K. Song, U. Manna, A. Fukuda and J. K. Vij; *Appl. Phys. Lett.*, 93, 142903-3 (2008), Antiferroelectric dielectric relaxation processes and the interlayer interaction in antiferroelectric liquid crystals.
- [57] U. Manna, J. K. Song, G. Power, and J. K. Vij; *Phys. Rev. E*, 78, 021711-8 (2008), Effect of cell surfaces on the stability of chiral smectic-C phases.
- [58] U. Manna, J. K. Song, G. Power, J. K. Vij; *Phys. Rev. E*, 78, 021711-8 (2008), Effect of cell surfaces on the stability of chiral smectic-C phases.
- [59] M. Buivydas, F. Gouda, G. Andersson, S. T. Lagerwall, B. Stembler, J. Bomelburg, G. Heppke, B. Gestblom; *Liq. Cryst.*, 23, 723- 739 (1997), Collective and non-collective excitations

in antiferroelectric and ferroelectric liquid crystals studied by dielectric relaxation spectroscopy and electro-optic measurements.

[60] S. Haldar, K. C. Dey, D. Sinha, P. K. Mandal, W. Haase, P. Kula; *Liq. Cryst.*, 39, 1196-1203 (2012), X-ray diffraction and dielectric spectroscopy studies on a partially fluorinated ferroelectric liquid crystal from the family of terphenyl esters.

[61] M. Marzec, A. Mikulko, S. Wrobel, R. Dabrowski, M. Darius and W. Haase; *Liq. Cryst.*, 31, 153–159 (2004), Alpha sub-phase in a new ferroelectric fluorinated compound.

[62] P. Nayek, S. Ghosh, S. Roy, T. P. Majumder, R. Dabrowski; *J. Mol. Liq.* 175, 91–96 (2012), Electro-optic and dielectric investigations of a perfluorinated compound showing orthoconic antiferroelectric liquid crystal.

[63] P. Arora, A. Mikulko, F. Podgornov, W. Haase; *Mol. Cryst. Liq. Cryst.*, 502, 1-8 (2009), Dielectric and electro-optic properties of new ferroelectric liquid crystalline mixture doped with carbon nanotubes.

[64] A. Mikulko, P. Arora, A. Glushchenko, A. Lapanik and W. Haase; *Euro Phys. Lett.*, 87, 27009/1-4 (2009), Complementary studies of BaTiO₃ nanoparticles suspended in a ferroelectric liquid-crystalline mixture.

[65] P. K. Mandal, B. R. Jaishi, W. Haase, R. Dabrowski, M. Tykarska, P. Kula; *Phase Transition*, 79, 223–235 (2006), Optical microscopy, DSC and dielectric relaxation spectroscopy studies on a partially fluorinated ferroelectric liquid crystalline compound MHPO(13F)BC.

[66] W. N. Thurmes, M. D. Wand, R. T. Vohra, K. M. More; *SPIE Conf. Proc.* 3015, 1-7 (1997), FLC materials for microdisplay applications.

[67] M. Marzec, S. Wrobel, E. Gondek, R. Dabrowski; *Mol. Cryst. Liq. Cryst.*, 410, 153–161 (2004), Room Temperature Antiferroelectric Phase Studied by Electrooptic Methods.

[68] F. Gouda, T. Carlsson, G. Andersson, S.T. Lagerwall, B. Stebler; *Liq. Cryst.*, 16, 315-322 (1994), Manifestation of biquadratic coupling in the smectic C* phase soft mode dielectric response.

- [69] M. Marzec, S. Wröbel, S. Hiller, A. M. Biradar, R. Dabrowski, B. Gestblom, W. Haase; *Mol. Cryst. Liq. Cryst.*, 302, 35-40 (1997), Dynamical properties of two ferroelectric phases of epoxy compound.
- [70] R. Eidenschink, T. Geelhaar, G. Andersson, A. Dahlgren, K. Flatischler, F. Gouda, S. T. Lagerwall, K. Skarp; *Ferroelectrics*, 84, 167-181 (1988), Parameter characteristics of a ferroelectric liquid crystal with polarization sign reversal.
- [71] A. K. Srivastava, R. Dhar, V. K. Agrawal, S. H. Lee, R. Dabrowski; *Liq. Cryst.*, 35, 1101–1108 (2008), Switching and electrical properties of ferro- and antiferroelectric phases of MOPB(H)PBC.
- [72] S. Essid, M. Manai, A. Gharbi, J. P. Marcerou, J. C. Rouillon; *Liq. Cryst.*, 32, 307–313, (2005), Electro-optical switching properties for measuring the parameters of a ferroelectric liquid crystal.

CHAPTER 6

OPM, SYNCHROTRON X-RAY DIFFRACTION AND DIELECTRIC STUDY ON A CHIRAL BIPHENYL CARBOXYLATE

Part of the work has been published in Materials Research Express., Vol. 1: pp. 035101–035113, 2014.

6.1 INTRODUCTION

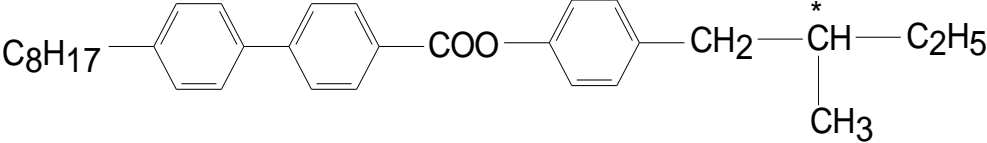
Liquid crystals are an important subclass of soft condensed matter and can be broadly described as ordered fluids formed from geometrically anisotropic molecules. In these self-assembling media on nanoscale level molecular ordering is intermediate between that of the crystalline solid and the isotropic liquid phases. There may be only orientational ordering (nematic) or one dimensional positional ordering with layered structure (smectic). Considering tilt of the constituent molecular long axis (known as director which is the average direction in which the molecules point) from the layer normal, hexatic bond orientational ordering, translational ordering within the smectic layers and interlayer correlation of this ordering [1,2] they are classified into SmA, SmC, SmB_{hex}, SmF, SmI, SmB_{cryst}, SmG, SmJ (SmG'), SmE, SmH and SmK (SmH') where in SmA, SmB_{hex}, SmB_{cryst} and SmE phases molecules are normal to the layers and in the remaining phases molecules are tilted within the layers. When the constituent molecules are chiral and the system is not racemic, tilted smectic phases are designated as SmC*, SmI*, etc; so also the nematic phase as N* (cholesteric phase). In some chiral systems another phase, known as blue phase, appears between the cholesteric phase (N*) and the isotropic phase in a narrow temperature range. Although all these phases are not usually observed in a single compound but some systems exhibit a large variety of them. Liquid crystals are, therefore, considered as an ideal system for studying the phenomena of phase transitions and critical behaviour. The chiral tilted phases also show ferroelectric behavior when the constituent molecules possess permanent dipole moment perpendicular to long axis and close to the chiral centre [3], being the only example of fluid ferroelectrics. However, when the helical structure is stable in free bulk sample, the tilt directions are continuously degenerate and hence there exists no net polarization. In a thin surface stabilized ferroelectric liquid crystal (SSFLC) cell, the helical structure is unwound spontaneously; continuous degeneracy is lifted and results in bistability [4]. Liquid crystalline compound containing blue phase has a number of interesting properties. As mentioned earlier, since blue phases are liquid phases, they exhibit a non-zero elastic shear modulus. The magnitude of the elastic shear modulus is about 10⁶ times smaller than that of a conventional solid [5]. In addition, the blue phases possess higher viscosity than either the helical or isotropic phase [5]. The blue phases have unique optical properties and some physical properties rarely associated with liquids due to their complicated lattice structure of double-twist tubes which make blue phases so fascinating and interesting. Now a days the blue

phase technology is used to obtain a better display of moving images (with frame rates of 100–120 Hz) to improve the temporal response of LCDs. Keeping these in view, a chiral liquid crystal system has been chosen to investigate which exhibit a large variety of tilted hexatic phases as well as blue phases. This is the only non-fluorinated compound investigated in the present dissertation.

6.2 COMPOUND STUDIED

Phase behavior, structure and dynamics of the chiral compound (S)-4-(2'-methylbutyl) phenyl-4-(n-octyl) biphenyl-4-carboxylate (abbreviated as MPOBC) has been studied by employing optical polarizing microscopy, synchrotron X-ray diffraction and frequency dependent dielectric spectroscopy techniques. Molecular structure of the investigated compound along with its abbreviated name and transition temperature (in °C) are given in the table 6.1.

Table 6.1: Molecular structure and phase transition temperatures of MPOBC

Name	Molecular structure with transition temperature
MPOBC	 <p style="text-align: center;">Cr 48 SmG* 63 SmJ* 65 SmF* 67 SmI* 71 SmC* 81 SmA* 136 N* 139 BP* 140 Iso</p>

The compound exhibits, other than crystalline and isotropic phases, four tilted hexatic (SmG^* , SmJ^* , SmF^* , SmI^*), one tilted synclonic phase (SmC^*), one orthogonal smectic phase (SmA^*), cholesteric phase (N^*) and blue phase (BP^*).

6.3 EXPERIMENTAL METHODS

Phase behavior and transition temperatures of MPOBC have been investigated by studying its topological defect structures under an Olympus BX41 polarizing microscope equipped with CCD camera, temperature regulation was made, within $\pm 0.1^\circ\text{C}$, using Mettler FP82 central processor and FP84 hot stage.

Mesophase structural investigation was made using synchrotron radiation facility (PETRA III beamline at P07 Physics Hutch station) at DESY, Hamburg. For this study, sample was taken in a Lindemann glass capillary of diameter 1.0 mm and very slowly cooled down from isotropic phase to the desired temperature to get aligned sample. 50 images of exposure time 0.2s was grabbed and averaged to get one diffraction image and such five images were collected at a particular temperature. All the physical parameters were averaged over these five image data. A Perkin Elmer 2D detector of pixel size $200 \times 200 \mu\text{m}$ and total size $400 \times 400 \text{mm}$ was used for image grabbing which was placed at 3.3 m away from the sample. QXRD program for PE Area Detectors (G. Jennings, version 0.9.8, 64 bit) was used for data acquisition and also for analyzing the images. Images were integrated using a step size of 0.002 to get intensity versus wave vector (Q) distribution.

Relaxation behavior of MPOBC was studied by measuring frequency dependent complex dielectric permittivity using a computer controlled impedance analyzer HIOKI 3532-50 (50Hz–5 MHz). Polyimide-coated homogeneous (HG) cells in the form of a parallel plate capacitor with low resistivity (about $20 \Omega/\square$) indium tin oxide (ITO) electrodes of $\sim 5 \mu\text{m}$ cell gap were used. The cells were filled by capillary action with samples in isotropic state and cell temperature was maintained within $\pm 0.1^\circ\text{C}$ using Eurotherm 2216e temperature controller. Very slow regulated cooling of the sample was made to get proper alignment. To find the dielectric increment and relaxation frequency of a particular mode, observed dielectric spectra, as mentioned in chapter 2, were fitted to the following complex dielectric permittivity proposed by Cole-Cole [6,7,8], which was modified to take into account the low and high frequency parasitic effects:

$$\varepsilon^* = \varepsilon' - i\varepsilon'' = \varepsilon_\infty + \sum_k \frac{\Delta\varepsilon_k}{1 + (i\omega\tau_k)^{1-\alpha_k}} - i \frac{\sigma}{\omega\varepsilon_0}$$

where $\Delta\varepsilon_k = \varepsilon_0 - \varepsilon_\infty$ is the dielectric increment, ε_0 and ε_∞ being the real part of the low and high frequency limit dielectric permittivities, τ_k is the relaxation time (inverse of critical angular frequency) and α_k is the asymmetry parameter signifying deviation from Debye type behavior of k-th mode relaxation process. σ is the conductivity of the cell due to charge impurities which contributes mainly in low frequency region.

Spontaneous polarization (P_S) was measured as a function of temperature by the reversal current method [9] using a triangular wave at 10 Hz obtained from an Agilent 3320A function generator. The amplitude of the applied voltage was 20 V_{pp}. A digital oscilloscope ((Tektronix TDS 2012B) was used to record the voltage drop across a standard resistor in series with the cell as a function of time. The area under the curve was determined from the stored image after creating an appropriate base line following procedure described before [10]. P_S was calculated using the expression $P_S = \int V dt / (2AR)$ where A is the active area of the cell and R is the resistance used to record the voltage–time curve.

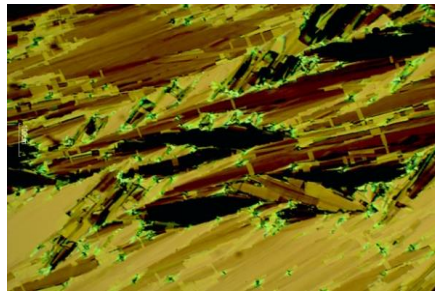
Since in an ac field the molecules switch around an imaginary cone through twice the tilt angle there by reversing the sign of the P_S , tilt of the molecules in smectic layers was determined by measuring the angle of rotation of the analyzer between two extinction conditions while observing, under polarizing microscope, switching of the molecules subjected to a 10 mHz 40 volt square wave pulse. This tilt is referred to as optical tilt. From synchrotron data tilt was also determined which is known as X-ray tilt.

6.4 RESULTS AND DISCUSSIONS

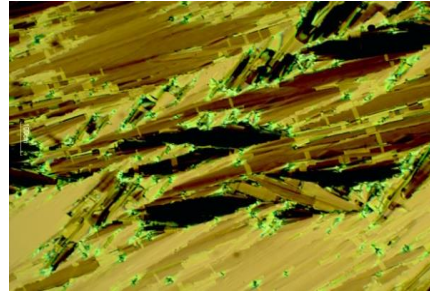
6.4.1 Optical Polarizing Microscopy

The compound MPOBC exhibits richly polymorphic behavior – as many as ten different phases are observed. Photo micrographs of textures of different phases observed under planar anchoring condition are shown in Figure 6.1. Molecules of MPOBC contain an asymmetric C* atom rendering chirality while the carbonyl (–C=O) functional group provides a transverse permanent electric dipole moment. Variant of mosaic textures are observed in SmG* and SmJ*

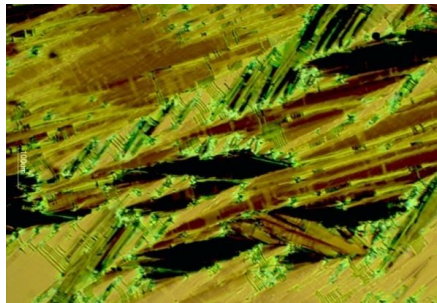
phases, they differ only slightly in colour; there is no indication of helical structure. Within the individual grains the optic axis is oriented uniformly and homogeneously, while discontinuous direction changes of the long molecular axes are encountered advancing from grain to grain, leading to differently coloured mosaic phases [11]. These two phases are soft crystal like with pseudo-hexagonal packing within the smectic layers, with long range bond orientational order as well as long range interlayer correlation. They differ only in the direction of tilt of the molecules, in SmG^* the tilt is towards the side of the hexagon while in SmJ^* it is towards the apex of the hexagon [12,13]. In the next two higher temperature smectic phases, SmF^* and SmI^* , textures change from the above phases, indication of helicoidal structure is now visible in the form of parallel equidistant lines, more in SmI^* than in SmF^* . Measured pitch values in the two phases estimated from the separation of helical lines are 5-10 μm . Unlike in MPOBC, usually only SmI^* phase is observed below SmC^* phase. In these two phases the molecular packing is also pseudo-hexagonal, but both the bond orientational order and the interlayer correlation are quasi long range in nature, in SmF^* the tilt is towards the side of the hexagon while in SmI^* it is towards the apex of the hexagon [14]. In SmC^* phase the texture is uniform throughout the field of view and existence of helicoidal structure is also evident throughout the sample. It transforms to typical fan shaped texture in orthogonal SmA^* phase, to oily streaks texture in cholesteric (N^*) phase, appearance of oily streaks at the expense of fan shaped texture is clearly seen at $\text{SmA}-\text{N}^*$ transition. Blue coloured platelet texture is observed in blue phase. This is definitely not BPIII^* phase or “fog phase”, it is difficult to ascertain whether it is a BPI^* or BPII^* phase both of which are cubic phases, the former being simple cubic whereas the later is body centered cubic. But since the lower temperature phase is a cholesteric phase this phase is likely to be a BPI^* phase [11, 15].



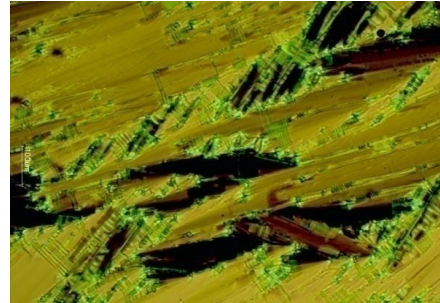
SmG* Phase (50°C)



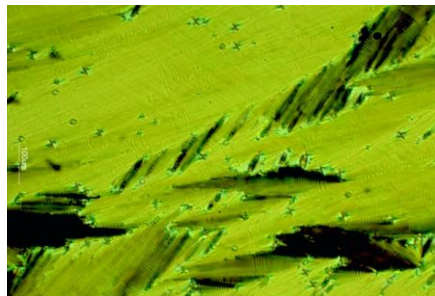
SmJ* Phase (64°C)



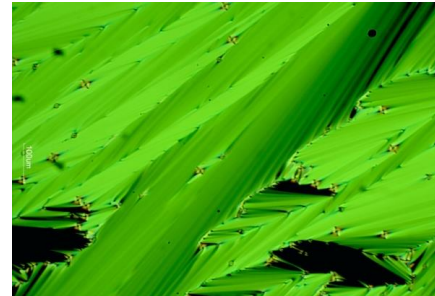
SmF* Phase (66°C)



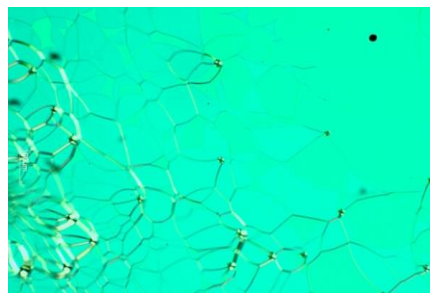
SmI* Phase (69°C)



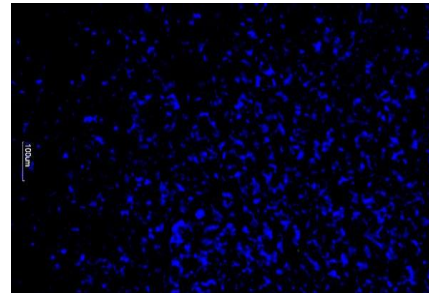
SmC* Phase (75°C)



SmA* Phase (100°C)



N* Phase (138°C)



Blue Phase (139.5°C)

Figure 6.1: Observed textures in MPOBC in different phases.

It may be of interest to point out that molecular structures of the compounds have pronounced effect on their phase behavior. While the present compound MPOBC shows eight different liquid crystalline phases, the compound DOBAMBC, the first ferroelectric liquid crystal [3], was having different molecular structure $[C_{10}H_{21}O.Ph.CHN.Ph.CH.CH.COO.CH_2.CH(CH_3).C_2H_5]$ from MPOBC, exhibits only one ferroelectric (SmC^*) and one paraelectric phase (SmA^*); on the other hand in the first antiferroelectric liquid crystal MHPOBC, having core structure similar to MPOBC, $[C_8H_{17}O.Ph.Ph.COO.Ph.COO.CH(CH_3).C_6H_{13}]$, three sub phases of ferroelectric SmC^* are found to exist between anticlinic SmC^*_A and orthogonal SmA^* phases [16]. When the six end carbon atoms of alkoxy chain of MHPOBC are fluorinated antiferroelectric phase is suppressed [10].

6.4.2 X-Ray Study

Since conventional X-ray scattering is not sensitive to the local environment of a molecule it cannot distinguish smectic liquid crystal phases that differ only with respect to the orientation of the molecules in successive layers like antiferroelectric SmC^*_A , ferroelectric SmC^* and various intermediate ferroelectric phases but it can distinguish smectic phases that differ with respect to the packing of molecules within the smectic layers. Although no external field, magnetic or electric, was used to align the sample, partial alignment was achieved due to surface interaction, with molecular axes perpendicular to beam direction. Diffraction photographs obtained in different phases are shown in Figure 6.2. Transition temperatures seen from X-ray study are found to be shifted to higher side by 1 to 2 degrees than those observed from optical microscopy study since two different temperature baths were used. In SmG^* phase one strong inner ring is present with quite strong second order diffraction feature signifying long range positional order across the smectic layers. One very strong outer ring with two distinct satellites on both sides is also observed in this phase characterizing two dimensional positional ordering within the smectic layers as depicted in Figure 6.3. Correlation length (ξ), defined as $\xi=2\pi/FWHM$

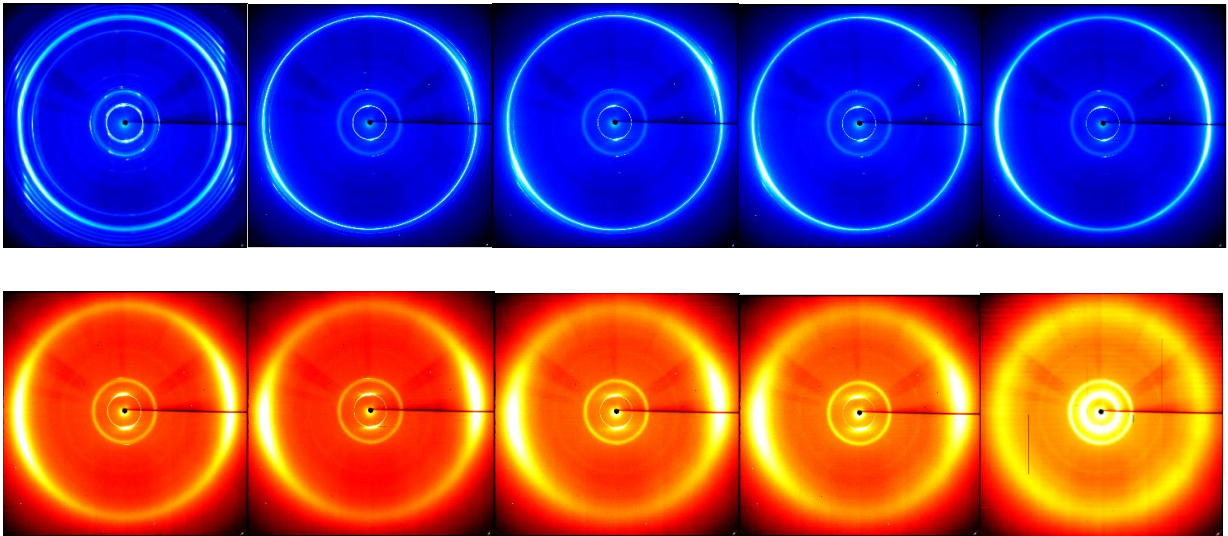


Figure 6.2: Diffraction photographs in Crystal, SmG*, SmJ*, SmF*, SmI*, SmC*, SmA*, N*, BP* and isotropic phases

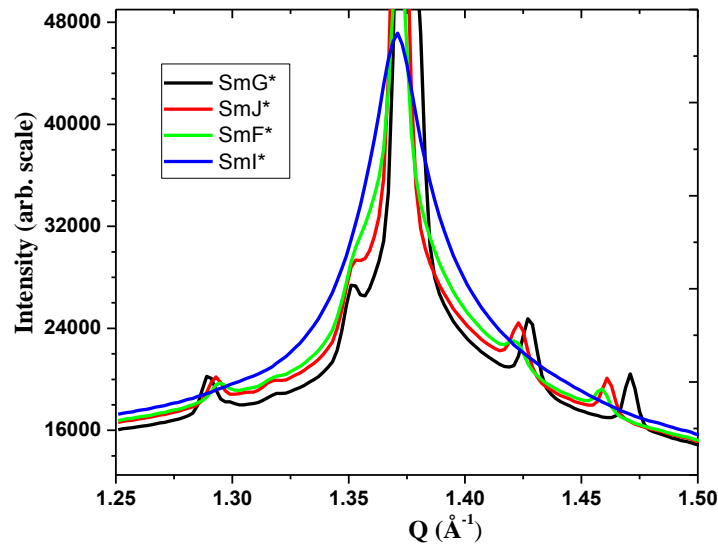


Figure 6.3: Profile of wide angle diffraction peak depicting ordering within smectic planes in hehatic phases at 55⁰C (SmG*), 64⁰C (SmJ*), 66⁰C (SmF*) and 68⁰C (SmI*)

where FWHM is the full width at half maxima in scattering vector (Q) of the relevant Bragg peak, is found to be 145 nm across the smectic layers and 65 nm within the layers. Diffraction features remain almost same in SmJ* phase, only the second order of the inner peak and the

satellites of the outer peak become less prominent and ξ decreases slightly both across (140 nm) and within the smectic layers (59 nm), decrease in molecular tilt angle is also observed. Quite strong second order inner diffraction peak (although less than those in SmG^* and SmJ^* phases) is observed but the satellites of the outer peak are very weak in SmF^* phase which means correlation across the smectic layers reduces slightly (134 nm) but within the layers it becomes half (30 nm). In SmI^* phase, a 30° rotation of outer maxima is distinctly observed which gives direct evidence of change of tilt direction of the molecules from the edge of the pseudo-hexagonal net towards its apex. Correlation lengths also reduce to 125 nm and 22 nm across and within the layers respectively. In-plane correlation lengths ranging from 5 to 20 nm has been reported from quasielastic light scattering experiment on thin film of SmI^* phase and also from X-ray measurements [17,18] in this compound. In ferroelectric SmC^* and paraelectric SmA^* phases correlation lengths across the smectic layers decreases slightly to 118 nm and 116 nm respectively, no positional ordering is observed within the layers and ξ reduces drastically to about 3 nm in both phases. Same trend is observed in cholesteric (N^*) phase. But in blue phase, correlation length along the director increases substantially to 134 nm from 113 nm in cholesteric phase. This is expected since the blue phase structures involve a twist of the director extending not only in one direction, such as in cholesteric phase, but in both directions perpendicular to the director generating what is known as double twist structure [19]. However, observed correlation length for MPOBC is substantially large than that observed in $\text{BP}_{\text{Sm}1}$ and $\text{BP}_{\text{Sm}2}$ phases (58 nm) of a different chiral compound [19]. Clear discontinuities are also observed at all phase transitions in d_{001} smectic layer spacing as shown in Figure 6.4. Present study therefore clearly depicts the temperature evolution of the different tilted hexatic smectic phases along with cholesteric and blue phase in a single compound. Tilt (τ) of the molecules with respect to smectic layer normal has also been calculated using the relation, $\tau = \arccos(d/d_A)$ where d_A is average layer spacing in SmA^* phase. Molecular tilt is found to decrease with temperature, in SmG^* and SmJ^* phases from 16.5° to 14.6° however, at the onset of SmF^* phase it increases slightly to 14.9° and then decreases up to 12.5° till the end of SmI^* phase. Thus discontinuous change in tilt is observed only when molecules change orientations from apex to edge of the in-plane hexagonal net. At the onset of SmC^* phase it again jumps up and then decreases with temperature as in previous hexatic smectic phases. Temperature variation of tilt is shown in Figure 6.5. It is further noted that tilt angle (12.54°) calculated as above at 72°C is found to be equal to that measured

directly from the film (12.5°) which justifies calculation of tilt angle, at least in SmC^* phase, taking average d_A . Our measured value in SmJ^* phase (14.6°) is less than reported (19°) from extinction measurement in a SSFLC cell under a polarizing microscope [20].

Average intermolecular distance (D), determined from outer peak (in SmG^* , SmJ^* , SmF^* and SmI^* phases from the main outer peak) is found to increase monotonically from 4.58 \AA to 4.79 \AA . However, no discontinuity is observed in D as observed in d_{001} spacing. D values observed in MPOBC is substantially less than the values (5.87 \AA and 6.89 \AA) observed in chiral terphenyl compounds having oligomethylene spacer and ester group in the chain part, discussed in chapter 5.

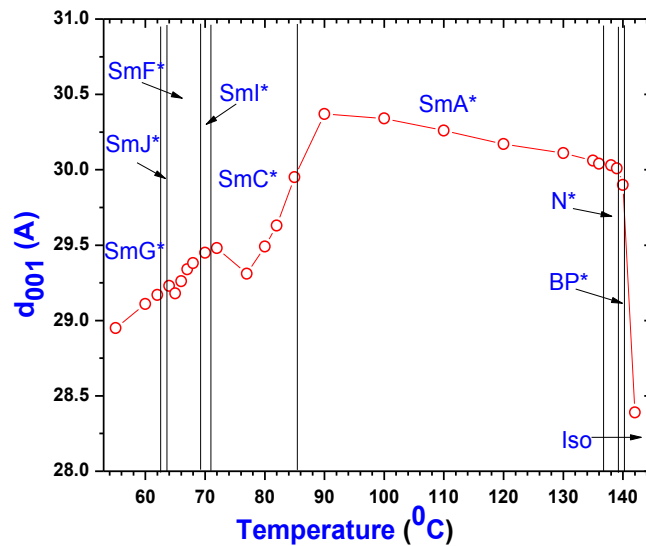


Figure 6.4: Layer spacing in smectic phases and apparent molecular length in cholesteric, blue and isotropic phases.

6.4.3 Optical Tilt

Optical tilt of the molecules in different phases has also been determined and depicted in Figure 6.5. Distinct discontinuities are observed at the phase transition points. In SmG^* phase tilt (τ) increases from 14.7° to 19.8° with temperature, in SmJ^* phase it increases further from 20.0° to 21.0° . However, in SmF^* phase tilt suddenly decreases to 17.0° and continue to decrease up to

13° . In SmI^* phase τ increases to 16.0° and then decreases to 14.8° . In SmC^* phase it again increases to 19° and then decreases with temperature to 3° . Thus except in SmG^* and SmJ^* phases molecular tilt decreases with temperature. Unlike in X-ray tilt clear discontinuities are observed in optical tilt at all transitions except at SmG^* - SmJ^* transition. Optical tilt reflects the angle between the direction of molecular core and the layer normal, since the principal axis of indicatrix coincides with the core direction. On the other hand, X-ray tilt gives the average direction of total populations of electrons of the molecules. Thus X-ray tilt is usually found to be larger than optical tilt and in the present compound MPOBC it is found to be true in SmC^* phase as reported in systems described in chapter 5 and as reported earlier in other systems [8,21], however, in higher ordered tilted phases (SmI^* and SmJ^*) opposite behavior is observed, such behavior has also been reported in SmC^* phase [22,23]. A crossover is found in SmG^* phase.

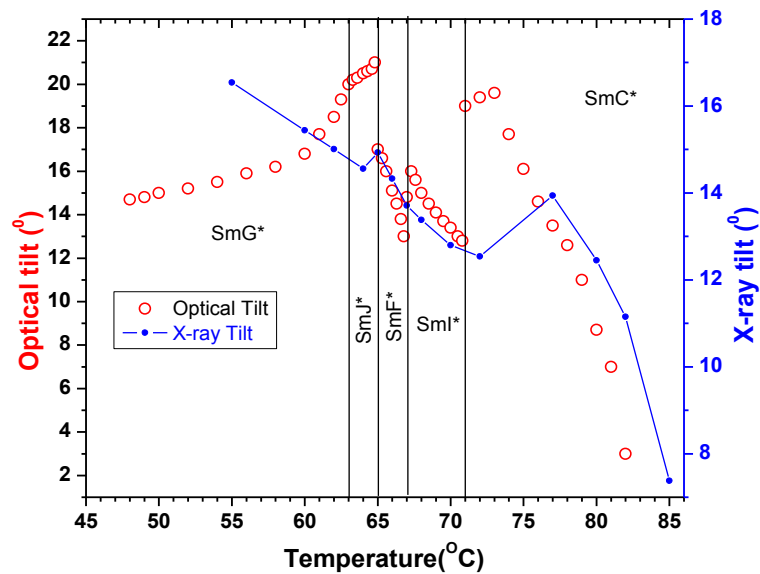


Figure 6.5: Temperature dependence of X-ray and optical tilt of MPOBC.

6.4.4 Spontaneous Polarization (P_s)

Measuring depolarization current using triangular wave method P_s has been measured in ferroelectric SmC^* phase. Although any chiral tilted phase may possess, due to symmetry consideration, spontaneous polarization, we could measure P_s only in SmC^* phase. No previous report on P_s measurement in SmG^* and SmJ^* phases are available, but P_s in SmI^* phase was reported [24]. In a two ring perfluorinated compound it was found that SmI^* phase exhibits almost 3 times larger spontaneous polarization than the high temperature ferroelectric SmC^* phase when the applied field is very high but at lower field P_s was less than in SmC^* phase. From optimized geometry of the molecule, obtained by molecular mechanics calculation using PM3 method of software Hyperchem (shown in Figure 6.6), dipole moment of the molecules is found to be 2.06 Debye which is rather small compared to other chiral liquid crystal forming compounds; for example dipole moments of 4F3R and 4F6R, discussed in chapter 5, are 4.25 Debye and 5.75 Debye respectively [8]. However, P_s was found to be quite high, maximum value being 237 nC/cm^2 and found to fall off rapidly with temperature. Heating and cooling data was found to be almost identical and data obtained during cooling are shown in Figure 6.7. Although increase of molecular lateral dipole moment normally leads to increased P_s but molecular rotations around their long axes and various intramolecular rotations in the mesophase play important role in the macroscopic P_s values.

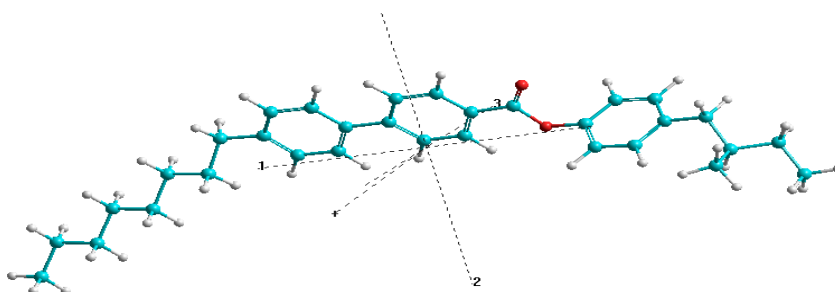


Figure 6.6: Optimized structure of MPOBC

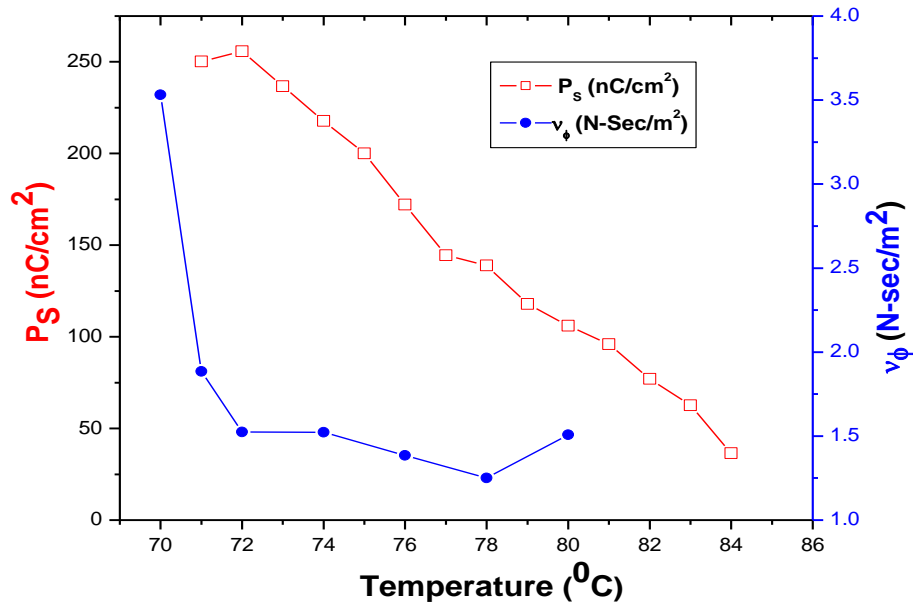


Figure 6.7: Temperature variation spontaneous polarization (P_s) and rotational viscosity γ_ϕ in SmC^* phase.

Using the following relation obtained from the generalized Landau theory [25]

$$\gamma_\phi = \frac{1}{4\pi\epsilon_0} \frac{1}{\Delta\epsilon f_c} \left(\frac{P_s}{\theta} \right)^2$$

it is possible to calculate rotational viscosity, which is related to rotations of the molecular directors about the smectic C^* cone and one of the most important parameters of the SmC^* phase that strongly influences the switchingtime between the field-induced states of FLCs, utilizing spontaneous polarization (P_s), tilt angle (θ), Goldstone mode critical frequency (f_c) and Goldstone mode dielectric strength ($\Delta\epsilon$) (discussed in next section). Temperature variation of calculated rotational viscosity has also been depicted in Figure 6.7. It was found to decrease sharply near SmI^*-SmC^* transition, then it decreases at slower rate and finally shows increasing trend near SmC^*-SmA^* transition which theoretically should diverge.

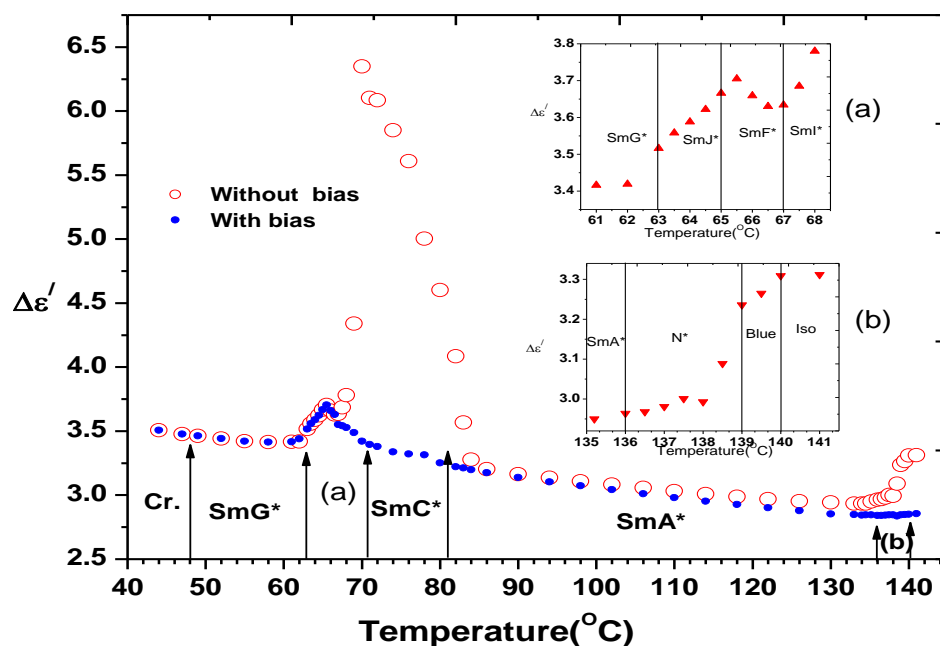


Figure 6.8: Temperature variation of dielectric increment with and without bias field. Magnified views are shown in the inset for (a) in hexatic phases and (b) in cholesteric and blue phases (without bias).

6.4.5 Frequency Dependent Dielectric Study Without Bias

Dielectric behavior of the compound has also been investigated in detail to study the dynamics of the molecules. Dielectric increment ($\Delta\epsilon$) exhibits discontinuous change at all the phase transitions as depicted in Figure 6.8. Transition temperatures between phases differ slightly from those observed from texture and dielectric study. Although long range BOO is established in SmG^* phase along with the establishment of a helical structure but in the measuring cell the helical structure may be suppressed due to strong surface interactions (observed texture supports this), so there might not be appreciable change in $\Delta\epsilon$ at Cr- SmG^* transition as observed and it decreases slightly with increasing temperature. On further heating, when SmJ^* phase is formed where molecular tilt changes from the side of the pseudo-hexagonal net towards the apex, reorientation of the director results in higher tilt and higher $\Delta\epsilon$. At SmJ^* - SmF^* transition since the tilt direction reverses, $\Delta\epsilon$ slightly decreases. On further heating at SmF^* - SmI^* transition tilt direction again changes from the side of the hexagon to apex, $\Delta\epsilon$ again increases. Due to

increased thermal energy, overcoming surface energy helical structure is established in SmC^* phase, greater director reorientation is possible as a result of reduced BOO and reduced coupling between local tilt and bond directions thus generating higher values of $\Delta\varepsilon$ in this phase. However, since molecular tilt in SmC^* is quite small (about 19° at the onset of SmC^* as obtained from optical study) and decreases rapidly with increasing temperature, $\Delta\varepsilon$ is found to decrease quite strongly with temperature. Within SmA^* phase $\Delta\varepsilon$ is small and decreases slightly with temperature. At the onset of cholesteric phase, since helical structure is established again, $\Delta\varepsilon$ increases, although the value is smaller than those observed in low temperature smectic phases because of the absence of the layered structure. On the formation of blue phase $\Delta\varepsilon$ increases further, showing a distinct discontinuity, since in blue phase double twist structure is established from a single twist structure in cholesteric phase.

From the absorption spectra one low frequency collective relaxation process is observed in all the tilted smectic phases except in SmG^* phase. In SmJ^* the process is very weak and the relaxation frequency remains constant with temperature at around 300Hz as shown in Figure 6.9. In SmF^* phase it increases rapidly up to 700Hz. In SmI^* phase it again remains constant at 800 Hz. In SmC^* phase the relaxation frequency again increase with temperature reaching up to 1400 Hz which is identified as Goldstone mode or phason mode associated with fluctuations of the phase angle of the director. One high frequency relaxation process is also observed in hexatic tilted phases which remain almost constant with temperature. On approaching SmC^* - SmI^* (or SmF^*) transition from above two collective director relaxation processes are discussed [26] – higher frequency one is related to amplitude fluctuation whereas the lower frequency one is related to the phase fluctuation of the bond orientational order (BOO) coupled with the polarization and tilt of the molecules. It has been predicted that BOO phason frequency should jump to a lower value at the transition and continue to decrease slowly with decreasing temperature. However, BOO amplitudon mode frequency should jump to a higher value at the transition and continue to increase strongly with decreasing temperature. No such theoretical prediction is available for the dynamic behavior of molecules in SmJ^* and SmG^* phases. Observed temperature variation of BOO related phason frequency in the vicinity of SmC^* - SmI^* transition of MPOBC is as predicted. But BOO amplitudon frequency was observed in all the tilted hexatic phases, it remains almost constant at 420 kHz instead of increasing with decreasing temperature and this mode persists even in SmC^* phase near transition. For a substance denoted

as C8OCOOC5, similar behavior of BOO phason frequency was reported and no amplitude mode was observed in that system [27]. Soft mode could be detected in SmA^* phase which increases with temperature from 130 kHz to 200 kHz. No molecular mode was possible to detect in the cholesteric or blue phase because either the mode is very weak or merged with the ITO peak, or the molecular mode in these phases are beyond the frequency measuring range.

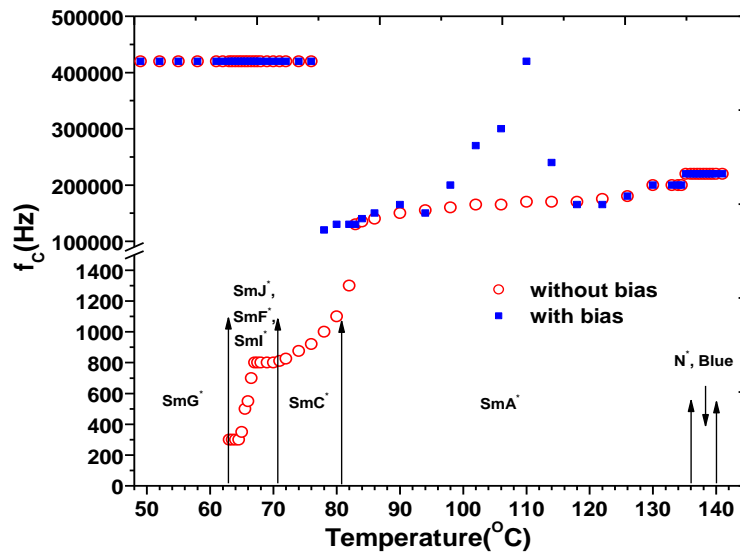


Figure 6.9: Observed critical frequencies with and without bias field in different phases of MPOBC.

6.4.6 Frequency Dependent Dielectric Study With Bias

Relaxation behavior was also studied by applying a dc bias field in addition to the measuring field. At all transitions discontinuous change is observed in dielectric increment ($\Delta\epsilon$) as was observed without bias (Figure 6.8). However, dielectric increment with bias is observed to be less throughout the mesomorphic range as expected. Within SmA^* phase it increases with decreasing temperature at substantially higher rate compared to non-bias case. It increases further in SmC^* phase and unlike in the without bias situation it continues to increase in SmI^* and SmF^* phases as has been observed in compound C8OCOOC5 [27]. In SmJ^* phase $\Delta\epsilon$ decreases when

temperature is lowered, similar behaviour is observed also in SmG^* phase initially, but it increases slightly on further cooling.

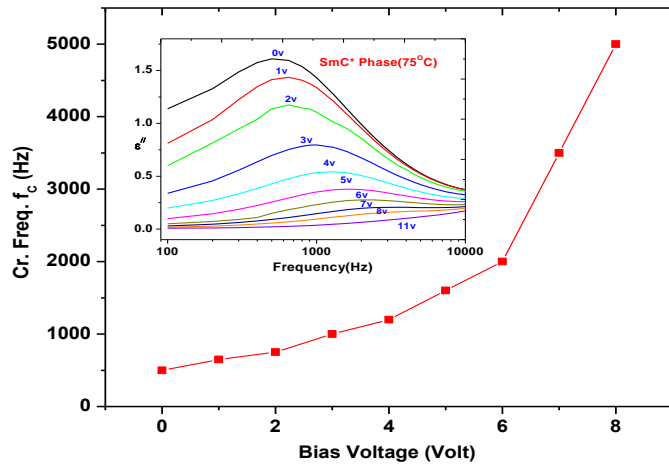


Figure 6.10: Effect of bias voltage on GM critical frequency in SmC^* phase (75°C)

In SmC^* phase Goldstone mode contribution to dielectric constant decreases with increasing bias field and at about 10 V Goldstone mode was completely suppressed which means that helicoidal structure is completely unwound at that voltage (Figure 6.10, inset). However with increasing bias Goldstone mode critical frequency increases from 500 Hz to about 5 kHz as depicted in Figure 6.10. This might be due to the fact that unwinding of helicoidal structure with bias hinders cooperative phase fluctuations of the molecules.

No BOO related phason mode was observed in the hexatic phases under bias field, however BOO amplitudon mode critical frequency remained similar to that observed without bias (Figure 6.9). In SmA^* phase soft mode relaxation frequency was found to increase from 130 kHz (82°C) to 420 kHz (110°C), then decreased to 165 kHz at 118°C and again increased to 200 kHz (130°C), whereas it increased smoothly 130 kHz (82°C) to 200 kHz (130°C) in without bias case. No plausible explanation is available yet for this anomalous behavior.

6.5 CONCLUSION

Phase behaviour, structure and molecular dynamics of the chiral liquid crystalline compound MPOBC have been investigated by optical polarizing microscopy, small and wide angle diffraction by synchrotron radiation and frequency dependent dielectric spectroscopy techniques. Compound exhibits richly polymorphic mesomorphic behavior within 48⁰C to 140⁰C. Other than crystalline and isotropic phases, it shows four tilted hexatic smectic phases (SmG*, SmJ*, SmF*, SmI*), one tilted synclinic SmC* phase, one normal smectic phase (SmA*) along with cholesteric (N*) and a blue phase (BP*). Difference in textures, which reveal topological defect structure, in SmG* and SmJ* phases and those of SmF* and SmI* is subtle. Clear evidence of helicoidal structure in the form of disclination lines is observed in SmI* and in SmC*. Blue coloured platelet texture is observed in BP* phase. Although no hexagonal symmetry was directly revealed from synchrotron study in the hexatic phases but these phases could be distinguished from the wide angle diffraction peak and its satellite structures and measuring the correlation lengths across and within the smectic layers. However, direct evidence of change of tilt direction of the molecules from the edge of the pseudo-hexagonal net (SmF*) towards its apex (SmI*) was observed. In blue phase, correlation length along the director increased substantially to 134 nm from 113 nm in cholesteric phase. Clear discontinuities were observed at the transitions of all the phases in d_{001} smectic layer spacing. Discontinuities were also observed in molecular tilts measured from diffraction and optical methods. Present study nicely depicted the temperature evolution of the different smectic phases along with cholesteric and blue phase in a single compound. Although from mechanics calculation dipole moment of the molecules was found to be rather low (2.06 Debye), the compound exhibited high spontaneous polarization (237 nC/cm²) in ferroelectric SmC* phase. Frequency dependent dielectric spectroscopic study also revealed discontinuous changes in dielectric increment at all the phase transitions. In hexatic phases dielectric absorption spectra revealed one low frequency relaxation process, related to the phase fluctuation of the bond orientational order, and one high frequency process related to amplitude fluctuation of the bond orientational order coupled with the polarization and tilt of the molecules. In SmC* phase Goldstone mode relaxation and in SmA* phase soft mode relaxation processes were detected. Dielectric increment with bias field was found to be less throughout the mesomorphic range compared to non-bias value. Helicoidal structure in SmC* phase could be completely unwound at 10 V bias.

6.6 REFERENCES

- [1] D. Demus and J. Goodby, Handbook of Liquid Crystals, Wiley-VCH Weinheim, (1998).
- [2] P. S. Pershan, Structure of Liquid Crystal Phases, World Scientific Singapore, (1988).
- [3] R. B. Meyer, L. Liebert, L. Strzelecki, P. Keller; J. Phys. (France) Lett., 36, L-69 (1975), Ferroelectric liquid crystals.
- [4] N. A. Clark and S. T. Lagerwall; Appl. Phys. Lett., 36, 899 (1980), Submicrosecond bistable electro-optic switching in liquid crystals.
- [5] D. C. Wright and N. D. Mermin; Rev. Mod. Phys., 66, 385 (1989), Crystalline liquids: the blue phases.
- [6] C. J. F. Botcher and P. Bordewijk; Theory of Electric Polarization Vol. I Elsevier, Amsterdam (1978).
- [7] Wrobel S, Dielectric relaxation spectroscopy, Relaxation phenomena — Liquid crystals, magnetic systems, polymers, high-TC superconductors, metallic glasses, Haase W. and Wrobel S Eds., Ch 1 Springer-Verlag Berlin-Heidelberg (2003).
- [8] D. Goswami, D. Sinha, A. Debnath, P.K. Mandal, S. K. Gupta, W. Haase, D. Ziobro and R. Dabrowski; J. Mol. Liq., 182, 95-101 (2013), Molecular and dynamical properties of a perfluorinated liquid crystal with direct transition from ferroelectric SmC* phase to isotropic phase.
- [9] K. Miyasato, S. Abe, H. Takezoe, A. Fukuda and E. Kuze; Jpn. J. Appl. Phys., 22, L661 (1983), Direct Method with Triangular Waves for Measuring Spontaneous Polarization in Ferroelectric Liquid Crystals.
- [10] P. K. Mandal, B. R. Jaishi, W. Haase, R. Dabrowski, M. Tykarska and P. Kula; Phase Trans., 79, 223-235 (2006), Optical microscopy, DSC and dielectric relaxation spectroscopy studies on a partially fluorinated ferroelectric liquid crystalline compound MHPO(13F)BC.
- [11] I. Dierking, Textures of Liquid Crystals Wiley-VCH, Weinheim, (2003).

- [12] A. J. Leadbetter, J. P. Gaughan, B. Kelly, G. W. Gray and J. Goodby; *J Phys. (France) Colloq.*, 40, C3-178 (1979), Characterisation and structure of some new smectic phases.
- [13] G. W. Gray and J. W. Goodby *Smectic Liquid Crystals, Textures and Structures*, Leonard Hill, Philadelphia, (1984).
- [14] P. A. C. Gane, A. J. Leadbetter and P. G. Wrighton; *Mol. Cryst. Liq. Cryst.*, 66, 247 (1981), Structure and Correlations in Smectic B, F and I Phases.
- [15] H. Stegmeyer, T. Blumel, K. Hiltrop, H. Onnusseit and F. Porsch; *Liq. Cryst.* 1, 3-28 (1986), Thermodynamic, structural and morphological studies on liquid-crystalline blue phases.
- [16] Jan P. F. Lagerwall, Per Rudquist, Sven T. Lagerwall and Frank Gießelmann; *Liq. Cryst.*, 30 399-414 (2003), On the phase sequence of antiferroelectric liquid crystals and its relation to orientational and translational order.
- [17] S. B. Dierker and R. Pindak; *Phys. Rev. Lett.*, 59, 1002 (1987), Dynamics of thin tilted hexatic liquid crystal films.
- [18] E. B. Sirota, P. S. Pershan, L. B. Sorensen and J. Collett; *Phys. Rev. Lett.*, 55, 2039 (1985), X-Ray Studies of Tilted Hexatic Phases in Thin Liquid-Crystal Films.
- [19] E. Grelet, B. Pansu, M-H Li and H. T. Nguyen; *Phys. Rev. Lett.*, 86, 3791 (2001), Structural Investigations on Smectic Blue Phases.
- [20] T. Uemura, Y. Ouchi, K. Ishikawa, H. Takezoe and A. Fukuda; *Jpn. J Appl. Phys.*, 24, L224 (1985), Optical Microscope Observation of Hexagonal Ordering in Surface Stabilized Ferroelectric Liquid Crystal Cells.
- [21] D. Ziobro, R. Dąbrowski, M. Tykarska, W. Drzewiński, M. Filipowicz, W. Rejmer, K. Kuśmierk, P. Morowiak and W. Piecek; *Liq. Cryst.*, 39, 1011 (2012), Synthesis and properties of new ferroelectric and antiferroelectric liquid crystals with a biphenyl benzoate rigid core.
- [22] W. Piecek, Z. Raszewski, P. Perkowski, J. Przedmojski, J. Kedzierski, W. Drzewinski, R. Dabrowski and J. Zielinski; *Ferroelectrics*, 310, 125 (2004), Apparent Tilt Angle and Structural

Investigations of the Fluorinated Antiferroelectric Liquid Crystal Material for Display Application.

[23] J. P. F. Lagerwall, A. Saipa, F. Giesselmann and R. Dabrowski; *Liq. Cryst.*, 31, 1175 (2004), On the origin of high optical director tilt in a partially fluorinated orthoconic antiferroelectric liquid crystal mixture.

[24] A. Mikułko, M. Wierzejska, M. Marzec, S. Wrobel, J. Przedmojski and W. Haase; *Mol. Cryst. Liq. Cryst.*, 477, 185 (2007), Ferroelectricity of Hexatic Phases.

[25] T. Carlsson, B. Zeks, C. Filipic, A. Levstik; *Phys. Rev. A*, 42, 877 (1990), Theoretical model of the frequency and temperature dependence of the complex dielectric constant of ferroelectric liquid crystals near the smectic-C*–smectic-A phase transition.

[26] M. Glogarova and I. Rychetsky; *Dielectric relaxation spectroscopy, Relaxation phenomena — Liquid crystals, magnetic systems, polymers, high-TC superconductors, metallic glasses*, W. Haase and S. Wrobel, Eds., Ch 5.3 Springer-Verlag Berlin-Heidelberg (2003).

[27] I. Rychetsky, D. Pocięcha, V. Dvorak, J. Mieczkowski, E. Gorecka and M. Glogarova; *J. Chem. Phys.*, 111, 1541 (1999), Dielectric behavior of ferroelectric liquid crystals in the vicinity of the transition into the hexatic phase.

CHAPTER 7

SUMMARY AND CONCLUSIONS

Now a days liquid crystal technology has a major effect in many areas of science and engineering especially in display technology. For successful applications of liquid crystals, studies on their structure-property relationships are extremely important. These studies also help in synthesizing better materials. Phase behavior and physical properties of fluorinated derivatives are found to be different from their hydrogenous analogues and often give rise to properties suitable for various applications. With this aim and objective various physical properties of a few fluorinated achiral and chiral liquid crystalline materials have been investigated using OPM, DSC, X-ray diffraction, optical birefringence, dielectric spectroscopy and electrooptic methods.

Three laterally fluorinated isothiocyanato terphenyl compounds (**2TP-3'F-4NCS**, **2TP-3'3F-4NCS** and **4TP-3',3F-4NCS**) and six phenyl bicyclohexyl based terminal fluorinated compounds (**3ccp-f**, **3ccp-ff**, **3ccp-fff**, **5ccp-f**, **5ccp-ff** and **5ccp-fff**) have been studied in the achiral system all of which exhibit nematic phase, in some cases also smectic phase. Two partially fluorinated biphenyl benzoate based chiral compounds (**4F3R** and **4F6R**), which exhibit ferroelectric and antiferroelectric phases, have also been investigated. Only one non-fluorinated biphenyl carboxylate based chiral compound (**MPOBC**) have also been studied which shows richly polymorphic behavior viz., four tilted hexatic smectic phases, one tilted synclinic smectic phase, one normal smectic phase along with cholesteric and blue phase.

From the detailed investigations on the first three isothiocyanato terphenyl compounds (**2TP-3'F-4NCS**, **2TP-3'3F-4NCS** and **4TP-3',3F-4NCS**) effect of increasing lateral fluorination and increasing chain length on various physical properties has been determined. It is observed that:

- ❖ With increasing fluorination (**2TP-3'F-4NCS** to **2TP-3'3F-4NCS**) nematic phase stability increases from 68⁰C to 108⁰C, but when chain length is also increased (**2TP-3'F-4NCS** to **4TP-3',3F-4NCS**) increase of thermal stability is less, 68⁰C to 85⁰C.
- ❖ Dipole moments of the molecules also show similar increasing trend, 5.57D to 6.68D to 6.29D as one move from the first to the third compound.
- ❖ Contrary to common perception that NCS compounds do not form dimers, presence of weak antiparallel correlation among the neighbouring molecules in all the three compounds has been observed from X-ray study. Calculated effective values of dipole moments and dipole-dipole correlation factor within nematic phase corroborate the above observation.

- ❖ All the three compounds show positive dielectric anisotropy. With increased lateral fluorination dielectric anisotropy slightly decreases, but it increases when chain length is also increased by two carbon atoms. As a result similar trend is observed in both threshold and driving voltages. Thus the doubly fluorinated ethyl compound is most easily switchable, however driving voltage for all the compounds is suitable for thin TFT based LC display cells.
- ❖ Splay elastic constants of the materials suggest that faster response is expected in the butyl compound compared to ethyl compounds.
- ❖ Flip-flop mode relaxation frequency in the nematic phase decreases with increasing fluorination and chain length while opposite behavior is observed in the smectic phase. Nature of absorption process is Debye type in all cases.
- ❖ All the compounds exhibit high birefringence, highest values being 0.373, 0.357 and 0.333 in the three compounds. Thus with increasing fluorination and increasing chain length the birefringence gradually decreases. These compounds are, therefore, expected to be very suitable for formulating high birefringence nematic mixtures for fast switching displays.

Effect of fluorination and increased chain length on the physical properties of six phenyl bicyclohexyl based terminal fluorinated compounds (**3ccp-f**, **3ccp-ff**, **3ccp-fff**, **5ccp-f**, **5ccp-ff** and **5ccp-fff**) has also been studied. 3-D crystal structure analysis of one of the compounds (**5ccp-fff**) has also been made. It is observed that

- ❖ All the compounds exhibit nematic phase, melting points and phase stability changes considerably with extent of fluorination and chain length.
- ❖ Molecular dipole moments increases from 1.93D to 3.37D with fluorination in both the propyl and pentyl based systems; increment in **f** to **ff** derivatives is more than in **ff** to **fff** derivatives. However, no change is observed with increased chain length.
- ❖ Molecular geometry and conformation, packing in the crystalline state and density, magnitude of molecular dipole moments and its orientation with molecular long axes of **5ccp-fff** differ from those in closely related singly and doubly fluorinated compounds **3ccp-f** and **3ccp-ff**. These differences are probably the cause of the substantial increase of melting point and decrease of nematic range in **5ccp-fff** compared to compounds **3ccp-f** and **3ccp-ff**.

- ❖ The facts that in the nematic phase apparent length of the molecules is more than the most extended molecular lengths, average values of dielectric constants are less than the extrapolated values of dielectric constants in isotropic phase, effective values of molecular dipole moments are less than free molecular dipole moments as well as magnitude of calculated values dipole-dipole correlation factors give conclusive evidence of existence of short range anti-parallel order in all these compounds as was observed in **NCS** compounds.
- ❖ All the compounds show moderately strong positive dielectric anisotropy. Increased fluoro substitution caused increased dielectric anisotropy; however, increased chain length resulted in opposite behavior but in lower degree.
- ❖ Improved switching characteristics (V_{th} and V_d) is observed in **3ccp** series compared to **5ccp** series and increased lateral fluorination resulted further improvement. However, driving voltage for all the compounds is suitable for thin TFT based LC display cells.
- ❖ Values of splay elastic constants suggest that faster response is expected in triply fluorinated compounds and response will be faster than the **NCS** compounds.
- ❖ Like the **NCS** compounds, only one strong dielectric absorption process (flip-flop mode) is exhibited by these compounds which are again almost Debye type.
- ❖ In low temperature region critical frequency decreases sharply from f to ff derivatives but increases from ff to fff derivatives.

From the detailed study on the two partially fluorinated biphenyl benzoate based chiral compounds (**4F3R** and **4F6R**) following points are worth noting:

- ❖ While **4F3R** exhibits only ferroelectric SmC^* phase over a broad temperature range, compound **4F6R** having three additional oligomethylene spacer groups, exhibit both anti-ferroelectric SmC_A^* phase and ferroelectric SmC^* phase.
- ❖ Both the compounds directly goes to isotropic phase from SmC^* phase which is not common in FLCs.
- ❖ Dipole moment of **4F6R** is found to be substantially higher than that of **4F3R** which might be the result of change of molecular conformation due increased oligomethylene spacer group.
- ❖ Clear discontinuities are observed at SmC_A^* - SmC^* transition in **4F6R** in layer spacing, X-ray tilt, dielectric increment and rotational viscosity.

- ❖ Only Goldstone mode relaxation behavior is observed in both the compounds, increase of dielectric strength and critical frequency with temperature has been explained in the light of generalized Landau model. GM is found to be of Cole-Cole type.
- ❖ No soft mode is observed in any case since the compounds directly melt into isotropic phase.
- ❖ The facts that the compounds show quite strong dipole moment, about 45° tilt angle, moderately strong polarization, low viscosity, micro-second range switching and are capable of forming room temperature ferroelectric phase in appropriate host mixture make the compounds suitable from application point of view.

Following conclusions are drawn from the investigation on the only non-fluorinated biphenyl carboxylate based chiral compound (**MPOBC**):

- ❖ Compounds exhibit richly polymorphic behavior from 48°C to 140°C .
- ❖ Within the crystalline and isotropic phase it shows four tilted hexatic phase (SmG^* , SmJ^* , SmF^* , SmI^*), one tilted synclonic phase (SmC^*), one normal smectic phase (SmA^*), cholesteric phase (N^*) and one blue phase (BP^*).
- ❖ Only subtle difference in textures is observed in SmG^* and SmJ^* phases and those in SmF^* and SmI^* . Clear evidence of helicoidal structure in the form of disclination lines is observed in SmI^* and in SmC^* . Blue coloured platelet texture is observed in BP^* phase.
- ❖ Synchrotron X-ray diffraction study nicely depicts the temperature evolution of different smectic phases along with the cholesteric and blue phase in a single compound.
- ❖ Direct evidence of change of tilt direction of the molecules from the edge of the pseudo-hexagonal net (SmF^*) towards its apex (SmI^*) is observed.
- ❖ Correlation lengths, across and within the smectic layers, change discontinuously in hexagonal phases. In the blue phase correlation length along the director increased substantially to 134 nm from 113 nm in cholesteric phase.
- ❖ Clear discontinuities were observed at the transitions of all the phases in d_{001} smectic layer spacing, in X-ray and optical tilt, as well as in dielectric increment.
- ❖ In hexatic phases two relaxation processes are observed - one low frequency process related to phase fluctuation in bond orientational order and one high frequency process related to amplitude fluctuation of the bond orientational order coupled with the polarization and tilt of the molecules.

- ❖ In SmC^* phase Goldstone mode relaxation and in SmA^* phase soft mode relaxation processes are observed. Helicoidal structure in SmC^* phase could be completely unwound at 10V bias.

APPENDIX A

LIST OF SELECTED BOOKS AND MONOGRAPHS ON LIQUID CRYSTALS

1. *Molecular Structure and Physical Properties of Liquid Crystals*, (Eds.) G. W. Gray, Academic Press (AP), 1962.
2. *The Physics of Liquid Crystals*, (Eds.) P. G. de Gennes, OUP London, 1974.
3. *Liquid Crystals & Plastic Crystals* Vols 1 and 2. Ed. G. W. Gray and P. A. Winsor, Ellis Horwood Ltd., 1974.
4. *Introduction to Liquid Crystals*. Ed. E. B. Priestley, P. J. Wojtowicz and P. Sheng, Plenum Press, 1975.
5. *Applications of Liquid Crystals*. Ed. G. Meier, E. Sackmann and J. G. Grabmaier, Springer Verlag, 1975.
6. *Liquid Crystals*, (Eds.) S. Chandrasekhar, CUP 1977.
7. *Liquid Crystals*. Solid State Physics Suppl. 14, (Ed.) L. Liebert, AP, 1978.
8. *Textures of Liquid Crystals*, (Ed.) D. Demus and L. Richter, Verlag Chemie, 1978.
9. *The Molecular Physics of Liquid Crystals*, (Eds.) G. R. Lukhurst and G. W. Gray, AP, NY, 1979.
10. *Liquid Crystals and Biological Structure*, (Ed.) G. H. Brown and J. J. Wolken, AP 1979.
11. *Liquid Crystals*, Proceedings of the International Conference held at Bangalore, in 1979, (Ed.) S. Chandrasekhar, HEYDEN, London (1980).
12. *Handbook of Liquid Crystals*, (Ed.) H. Kelker and R. Hatz, Verlag Chemie, 1980.
13. *Physical Properties of Liquid Crystalline Materials*, (Ed.) W. H. de Jeu, Gordon and Breach Science Publishers, 1980.
14. *Polymeric Liquid Crystals*, (Ed.) A. Ciferri, W. R. Krigbaum and Robert B. Meyer, AP, 1982.
15. *Advances in Liquid Crystals* Vol. 1-6, Ed. Glenn H. Brown, AP 1978-1983.
16. *Smectic Liquid Crystals*, (Ed.) G. W. Gray and J. W. Goodby, Glasgow, Leonard Hill, 1984.

17. *Thermotropic liquid crystals*, (Ed.) G. W. Gray, Wiley, Chichester, 1987.
18. *Thermotropic Liquid Crystals, Fundamentals*. (Ed.) G. Vertogen and W. H. de Jeu, Springer-Verlag 1988.
19. *Structure of Liquid Crystal Phases*, Lecture Notes in Physics - Vol. 23, (Ed.) P. S. Pershan World Scientific 1988.
20. *Liquid Crystals: Nature's Delicate Phase of Matter* (Eds.) P. J. Collings, (Princeton Press, Princeton, 1990.
21. *Liquid Crystal: Nature's Delicate Phase of Matter*, Peter J. Collings, (Princeton Press, Princeton, 1990.
22. *Liquid Crystals Application and Uses*, Vol. 1-3. (Ed.) B. Bahadur, World Scientific, 1990-1992.
23. *Thermophysical Properties of Liquid Crystals*, (Ed.) A. L. Tsykalo, Gordon and Breach Science Publishers, 1991.
24. *Ferroelectric Liquid Crystals: Principles, Properties and applications*, (Eds.), J. W. Goodby, R. Blinc, N. A. Clark, S. T. Lagerwall, M. A. Osipov, S. A. Pikin, T. Sakurai, K. Yoshino and B. Zeks, Gordon & Breach, Philadelphia, 1991.
25. *Liquid Crystals, Second edn.*, (Eds.) S. Chandrasekhar, Cambridge University Press, 1992.
26. *The Physics of Liquid Crystals*. 2nd ed., (Ed.) P. G. de Gennes and J. Prost, OUP (Clarendon) London, 1993.
27. *Liquid Crystals in the Nineties and Beyond*, (Ed.) S. Kumar, World Scientific, 1995.
28. *The Surface Physics of Liquid Crystals*. (Ed.) A. A. Sonin, Gordon and Breach Science Publishers, 1995.
29. *Introduction to Liquid Crystals Chemistry and Physics*. (Eds.) P. J. Collings and M. Hird, Taylor & Francis, 1997.
30. *The Optics of Thermotropic Liquid Crystals*, (Ed.) S. Elston and R. Sambles, Taylor & Francis, 1998.
31. *Handbook of Liquid Crystals*. Vol. 1 "Fundamentals", 2A "Low Molecular Weight Liquid Crystals I", 2B "Low Molecular Weight Liquid Crystals II", 3 "High Molecular Weight Liquid Crystals", (Ed.) D. Demus, J. Goodby, G. W. Gray, H.-W. Spiess and V. Vill, WILEY-VCH, Verlag GmbH, Weinheim, FRG, 1998.
32. *Ferroelectric and antiferroelectric Liquid Crystals*, (Eds.) S.T. Lagerwall, Weinheim, Wiley-VCH, 1999.

- 33.** *The Physics of Ferroelectric and Antiferroelectric Liquid Crystals*, (Eds.) I. Musevic, R. Blinc and B. Zeks, Singapore, (World Scientific, Singapore 2000).
- 34.** *Physical properties of liquid crystals*, Eds. D. A. Dunmur, A. Fukuda and G. R. Luckhurst, INSPEC, London, 2001.
- 35.** *Principles and Applications of Ferroelectric and Related Materials*, (Ed.) M.E. Lines and A.M. Glass, Oxford University Press: Oxford, 2001.
- 36.** *Textures of liquid crystals*, (Eds.) I. Dierking, WILEY-VCH, GmbH & Co. KGaA, 2003.
- 37.** *Relaxation phenomena – Liquid crystals, magnetic systems, polymers, high-TC superconductors, metallic glasses*, (Eds.) W. Haase and S. Wrobel, (Springer-Verlag, Berlin-Heidelberg), 2003.
- 38.** *Crystals That Flow: Classic Papers from the History of Liquid Crystals*, (Ed.) T. J. Sluckin, D. A. Dunmur and H. Stegemeyer, 2004.

APPENDIX B

LIST OF PUBLICATIONS

1. Smectic layer spacing, average intermolecular distance and spontaneous polarization of room temperature FLC mixtures; S. Haldar, **D. Sinha**, D. Goswami, P. K. Mandal, K. C. Dey and A. Lapanik; **Molecular Crystals and Liquid Crystals**; Vol. 547, pp. 25-32 (2011).
2. X-ray diffraction and dielectric spectroscopy studies on a partially fluorinated ferroelectric liquid crystal from the family of terphenyl esters; S. Haldar, K.C. Dey, **D. Sinha**, P.K. Mandal, W. Haase and P. Kula; **Liquid Crystals**; Vol. 39, No. 10, pp. 1196-1203 (2012).
3. On the nature of molecular associations, static permittivity and dielectric relaxation in a uniaxial nematic liquid crystal; **D. Sinha**, D. Goswami, P. K. Mandal, Ł. Szczucinski and R. Dabrowski; **Molecular Crystals and Liquid Crystals**; Vol. 562, pp. 156–165 (2012).
4. Effect of molecular conformation on the mesogenic properties of a partially fluorinated nematogenic compound investigated by X-ray diffraction and dielectric measurements; S. Haldar, **D. Sinha**, P. K. Mandal, K. Goubitz and R. Peschar; **Liquid Crystals**; Vol. 40, No. 5, pp. 689–698 (2013).
5. Molecular and dynamical properties of a perfluorinated liquid crystal with direct transition from ferroelectric SmC* phase to isotropic phase; D. Goswami, **D. Sinha**, A. Debnath, P.K. Mandal, S.K. Gupta, W. Haase, D. Ziobro, R. Dabrowski; **Journal of Molecular Liquids**; Vol. 182, 95–101 (2013).
6. High birefringence laterally fluorinated terphenyl isothiocyanates: Structural, optical and dynamical properties; **D. Sinha**, P. K. Mandal and R. Dabrowski; **Physica B**; Vol. 441, pp. 100-106 (2014).
7. Hexatic and blue phases in a chiral liquid crystal: optical polarizing microscopy, synchrotron radiation and dielectric study; **D. Sinha**, A. Debnath and P. K. Mandal; **Materials Research Express**; Vol. 1 (035101), pp. 1-13 (2014).

8. Structural, optical and dynamical properties of a high birefringence laterally fluorinated terphenyl isothiocyanate; **D. Sinha**, P. K. Mandal and R. Dabrowski; **Phase Transitions**; Vol. 88, No. 2, pp. 153-168 (2015).

BIBLIOGRAPHY

CHAPTER 1:

- [1] G. Durand and J. D. Lister; *Ann. Rev. Mate. Sci.*, 23, 269 (1973), Recent advances in liquid crystals.
- [2] T. J. Sluckin, D. A. Dunmur and H. Stegemeyer, *Crystals That Flow: Classic Papers from the History of Liquid Crystals*, History of Physics Group Newsletter, Institute of Physics (2006).
- [3] O. Lehmann; *Z. physik. Chem.* 4, 462- 472 (1889), Fließende Kristalle.
- [4] F. Reinitzer; *Monatshefte fur Chemie.*, 9, 421-441(1888), Beitrage Zur Kenntnis des Cholesterins.
- [5] G. Freidel; *Ann. Physique (Paris)*, 18, 273 (1922), Les états mésomorphes de la matière.
- [6] V. Vill; *Liq. Cryst 3.4 Database*, LC publisher GmbH, hamburg, May (2000).
- [7] H. Kelker and R. Hatz; *Verlag Chemie*, Chapter 1 (1980), *Hand Book of Liquid Crystals*.
- [8] H. Kelker; *Mol. Cryst. Liq. Cryst.*, 21, 1 (1973), History of liquid crystals.
- [9] H. Kelker and P. M. Knoll; *Liquid. Cryst.* 5(1), 19 (1989), Plenary Lecture: Some pictures of the history of liquid crystals.
- [10] G. W. Gray; *Mol. Cryst. Liq. Cryst.*, 63, 3 (1981), Comments on some recent development in the field of liquid crystals.
- [11] G. W. Gray; *Liq. Cryst.*, 24(1), 5 (1998), Reminiscences from a life with liquid crystals.
- [12] P. J. Coolings and M. Hird, *Introduction to Liquid Crystals Chemistry and Physics*, Taylor & Francis (1998).
- [13] G. W. Gray and H. Finkelmann in *Polymeric Liquid Crystals*, ed. A. Ciferri, W. R. Krigbaum and Robert B. Meyer, AP, chap-1 and chap-2 respectively (1982).
- [14] D. Demus; *Mol. Cryst. Liq. Cryst.*, 364, 25 (2001), One century liquid crystal chemistry: from Vorlander's rods to disks, stars and dendrites and G. W. Gray in *Handbook of Liquid Crystals. Vol. 1 (Fundamentals)*, Ed. D. Demus, J. W. Goodby, G. W. Gray, H.-W. Spiess and V. Vill, Introduction and Historical Development, WILEY-VCH, Verlag GmbH, Weinheim, FRG (1998).
- [15] S. Chandrasekhar, B. K. Sadashiva and K. A. Suresh; *Pramana*, 9, 471- 480 (1977), Liquid crystals of disc-like molecules.
- [16] J. Billard, J. C. Dubois, T. H. Nguyen and A. Zann; *Nouveau J. Chim.* 2, 535-540 (1978), Une mésophase disquotique.
- [17] *Liquid Crystals Application and Uses Vol. 1-3*. Ed. B. Bahadur, World Scientific, (1990-1992).
- [18] G. W. Brown, J. W. Doane and V. D. Neff, *A Review of the Structure and Physical Properties of Liquid Crystals*. CRC Press, Cleveland, Ohio (1971).
- [19] J. W. Goodby; *Liq. Cryst.* 24, 25-38 (1998), Liquid crystals and life.
- [20] P. G. de Gennes; "The Physics of Liquid Crystals", Clarendon Press, Oxford (1974); P. G. de Gennes and J. Prost, 2nd ed. Clarendon Press, Oxford (1993).
- [21] L. A. Madsen, T. J. Dingemans, M. Nakata, E. T. Samulski; *Phys. Rev. Lett.* 92 (14) (2004), Thermotropic Biaxial Nematic Liquid Crystals.

- [22] A. de Vries; *Mol. Cryst. Liq. Cryst.*, 10, 31 (1970), Evidence for the Existence of More Than One Type of Nematic Phase.
- [23] A. de Vries; *Mol. Cryst. Liq. Cryst.*, 10, 219 (1970), X-Ray Photographic Studies of Liquid Crystals I. A Cybotactic Nematic Phase and A. de Vries, in *Proc. of the International Liquid Crystal Conference, Bangalore, December, Pramana Supplement I*, 93 (1973), X-Ray Studies of Liquid Crystals: V. Classification of Thermotropic Liquid Crystals and Discussion of Intermolecular Distances.
- [24] P. E. Cladis; *Phys. Rev. Lett.*, 35, 48-51 (1975), New Liquid-Crystal Phase Diagram.
- [25] G. W. Gray, *Molecular Structure and the Properties of Liquid Crystals*, Academic Press, London (1962).
- [26] P. S. Pershan, *Structure of Liquid Crystals Phases*, World Scientific Lecture Note in Physics, Vol 23, World Scientific, Singapore (1988).
- [27] G. W. Gray and J. W. Goodby, Eds., *Smectic Liquid Crystals, Textures and Structures*, Leonard - Hill, Philadelphia (1984).
- [28] A. J. Leadbetter in *Thermotropic Liquid Crystals, Critical Reports on Applied Chemistry*, Vol. 22, G. W. Gray(Ed.), Wiley, Chichester, p1 (1987).
- [29] A. de Vries in *Liquid Crystals, The Fourth State of Matter* (Ed. F. D. Saeva), Marcell Dekker, New York, p1 (1972).
- [30] A. de Vries, *Mol. Cryst. Liq. Cryst.*, 63, 215(1981), A Structural Classification of Smectic Liquid Crystals.
- [31] J. Doucet in *The Molecular Physics of Liquid Crystals*, Eds. G. R. Luckhurst and G. W. Gray, Academic Press, London, p317 (1979).
- [32] L. V. Azaroff, *Mol. Cryst. Liq. Cryst.*, 60, 73(1980), X-Ray Diffraction by Liquid Crystals.
- [33] D. Demus, J. W. Goodby, G. W. Gray and H. Sackmann, *Mol. Cryst. Liq. Cryst.*, 56, 311(1980), Recommendation for The Use of The Code Letters G And H for Smectic Phases.
- [34] J. W. Goodby and G. W. Gray, *Mol. Cryst. Liq. Cryst.*, 41, 145-150 (1978), Some New Smectic F Materials.
- [35] R. M. Richardson, A. J. Leadbetter and J. C. Frost, *Mol. Phys.*, 45, 1163 (1982), A comparative study of the molecular motions in the three smectic phases of isobutyl 4(4' phenylbenzylideneamino) cinnamate using incoherent neutron scattering.
- [36] A. J. Leadbetter, J. C. Frost, J. P. Gaughan, and M. A. Mazid, *J. Phys. (Paris)*, 40, C3-185-C3-192 (1979), The structure of the crystal, smectic E and smectic B forms of IBPBAC.
- [37] J. W. Goodby in *Handbook of Liquid Crystals*, Eds. D. Demus, J. Goodby, G.W. Gray, H.-W. Spiess and V. Vill, Vol. 2A, Wiley-VCH, Verlag GmbH, Weinheim, FRG, p7 (1998).
- [38] F. Hardouin, A. M. Levelut, J. Bennattar and G. Sigaud; *Solid State Comm.*, 33, 337-340 (1980), X-rays investigations of the smectic A1 - smectic A2 transition.
- [39] A. J. Leadbetter, J. L. Durrant and M. Rugman; *Mol. Cryst. Liq. Cryst. Lett.*, 34, 231 (1977), The Density Of 4 n-Octyl-4-Cyano-Biphenyl (8CB).
- [40] A. J. Leadbetter, J. C. Frost, J.P. Gaughan, G.W. Gray and A. Mosley; *J. Phys. (Paris)*, 40, 375-380 (1979), The structure of smectic A phases of compounds with cyano end groups.
- [41] F. Hardouin, G. Sigaud, N. H. Tinh, A.F. Achard; *J. Phys. (Paris) Lett.*, 42, 63-66 (1981), A fluid smectic A antiphase in a pure nitro rod-like compound.

- [42] J. Prost; *Advances in Physics*, 33, 1-46 (1984), The smectic state.
- [43] P. S. Pershan, *Structure of Liquid crystals*, World Scientific, Singapore (1988).
- [44] B. R. Ratna, R. Shashidhar and V. N. Raja, *Phys. Rev. Lett.*; 55(14), 1476 (1985), Smectic-A phase with two collinear incommensurate density modulations.
- [45] S. T. Wang, S. L. Wang, X. F. Han, Z. Q. Liu, S. Findeisen, W. Weissflog and C. C. Huang; *Liq. Cryst.*, 32, 5, 609–617 (2005), Optical studies on two tilted smectic phases of meta-substituted three-ring liquid crystal compounds.
- [46] A. L. Tsykalo, *Thermophysical properties of liquid crystals*, Gordon and Breach Science Publishers (1991).
- [47] R. Pindak, D. E. Moncton, S. C. Davey and J. W. Goodby; *Phys. Rev. Lett.*, 46, 1135 (1981), X-Ray Observation of a Stacked Hexatic Liquid-Crystal B Phase.
- [48] D. E. Moncton and R. Pindak in *Ordering in Two Dimensions* (Ed. S. K. Sinha), North Holland, New York, p83 (1980).
- [49] A. J. Leadbetter, J. C. Frost, M. A. Mazid; *J. Phys. (Paris) Lett.*, 40, 325-329 (1979), Interlayer correlations in smectic B phases.
- [50] P. S. Pershan, G. Aeppli, J. D. Litster and R. J. Birgeneau; *Mol. Cryst. Liq. Cryst.*, 67, 205(1981), High-Resolution X-ray Study of the Smectic A-Smectic B Phase Transition and the Smectic B Phase in Butyloxybenzylidene Octylaniline.
- [51] D. E. Moncton, and R. Pindak; *Phys. Rev. Lett.*, 43, 701(1979), Long-Range Order in Two- and Three-Dimensional Smectic-B Liquid-Crystal Films.
- [52] P. A. C. Gane, A. J. Leadbetter and P.G. Wrighton; *Mol. Cryst. Liq. Cryst.*, 66, 247-266 (1981), Structure and Correlations in Smectic B, F and I Phases.
- [53] S. Diele, D. Demus and H. Sackmann; *Mol. Cryst. Liq. Cryst. Lett.*, 56, 217 (1980), X-Ray Studies in the n-Pentyl 4-[4-n-Dodecyl-Oxybenzylidene-Amino]-Cinnamate in the S_1 Phase.
- [54] J. J. Benattar, F. Moussa, M. Lambert; *J. Phys. (Paris) Lett.*, 42, 67-70 (1981), Two kinds of two-dimensional order : the SmF and SmI phases.
- [55] A. M. Levelut, J. Doucet and M. Lambert; *J. Phys.*, (Paris), 35, 773-779 (1974), X-ray study of the nature of the smectic B mesophases and of the solid-smectic B phase transition.
- [56] J. Doucet, P. Keller, A.M. Levelut and P. Porquet; *J. Phys. (Paris)*, 39, 548-553 (1978), Evidence of two new ordered smectic phases in ferroelectric liquid crystals.
- [57] A. J. Leadbetter, M. A. Mazid, R. M. Richardson, in *Liquid Crystals*, Ed. S. Chandrasekhar, Heyden, London, p65 (1980).
- [58] J. L. Fergason; *Sci. Am.*, 211, 76-85 (1964), Liquid Crystals.
- [59] D. Demus, J. Goodby, G.W. Gray, H.-W. Spiess and V. Vill, *Handbook of Liquid Crystals*, Ch. IV and V, Vol. 2A, Wiley-VCH, Verlag GmbH, Weinheim, FRG (1998).
- [60] F. D. Saeva; *Mol. Cryst. Liq. Cryst.*, 23, 171-177 (1973), On the Relationship between Cholesteric and Nematic Mesophases.

- [61] T. Nakagiri, H. Kodama and K.K. Kobayashi; *Phys. Rev. Lett.*, 27, 564-567 (1971), Helical Twisting Power in Mixtures of Nematic and Cholesteric Liquid Crystals*.
- [62] I. G. Chistiyakov; *Sov. Phys. Usp.*, 9, 551-573 (1967), Liquid Crystals.
- [63] A. Saupe; *Angew. Chem. Intl. Edn.* 7, 97-112 (1968), Recent Results in the Field of Liquid Crystals.
- [64] A. Hochbaum, Fluorescent Guest-Host in Scattering Liquid crystals and New Physical Phenomena in Thin Liquid Crystal Films (Ph.D. Thesis), Temple University, p.5 (1980).
- [65] J. J. Wysocki, J. Adams and W. Hasse; *Phys. Rev. Lett.*, 20, 1024-1025 (1968), Electric-Field-Induced phase change in cholesteric liquid crystals.
- [66] H. Baessler and M. M. Labes; *Phys. Rev. Lett.*, 21, 1791-1793 (1968), Relationship Between Electric Field Strength and Helix Pitch in Induced Cholesteric-Nematic Phase Transitions.
- [67] O. Lehmann; *Z Phys. Chem*, 56, 750 (1906).
- [68] Harry J Coles, Pivnenko, N. Mikhail; *Nature* 436 (7053), 997–1000 (2005), Liquid crystal 'blue phases' with a wide temperature range.
- [69] Jun Yamamoto, Isa Nishiyama, Miyoshi Inoue, Hiroshi Yokoyama; *Nature*, 437 (7058): 525 (2005), Optical isotropy and iridescence in a smectic blue phase.
- [70] R. M. Hornreich and S. Shtrikman; *J. Physique*, 41, 335-340 (1980), A body-centered cubic structure for the cholesteric blue phase.
- [71] H. Kikuchi, M. Yokota, Y. Hisakado, H Yang, T. Kajiyama; *Nature Materials*, 1 (1): 64–8 (2002), Polymer-stabilized liquid crystal blue phases.
- [72] R. B. Meyer, L. Liebert, L. Strzelecki and P. Keller; *J. Phys. Lett.* 36, L69-L71 (1975), Ferroelectric liquid crystals.
- [73] S. Pirke and M. Glogorova in *Ferroelectric – Physical Effects*; Ed, M. Lallart, INTECH, Rijeka, Croatia (2011).
- [74] S. Pirkl and M. Glogarova; *Intech*, Croatia (2011), Ferroelectric liquid crystals with high spontaneous polarization.
- [75] R. B. Meyer; *Mol. Cryst. Liq. Cryst.*, 40, 33-48 (1977), Ferroelectric liquid crystals: A review.
- [76] Yu. P. Panarin, O. Kalinovskaya & J. K. Vij; *Liquid Crystals*, Vol. 25, No. 2, 241- 252 (1998), The investigation of the relaxation processes in antiferroelectric liquid crystals by broad band dielectric and electro-optic spectroscopy.
- [77] A. D. L. Chandani, E. Gorecka, Y. Ouchi, H. Takezoe, and A. Fukuda; *Jpn. J. Appl. Phys.* 28(7), L1265 (1989), Antiferroelectric Chiral Smectic Phases Responsible for the Trislable Switching in MHPOBC.
- [78] H. Hiraoka, A. D. L. Chandani, E. Gorecka, Y. Ouchi, H. Takezoe and A. Fukuda; *Jpn. J. Appl. Phys.* 29(8), L1473 (1990), Electric-Field-Induced Transitions among Antiferroelectric, Ferrielectric and Ferroelectric Phases in a Chiral Smectic MHPOBC.
- [79] J. P. F. Lagerwall, P. Rudquist, S. T. Lagerwall and F. Gießelmann; *Liq. Cryst.*, 30, 399-414 (2003), On the phase sequence of antiferroelectric liquid crystals and its relation to orientational and translational order.
- [80] K. Miyachi and A. Fukuda, in *Handbook of Liquid Crystals*, Eds. D. Demus, J. Goodby,

G.W. Gray, H.-W. Spiess and V. Vill, Vol. 2B, Wiley-VCH, Verlag GmbH, Weinheim, FRG, Ch. 3 (1998).

[81] J. Dijon in *Liquid Crystal Application and Uses* (Ed. B. Bahadur), Vol. I, World Scientific, Singapore, p 305 (1990).

[82] N. A. Clark and S. T. Lagerwall; *Appl. Phys. Lett.*, 36, 899-901(1980), Submicrosecond bistable electrooptic switching in liquid crystals.

[83] D. Armitage, J. I. Thakara and W. D. Eades; *Ferroelectrics*, 85, 291-302 (1988), Ferroelectric liquid-crystal devices and optical processing.

[84] M. Hird; *Liq. Cryst.*, 38, 1467–1493 (2011), Invited topical review (Ferroelectricity in liquid crystals - materials, properties and applications).

[85] A. N. Cammidge and R. J. Bushby in *Handbook of Liquid Crystals*, Eds. D. Demus, J. Goodby, G.W.Gray, H.-W. Spiess and V. Vill, Vol. 2B, Wiley-VCH, Verlag GmbH, Weinheim, FRG, Ch.VII (1998).

[86] S. Kumar; *Liquid Crystals*, 31, 1037-1059 (2004), Recent developments in the chemistry of triphenylene-based discotic liquid crystals.

[87] M. Schadt and W. Helfrich; *Appl. Phys. Lett.* 18(4), 127 (1971), Voltage-dependent optical activity of a twisted nematic liquid crystal.

[88] T. J. Scheffer and J. Nehring; *Appl. Phys. Lett.* 45(10), 1021 (1984), A new, highly multiplexable liquid crystal display.

[89] H. Xu, D. Hartono and K. -L. Yang, *Liquid Crystals*, 37 (10), 1269–1274 (2010), Detecting and differentiating *Escherichia coli* strain TOP10 using optical textures of liquid crystals.

[90] J. Akaogi, Y. Koizumi, M. Ono and H. Furue; *Mol. Cryst. Liq. Cryst.*, 596, 106–112 (2014), Application of Ferroelectric Liquid Crystals to Optical Devices.

[91] J. S. Patel and Seong-Woo Suh; *Journal of the Korean Physical Society*, 32, S1048-S1051 (1998), Ferroelectricity in Liquid Crystals and Its Applications.

[92] C. L. Khetrpal in *Liquid Crystals in the Nineties and Beyond*, Ed. S. Kumar, World Scientific, p 435 (1995).

[93] B. Bahadur in *Handbook of Liquid Crystals*, Eds. D. Demus, J. Goodby, G.W. Gray, H.-W. Spiess and V. Vill, Vol. 2A, Wiley-VCH, Verlag GmbH, Weinheim, FRG, p257 (1998).

CHAPTER 2:

- [1] M. Born; Sitzb. kgl. preub. Akad. Wiss., 614 (1916), Theorie der flussigen Kristalle und des electrischen Kerr Effects in Flussigkeiten.
- [2] P. G. de Gennes; The Physics of Liquid Crystals, Clarendon Press, Oxford (1974); P. G. de Gennes and J. Prost, 2nd ed. Clarendon Press, Oxford (1993).
- [3] A. L. Tsykalo; Thermophysical properties of liquid crystals, Gordon and Breach Science Publishers, (1991).
- [4] S. Chandrasekhar, Liquid Crystals, 2nd Edn., Cambridge University Press, Cambridge, (1992).
- [5] I. Musevic, R. Blinc and B. Zeks's, The Phases of Ferroelectric and Antiferroelectric Liquid Crystals, World Scientific, Singapore (2000).
- [6] W. Maier and A. Saupe, Z. Naturforsch 13a, 564 (1958), Eine einfach molekularstatische theorie der nematischen kristallinflussign phase, Dispersionswechselwirkung; W. Maier, and A. Saupe, Z. Naturforsch, 14a, 882 (1959), Eine einfach molekularstatische theorie der nematischen kristallinflussign phase. Teil I; W. Maier, and A. Saupe, Z. Naturforsch, 15a, 287 (1960), Eine einfach molekularstatische theorie der nematischen kristallinflussign phase. Teil II; A. Saupe and W. Maier, Z. Naturforsch, 16a, 816 (1961), Methoden zur Bestimmung des Ordnungsgrades nematischer Schichten; W Maier, Angew. Chem. 73, 660 (1961), Struktur und Eigenschaften nematisscher Phasen.
- [7] A. L. Tsykalo, Thermophysical Properties of Liquid Crystals, Gordon and Breach Science Publishers, p27 (1991).
- [8] K. K. Kobayashi; Phys. Lett. A, 31, 125-126 (1970), On the theory of translational and orientational melting with application to liquid crystals.
- [9] W. L. McMillan; Phys. Rev. A 4, 1238-1246 (1971), Simple molecular model for the smectic A phase of liquid crystals.
- [10] W. L. McMillan; Phys. Rev.A 6, 936 (1972), X-Ray Scattering from Liquid Crystals. I. Cholesteryl Nonanoate and Myristate.
- [11] A. L. Tsykalo, Thermophysical Properties of Liquid Crystals, Gordon and Breach Science Publishers, p 164 (1991).
- [12] R. J. Meyer and W. L. McMillan; Phys. Rev. A, 9, 899 (1974), Simple molecular theory of the smectic C, B, and H phases.
- [13] S. Chandrashekar; Liquid crystals, Cambridge University Press (1977).
- [14] G. Vertogen and W. H. de Jeu; Thermotropic Liquid crystals, Fundamentals. Springer-Verlag, Berlin (1988).
- [15] P. J. Collings and Michael Hird; Introduction to Liquid Crystals Chemistry and Physics. Taylot and Francis (1998).
- [16] G. R. Luckhurst; Molecular Phphysics of Liquid Crystals, Academic Press (1979).
- [17] R. L. Humphries, P. G. James and G. R. Luckhurst; J. Chem. Soc., Faraday Trans. 2, 68, 1031 – 1044 (1972), Molecular field treatment in nematics.

- [18] K. K. Kobayashi; J. Phys. Soc. (Japan), 29, 101 (1970), Theory of Translational and Orientational Melting with Application to Liquid Crystals I.
- [19] K. K. Kobayashi; Mol. Cryst. Liq. Cryst., 13, 137 (1971), Theory of Translational and Orientational Melting with Application to Liquid Crystals.
- [20] B. K. Vainstein; Diffraction of X-rays by Chain Molecules, Elsevier, Amsterdam (1966).
- [21] H. Kelkar and R. Hatz; Handbook of Liquid Crystals, Verlag Chemie, Ch. 5 (1980).
- [22] P. S. Pershan; Structure of Liquid Crystalline Phases, World Scientific, Singapore (1988).
- [23] G. Ungar in Physical properties of liquid crystals, D. A. Dunmur, A. Fukuda and G. R. Luckhurst (Eds.), INSPEC, London, Ch. 4.1 (2001).
- [24] G. Vertogen and W. H. de Jeu (Eds.), Thermotropic Liquid Crystals Fundamentals., Springer-Verlag, p-207 (1988).
- [25] G. R. Luckhurst in Liquid Crystals & Plastic Crystals (Eds. G. W. Gray and P. A. Winsor), Ellis Horwood Limited, Vol 2, p-144 (1974).
- [26] C. L. Khetrpal and A. C. Kunwar in Advances in Liquid Crystals, Vol. 1-6, Ed. Glenn H. Brown, p-173, AP (1983).
- [27] V. D. Neff in Liquid Crystals & Plastic Crystals (Ed. G. W. Gray and P. A. Winsor), Ellis Horwood Limited, Vol 2, p-231 (1974).
- [28] S. J. Gupta, R. A. Gharde and A. R. Tripathi; Mol. Cryst. Liq. Cryst., 364, 461- 468 (2001), Phase Transition Temperatures of LCs using Fabry-Perot Etalon.
- [29] D. Demus, Textures of liquid crystals, Verlag Chemie Weinheim, New York (1978).
- [30] I. Dierking, Textures of liquid crystals WILEY-VCH, GmbH & Co. KGaA p-16 (2003).
- [31] A. J. Slaney, K. Takatohi and J. W. Goodby in The Optics of Thermotropic Liquid Crystals, Ed. S. Elston and R. Sambles, Taylor & Francis (1998), Defect textures in liquid crystals.
- [32] Y. Bouligand in Handbook of Liquid Crystals. Vol. 1 (Fundamentals), Ed. D. Demus, J. Goodby, G. W. Gray, H.-W. Spiess and V. Vill, WILEY-VCH, Verlag GmbH, Weinheim, FRG (1998), Defects and textures.
- [33] B. Jha and R. Paul; Proc. Nucl. Phys. and Solid State Phys. Symp., India . 19C, 491 (1976) A Design for High Temperature X-ray Camera for the Study of Liquid Crystals in a Magnetic Field.
- [34] B. Jha, S. Paul, R. Paul and P. Mandal; Phase Transitions, 15, 39-48 (1989), Order parameters of some homologue cybotactic nematics from X-ray diffraction measurements.
- [35] S. Diele. P. Brand and H. Sackmann; Mol. Cryst. Liq. Cryst., 16, 105-116 (1972), X-ray Diffraction and Polymorphism of Smectic Liquid Crystals I. A-, B- and C-modifications.
- [36] A. de Vries; Pramana, Suppl. No. 1, 93 (1975), X-Ray Studies of Liquid Crystals: V, Classification of Thermotropic Liquid Crystals and Discussion of Intermolecular Distances.

- [37] A. de Vries, A. Ekachi and N. Sielberg; *J. de Phys.*, 40, C3-147 (1979), X-Ray Studies of Liquid Crystals VI. The Structure of the Smectic A, C, Bn and Bt Phases of Trans-1, 4-Cyclohexane-DI-NOctyloxybenzoate.
- [38] A. J. Leadbetter, J. Prost, J. P. Gaughan and M. A. Mazid; *J. de Phys.*, 40, C3-185 – C3-193 (1979), The structure of the crystal, SmE and SmB forms of IBPBAC.
- [39] A. J. Leadbetter and P. G. Wrighton; *J. de Phys.*, 40, C3-234 – C3-242 (1979), Order parameters in S_A , S_C , and N phases by X-ray diffraction.
- [40] V. M. Sethna, A. de Vries and N. Spielberg; *Mol. Cryst. Liq. Cryst.*, 62, 141-153 (1980), X-Ray Studies of Liquid Crystals VIII: A Study of the Temperature Dependence of the Directly Observed Parameters of the Skewed Cybotactic Nematic Phase of Some Bis-(4'-n-Alkoxybenzal) -2-Chloro-1,4-Phenylenediamines.
- [41] L.V. Azaroff and C. A. Schuman; *Mol. Cryst. Liq. Cryst.*, 122, 309-319 (1985), X-Ray Diffraction by Cybotactic Nematics.
- [42] A. de Vries; *Mol. Cryst. Liq. Cryst.*, 131, 125-145 (1985), The Use of X-Ray Diffraction in the Study of Thermotropic Liquid Crystals with Rod-Like Molecules.
- [43] P. Mandal, M. Mitra, S. Paul and R. Paul; *Liq. Cryst.*, 2, 183-193 (1987), X-Ray Diffraction and Optical Studies of an Oriented Schiff's Base Liquid Crystal.
- [44] A. de Vries; *Mol. Cryst. Liq. Cryst.*, 10, 219-236 (1970), X-ray photographic studies of liquid crystals I. A cybotactic nematic phase.
- [45] A. de Vries; *Mol. Cryst. Liq. Cryst.*, 11, 361-383 (1970), X-Ray Photographic Studies of Liquid Crystals II. Apparent Molecular Length and Thickness in Three Phases of Ethyl-p-Ethoxybenzal-p-Aminobenzoate.
- [46] C. Kittel; *Intro to Solid State Physics*, Wiley Eastern, Chapter 2 (1976).
- [47] G. Pelzl in *Handbook of Liquid Crystals. Vol. 1 (Fundamentals)*, Ed. D. Demus, J. Goodby, G. W. Gray, H.-W. Spiess and V. Vill, WILEY-VCH, Verlag GmbH, Weinheim, FRG (1998).
- [48] D. A. Dunmur in *The Optics of the Thermotropic Liquid Crystals*. Ed. S. Elston and R. Sambles, Taylor & Francis (1998).
- [49] S. M. Kelly, M. O'Neill; Chapter 1, *Liquid Crystals For Electro-optic Applications*.
- [50] A. K. Zeminder, S. Paul and R. Paul; *Mol. Cryst. Liq. Cryst.* 61, 191-206 (1980), Refractive Indices and Orientational Order Parameter of Five Liquid Crystals in Nematic Phase.
- [51] M. F. Vuks; *Optics and Spectroscopy*, 20, 361-368, (1966), Determination of optical anisotropy of aromatic molecules from the double refraction of crystals.

- [52] H. E. J. Neugebauer, *J. Canad. Phys.*, 32, 1-8 (1954), Clausius-Mossotti equation for certain types of anisotropic crystals.
- [53] S. Chandrasekhar; *Liquid Crystals*, second edn., Cambridge University Press, Cambridge, p39, (1992).
- [54] W. H. de Jeu, *Physical Properties of Liquid Crystalline Materials*, Ed G. Gray, Gordon and Breach, Vol. 1, p 41 (1980).
- [55] P. G. de Gennes; *Mol. Cryst. Liq. Cryst.* 12, 193-214 (1971), Short Range Order Effects in the Isotropic Phase of Nematics and Cholesterics.
- [56] I. Haller, H. A. Huggins, H. R. Lilienthal and T. R. McGuire; *J. Phys. Chem.*, 77, 950 (1973), Order-Related Properties of Some Nematics; I. Haller; *Jappl. Phys. Lett.*, 24, 349 (1974), Alignment and wetting properties of Nematics.
- [57] K. Toriyama, K. Suzuki, T. Nakagomi, T. Ishibashi and K. Odawara; *J. de Phys*, 40, C3-317 (1979), A design of liquid crystal material for multiplexed liquid crystal display.
- [58] D. A. Dunmur and W. H. Miller; *Mol. Cryst. Liq. Cryst.*, 60, 281-283 (1980), Dipole-Dipole Correlation in Nematic Liquid Crystals.
- [59] R. E. Michel and G. W. Smith; *J. Appl. Phys.* 45, 3234 (1974), Dependence of birefringence threshold voltage on dielectric anisotropy in a nematic liquid crystals.
- [60] C. J. F. Böttcher, *Theory of Electric Polarization*, 2nd edition, Vol I (1973) and C. J. F. Böttcher and P. Bordewijk, 2nd edition, Elsevier Scientific Publishing Co., Vol II (1978).
- [61] W. H. de Jeu and T. W. Lathouwers; *Z. Naturforsch* 29a, 905 (1974), Dielectric constants and molecular structure of nematics. I. Terminally substituted azobenzene and azoxybenzenes.
- [62] W. Maier and G. Meier, *Z. Naturforsch*; 16a, 262 (1961), Einfache Theorie der dielektrischen Eigenschaften von homogen orientierten nematischen Phasen.
- [63] L. Onsager; *J. Am. Chem. Soc.*, 58, 1486-1493 (1936), Electric Moments of Molecules in Liquids.
- [64] L. Bata and A. Buka; *Mol. Cryst. Liq. Cryst.* 63, 307 (1981), Dielectric Permittivity and Relaxation Phenomena in smectic Phases.
- [65] H. Fröhlich, *Theory of Dielectrics*. Clarendon Press, Oxford (1949); H. Fröhlich, *J. Chem. Phys.*, 22, 1804 (1954).
- [66] P. Bordewijk; *Physica*, 69, 422-432 (1973), On the derivation of the Kirkwood-Fröhlich equation.

- [67] P. Bordewijk; *Physica*, 75, 146-156 (1974), Extension of the Kirkwood-Fröhlich theory of the static dielectric permittivity to anisotropic liquids.
- [68] P. Bordewijk and W. H. de Jeu; *J. Chem. Phys.* 68 (1), 116 (1978), Calculation of dipole correlation factors in liquid crystals with use of a semiempirical expression for the internal field.
- [69] W. H. de Jeu and P. Bordewijk; *J. Chem. Phys.* 68 (1), 109 (1978), Physical studies of nematic azoxybenzenes. II. Refractive indices and the internal field.
- [70] W. H. de Jeu, T. W. Lathouwers and P. Bordewijk; *Phys. Rev. Lett.* 32, 40 (1974), Dielectric properties of n and S_A p,p/-di-n-heptylazoxybenzene.
- [71] W. H. de Jeu, J. W. A. Goosens and P. Bordewijk; *J. Chem. Phys.* 61, 1985(1974), Influence of smectic order on the static dielectric permittivity of liquid crystals.
- [72] P. Debye, *Polar molecules*, Dover Pub. Inc., NX (1929).
- [73] C. J. F. Böttcher and P. Bordewijk, Ed., *Theory of Electric Polarization*, Vol II, Dielectric in time-dependent fields, Elsevier, Scientific Publishing Co. (1973).
- [74] S. Havriliak and S. Negami; *J. Polime*, 8, 161-210 (1967), A complex plane representation of dielectric and mechanical relaxation processes in some polymers.
- [75] A. Wurflinger; *Int. Rev. Phys. Chem.*, 12, 89 (1993), Dielectric studies under pressure on plastic and liquid crystals.
- [76] W. Haase, H. Pranoto, F. J. Bormuth, *Ber. Bunsenges. Phys. Chem.*, 89, 1229-1234 (1985), Dielectric Properties of Some Side Chain Liquid Crystalline Polymers.
- [77] F. J. Bormuth, Ph.D. Thesis, Technische Hochschule, Darmstadt (1998).
- [78] V. I. Minkin, O. A. Osipov, Y. A. Zhdanov, *Dipole Moments in Organic Chemistry*, New York- London, (1970).
- [79] A. K. Jonscher, *Dielectric Relaxation In Solids*, Chelsea Dielectric Press, London (1983).
- [80] S. Wrobel, B. T. Gowda, W. Haase, *J. Chem. Phys.*, 106 (10), 5904 (1997), Dielectric study of phase transitions in 3-nitro-4-chloro-aniline.
- [81] V. K. Agarwal and A. H. Price; *Mol. Cryst. Liq. Cryst.*, 98, 193-200 (1983), Dielectric Relaxation and Order Parameters in Mixtures of 4-cyanobiphenyl and MBBA.
- [82] V. V. Daniel, *Dielectric Relaxation*, Academic Press, London and N.Y. (1967).

- [83] K. S. Cole and R. H. Cole; *J. Chem. Phys.* 9, 341-351 (1941), Dispersion and Absorption in Dielectrics I. Alternating Current Characteristics.
- [84] J. Hatano, Y. Hakanai, H. Furue, H. Uehara, S. Saito, and K. Murashiro, *Jpn. J. Appl. Phys.*, 33, 5498-5502 (1994), Phase Sequence in Smectic Liquid Crystals Having Fluorophenyl Group in the Core.
- [85] S. Merino, M. R. de la Fuente, Y. Gonzalez, M. A. Perez Jubindo, M. B. Ros, J. A. Puertolas; *Phys. Rev.*, E 54, 5169-5177 (1996), Broadband dielectric measurements on the (R)-1-methylheptyl-6-(4'-decyloxybenzoyloxy)-2-naphthalene carboxylate antiferroelectric liquid crystal.
- [86] A. Fafara, B. Gestblom, S. Wrobel, R. Dabrowski, W. Drzewinski, D. Kilian, W. Haase; *Ferroelectrics*, 212, 79-90 (1998), Dielectric spectroscopy and electrooptic studies of new MHPOBC analogues.
- [87] M. Marzec, R. Dabrowski, A. Fafara, W. Haase, S. Hiller and S. Wrobel; *Ferroelectrics*, 180,127-135(1996), Gold-stone mode and Domain mode relaxation in ferroelectric phases of 4'-[(S,S) - 2,3 - epoxyhexyloxy] Phenyl 4 (Decyloxy) Benzoate (EHPDB).
- [88] H. Uehara, Y. Hakanai, J. Hatano, S. Saito and K. Murashiro; *Jpn. J. Appl. Phys.*, 34, 5424-5428 (1995), Dielectric Relaxation Modes in the Phases of Antiferroelectric Liquid Crystals.
- [89] M. Buivydas, S. T. Lagerwall, F. Gouda, R. Dubal, A. Takeichi; *Ferroelectrics*, 212, 55-65 (1998), The dependence of polarization and dielectric biaxiality on the enantiomeric excess in chiral dopant added to a smectic C host mixture.
- [90] H. Kresse, H. Schmalfluss, W. Weissflog, C. Tschierske, A. Hauser; *Mol. Cryst. Liq. Cryst.*, 366, 505-517 (2001), Dielectric Characterization of Bn Phases.
- [91] W. Kuczynski, Electrooptical studies of relaxation processes in ferroelectric liquid crystals, in: W. Haase, S. Wrobel (Eds), *Relaxation phenomena* –Springer-Verlag, Berlin-Heidelberg, pp 422-444 (2003), Liquid crystals, magnetic systems, polymers, high-TC superconductors, metallic glasses.
- [92] A. M. Biradar, S. Wrobel and W. Haase; *Phys. Rev. A*, 39 2693-2702 (1989), Dielectric relaxation in the smectic-A* and smectic-C* phases of a ferroelectric liquid crystal.
- [93] J. K. Ahuja and K. K. Raina; *Jpn. J. Appl. Phys.*, 39, 4076-4081 (2000), Polarization Switching and Dielectric Relaxations in Ferroelectric Liquid Crystals.
- [94] Y. P. Panarin, O. Kalinovskaya, J. K. Vij and J. W. Goodby; *Phys. Rev. E*, 55, 4345-4353 (1997), Observation and investigation of the ferroelectric subphase with high qT parameter.
- [95] I.-S. Baik, S. Y. Jeon, S. H. Lee, K. A. Park, S. H. Jeong, K. H. An, and Y. H. Lee; *Appl. Phys. Lett.* 87, 263110 (2005), Electrical-field effect on carbon nanotubes in a twisted nematic liquid crystal cell.

- [96] F. Haraguchi, K.-I Inoue, N. Toshima, S. Kobayashi, and K. Takatoh; *Jpn. J. Appl. Phys.* 46, L796 (2007), Reduction of the Threshold Voltages of Nematic Liquid Crystal Electrooptical Devices by Doping Inorganic Nanoparticles.
- [97] F. C. Frank; *Disc. Faraday Soc.*, 25, 19-28 (1958), On the theory of liquid crystals.
- [98] I. W. Stewart, *The Static and Dynamic Continuum Theory of Liquid Crystals*, Taylor and Francis, London (2004).
- [99] B. Kundu, S. K. Pal, S. Kumar, R. Pratibha, N.V. Madhusudana; *Phys. Rev. E: Stat. Nonlinear Soft Matter Phys.* 82, 061703 (2010), Splay and bend elastic constants in the nematic phase of some disulfide bridged dimeric compounds.
- [100] M. Hird; *Liq. Cryst.*, 38, 1467–1493 (2011), Invited topical review (Ferroelectricity in liquid crystals - materials, properties and applications).
- [101] C. B. Sawyer and C. H. Tower; *Phys. Rev.* 35, 269-273 (1930), Rochelle Salt as a Dielectric.
- [102] W. J. Merz; *Phy. Rev.* 95(3), 690-698 (1954), Domain Formation and Domain Wall Motions in Ferroelectric BaTiO₃ Single Crystals; Y. Ouchi, T. Uemura, H. Takezoe and A. Fukuda; *Jpn. J. Appl. Phys.*, 24 (4), L235- L238 (1985), Correspondence between Stroboscopic Micrographs and Spontaneous Polarization Measurements in Surface Stabilized Ferroelectric Liquid Crystal Cells.
- [103] W. J. Merz; *J. Appl. Phys.* 27(8), 938-943 (1956), Switching Time in Ferroelectric BaTiO₃ and Its Dependence on Crystal Thickness.
- [104] H. D. Megaw; *Acta Cryst.*, 7,187-194 (1954), Ferroelectricity and crystal structure II.
- [105] M. E. Lines and A. M. Glan; Oxford, Clarendon 128 (1977), *Principles and Applications of Ferroelectric and Related Materials*.
- [106] K. Miyasato, S. Abe, H. Takezoe, A. Fukuda and E. Kuze; *Jpn. J. Appl. Phys.* 22 (10), L661-L663 (1983), Direct Method with Triangular Waves for Measuring Spontaneous Polarization in Ferroelectric Liquid Crystals.
- [107] S. Kaur, A. K. Thakur, R. Chauhan, S. S. Bawa and A. M. Biradar; *Physica B*, 352, 337-341 (2004), The effect of rotational viscosity on the memory effect in ferroelectric liquid crystal.
- [108] S. S. Bawa, A. M. Biradar and S. Chandra; *Jpn. J. Appl. Phys.* 25(6), L446 (1986), Frequency Dependent Polarization Reversal and the Response Time of Ferroelectric Liquid Crystal by Triangular Wave Method.
- [109] J-Z. Zue, M. A. Handschy and N. A. Clark; *Ferroelectrics*, 73, 305-314 (1987), Electrooptic response during switching of a ferroelectric liquid crystal cell with uniform director orientation.

- [110] K. Skarp, I. Dahl, S. T. Lagerwall and B. Stebler; *Mol. Cryst. Liq. Cryst.*, 114, 283-297 (1984), Polarization and Viscosity Measurements in a Ferroelectric Liquid Crystal by the Field Reversal Method.
- [111] T. Carlsson, B. Zeks, C. Filipic, A. Levstik; *Physical Review A*, 42, 877-889 (1990), Theoretical model of the frequency and temperature dependence of the complex dielectric constant of ferroelectric liquid crystals near the smectic C* - smectic A phase transition.
- [112] J. D. Bernal and D. Crowfoot; *Trans. Farad. Soc.*, 29, 1032-1049 (1933), Crystalline phases of some substances studied as liquid crystals.
- [113] P. Mandal and S. Paul; *Mol. Cryst. Liq. Cryst.*, 131, 223-235 (1985), X-Ray Studies on the Mesogen 4'-n-Pentyloxy-4-Biphenylcarbonitrile (5OCB) in the Solid Crystalline State.
- [114] P. Mandal, S. Paul, H. Schenk and K. Goubitz; *Mol. Cryst. Liq. Cryst.*, 135, 35-48 (1986), Crystal and Molecular Structure of the Nematogenic Compound 4-Cyanophenyl-4'-n-Heptylbenzoate (CPHB).
- [115] P. Mandal, B. Majumdar, S. Paul, H. Schenk and K. Goubitz; *Mol. Cryst. Liq. Cryst.*, 168, 135-146 (1989), An X-ray Study of Cyanophenyl Pyrimidines, Part I - Crystal Structure of PCCPP.
- [116] P. Mandal, S. Paul, C. H. Stam and H. Schenk; *Mol. Cryst. Liq. Cryst.*, 180, 369-378 (1990), X-Ray Studies of Cyanophenyl Pyrimidines Part II The Crystal and Molecular Structure of 5-(4-Ethylcyclohexyl)-2-(4-Cyanophenyl) Pyrimidine.
- [117] S. Gupta, P. Mandal, S. Paul, M. de Wit, K. Goubitz and H. Schenk; *Mol. Cryst. Liq. Cryst.*, 195, 149-159 (1991), An X-Ray Study of Cyanophenylpyrimidines Part III. Crystal Structure of 5-(trans-4-Heptylcyclohexyl)-2-(4-Cyanophenyl) Pyrimidine.
- [118] P. Mandal, S. Paul, H. Schenk and K. Goubitz; *Mol. Cryst. Liq. Cryst.*, 210, 21-30 (1992), Crystal and Molecular Structure of a Cybotactic Nematic Compound bis-(4'-n-Butoxybenzal)-2-Chloro-1,4-Phenylenediamine.
- [119] P. Mandal, S. Paul, K. Goubitz and H. Schenk; *Mol. Cryst. Liq. Cryst.*, 258, 209-216 (1995), X-ray Structural Analysis of a Mesogenic Compound N,N'-Bis-(p Butoxybenzylidene)- α , α' -bi - p-Toluidine.
- [120] A. Nath, S. Gupta, P. Mandal, S. Paul and H. Schenk; *Liq. Cryst.*, 20, 765-770 (1996), Structural analysis by X-ray diffraction of a non-polar alkenyl liquid crystalline compound.
- [121] B. R. Jaishi, P. K. Mandal, K. Goubitz, H. Schenk, R. Dabrowski and K. Czuprynski; *Liq. Cryst.*, 30, 1327-1333 (2003), The molecular and crystal structure of a polar mesogen 4-cyanobiphenyl-4'-hexylbiphenyl carboxylate.
- [122] P. A. C. Gane and A. J. Leadbetter; *Mol. Cryst. Liq. Cryst.*, 78, 183-200 (1981), The Crystal and Molecular Structure of N-(4-n octyloxy benzylidene) -4'-butylaniline (80.4) and the Crystal-Smectic G Transition.

- [123] L. Malpezzi, S. Bruckner, D. R. Ferro and G. R. Luckhurst; *Liq. Cryst.*, 28, 357-363 (2001), Crystal structure and packing analysis of the liquid crystal dimer α,ω -bis(4-cyanobiphenyl-4'-yloxy)octane.
- [124] M. A. Sridhar, N. K. Lokanath, J. Shashidhara Prasad, C. V. Yelamagad and Varshney, *Liq. Cryst.*, 28, 45-49 (2001), Crystal structure of a cholesterol-based dimesogen.
- [125] V. K. Gupta, P. Bhandhoria, M. Kalyan, M. Mathews and C. V. Yelamagad; *Liq. Cryst.*, 32, 741-747 (2005), Crystal structure of a liquid crystal non-symmetric dimer: cholesteryl 4-[4-(4-n-butylphenylethynyl)phenoxy]butanoate.
- [126] L. Walz, F. Nepveu and W. Haase; *Mol. Cryst. Liq. Cryst.*, 148, 111-121 (1987), Structural Arrangements of the Mesogenic Compounds 4-Ethyl-4'-(4''-pentylcyclohexyl) biphenyl and 4-Ethyl-2'-fluoro-4'-(4''-pentylcyclohexyl) biphenyl (BCH's) in the Crystalline State.
- [127] P. S. Patil, V. Shettigar, S. M. Dharmaprakash, S. Naveen, M. A. Sridhar and J. Shashidhara Prasad, *Mol. Cryst. Liq. Cryst.*, 461, 123-130 (2007), Synthesis and Crystal Structure of 1-(4-fluorophenyl)-3-(3,4,5-trimethoxyphenyl)-2-propen-1-one.
- [128] R. F. Bryan, Proceedings of the Pre-Congress Symposium on Organic Crystal Chemistry, Poznan, Poland, 105 (1979); *J. Structural Chem.*, 23, 128 (1982).
- [129] W. Haase and M. A. Athanassopoulou; *Liquid Crystals*, D.M.P. Mingos (Ed.), Springer-Verlag, Vol. I, pp. 139-197 (1999).
- [130] S. Biswas, S. Haldar, P. K. Mandal, K. Goubitz, H. Schenk, and R. Dabrowski; *Cryst. Res. Technol.* 42, 10, 1029-1035 (2007), Crystal structure of a polar nematogen 4-(trans-4-undecylcyclohexyl) isothiocyanatobenzene.
- [131] S. Haldar, S. Biswas, P. K. Mandal, K. Goubitz, H. Schenk and W. Haase; *Mol. Cryst. Liq. Cryst.*, 490, 80-87 (2008), X-Ray Structural Analysis in the Crystalline Phase of a Nematogenic Fluoro-Phenyl Compound.
- [132] S. Haldar, P. K. Mandal, S. J. Prathap, T. N. Guru Row and W. Haase; *Liq. Cryst.*, 35, 11, 1307-1312 (2008), X-ray studies of the crystalline and nematic phases of 49-(3,4,5-trifluorophenyl)-4-propylbicyclohexyl.
- [133] P. Das, A. N. Biswas, S. Acharya, A. Choudhury, P. Bandyopadhyay, P. K. Mandal and S. Upreti; *Mol. Cryst. Liq. Cryst.*, 501, 53-61 (2009), Structure of Liquid Crystalline 1-Phenyl-3-{4-[4-(4-octyloxybenzoyloxy)phenyloxycarbonyl]phenyl}triazene-1-oxide at Low Temperature.
- [134] B. K. Vainshtein, *Diffraction of X-rays by Chain Molecules*, Elsevier, Amsterdam, p12 (1966).
- [135] M. F. C. Ladd and R. A. Palmer, *Theory and practice of Direct methods in Crystallography*, Plenum Pub. Co., N. Y., (1980).

- [136] G. Germain, P. Main and M. M. Woolfson; *Acta Cryst.*, B26, 274-285 (1970), On the application of phase relationships to complex structures.
- [137] H. Schenk and C. T. Kiers, *Simpel 83*, an automatic direct method program package, University of Amsterdam (1983); H. Schenk; *Recl. Trav. Chim. Pays-bas*, 102, 1(1983).
- [138] G. M. Sheldrick, *Direct method package program*, University of Gottingen, Germany (1993).
- [139] S. R. Hall and J. M. Stewart, *XTAL*, University of Western Australia and Maryland (1989).
- [140] A. Altomere, G. Cascarano, C. Giacovazzo, A. Guagliardi, M. C. Burla, G. Polidori and M. Camalli, *The SIR 92 Programme* (1992).
- [141] P. S. White, *PC Version of NRCVAX (88)*, University of New Brunswick, Canada (1988).
- [142] Yao Jia-Xing, Zheng Chao-de, Quian Jin-Zi, Han Fu-Son, Gu Yuan-Zin and Fan Hai-Fu, *SAPI: A Computer Program for Automatic Solution of Crystal Structures from X-ray Data*, Institute of Physics, Academia Sinica, Beijing (1985).
- [143] C. J. Gilmore, *J. App. Cryst.*, 17, 42-46 (1984), *MITHRIL*-an integrated direct-methods computer program.
- [144] H. Hauptman and J. Karle, *Acta Cryst.*, 9, 45-55 (1956), Structure invariants and seminvariants for noncentrosymmetric space groups; *ibid.*, 12, 93-97 (1959); Seminvariants for centrosymmetric space group with conventional centered cells.
- [145] J. Karle and H. Hauptman, *Acta Cryst.*, 14, 217-223 (1961), Seminvariants for non-centrosymmetric space groups with conventional centered cells.
- [146] J. Karle and I. L. Karle, *Acta Cryst.*, 21, 849-859 (1966), The symbolic addition procedure for phase determination for centrosymmetric and non-centrosymmetric crystals.
- [147] H. Schenk (Ed), *Direct Methods in Solving Crystal Structures*, NATO ASI Series, Plenum Press, New York (1991).
- [148] G. H. Stout and L. H. Jensen, *X-ray Structure Determination*, Macmillan, New York p195 (1968).
- [149] A. J. C. Wilson, *Nature*, 150, 152 (1942), Determination of Absolute from Relative X-Ray Intensity Data.
- [150] W. Cochran and M. M. Woolfson, *Acta Cryst.*, 8, 1-12 (1955), "The theory of sign relations between structure factors".
- [151] W. Cochran, *Acta Cryst.*, 8, 473-478 (1955), Relations between the phases of structure factors.

[152] J. Karle and H. Hauptman, *Acta Cryst.*, 9, 635-651 (1956), A theory of phase determination for the four types of non-centrosymmetric space groups.

[153] M. J. Buerger, *Crystal Structure Analysis*, Wiley, New York (1960).

[154] G. H. Stout and L. H. Jensen, *X-ray Structure Determination*, Macmillan, New York, p353 (1968).

CHAPTER 3:

[1] S. Gauza, H. Wang, C. H. Wen, S. T. Wu, A. Seed and R. Dabrowski; *Jpn. J. Appl. Phys.*, 42, 3463 (2003), High Birefringence Isothiocyanato Tolane Liquid Crystals.

[2] J. S. Gasowska, S. J. Cowling, M. C. R. Cockett, M. Hird, R. A. Lewis, E. P. Raynes and J. W. Goodby; *J. Mater. Chem.*, 20, 299 (2010), The influence of an alkenyl terminal group on the mesomorphic behaviour and electro-optic properties of fluorinated terphenyl liquid crystals.

[3] A. Mori, M. Hashimoto and S. Ujiie; *Liq. Cryst.*, 38, 263 (2011), Effects of a semi-fluorinated side chain and a lateral polar group on mesomorphic properties of 5-cyanotroponoids and benzonitriles.

[4] D. Demus, Y. Goto, S. Swada, E. Nakagawa, H. Saito and R. Tarao; *Mol. Cryst. Liq. Cryst.*, 260, 1 (1995), Trifluorinated Liquid Crystals for TFT Displays.

[5] T. Nishi, A. Matsubara, H. Okada, H. Onnagawa, S. Sugimori, and K. Miyashita; *Jpn. J. Appl. Phys.*, 34, 236 (1995), Relationship between Molecular Structure and Temperature Dependence of Threshold Voltage in Fluorinated Liquid Crystals.

[6] V. F. Petrov; *Liq. Cryst.*, 19, 729 (1995), Liquid crystals for AMLCD and TFT-PDLC applications.

[7] S. Gauza, X. Zhu, W. Piecek, R. Dabrowski, S. T. Wu; *J. Disp. Technol.* 3 (3), 250-252 (2007), Fast Switching Liquid Crystals for Color-Sequential LCDs.

[8] M. Schadt, W. Helfrich; *Appl. Phys. Lett.*, 18, 127 (1971), Voltage-dependent optical activity of a twisted nematic liquid crystal.

[9] K. Nishiyama, M. Okita, S. Kawaguchi, K. Teranishi, R. Takamatsu; *SID Tech. Dig.* 36, 132 (2005), 32" WXGA LCD TV using OCB Mode, Low Temperature p-Si TFT and Blinking Backlight Technology.

[10] G. Harbers, C. Hoelen, *SID Tech. Dig.* 32, 702 (2001), High Performance LCD Back lighting using High Intensity Red, Green and Blue Light Emitting Diodes.

[11] D. P. Resler, D. S. Hobbs, R. C. Sharp, L. J. Friedman, T.A. Dorschner; *Opt. Lett.* 21 (9), 689 (1996), High-efficiency liquid-crystal optical phased-array beam steering.

[12] J. Y. Hardeberg, F. Schmitt, H. Brettel; *Opt. Eng.* 41 (10), 2532 (2002), Multispectral color image capture using a liquid crystal tunable filter.

[13] H. C. Lin, Y. H. Lin; *Opt. Express*, 20 (3), 2045 (2012), An electrically tunable-focusing liquid crystal lens with a low voltage and simple electrodes.

- [14] T.T. Ru, C.C. Yuan, R.P. Pan, C.L. Pan, X.C. Zhang; *IEEE Microwave Wireless Compon. Lett.* 14 (2) (2004), Electrically controlled room temperature terahertz phase shifter with liquid crystal.
- [15] R. L. Sutherland, V. P. Tondiglia, L.V. Natarajan; *Appl. Phys. Lett.* 64, 1074 (1994), Electrically switchable volume gratings in polymer-dispersed liquid crystals.
- [16] N. Mizoshita, K. Hanabusa, T. Kato; *Adv. Funct. Mater.* 13, 313 (2003), Fast and High-Contrast Electro-optical Switching of Liquid-Crystalline Physical Gels: Formation of Oriented Microphase-Separated Structures.
- [17] Y. H. Fan, H. W. Ren, S. T. Wu; *Appl. Phys. Lett.* 82, 2945 (2003), Normal-mode anisotropic liquid-crystal gels.
- [18] M. Hird; *Chem. Soc. Rev.*, 2007; 36, 2070, Fluorinated liquid crystals – properties and applications.
- [19] J. A. Malecki and J. Nowak; *J. Molecular Liquids*, vol. 81, 245-252 (1999), Intermolecular interactions in benzene solutions of 4-heptyl-3'-cyano-biphenyl studied with non-linear dielectric effects.
- [20] S. Gauza, J. Li, S. T. Wu, A. Spadlo, R. Dabrowski, Y. N. Tzeng, K. L. Cheng, *Liq. Cryst.* 32(8), 1077 (2005), High birefringence and high resistivity isothiocyanate-based nematic liquid crystal mixtures.
- [21] S. Gauza, S. T. Wu, A. Spadlo, R. Dabrowski, *J. Disp. Technol.* 2(3), 247 (2006), High performance room temperature nematic liquid crystals based on laterally fluorinated isothiocyanato-tolanes.
- [22] D. Sinha, D. Goswami, P. K. Mandal, Ł. Szczucinski, R. Dabrowski; *Mol Cryst Liq Cryst.*, 562,156 (2012), On the nature of molecular associations, static permittivity and dielectric relaxation in a uniaxial nematic liquid crystal.
- [23] B. Jha, S. Paul, R. Paul, P. Mandal; *Phase Transitions*, 15, 39 (1989), Order parameters of some homologue cybotactic nematics from X-ray diffraction measurements.
- [24] A. de Vries; *Mol Cryst Liq Cryst.*, 10, 31 (1970), Evidence for the existence of more than one type of nematic phase.
- [25] B. R. Jaishi, P. K. Mandal; *Liq Cryst.*, 33, 753 (2006), Optical microscopy, DSC and X-ray diffraction studies in binary mixtures of 4-pentyloxy-4'-cyanobiphenyl with three 4,4'-di(alkoxy) azoxybenzenes.
- [26] P.G. de Gennes; *Mol. Cryst. Liq. Cryst.*, 12, 193 (1971), Short range order effects in the isotropic phase of nematics and cholesterics.
- [27] H. E. J. Neugebauer; *Canad. J. Phys.*, 32, 1-8 (1954), Clarius-Mossoti equation for certain types of anisotropic crystals.
- [28] Hyperchem 6.03, Hypercube Inc., Gainesville, FL, USA.
- [29] S. Biswas, S. Haldar, P. K. Mandal, K. Goubitz, H. Schenk and R. Dabrowski, *Crystal Research and Technology*, Vol. 42, No.10, P. 1029 – 1035 (2007), Crystal structure of a polar nematogen 4-(trans-4'-undecylcyclohexyl) isothiocyanatobenzene.
- [30] E. Megnassan and A. Proutier; *Mol. Cryst. Liq. Cryst.*, 108, 245-254 (1984), Dipole Moments and Kerr Constants of 4-n-Alkyl-4'-Cyanobiphenyl Molecules (From 1CB to 12CB) Measured in Cyclohexane Solutions.
- [31] P. Sarkar, P. Mandal, S. Paul, R. Paul; *Liq. Cryst.*, Vol. 30, No. 4, 507–527 (2003), X-ray diffraction, optical birefringence, dielectric and phase transition properties of the long homologous series of nematogens 4-(trans-4'-n-alkylcyclohexyl) isothiocyanatobenzenes.

- [32] A de Vries; *Mol Cryst Liq Cryst.*, 10, 219 (1970), X-ray photographic studies of liquid crystals I. A cybotactic nematic phase.
- [33] P. Sarkar, P. Mandal, S. Paul, R. Dabrowski, K. Czuprynski; *Liq.Cryst.* 30 (4), 507 (2003), X-ray diffraction, optical birefringence, dielectric and phase transition properties of the long homologous series of nematogens 4-(trans-4'-n-alkylcyclohexyl) isothiocyanatobenzenes.
- [34] S. Haldar, S. Barman, P. K. Mandal, W. Haase, R. Dabrowski; *Mol. Cryst. Liq.Cryst.*, 528, 81-95 (2010), Influence of Molecular Core Structure and Chain Length on the Physical Properties of Nematogenic Fluorobenzene Derivatives.
- [35] W. L. McMillan; *Phys. Rev A*, 4, 1238-1246 (1971), Simple molecular model for the smectic A phase of liquid crystals.
- [36] W. L. McMillan; *Phys. Rev A*, 6, 936 (1972), X-Ray Scattering from Liquid Crystals. I. Cholesteryl Nonanoate and Myristate.
- [37] P. Sarkar, P. Mandal, S. Paul, R. Dabrowski, K. Czuprynski; *Liq Cryst.* 30 (4), 507 (2003), X-ray diffraction, optical birefringence, dielectric and phase transition properties of the long homologous series of nematogens 4-(trans-4'-n-alkylcyclohexyl) isothiocyanatobenzenes.
- [38] A. J. Leadbetter, R. M. Richardson, C. N. Cooling; *J Phys (Paris)*, 36 (C1), 37 (1975), The structure of a number of nematogens.
- [39] P. K. Sarkar, S. Paul, P. Mandal; *Mol Cryst Liq Cryst.*, 265, 249 (1995), Small angle X-ray scattering studies on smectic and nematic phases of a toluidine compound.
- [40] N. V. Madhusudana, S. Chandrasekhar; *Pramana Suppl.*, 1, 57 (1975), The role of permanent dipoles in nematic order.
- [41] S. Haldar, S. Biswas, P. K. Mandal, K. Goubitz, H. Schenk and W. Haase; *Mol. Cryst. Liq. Cryst.*, 490, 80-87 (2008), X-Ray Structural Analysis in the Crystalline Phase of a Nematogenic Fluoro-Phenyl Compound.
- [42] S. Haldar, P. K. Mandal, S.J. Prathap, T. N. Guru Row and W. Haase; *Liq. Cryst.*, 35, 1307-1312 (2008), X-ray studies of the crystalline and nematic phases of 49-(3,4,5-trifluorophenyl)-4-propylbicyclohexyl.
- [43] S. Biswas, S. Haldar, P. K. Mandal, K. Goubitz, H. Schenk, R. Dabrowski; *Crystal Res Technol.*, 42(10), 1029-1035 (2007), Crystal structure of a polar nematogen 4-(trans-4-undecylcyclohexyl) isothiocyanatobenzene.
- [44] H. Ishikawa, A. Toda, H. Okada, H. Onnagawa, S. Sugimori; *Liq. Cryst.*, 22, 743 (1997), Relationship between order parameter and physical constants in fluorinated liquid crystals.
- [45] S. Urban, P. Kula, A. Spadlo, M. Geppi, A. Marini; *Liq.Cryst.*, 37, 1321 (2010), Dielectric properties of selected laterally fluoro-substituted 4,4''-dialkyl, dialkoxy and alkyl-alkoxy [1:1';4':1''] terphenyls.
- [46] P. Bordewijk, *Physica*, 75, 146 (1974), Extension of the Kirkwood-Frölich Theory of the Static dielectric Permittivity to anisotropic Liquids.
- [47] N. V. Madhsudana, B. S. Srikanta, R. Subramanya, M. Urs, *Mol. Cryst. Liq. Cryst.* 108, 19 (1984), Comparative X-ray and dielectric studies on some structurally related smectogenic compounds.

- [48] J. Schacht, P. Zugenmaier, M. Buivydas, L. Komitov, B. Stebler, S. T. Lagerwall, F. Gouda, F. Horii; *Phys Rev E.*, 61, 3926 (2000), Intermolecular and intramolecular reorientations in nonchiral smectic liquid-crystalline phases studied by broadband dielectric spectroscopy.
- [49] S. Urban, R. Dabrowski, J. Dziaduszek, J. Janik, J. K. Moscicki; *Liq. Cryst.* 26, 1817 (1999), Mesomorphic and dielectric properties of fluorosubstituted isothiocyanates with different bridging groups.
- [50] L. Benguigui; *Phys. Rev. A*, 28, 1852 (1983), Dielectric relaxation in the crystalline smectic-B phase.
- [51] M. Gu, Y. Yin, S. V. Shiyankovskii, O. D. Lavrentovich; *Phys Rev E.*, 76, 061702 (2007), Effects of dielectric relaxation on the director dynamics of uniaxial nematic liquid crystals.
- [52] H. Baessler, R. B. Beard, M. M. Labes; *J Chem Phys.*, 52, 2292 (1970), Dipole Relaxation in a Liquid Crystal.
- [53] J. Czub, R. Dabrowski, J. Dziaduszek, S. Urban; *Phase Transition*, 82, 485-495 (2009), Dielectric properties of ten three-ring LC fluorosubstituted isothiocyanates with different mesogenic cores.
- [54] A. C. Diogo, A. F. Martins; *J Phys (Paris).*, 43, 779 (1982), Order parameter and temperature dependence of the hydrodynamic viscosities of nematic liquid crystals.
- [55] S. Arrhenius; *Z Phys Chem.*, 4, 226 (1889), On the reaction rate of the inversion of non-refined sugar upon souring.
- [56] B. Kundu, S. K. Pal, S. Kumar, R. Pratibha, N. V. Madhusudana; *Physical Review E.*, 82, 061703 (2010), Splay and bend elastic constants in the nematic phase of some disulfide bridged dimeric compounds.
- [57] R. Dhar, A. S. Pandey, M. B. Pandey, S. Kumar and R. Dabrowski; *Applied Physics Express* 1, 121501 (2008), Optimization of the display parameters of a room temperature twisted nematic display material by doping single-wall carbon nanotubes.
- [58] M. D. Gupta, A. Mukhopadhyay, S. K. Roy, R. Dabrowski; *J Appl Phys.*, 113, 053516 (2013), High birefringence liquid crystal mixtures: Optical properties and order parameter.
- [59] E. Nowinowski-Kruszelnicki, J. Kedzierski, Z. Raszewski, L. Jaroszewicz, R. Dabrowski, M. Kojdecki, W. Piecek, P. Perkowski, K. Garbat, M. Olifierczuk, M. Sutkowski, Karolina Ogrodnik, P. Morawiak, E. Miszczyk; *Optica Applicata*, Vol. XLII, No. 1, oal20116 (2012), High birefringence liquid crystal mixtures for electro-optical devices.
- [60] H. S. Subramanyam, C. S. Prabha and D. Krishnamurti; *Mol. Cryst. Liq. Cryst.*, 28, 201 (1974), Optical Anisotropy of Nematic Compounds.
- [61] M. Mitra, S. Paul and R. Paul; *Pramāna J. Phys.*, 29, 409 (1987), Optical Birefringence and Order Parameter of Three Nematogens.
- [62] N. V. Madhusudana, *Mol. Cryst. Liq. Cryst.*, 59, 117 (1980), Polarization Field and Orientational Order in Liquid Crystals.

CHAPTER 4:

- [1] B. Bahadur, (1991). *Liquid Crystals Applications and Uses*, World Sci.: Singapore.
- [2] G. H. Heilmeyer and L. A. Zanoni; *Appl. Phys. Lett.* 13, 91 (1968), Guest-host interactions in nematic liquid crystals: a new electro-optic effect.
- [3] S. Marino, M. Castriota, V. Bruno, E. Cazzanelli, G. Strangi, C. Versace and N. Scaramuzza; *J. Appl. Phys.*, 97, 013523 (2005), Changes of the electro-optic response of nematic liquid crystal cells due to inserted titania-vanadia films.
- [4] M. Oh-e and K. Kondo; *Appl. Phys. Lett.*, 69, 623 (1996), Response mechanism of nematic liquid crystals using the in-plane switching mode.
- [5] R. Muenster, M. Jarasch, X. Zhuang and Y. R. Shen; *Phys. Rev. Lett.*, 78, 42 (1997), Dye-Induced Enhancement of Optical Nonlinearity in Liquids and Liquid Crystals.
- [6] Y. Goto, T. Ogawa, S. Swada and S. Sugimori; *Mol. Cryst. Liq. Cryst.*, 209, 1–7 (1991), Fluorinated Liquid Crystals for Active Matrix Displays.
- [7] D. Demus, Y. Goto, S. Sawada, E. Nakagawa, H. Saito, R. Tarao; *Mol Cryst Liq Cryst.*, 260, 1–21(1995), Trifluorinated liquid crystals for TFT displays.
- [8] T. Nishi, A. Matsubara, H. Okada, H. Onnagawa, S. Sugimori, K. Miyashita; *Jpn J Appl Phys.*, 34, 236–239 (1995), Relationship between molecular structure and temperature dependence of threshold voltage in fluorinated liquid crystals.
- [9] V. F. Petrov; *Liq Cryst.*, 19, 729–741 (1995), Liquid crystals for AMLCD and TFTPDLCD applications; V. F. Petrov, Sofia I. Torgova ; Ludmila A. Karamysheva ; Shunsuke Takenaka; *Liq. Cryst.*, 26, 1141-1162 (1999), The trans-1,4-cyclohexylene group as a structural fragment in liquid crystals.
- [10] S. Gauza, H. Wang, C. H. Wen, S. T. Wu, A. Seed, R. Dabrowski; *Jpn J Appl Phys.*, 42, 3463–3466 (2003), High birefringence isothiocyanato tolane liquid crystals.
- [11] J. S. Gasowska, S. J. Cowling, M. C. R. Cockett, M. Hird, R. A. Lewis, E. P. Raynes, J. W. Goodby; *Mater Chem.*, 20, 299–307 (2010), The influence of an alkenyl terminal group on the mesomorphic behavior and electro-optic properties of fluorinated terphenyl liquid crystals.
- [12] H. Ishikawa, A. Toda, H. Okada, H. Onnagawa, S. Sugimori; *Liq Cryst.*, 22, 743–747 (1997), Relationship between order parameter and physical constants in fluorinated liquid crystals.
- [13] M. Hird; *Chem Soc Rev.*, 36, 2070–2095 (2007), Fluorinated liquid crystals – properties and applications.
- [14] M. Klasen, M. Bremer, A. Gotz, A. Manabe, S. Naemura, K. Tarumi; *Jpn J Appl Phys.*, 37, L945–L948 (1998), Calculation of optical and dielectric anisotropy of nematic liquid crystals.
- [15] K. Hori, M. Maeda, M. Yano, M. Kunugi; *Liq Cryst.*, 38, 287–293 (2011), The effect of fluorination (2): dependence of alkyl chain length on the crystal structures of mesogenic alkyl 4-[2-(perfluorohexyl) ethoxy] benzoates.

- [16] M. R. Cargill, G. Sandford, A. J. Tadeusiak, G. D. Love, N. Hollfelder, F. Pleis, G. Nelles, P. Kilickiran; *Liq Cryst.*, 38, 1069–1078 (2011), Highly fluorinated biphenyl ether systems as dopants for fastresponse liquid crystal display applications.
- [17] S. Haldar, K. C. Dey, D. Sinha, P. K. Mandal, W. Haase, P. Kula; *Liq Cryst.*, 39, 1196–1203 (2012), X-ray diffraction and dielectric spectroscopy studies on a partially fluorinated ferroelectric liquid crystal from the family of terphenyl esters.
- [18] E. Bartmann, D. Dorsch, U. Finkenzeller, H. A. Kurmeier and E. Poetsch; *Freiburger Arbeitstagung Flüssigkristalle*, 19, P8 (1990).
- [19] U. Finkenzeller, A. Kurmeier and E. Poetsch; *Freiburger Arbeitstagung Flüssigkristalle*, 18, P17 (1989).
- [20] P. Kirsch, S. Naemura and K. Tarumi; *Freiburger Arbeitstagung Flüssigkristalle*, 27, P45 (1998).
- [21] K. Tabayashi and K. Akasaka; *Liq. Cryst.*, 26, 127-129 (1999), Preliminary communication Natural abundance ^2H NMR for liquid crystal studies: deuterium isotope effect on microscopic order.
- [22] H. Ishikawa, A. Toda, A. Matsubara, T. Nishi, H. Okada, H. Onnagawa, S. Sugimori and K. Miyashita; 20th Jpn. Symp. *Liq. Cryst.*, Nagoya 1G505 (1994).
- [23] D. A. Dunmur, R. Hanson, H. Okada, H. Onnagawa, S. Sugimori and K. Toriyama; *Asia Display' 95 Proceeding*, S22-2, 563 (1995), Effect of Intermolecular Interactions on Threshold Voltages for TN and TFT LC-Displays: Dipole Association in F-Substituted Cyclohexyl cyclohexyl benzenes.
- [24] S. Biswas, S. Haldar, P. K. Mandal, W. Haase; *Liq Cryst.*, 34, 365–372 (2007), X-ray diffraction and optical birefringence studies on four nematogenic difluorobenzene derivatives.
- [25] S. Haldar, S. Barman, P. K. Mandal, W. Haase, R. Dabrowski; *Mol Cryst Liq Cryst.*, 528, 81–95 (2010), Influence of molecular core structure and chain length on the physical properties of nematogenic fluorobenzene derivatives.
- [26] I. C. Khoo and S. T. Wu; *Optics and Nonlinear Optics of Liquid Crystals*, World Scientific: Singapore, (1993).
- [27] L. M. Blinov, V. G. Chigrinov; *Electro-Optic Effects in Liquid Crystal Materials*, Springer: New York, (1996).
- [28] M. Schadt; *Annu. Rev. Mater. Sci.*, 27, 305–379 (1997), Liquid crystal materials and liquid crystal displays.
- [29] B. Kundu, S. K. Pal, S. Kumar, R. Pratibha, N. V. Madhusudana; *Phys Rev E.*, 82, 061703-1–061703-9 (2010), Splay and bend elastic constants in the nematic phase of some disulfide bridged dimeric compounds.
- [30] H. Kresse; Dynamic dielectric properties of nematics. In: Dunmur, DA, Fukuda, A, Luckhurst, GR, editors. *Physical properties of liquid crystals: nematics*. London: INSPEC; 2001. p. 277–287.
- [31] H. Kresse; Dielectric properties of nematic liquid crystals. In: Demus, D, Goodby, J, Gray, GW, Spiess HW, Vill, V, editors. *Handbook of liquid crystals*. Vol. 2A. Weinheim, FRG: Wiley-VCH, Verlag GmbH, p. 91–112 (1998).
- [32] W. H. de Jeu, T. W. Lathouwers, D. Constants; *ZNaturforsch*, 29a, 905–911 (1974), Molecules structure of nematic liquid crystals. I. Terminally substituted azobenzene and azoxybenzenes.

- [33] J. Schacht, P. Zugenmaier, M. Buivydas, L. Komitov, B. Stebler, S. T. Lagerwall, F. Gouda, F. Horii; *Phys Rev E.*, 61, 3926–3935 (2000), Intermolecular and intramolecular reorientations in nonchiral smectic liquid-crystalline phases studied by broadband dielectric spectroscopy.
- [34] D. A. Dunmur, W. H. Miller; *Mol Cryst Liq Cryst.*, 60, 281–292 (1980), Dipole–Dipole correlation in nematic liquid crystals.
- [35] S. Haldar, D. Sinha, P. K. Mandal, K. Goubitz and R. Peschar; *Liquid Crystals*, Vol. 40, No. 5, 689–698 (2013), Effect of molecular conformation on the mesogenic properties of a partially fluorinated nematogenic compound investigated by X-ray diffraction and dielectric measurements.
- [36] S. Haldar, P. K. Mandal, K. Goubitz, H. Schenk, W. Haase; *Mol Cryst Liq Cryst.*, 490, 80–87 (2008), X-ray structural analysis in the crystalline phase of a nematogenic fluoro-phenyl compound.
- [37] S. Haldar, P. K. Mandal, S. J. Prathap, T. N. Guru Row, W. Haase; *Liq Cryst.*, 35, 1307–1312 (2008), X-ray studies of the crystalline and nematic phases of 4₋-(3,4,5-trifluorophenyl)-4- propylbicyclohexyl.
- [38] W. Haase, M. A. Athanassopoulou; Vol. I. Berlin: Springer, p. 139–197 (1999), Crystal structures of LC mesogens. In: Mingos, M, editor. *Structure and bonding*.
- [39] M. Hird and K. J. Toyne; *Mol. Cryst. Liq. Cryst.*, 323, 1–67 (1998), Fluoro Substitution in Thermotropic Liquid Crystals.
- [40] V. Vill; *Liq. Cryst. Database*, Version 4.4 , LCI Publisher, GmbH, Hamburg (2003) and references therein.
- [41] L. Bata and A. Buka; *Mol. Cryst. Liq. Cryst.*, 63, 307–320 (1981), Dielectric Permittivity and Relaxation Phenomena in smectic Phases.
- [42] R. deGelder, R. A. G. de Graaff, H. Schenk; *Acta Cryst.*, A49, 287–293 (1993), Automatic determination of crystal structures using Karle-Hauptman matrices.
- [43] D. T. Cromer, J. B. Mann; *Acta Cryst.*, 24A, 321–324 (1968), X-ray scattering factors computed from numerical Hartree–Fock wave functions.
- [44] International Union of Crystallography. *International tables for X-ray crystallography*. Vol. IV, Birmingham: Kynoch Press, pp. 55 (1974).
- [45] D. T. Cromer, D. Liberman; *J Chem Phys.*, 53, 1891–1898 (1970), Relativistic calculation of anomalous scattering factors for X-rays.
- [46] S. R. Hall, D. J. du Boulay, R. Olthof-Hazekamp, editors. *XTAL3.7 system*. Lamb: University of Western Australia (2000).
- [47] Spek AL. *PLATON*, An integrated tool for the analysis of the results of a single crystal structure determination. *Acta Cryst.*, A46, C–34 (1990).
- [48] Hyperchem 6.03, Hypercube Inc., Gainesville, FL, USA.
- [49] P. Sarkar, P. K. Mandal, S. Paul, R. Paul; *liq. Cryst*, Vol. 30, No. 4, 507–527 (2003), X-ray diffraction, optical birefringence, dielectric and phase transition properties of the long homologous series of nematogens 4-(trans-4 ∞ -n-alkylcyclohexyl) isothiocyanatobenzenes.

- [50] E. Megnassan and A. Proutierre; *Mol. Cryst. liq. Cryst.*, 108, 245 (1984), Dipole Moments and Kerr Constants of 4-n Alkyl-4'-Cyanobiphenyl Molecules (From 1CB to 12CB) Measured in Cyclohexane Solutions.
- [51] K. P. Gueu, E. Megnassan and A. Proutierre; *Mol. Cryst. liq. Cryst.*, 132, 303 (1986), Dipole Moments of 4-n Alkyl-4'-Cyanobiphenyl Molecules (from OCB to 12CB) Measurement in Four Solvents and Theoretical Calculations.
- [52] W. Haase, H. Paulus, R. Pendzialek; *Mol. Cryst. Liq. Cryst.*, 100: 211-221 (1983), Solid State Polymorphism in 4-Cyano-4'-n-Propyl biphenyl and X-Ray Structure Determination of the Higher Melting Modification.
- [53] B. R. Jaishi, P. K. Mandal, K. Goubitz, H. Schenk, R. Dabrowski, K. Czuprynski; *Liq. Cryst.*, 30, 1327-1333 (2003), The molecular and crystal structure of a polar mesogen 4-cyanobiphenyl-4'-hexylbiphenyl carboxylate.
- [54] S. Biswas, S. Haldar, P. K. Mandal, K. Goubitz, H. Schenk, R. Dabrowski; *Cryst. Res. Technol.*, 42, 1029-1035 (2007), Crystal structure of a polar nematogen 4-(trans-4- undecylcyclohexyl) isothiocyanatobenzene.
- [55] L. Walz, W. Haase, R. Eidenschink; *Mol. Cryst. Liq. Cryst.*, 168, 169-182 (1989), The Crystal and Molecular Structures of Four Homologous, Mesogenic trans,trans-4,4'-dialkyl-(1 α ,1'-bicyclohexyl)-4 β -carbonitril (CCN's).
- [56] S. Gupta, P. Mandal, S. Paul, K. Goubitz, M. de Wit, H. Schenk; *Mol. Cryst. Liq. Cryst.*, 195, 149-159 (1991), An X-Ray Study of Cyanophenylpyrimidines Part III. Crystal Structure of 5-(trans-4-Heptylcyclohexyl)-2-(4-Cyanophenyl) Pyrimidine.
- [57] A. Nath, S. Gupta, P. Mandal, S. Paul, H. Schenk; *Liq. Cryst.*, 20, 765-770 (1996), Structural analysis by X-ray diffraction of a non-polar alkenyl liquid crystalline compound.
- [58] P. Mandal, S. Paul, H. Schenk, K. Goubitz; *Mol. Cryst. Liq. Cryst.*, 210: 21-30 (1992), Crystal and Molecular Structure of a Cybotactic Nematic Compound bis-(4'-n-Butoxybenzal)-2-Chloro-1,4-Phenylenediamine.
- [59] P. Mandal, S. Paul, H. Schenk, K. Goubitz; *Mol. Cryst. Liq. Cryst.*, 135, 35-48 (1986), Crystal and Molecular Structure of the Nematogenic Compound 4-Cyanophenyl-4'-n-Heptylbenzoate (CPHB).
- [60] P. Mandal, S. Paul; *Mol. Cryst. Liq. Cryst.*, 131, 223-235 (1985), X-Ray Studies on the Mesogen 4'-n-Pentyloxy-4-Biphenylcarbonitrile (5OCB) in the Solid Crystalline State.
- [61] L. Walz, F. Nepveu, W. Haase; *Mol. Cryst. Liq. Cryst.*, 148, 111-121 (1987), Structural Arrangements of the Mesogenic Compounds 4-Ethyl-4'-(4''-pentylcyclohexyl)biphenyl and 4-Ethyl-2'-fluoro-4'-(4''-pentylcyclohexyl)biphenyl (BCH's) in the Crystalline State.
- [62] P. S. Patil, V. Shettigar, S. M. Dharmaprasad, S. Naveen, M. A. Sridhar, J. S. Prasad; *Mol. Cryst. Liq. Cryst.*, 461, 123-130 (2007), Synthesis and Crystal Structure of 1-(4-fluorophenyl)-3-(3,4,5-trimethoxyphenyl)-2-propen-1-one.
- [63] S. Haldar; S. Barman; P. K. Mandal; W. Haase; R. Dabrowski; *Mol. Cryst. Liq. Cryst.*, Vol. 528, 81-95 (2010), Influence of Molecular Core Structure and Chain Length on the Physical Properties of Nematogenic Fluorobenzene Derivatives.
- [64] A. J. Leadbetter, R. M. Richardson, C. N. Colling; 36, C1-37-C1-43 (1975), The structure of a number of nematogens. *J Phys (Paris)*.
- [65] S. Gupta, G-P Chang-Chien, W-S Lee, R. Centore, S. P. Sen Gupta; *Liq Cryst.*, 29, 657-661 (2002), Crystal structure of the mesogenic alkene monomer, 3-[4-(4-ethylbiphenyl)]-1-propene.

- [66] B. R. Ratna, R. Shashidhar; *Mol Cryst Liq Cryst.*, 42, 113–125 (1977), Dielectric studies on liquid crystals of strongly positive dielectric anisotropy.
- [67] B. R. Ratna, R. Shashidhar; *Mol Cryst Liq Cryst.*, 45, 103–116 (1978), Dielectric properties of some nematics of positive dielectric anisotropy.
- [68] M. Schadt; *J Chem Phys.*, 56, 1494–1497 (1972), Dielectric properties of some nematic liquid crystals with strong positive dielectric anisotropy.
- [69] N. V. Madhusudana, S. Chandrasekhar; *Pramana.*, 1, 57–68 (1975), The role of permanent dipoles in nematic order.
- [70] P. Bordewijk; *Physica.*, 75, 146 (1974), Extension of the Kirkwood-Fröhlich theory of the static dielectric permittivity to anisotropic liquids.
- [71] M. Gu, Y. Yin, S. V. Shiyankovskii, O. D. Lavrentovich; *Phys Rev E.*, 76, 061702 (2007), Effects of dielectric relaxation on the director dynamics of uniaxial nematic liquid crystals.
- [72] H. Baessler, R. B. Beard, M. M. Labes; *J Chem Phys.*, 52, 2292 (1970), Dipole Relaxation in a Liquid Crystal.
- [73] A. C. Diogo, A. F. Martins; *J Phys (Paris)*, 43, 779 (1982), Order parameter and temperature dependence of the hydrodynamic viscosities of nematic liquid crystals.
- [74] S. Arrhenius; *Z Phys Chem.*, 4, 226 (1889), On the reaction rate of the inversion of non-refined sugar upon souring.

CHAPTER 5:

- [1] R. B. Meyer, Paper presented at the 5th Int. Liquid Crystal Conf., Stockholm, June, (1974); R. B. Meyer, L. Liebert, L. Strzelecki and P. Kelker, *J Phys (Paris) Lett.*, 36, L69 (1975), Ferroelectric liquid crystals.
- [2] A. D. L. Chandani, Y. Ouchi, H. Takezoe, A. Fukuda, K. Terashima, K. Furukawa and A. Kishi; *Jpn. J. Appl. Phys. Part 2*, 28, L1261 (1989), Novel Phases Exhibiting Tristable Switching.
- [3] Y. Izozaki, T. Fujikawa, H. Takezoe, A. Fukuda, T. Hagiwara, Y. Suzuki and I. Kawamura, *Phys. Rev. B*; 48, 13439 (1993), Devil's staircase formed by competing interactions stabilizing the ferroelectric smectic-C* phase and the antiferroelectric smectic-C_A* phase in liquid crystalline binary mixtures.
- [4] J. P. F. Lagerwall, D. D. Parghi, D. Kruerke, F. Gouda, and P. Jagemalm, *Liq. Cryst.*, 29, 163 (2002), Phases, phase transitions and confinement effects in a series of antiferroelectric liquid crystals.
- [5] J. P. F. Lagerwall, P. Rudquist, and S.T. Lagerwall; *Liq. Cryst.*, 30, 399 (2003), On the phase sequence of antiferroelectric liquid crystals and its relation to orientational and translational order.
- [6] E. Gorecka, D. Pocięcha, M. Čepič, B. Žekš, R. Dabrowski; *Phys. Rev. E*, 65, 061703 (2002), Enantiomeric excess dependence of the phase diagram of antiferroelectric liquid crystals.
- [7] I. C. Sage, Applications, in: D. Demus, J. Goodby, G.W. Gray, H.W. Spiess, V. Vill (Eds.), *Handbook of Liquid Crystals Vol. I – Fundamentals*, Wiley-Vch., Weinheim, pp. 731-762 (1998).

- [8] M. Hird; *Liq. Cryst.*, 38, 1467–1493 (2011), Ferroelectricity in liquid crystals-materials, properties and applications.
- [9] P. J. Collings, Ferroelectric liquid crystals: The 2004 Benjamin Franklin Medal in Physics presented to Robert B. Meyer of Brandeis University, *J. Frankl. Inst.* 342, 599–608 (2005).
- [10] J. Wen, M. Tian, Q. Chen, *Liq. Cryst.* 16, 445-453 (1994), Novel fluorinated liquid crystals. II. The synthesis and phase transitions of a novel type of ferroelectric liquid crystals containing 1,4-tetrafluorophenylene moiety.
- [11] Y. Xu, W. Wang, Q. Chen, J. Wen; *Liq. Cryst.*, 21, 65-71 (1996), Synthesis and transition temperatures of novel fluorinated chiral liquid crystals containing 1,4-tetrafluorophenylene units.
- [12] R. Dąbrowski, J. Gąsowska, J. Otón, W. Piecek, J. Przedmojski, M. Tykarska; High tilted antiferroelectric liquid crystalline materials, *Disp.* 25, 9-19 (2004).
- [13] R. Dąbrowski, P. Kula, Z. Raszewski, W. Piecek, J. M. Otón, A. Spadło; *Ferroelectrics*, 395 116-132 (2010), New orthoconic antiferroelectrics useful for applications.
- [14] D. Ziobro, R. Dąbrowski, M. Tykarska, W. Drzewiński, M. Filipowicz, W. Rejmer, K. Kuśmierk, P. Morowiak, W. Piecek; *Liq. Cryst.* 39, 1011-1032 (2012), Synthesis and properties of new ferroelectric and antiferroelectric liquid crystals with a biphenyl benzoate rigid core.
- [15] H. T. Nguyen, J. C. Rouillon, A. Babeau, J. P. Marcerou, G. Sigaud; *Liq. Cryst.* 26, 1007-1019 (1999), Synthesis, properties and crystal structure of chiral semiperfluorinated liquid crystals with ferro and anticlinic smectic phases.
- [16] R. Dabrowski, *Ferroelectrics*, 243, 1-18 (2000), Liquid crystals with fluorinated terminal chains and antiferroelectric properties.
- [17] S. Seomun, T. Gouda, Y. Takanishi, K. Ishikawa, H. Takezoe; *Liq. Cryst.* 26, 151-161(1999), Bulk optical properties in binary mixtures of antiferroelectric liquid crystal compounds showing V-shaped switching.
- [18] J. V. Selinger, P. J. Collings, R. Shashidhar; *Phys. Rev. E* 64, 061705/1-9 (2001), Field-dependent tilt and birefringence of electroclinic liquid crystals: Theory and experiment.
- [19] W. M. Zoghaib, C. Carboni, A. K. George, S. AL-Manthari, A. Al-Hussaini, F. Al-Futaisi, , *Mol. Cryst. Liq. Cryst.* 542, 123–131 (2011), Novel fluorinated ferroelectric organosiloxane liquid crystals.
- [20] J. Naciri, C. Carboni, A. K. George; *Liq. Cryst.*, 30, 219-225 (2003), Low transition temperature organosiloxane liquid crystals displaying a de Vries smectic A phase.
- [21] J. Naciri, J. Ruth, G. Crawford, R. Shashidhar, B. R. Ratna; *Chem. Mater.*, 7, 1397-1402 (1995), Novel ferroelectric and electroclinic organosiloxane liquid crystals.
- [22] J. Dziaduszek, R. Dabrowski, K. Czuprynski, N. Bennis; *Ferroelectrics.*, 343, 3–9 (2006), Ferroelectric Compounds with Strong Polar Cyano Group in Terminal Position.
- [23] Z. Li, P. Salamon, A. Jakli, K. Wang, C. Qin, Q. Yang, C. Liu and J. Wen; *Liq. Cryst.*, 37 427–433 (2010), Synthesis and mesomorphic properties of resorcylic di[4-(4-alkoxy-2,3-diflorophenyl)ethynyl] benzoate liquid crystals.
- [24] Y. Yang, H. Li, J. Wen; *Liq. Cryst.*, 34, 975-979 (2007), Synthesis and mesomorphic properties of chiral fluorinated liquid crystals.

- [25] N. Shiratori, A. Yoshizawa, I. Nishiyama, M. Fukumasa, A. Yokoyama, T. Hirai, M. Yamane; *Mol. Cryst. Liq. Cryst.* 199, 129-140 (1991), New Ferroelectric Liquid Crystals Having 2-Fluoro-2-Methyl Alkanoyloxy Group.
- [26] A. Fafara, B. Gestblom, S. Wróbel, R. Dabrowski, W. Drzewiński, D. Kilian, W. Haase; *Ferroelectrics*, 212, 79-90 (1998), Dielectric spectroscopy and electrooptic studies of new MHPOBC analogues.
- [27] D. M. Potukuchi, A. K. George, C. Carboni, S. H. Alharthi, J. Naciri; *Ferroelectrics*, 300, 79-93 (2004), Low Frequency Dielectric Relaxation, Spontaneous Polarization, Optical Tilt Angle and Response Time Investigations in a Flourinated Ferroelectric Liquid Crystal, N125F2(R*).
- [28] D. M. Potukuchi, A. K. George; *Mol. Cryst. Liq. Cryst.*, 487, 92–109 (2008), Phase Transitions and Characterization in a Chiral Smectic-A_{de Vries} Liquid Crystal by Low-Frequency Dielectric Spectroscopy.
- [29] P. K. Mandal, S. Haldar, A. Lapanik, W. Haase; *Jpn. J. Appl. Phys.*, 48, 011501-6 (2009), Induction and enhancement of ferroelectric smectic C* phase in multi-component room temperature mixtures.
- [30] K. Hiraoka, A. Taguchi, Y. Ouchi, H. Takezoe and A. Fukuda; *Jpn. J. Appl. Phys.*, 29, 1473-1476 (1990), Electric-Field-Induced Transitions among Antiferroelectric, Ferrielectric and Ferroelectric Phases in a Chiral Smectic MHPOBC.
- [31] A. M. Biradar, S. Wróbel, and W. Haase; *Phys. Rev. A*, 39, 2693-2702 (1989), Dielectric relaxation in the smectic-A* and smectic-C* phases of a ferroelectric liquid crystal.
- [32] T. Carlsson, B. Zeks, C. Filipic, A. Levstik; *Phys. Rev. A*, 42, 877–889 (1990), Theoretical model of the frequency and temperature dependence of the complex dielectric constant of ferroelectric liquid crystals near the smectic-C* - smectic-A phase transition.
- [33] B. Zeks, M. Cepic, in *Relaxation Phenomena: Liquid Crystals, Magnetic Systems, Polymers, High-TC Superconductors, Metallic Glasses*; W. Haase, S. Wrobel, Eds. Springer Verlag: Berlin–Heidelberg, p 477 (2003).
- [34] M. Buivydas, F. Gouda, S. T. Lagerwall, B. Stebler; *Liq. Cryst.*, 18, 879–886 (1995), The molecular aspect of the double absorption peak in the dielectric spectrum of the antiferroelectric liquid crystal phase.
- [35] Hyperchem 6.03, Hypercube Inc., Gainesville, FL, USA.
- [36] S. Haldar, S. Barman, P. K. Mandal, W. Haase, R. Dabrowski; *Mol. Cryst. Liq. Cryst.*, 528, 81-95 (2010), Influence of molecular core structure and chain length on the physical properties of nematogenic fluorobenzene derivatives.
- [37] P. Sarkar, P. Mandal, S. Paul, R. Paul, R. Dabrowski, K. Czuprynski; *Liq. Cryst.*, 30, 507-527 (2003), X-ray diffraction, optical birefringence, dielectric and phase transition properties of the long homologous series of nematogens 4-(trans-4'-n-alkylcyclohexyl) isothiocyanatobenzenes.
- [38] D. Sinha, D. Goswami, P. K. Mandal, Ł. Szczucinski, R. Dabrowski; *Mol. Cryst. Liq. Cryst.* 562, 156-165 (2012), On the nature of molecular associations, static permittivity and dielectric relaxation in a uniaxial nematic liquid crystal.
- [39] U. Manna, R. M. Richardson, A. Fukuda, J.K. Vij; *Phys. Rev. E*, 81, 050701–4 (2010), X-ray diffraction study of ferroelectric and antiferroelectric liquid crystal mixtures exhibiting de Vries SmA*-SmC* transitions.
- [40] S. T. Lagerwall, *Ferroelectric liquid crystals* in : D. Demus, J. Goodby, G.W. Gray, H. W. Spiess, V. Vill (Eds.), *Handbook of Liquid Crystals Vol. 2B – Low molecular weight liquid crystals*, Wiley-Vch., Weinheim, pp 515-664 (1998).

- [41] W. Piecek, Z. Raszewski, P. Perkowski, J. Przedmojski, J. Kedzierski, W. Drzewinski, R. Dabrowski, J. Zielinski; *Ferroelectrics*, 310, 125–129 (2004), Apparent tilt angle and structural investigations of the fluorinated antiferroelectric liquid crystal material for display application.
- [42] J. P. F. Lagerwall, A. Saipa, F. Giesselmann, R. Dabrowski; *Liq. Cryst.* 31, 1175–1184 (2004), On the origin of high optical director tilt in a partially fluorinated orthoconic antiferroelectric liquid crystal mixture.
- [43] K. D'havé, P. Rudquist, S.T. Lagerwall, H. Pauwels, W. Drzewinski, R. Dabrowski; *Appl. Phys. Lett.*, 76, 3528-3530 (2000), Solution of the dark state problem in antiferroelectric liquid crystal displays.
- [44] W. K. Robinson, C. Carboni, P. Kloess, S. P. Perkins, H. J. Coles; *Liq. Cryst.*, 25, 301–307 (1998), Ferroelectric and antiferroelectric low molar mass organosiloxane liquid crystals.
- [45] E. P. Haridas, S. S. Bawa, A. M. Biradar, S. Chandra, *Jpn. J. Appl. Phys.*, 34, 3602-3606 (1995), Anisotropic surface anchoring conditions for gray-scale capability in high-tilt-angle ferroelectric liquid crystal.
- [46] R. Blinc, B. Zeks; *Phys. Rev. A*. 18, 740-745 (1978), Dynamics of helicoidal ferroelectric smectic-C* liquid crystals.
- [47] T. Carlsson, B. Zeks, C. Filipic, A. Levstik; *Physical Review A*, 42, 877–889 (1990), Theoretical model of the frequency and temperature dependence of the complex dielectric constant of ferroelectric liquid crystals near the smectic–smectic-A phase transition.
- [48] N. A. Clark, S. T. Lagerwall, Introduction to ferroelectric liquid crystals, in: J.W. Goodby, R. Blinc, N. A. Clark, S. T. Lagerwall, M.A. Osipov, S.A. Pikin, T. Sakurai, K. Yoshino, B. Zeks (Eds), *Ferroelectric Liquid Crystals Principles, Properties and Applications*, Gordon and Breach, Philadelphia, 1991, pp. 1-97.
- [49] D. Goswami, P. K. Mandal, R. Dabrowski; to be published.
- [50] S. Sato, J. Hatano, S. Tatemori, H. Uehara, S. Saito, E. Okabe; *Mol. Cryst. Liq. Cryst. A* 328, 411-418 (1999), Antiferroelectricity of a Chiral Smectic Liquid Crystal Having Three Isolated Phenyl Rings in the Core.
- [51] M. Marzec, W. Haase, E. Jakob, M. Pfeiffer, S. Wróbel; *Liquid Crystals*, 14, 1967- 1976 (1993), The existence of four dielectric modes in the planar oriented SmC* phase of a fluorinated substance.
- [52] S. Wróbel, G. Cohen, D. Davidov, W. Haase, M. Marzec, M. Pfeiffer; *Ferroelectrics*, 166, 211–222 (1995), Dielectric, electro optic and X-ray studies of a room temperature ferroelectric mixture.
- [53] J. M. Czerwiec, R. Dabrowski, K. Garbat, M. Marzec, M. Tykarska, A. Wawrzyniak, S. Wróbel; *Liquid Crystals*, 39, 1503–1511 (2012), Dielectric and electro-optic behaviour of two chiral compounds and their antiferroelectric mixtures.
- [54] Y. P. Panarin, O. Kalinovskaya, J. K. Vij, and J. W. Goodby; *Phys. Rev. E*, 55, 4345-4353 (1997), Observation and investigation of the ferroelectric subphase with high qT parameter.
- [55] Y. P. Panarin, O. Kalinovskaya, and J. K. Vij; *Liq. Cryst.*, 25, 241-252 (1998), The investigation of the relaxation processes in antiferroelectric liquid crystals by broad band dielectric and electro-optic spectroscopy.
- [56] J. K. Song, U. Manna, A. Fukuda and J. K. Vij; *Appl. Phys. Lett.*, 93, 142903-3 (2008), Antiferroelectric dielectric relaxation processes and the interlayer interaction in antiferroelectric liquid crystals.
- [57] U. Manna, J. K. Song, G. Power, and J. K. Vij; *Phys. Rev. E*, 78, 021711-8 (2008), Effect of cell surfaces on the stability of chiral smectic-C phases.

- [58] U. Manna, J. K. Song, G. Power, J. K. Vij; *Phys. Rev. E*, 78, 021711-8 (2008), Effect of cell surfaces on the stability of chiral smectic-C phases.
- [59] M. Buivydas, F. Gouda, G. Andersson, S. T. Lagerwall, B. Stember, J. Bomelburg, G. Heppke, B. Gestblom; *Liq. Cryst.*, 23, 723- 739 (1997), Collective and non-collective excitations in antiferroelectric and ferroelectric liquid crystals studied by dielectric relaxation spectroscopy and electro-optic measurements.
- [60] S. Haldar, K. C. Dey, D. Sinha, P. K. Mandal, W. Haase, P. Kula; *Liq. Cryst.*, 39, 1196-1203 (2012), X-ray diffraction and dielectric spectroscopy studies on a partially fluorinated ferroelectric liquid crystal from the family of terphenyl esters.
- [61] M. Marzec, A. Mikulko, S. Wrobel, R. Dabrowski, M. Darius and W. Haase; *Liq. Cryst.*, 31, 153–159 (2004), Alpha sub-phase in a new ferroelectric fluorinated compound.
- [62] P. Nayek, S. Ghosh, S. Roy, T. P. Majumder, R. Dabrowski; *J. Mol. Liq.* 175, 91–96 (2012), Electro-optic and dielectric investigations of a perfluorinated compound showing orthoconic antiferroelectric liquid crystal.
- [63] P. Arora, A. Mikulko, F. Podgornov, W. Haase; *Mol. Cryst. Liq. Cryst.*, 502, 1-8 (2009), Dielectric and electro-optic properties of new ferroelectric liquid crystalline mixture doped with carbon nanotubes.
- [64] A. Mikulko, P. Arora, A. Glushchenko, A. Lapanik and W. Haase; *Euro Phys. Lett.*, 87, 27009/1-4 (2009), Complementary studies of BaTiO₃ nanoparticles suspended in a ferroelectric liquid-crystalline mixture.
- [65] P. K. Mandal, B. R. Jaishi, W. Haase, R. Dabrowski, M. Tykarska, P. Kula; *Phase Transition*, 79, 223–235 (2006), Optical microscopy, DSC and dielectric relaxation spectroscopy studies on a partially fluorinated ferroelectric liquid crystalline compound MHPO(13F)BC.
- [66] W. N. Thurmes, M. D. Wand, R. T. Vohra, K. M. More; *SPIE Conf. Proc.* 3015, 1-7 (1997), FLC materials for microdisplay applications.
- [67] M. Marzec, S. Wrobel, E. Gondek, R. Dabrowski; *Mol. Cryst. Liq. Cryst.*, 410, 153–161 (2004), Room Temperature Antiferroelectric Phase Studied by Electrooptic Methods.
- [68] F. Gouda, T. Carlsson, G. Andersson, S.T. Lagerwall, B. Stebler; *Liq. Cryst.*, 16, 315-322 (1994), Manifestation of biquadratic coupling in the smectic C* phase soft mode dielectric response.
- [69] M. Marzec, S. Wröbel, S. Hiller, A. M. Biradar, R. Dabrowski, B. Gestblom, W. Haase; *Mol. Cryst. Liq. Cryst.*, 302, 35-40 (1997), Dynamical properties of two ferroelectric phases of epoxy compound.
- [70] R. Eidenschink, T. Geelhaar, G. Andersson, A. Dahlgren, K. Flatischler, F. Gouda, S. T. Lagerwall, K. Skarp; *Ferroelectrics*, 84, 167-181 (1988), Parameter characteristics of a ferroelectric liquid crystal with polarization sign reversal.
- [71] A. K. Srivastava, R. Dhar, V. K. Agrawal, S. H. Lee, R. Dabrowski; *Liq. Cryst.*, 35, 1101–1108 (2008), Switching and electrical properties of ferro- and antiferroelectric phases of MOPB(H)PBC.
- [72] S. Essid, M. Manai, A. Gharbi, J. P. Marcerou, J. C. Rouillon; *Liq. Cryst.*, 32, 307–313, (2005), Electro-optical switching properties for measuring the parameters of a ferroelectric liquid crystal.

CHAPTER 6:

- [1] D. Demus and J. Goodby, Handbook of Liquid Crystals, Wiley-VCH Weinheim, (1998).
- [2] P. S. Pershan, Structure of Liquid Crystal Phases, World Scientific Singapore, (1988).
- [3] R. B. Meyer, L. Liebert, L. Strzelecki, P. Keller; J. Phys. (France) Lett., 36, L-69 (1975), Ferroelectric liquid crystals.
- [4] N. A. Clark and S. T. Lagerwall; Appl. Phys. Lett., 36, 899 (1980), Submicrosecond bistable electro-optic switching in liquid crystals.
- [5] D. C. Wright and N. D. Mermin; Rev. Mod. Phys., 66, 385 (1989), Crystalline liquids: the blue phases.
- [6] C. J. F. Botcher and P. Bordewijk; Theory of Electric Polarization Vol. I Elsevier, Amsterdam (1978).
- [7] Wrobel S, Dielectric relaxation spectroscopy, Relaxation phenomena — Liquid crystals, magnetic systems, polymers, high-TC superconductors, metallic glasses, Haase W. and Wrobel S Eds., Ch 1 Springer-Verlag Berlin-Heidelberg (2003).
- [8] D. Goswami, D. Sinha, A. Debnath, P.K. Mandal, S. K. Gupta, W. Haase, D. Ziobro and R. Dabrowski; J. Mol. Liq., 182, 95-101 (2013), Molecular and dynamical properties of a perfluorinated liquid crystal with direct transition from ferroelectric SmC* phase to isotropic phase.
- [9] K. Miyasato, S. Abe, H. Takezoe, A. Fukuda and E. Kuze; Jpn. J. Appl. Phys., 22, L661 (1983), Direct Method with Triangular Waves for Measuring Spontaneous Polarization in Ferroelectric Liquid Crystals.
- [10] P. K. Mandal, B. R. Jaishi, W. Haase, R. Dabrowski, M. Tykarska and P. Kula; Phase Trans., 79, 223-235 (2006), Optical microscopy, DSC and dielectric relaxation spectroscopy studies on a partially fluorinated ferroelectric liquid crystalline compound MHPO(13F)BC.
- [11] I. Dierking, Textures of Liquid Crystals Wiley-VCH, Weinheim, (2003).
- [12] A. J. Leadbetter, J. P. Gaughan, B. Kelly, G. W. Gray and J. Goodby; J Phys. (France) Colloq., 40, C3-178 (1979), Characterisation and structure of some new smectic phases.
- [13] G. W. Gray and J. W. Goodby Smectic Liquid Crystals, Textures and Structures, Leonard Hill, Philadelphia, (1984).
- [14] P. A. C. Gane, A. J. Leadbetter and P. G. Wrighton; Mol. Cryst. Liq. Cryst., 66, 247 (1981), Structure and Correlations in Smectic B, F and I Phases.
- [15] H. Stegmeyer, T. Blumel, K. Hiltrop, H. Onnuseit and F. Porsch; Liq. Cryst. 1, 3-28 (1986), Thermodynamic, structural and morphological studies on liquid-crystalline blue phases.
- [16] Jan P. F. Lagerwall, Per Rudquist, Sven T. Lagerwall and Frank Gießelmann; Liq. Cryst., 30 399-414 (2003), On the phase sequence of antiferroelectric liquid crystals and its relation to orientational and translational order.
- [17] S. B. Dierker and R. Pindak; Phys. Rev. Lett., 59, 1002 (1987), Dynamics of thin tilted hexatic liquid crystal films.
- [18] E. B. Sirota, P. S. Pershan, L. B. Sorensen and J. Collett; Phys. Rev. Lett., 55, 2039 (1985), X-Ray Studies of Tilted Hexatic Phases in Thin Liquid-Crystal Films.

- [19] E. Grelet, B. Pansu, M-H Li and H. T. Nguyen; *Phys. Rev. Lett.*, 86, 3791 (2001), Structural Investigations on Smectic Blue Phases.
- [20] T. Uemura, Y. Ouchi, K. Ishikawa, H. Takezoe and A. Fukuda; *Jpn. J Appl. Phys.*, 24, L224 (1985), Optical Microscope Observation of Hexagonal Ordering in Surface Stabilized Ferroelectric Liquid Crystal Cells.
- [21] D. Ziobro, R. Dąbrowski, M. Tykarska, W. Drzewiński, M. Filipowicz, W. Rejmer, K. Kuśmierk, P. Morowiak and W. Piecek; *Liq. Cryst.*, 39, 1011 (2012), Synthesis and properties of new ferroelectric and antiferroelectric liquid crystals with a biphenyl benzoate rigid core.
- [22] W. Piecek, Z. Raszewski, P. Perkowski, J. Przedmojski, J. Kedzierski, W. Drzewinski, R. Dabrowski and J. Zielinski; *Ferroelectrics*, 310, 125 (2004), Apparent Tilt Angle and Structural Investigations of the Fluorinated Antiferroelectric Liquid Crystal Material for Display Application.
- [23] J. P. F. Lagerwall, A. Saipa, F. Giesselmann and R. Dabrowski; *Liq. Cryst.*, 31, 1175 (2004), On the origin of high optical director tilt in a partially fluorinated orthoconic antiferroelectric liquid crystal mixture.
- [24] A. Mikułko, M. Wierzejska, M. Marzec, S. Wrobel, J. Przedmojski and W. Haase; *Mol. Cryst. Liq. Cryst.*, 477, 185 (2007), Ferroelectricity of Hexatic Phases.
- [25] T. Carlsson, B. Zeks, C. Filipic, A. Levstik; *Phys. Rev. A*, 42, 877 (1990), Theoretical model of the frequency and temperature dependence of the complex dielectric constant of ferroelectric liquid crystals near the smectic-C*-smectic-A phase transition.
- [26] M. Glogarova and I. Rychetsky; *Dielectric relaxation spectroscopy, Relaxation phenomena — Liquid crystals, magnetic systems, polymers, high-TC superconductors, metallic glasses*, W. Haase and S. Wrobel, Eds., Ch 5.3 Springer-Verlag Berlin-Heidelberg (2003).
- [27] I. Rychetsky, D. Pocięcha, V. Dvorak, J. Mieczkowski, E. Gorecka and M. Glogarova; *J. Chem. Phys.*, 111, 1541 (1999), Dielectric behavior of ferroelectric liquid crystals in the vicinity of the transition into the hexatic phase.

INDEX

A

Achiral, 6, 23, 24, 65, 66, 67
Activation energy, 128, 130, 180, 212, 213
Apparent molecular length, 45, 49, 51, 61, 105, 111
Anisotropic, 22, 34, 36, 39, 56, 120, 126, 139
Antiferroelectric, 9, 18, 34, 64, 191, 200
Arrhenius law, 128, 180

B

Bicyclohexyl, 110, 112, 146
Blue phase, 15, 192, 227, 228, 234, 240
Bragg angle, 50

C

Chiral, 6, 14, 16, 51, 65, 191
Chiral dopant, 93
Cholesteric phase, 14, 227, 229, 241, 252
Cole-cole function, 65, 123, 203
Cole-cole plot, 64, 124, 173, 203
Collective mode, 192
Crystalline state, 3, 35, 57, 147, 161
Cyclohexyl, 112, 115

D

Debye type, 64, 125, 137, 173, 181, 230
Differential scanning calorimetry, 45, 47
Dielectric anisotropy, 23, 57, 60, 106, 130, 250
Dielectric permittivity, 63, 71, 115, 146, 173, 195
Dielectric relaxation, 66, 93, 122, 147, 203
Diffraction, 14, 41, 48, 50, 161, 198
Display, 19, 22, 102, 147, 249
Dipolar, 23, 124
Dipole correlation factor, 59, 120, 137, 150, 181, 249, 251

E

Electron density, 41, 79, 150
Electric field, 14, 17, 35, 69, 74, 193

F

Ferroelectric, 9, 13, 16, 22, 74, 191, 199, 209, 221
Ferroelectric liquid crystal, 16, 22, 74, 191, 227
Ferroelectric phase, 13, 23, 197, 203, 212
Fluorination, 102, 103, 106, 116, 126, 135, 162, 179, 214, 249
Frequency, 22, 51, 64, 105, 172, 208, 240

G

Goldstone mode, 68, 78, 192, 217
Gold cell, 70, 105

H

Host mixture, 93, 216, 252
Homogeneous, 7, 36, 105, 229
Homeotropic, 46, 70, 105, 161

I

Intermolecular spacing, 51
Intermolecular interaction, 35, 103
Isotropic, 4, 23, 53, 150

L

Liquid crystal display, 19, 57, 103, 146
Liquid crystalline phase, 4, 41, 107, 192, 233

M

Mesophase, 8, 16, 21, 45, 137, 238
Molecular dipole moment, 59, 64, 110, 120, 181, 250
Molecular packing, 45, 112, 231
Molecular structure, 4, 23, 85, 153, 233

N

Nematic phase, 6, 14, 36, 105, 122, 216
Neugebauer, 55, 106
Nonlinear, 199

O

Optical birefringence, 52, 106, 131, 180, 249
Orientational distribution function, 37, 45
Orientational order parameter, 35, 45, 56, 106, 134

R

Relaxation frequency, 64, 78, 124, 173, 181, 207, 241
Relaxation mode, 67, 192, 203
Relaxation process, 63, 66, 128, 137, 180, 230, 241
Rotational viscosity, 75, 77, 78, 102, 193, 208, 239, 251

S

Smectic phase, 8, 16, 49, 67, 102, 107, 126, 135, 217
Spontaneous polarization, 16, 65, 74, 75, 192, 209, 214, 230, 238
Switching time, 73, 77, 131, 170, 193, 209, 212
Symmetry operation, 160

T

Thermotropic, 4, 6
Tilt angle, 10, 20, 45, 68, 78, 192, 201, 235
Transition temperature, 5, 23, 45, 69, 104, 193, 207, 216
Translational order, 8, 40, 49, 227

V

Vuks, 55

X

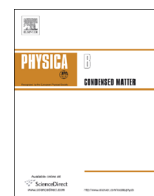
X-ray diffraction, 7, 14, 41, 48, 51, 110, 137, 171, 202, 249
X-ray photograph, 48, 74, 105, 198
X-ray scattering, 48, 105, 194, 233



ELSEVIER

Contents lists available at ScienceDirect

Physica B

journal homepage: www.elsevier.com/locate/physb

High birefringence laterally fluorinated terphenyl isothiocyanates: Structural, optical and dynamical properties

D. Sinha^a, P.K. Mandal^{a,*}, R. Dabrowski^b

^a Department of Physics, University of North Bengal, Siliguri 734013, India

^b Institute of Chemistry, Military University of Technology, 00-908 Warsaw, Poland

ARTICLE INFO

Article history:

Received 15 November 2013

Received in revised form

4 January 2014

Accepted 9 February 2014

Available online 19 February 2014

Keywords:

High birefringence isothiocyanato terphenyls

Low driving voltage

Dipole–dipole correlation factor

Molecular association

Order parameter

ABSTRACT

High birefringence liquid crystals are important for fast switching display and various other applications. One such singly fluorinated isothiocyanato terphenyl compound 2TP-3'F-4NCS which exhibits very broad range nematic (68 °C) and a narrow range smectic phase have been studied by X-ray, dielectric and optical methods. Optical birefringence and order parameters of its doubly fluorinated homologue 2TP-3',3F-4NCS have also been determined. Contrary to common perception weak antiparallel correlation of molecules is observed in both the compounds. Observed dielectric anisotropy (around 11), though less than cyano compounds, is strong enough to ensure a driving voltage suitable for thin (< 2 μm) TFT based LC display cell. Measured splay elastic constant suggests that singly fluorinated compound will exhibit faster response. Flip-flop mode relaxation is observed lowest at 510 kHz and 2.81 MHz respectively in the doubly and singly fluorinated compound. Thus the singly fluorinated compound excludes the possibility of undesirable energy absorption below MHz range applications. Above all both the compounds exhibit high birefringence, highest values being 0.373 and 0.357 respectively in the singly and doubly fluorinated compounds. Although Δn decreases with temperature it is found to be greater than 0.3 till 164 °C in 2TP-3'F-4NCS and 136 °C in 2TP-3',3F-4NCS. In addition, both the compounds exhibit high value of order parameters in low temperature region. These two compounds are, therefore, expected to be very suitable for formulating high birefringence nematic mixtures for fast switching displays.

© 2014 Elsevier B.V. All rights reserved.

1. Introduction

Response time of a nematic liquid crystal (LC) based display device is proportional to rotational viscosity and square of the display cell thickness [1]. But reduced cell thickness (d) necessitates high birefringence material to attain the appropriate optical path given by Gooch–Tarry first minima condition ($d \cdot \Delta n = \sqrt{3}\lambda/2$) in a twisted nematic cell [2]. Fast response time is especially important for color-sequential liquid crystal displays (LCDs) using blinking backlight [3] or primary-color (RGB) light-emitting diodes (LEDs) [4,5]. In the RGB LED-backlit color-sequential LCDs, the pigment color filters can be eliminated, which not only reduces the LCD cost but also triples the device resolution. High Δn materials ($0.3 < \Delta n < 0.5$) are also useful in non-display applications like laser beam steering [6], tunable colour filters [7], focus tunable lens [8], electrically controlled phase shifter in GHz and THz region [9]. High birefringence also enhances the display

brightness and contrast ratio of polymer-dispersed liquid crystals (PDLC), holographic PDLC, cholesteric LCD and LC gels [10–13]. In order to meet the demand for faster electro-optic response in nematic liquid crystal based display devices, new high birefringence (Δn) materials are, therefore, synthesized and their properties are studied in both pure and mixture state. Cyano (CN) and isothiocyanato (NCS) are two commonly employed polar groups for elongating the molecular conjugation in biphenyls, terphenyls or tolanes. As a result of longer p -electron conjugation, the NCS-based LC compounds exhibit a larger birefringence than the corresponding CN compounds. Moreover, due to lower dipole moment of NCS group ($\mu = 3.7$ D) compared to CN group ($\mu = 3.9$ D), viscosity of the NCS compounds is observed to be lower than the nitrile based systems. This is thought to be due to formation of dimmers as a result of strong intermolecular interactions between the nitrile groups which is less probable in isothiocyanato systems. However, a major concern of the CN- and NCS-based LC materials is their relatively low resistivity because of ion trapping near the polyimide alignment interfaces in device structure. Low resistivity leads to a low voltage holding ratio resulting in increased image flickering in thin film transistor (TFT)

* Corresponding author. Tel.: +91 94344 93795; fax: +91 3532 699 001.

E-mail addresses: mandal_pradip@yahoo.com, pradip.mandal@gmail.com (P.K. Mandal).

addressed liquid crystal displays. Fluorinated NCS compounds show high resistivity, at the same time they retain high birefringence. Moreover, lateral fluorine substitution in the core substantially reduces melting point and hinders formation of smectic phases because of increased lateral force due to increased volume effect and lateral dipole moment. For example, laterally singly fluorinated terphenyl isothiocyanato compound 2TP-3'-F-4NCS exhibits both smectic and nematic phase (Cr 102.5 °C SmA 120.5 °C N 188.2 °C I). Introduction of another lateral fluorine atom in the core (2TP-3',3F-4NCS) results in sharp decrease of melting point and complete suppression of smectic phase although clearing point remains same (Cr 80.2 °C N 188 °C I). Molecular formulae of both the compounds are given in Fig. 1. Results of optical polarizing microscopy, X-ray diffraction and dielectric spectroscopy studies on the nematogenic 2TP-3',3F-4NCS have recently been published [14]. In this paper we communicate high optical birefringence and order parameters of both the compounds along with X-ray and dielectric properties of singly fluorinated smectogenic compound 2TP-3'-F-4NCS. Eutectic mixtures of high birefringence nematogenic compounds are developed in order to satisfy various other physical properties including wide phase range, smectic compounds are also used in such mixture formulation [1,15,16]. In this respect both the compounds are expected to be very useful in such mixture formulation.

2. Experimental methods

The phase behavior of 2TP-3'-F-4NCS was studied under an Olympus BX41 polarizing microscope, temperature was regulated within ± 0.1 °C using Mettler FP 82 central processor and FP84 hot stage. Small and wide angle X-ray scattering measurements on randomly oriented samples were made using Ni filtered $\text{CuK}\alpha$ radiation and a custom built high temperature camera; X-ray photographs were scanned in 24 bit RGB colour format using HP2400C scanner and analyzed following procedures as detailed in earlier publications [14,17–19]. Intensity distribution, obtained from the linear scan of X-ray photographs along the equatorial and meridional diffraction peaks, was used to determine average intermolecular distance (D) and apparent molecular length (l) in nematic phase or smectic layer spacing (d) with an accuracy of 0.02 Å and 0.1 Å, respectively. Static and frequency dependent dielectric properties have been studied using computer controlled impedance analyzers HIOKI 3532-50 (50 Hz–5 MHz) and HP 4192A (100 Hz–13 MHz). Low resistivity (about $20 \Omega/\square$) polyimide-coated homogeneous (HG) cells in the form of a parallel plate capacitors with indium tin oxide (ITO) electrodes of $\sim 5 \mu\text{m}$ cell gap were used for static dielectric measurements. By applying sufficient DC bias field ($\sim 5 \text{ V } \mu\text{m}^{-1}$) homeotropic (HT) alignment of the molecules was achieved in the same cell. Perpendicular and parallel components of the dielectric constants were obtained from capacitive measurements in HG and HT cells, respectively. On the other hand, custom-built gold cells of thickness $\sim 19 \mu\text{m}$ were used for frequency dependent complex dielectric permittivity measurements. In both cases, the cells were filled by capillary action with samples in isotropic state and cell temperature was maintained within ± 0.1 °C using Eurotherm 2216e temperature controller. Very slow regulated cooling of the sample was made to get proper alignment.

Temperature dependent refractive indices were measured with He–Ne laser source ($\lambda=633 \text{ nm}$) using Chatelain–Wedge principle. Thin prisms, with angles $\sim 1^\circ$, were constructed using optically flat glass slides rubbed with polyvinyl alcohol solution (1%) in such a way that the molecules are aligned with nematic director lying parallel to the edge of the wedge. Prisms were filled with samples

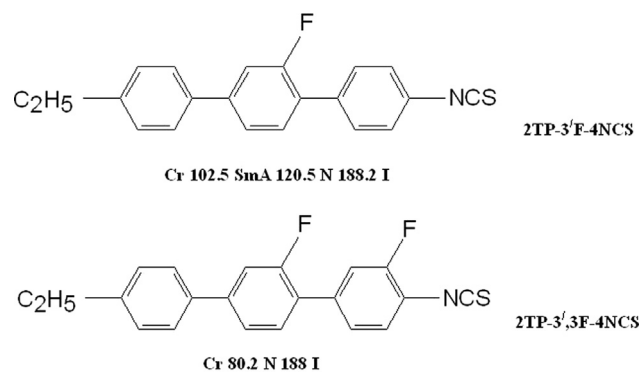


Fig. 1. Molecular structures and phase behaviour of the compounds under investigation.

in isotropic phase and cooled down very slowly. From the measured angular deflections of the ordinary and extraordinary rays on a graduated scale placed at around 5.0 m away from the sample, respective refractive indices (n_o and n_e) were determined as function of temperature. The density was measured at different temperatures using a dilatometer of capillary type, a travelling microscope, and a temperature controller; correction for glass expansion was made. The temperature was controlled within ± 0.5 °C in both cases and the accuracy of density and refractive index measurement was 0.001.

Molecules in the nematic phase have no positional correlation but they do have long-range orientational ordering. The extent of ordering is usually qualified by orientational order parameters (OOPs), which are uniaxial and are expressed by a traceless symmetric tensor of rank 2. Many physical properties like optical birefringence, dielectric anisotropy, threshold voltage for switching, etc., which are important device parameters, depend upon the OOPs. Orientational order parameter $\langle P_2 \rangle$ was calculated using the principal molecular polarizabilities α_o and α_e , perpendicular and parallel to the direction of optic axis, following de Gennes relation [20].

$$\langle P_2 \rangle = \frac{\alpha_e - \alpha_o}{\alpha_{\parallel} - \alpha_{\perp}}$$

α_o and α_e were calculated using the following Lorenz–Lorentz equations modified for anisotropic systems by Neugebauer [21].

$$\frac{1}{\alpha_e} + \frac{2}{\alpha_o} = \frac{4\pi N}{3} \left[\frac{n_e^2 + 2}{n_e^2 - 1} + \frac{2(n_o^2 + 2)}{n_o^2 - 1} \right]$$

$$\alpha_e + 2\alpha_o = \frac{9}{4\pi N} \left[\frac{n^2 - 1}{n^2 + 2} \right]$$

α_{\parallel} and α_{\perp} are the principal polarizabilities parallel and perpendicular to the long axes of the molecules in the perfectly ordered crystalline state where $\langle P_2 \rangle = 1$, which are difficult to measure experimentally. Haller's extrapolation procedure [22] was used to get those values.

3. Results and discussion

3.1. Optical polarization microscopy

Observed textures, topological defect structures observed under optical polarizing microscope, confirmed presence of SmA phase over 18 °C as well as broad range nematic phase exceeding 67 °C, transition temperatures are shown in Fig. 1. Observed focal conic texture in SmA phase and schlieren texture in nematic phase are shown in Fig. 2.

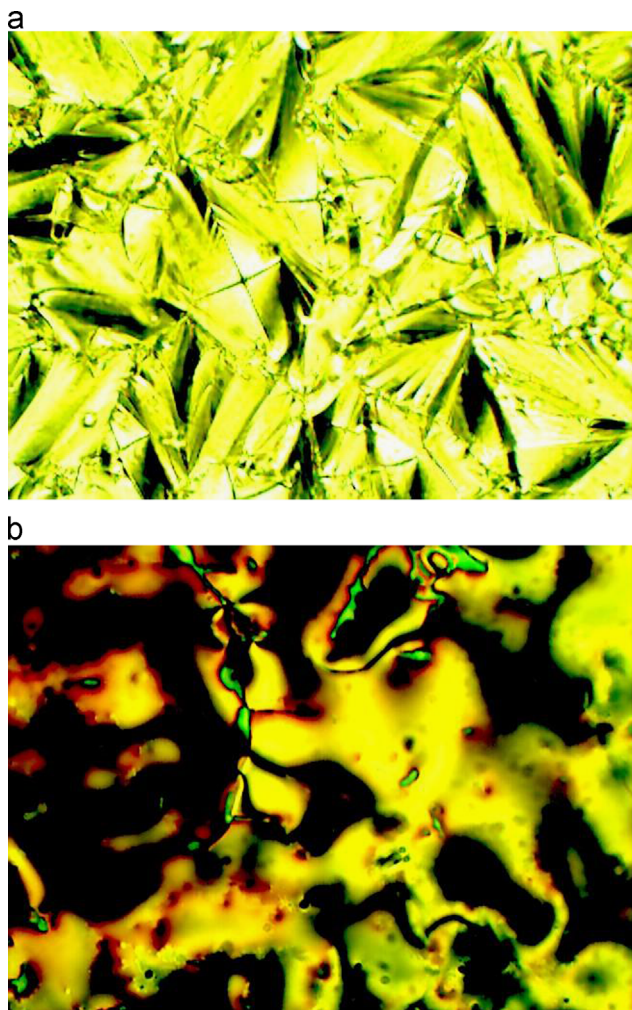


Fig. 2. Textures observed in SmA Phase (108 °C) and Nematic Phase (180 °C) of 2TP-3'F-4NCS.

3.2. X-ray diffraction study

Typical X ray diffraction photographs in SmA and nematic phases of 2TP-3'F-4NCS are shown in Fig. 3. The photographs contained two major diffraction maxima. Layer structure in SmA phase is clearly visible in the form of sharp inner ring compared to the nematic pattern. The inner ring is related to the layer spacing (d) in the smectic phase and the apparent length of the molecule (l) in the nematic phase. The diffused outer ring arises due to interaction of the neighboring molecules in a plane perpendicular to the molecular axis providing average intermolecular distance (D). These values were calculated using the relations given by de Vries [23]. Temperature variations of average intermolecular distance, apparent molecular length and layer spacing are depicted in Fig. 4.

It is evident that D increases with temperature indicating a slight decrease in molecular packing. From the fitted curves clear discontinuities are observed at SmA–N transition signifying first order phase transition. Average intermolecular distances are found to be slightly less in singly fluorinated 2TP-3'F-4NCS compared to those observed in the doubly fluorinated 2TP-3',3F-4NCS [14], average values being 5.5 Å and 5.66 Å, respectively. This is expected since introduction of additional F-atom in the core benzene ring increases lateral volume. This is further supported by the fact that in several homologues of non-fluorinated phenyl cyclohexyl based isothiocyanates D -values were found to vary

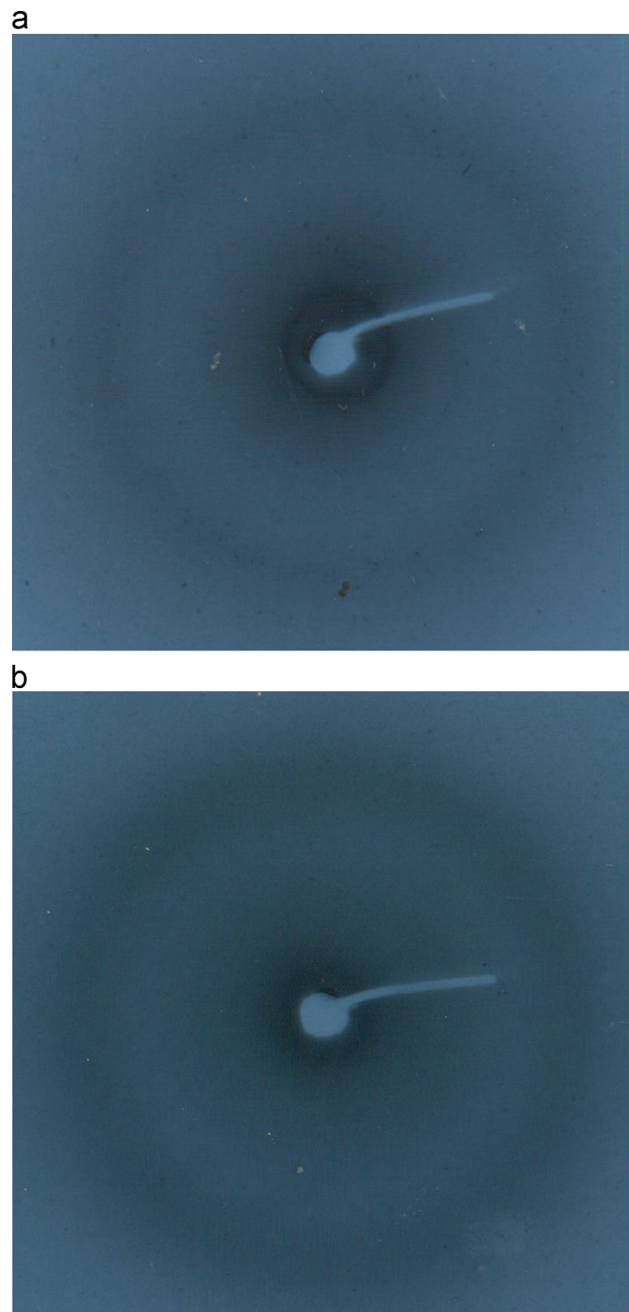


Fig. 3. X-ray diffraction photographs in SmA phase (110 °C) and nematic phase (125 °C).

from 5.06 Å to 5.12 Å [24], much less compared to the fluorinated molecules. D was observed as 5.48 Å when one lateral fluorine atom was present in the benzene ring of a terminally fluorinated nematogenic bicyclohexyl phenyl compound, whereas it increased to 5.60 Å when two lateral fluorine atoms were connected on opposite sides of the benzene ring [25]. Therefore, present observation on D is consistent with previous reported data of structurally similar compounds.

The smectic layer spacing (d) is found to increase from 19.45 Å to 24.91 Å while effective length of the molecules (l) increases from 24.99 Å to 29.65 Å in nematic phase as shown in Fig. 4. In this case also clear discontinuities are observed at SmA–N transition. Optimized geometry, obtained from molecular mechanics calculation using semi-empirical PM3 method in Hyperchem [26], yielded a dipole moment of 5.57 Debye and molecular length

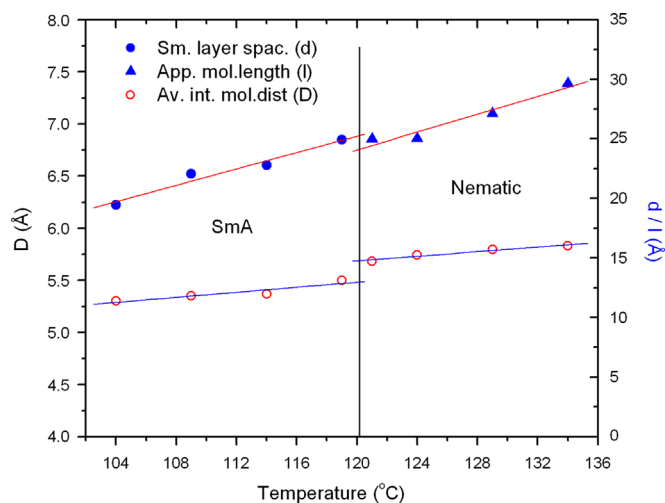


Fig. 4. Variation of average intermolecular distance (D), smectic layer spacing (d) and apparent molecular length (l) with temperature.

18.56 Å. Thus, the effective length of the molecules in N phase and layer spacing in smectic phase are considerably higher than molecular length. Similar observation was reported in doubly fluorinated 2TP-3',3F-4NCS [14] and in non-fluorinated isothiocyanobenzenes [24]. This suggests presence of some sort of molecular association among the neighboring molecules, usually antiparallel molecular associations are suggested in molecules having terminal polar groups [27], no such association is observed in systems having no terminal polar groups from either X-ray study or dielectric study [28,29]. It may further be noted that parallel and perpendicular component of dipole moments are 5.48 D and 1.02 D respectively in 2TP-3' F-4NCS whereas in 2TP-3',3F-4NCS the values are 6.39 D and 1.95 D, respectively. Thus although the present molecules are not strictly axially polar but axial dipole moments are much stronger than the transverse components resulting in antiparallel associations. With increasing temperature thermal energy probably helps to overcome the dipolar interaction partially, thereby increasing the apparent molecular length. Antiparallel associations in NCS compounds were also confirmed from crystal structure analysis of eleventh member of phenyl cyclohexyl isithiocyanates [30].

3.3. Static dielectric study

In order to determine switching voltage required to switch molecular alignment from planar (HG) to homeotropic (HT) configuration, dielectric constant was measured as a function of DC bias voltage across the cell. The switching characteristic in nematic phase is shown in Fig. 5. Voltage at which the real part of dielectric permittivity increases by 10% from its minimum value is called threshold voltage (V_{th}) and at which it reaches 90% of the maximum value is termed as driving voltage (V_d) [14]. For 2TP-3',3F-4NCS these were found to be 4.52 V and 9.6 V respectively in a cell of thickness 5 μm . Driving field is found to be 2.2 $\text{V}\mu\text{m}^{-1}$ in the singly fluorinated 2TP-3' F-4NCS, considerably higher than in the doubly fluorinated compound (1.9 $\text{V}\mu\text{m}^{-1}$). However, driving voltage for both the compounds is suitable for thin (< 2 μm) TFT based LC display cells. Nevertheless, 5 $\text{V}\mu\text{m}^{-1}$ field was used for switching from HG to HT configuration while measuring $\epsilon_{||}$ and ϵ_{\perp} .

Variation of principal dielectric constants with temperature is shown in Fig. 6. From the figure it is clear that $\epsilon_{||}$ decreases slowly with increasing temperature whereas ϵ_{\perp} remains almost constant. Average value of the dielectric constant ϵ_{av} , defined as $(\epsilon_{||} + 2\epsilon_{\perp})/3$, also remains almost independent of temperature as shown in

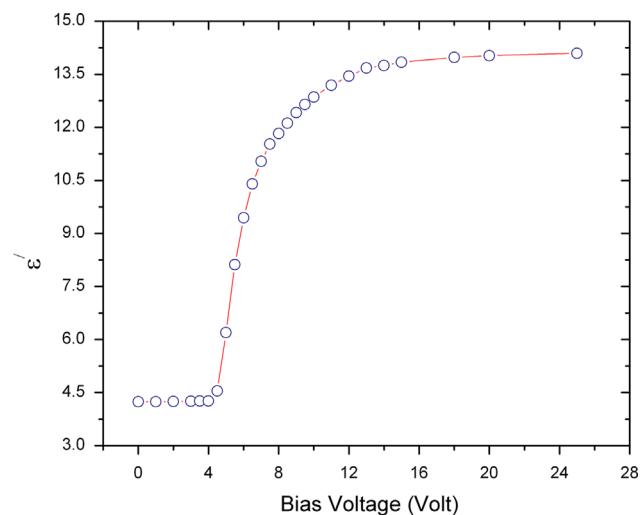


Fig. 5. Real part of dielectric constant (ϵ') as function of bias voltage at 10 kHz in 5 μm thick ITO cell at 123 $^{\circ}\text{C}$.

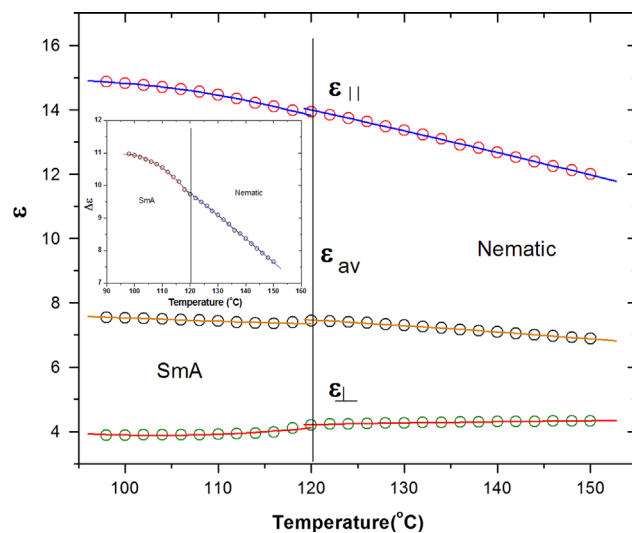


Fig. 6. Variation of static dielectric constants as a function temperature at 10 kHz in ITO cell in 2TP-3'F-4NCS.

Fig. 6. Slight discontinuity is observed in the dielectric parameters at SmA–N transition although not as prominent as observed in X-ray study. Since the molecules possess quite strong axial dipole moment, $\epsilon_{||}$ is found to be large (about 15 near Cr–N transition) compared to ϵ_{\perp} (about 4) whereas corresponding values for 2TP-3',3F-4NCS were about 17 and 6. This is due to the fact that the dipole moments along and perpendicular to molecular axes are large in later than in the former as noted earlier.

Temperature variation of dielectric anisotropy ($\Delta\epsilon = \epsilon_{||} - \epsilon_{\perp}$) is also shown in Fig. 6 as inset. It is found to decrease with temperature, decrement rate is, however, less in smectic than in nematic phase. Observed $\Delta\epsilon$ near Cr–SmA transition is 11 and near SmA–N transition it is 9.7 which is slightly less than in 2TP-3',3F-4NCS where it was 10.6 near Cr–N transition.

Following Bordewijk theory [31] of anisotropic dielectrics effective value of dipole moment in smectic and nematic phase were calculated and found respectively to be 5.37 D and 5.40 D whereas free molecule dipole moment was 5.57 D again suggesting antiparallel correlation of molecules. Although it was thought before that NCS compounds do not form dimers [16] like the CN compounds but X-ray study in crystalline and mesophase as well as dielectric study confirms formation of dimers in NCS

compounds. To obtain a quantitative measure of this correlation, dipole–dipole correlation factor g_λ , defined as follows, was calculated following the procedure of Bata and Buka [32]

$$g_\lambda = \frac{\left\langle \sum_{i \neq j} (\mu_\lambda)_i (\mu_\lambda)_j \right\rangle}{\langle \mu_\lambda^2 \rangle}$$

where correlation factor g_λ takes into account the correlation between the neighbouring dipole moments only and the subscript λ refers to axes \parallel and \perp to the nematic director. It is noted that $g_\lambda=1$ signifies no correlation at all (monomeric system), $g_\lambda=0$ means perfect antiparallel correlation and $g_\lambda=2$ means perfect parallel correlation. g_\parallel was found to be 0.35 in smectic phase and 0.40 in nematic phase signifying weak antiparallel correlation of the components of dipole moments along the molecular axes in nematic phase, correlation slightly improves in smectic phase. Corresponding values of g_\perp were 0.88 and 0.95 suggesting almost no antiparallel correlation of the perpendicular components of the dipole moments. Calculation of g_λ in 2TP-3'F-4NCS reveals that antiparallel correlation is slightly more in this system than the singly fluorinated compound. Effective value of dipole moment in this system is also found to be less (6.01 D) than the free molecule dipole moment (6.68 D).

Splay elastic constant (K_{11}), another important parameter for switching, was calculated using the following formula derived for Fredericksz transition [33]

$$K_{11} = \frac{\epsilon_0 \Delta \epsilon V_{th}^2}{\pi^2}$$

where $\epsilon_0=8.85 \text{ pF m}^{-1}$ is the dielectric permittivity in free space. It is, as expected, found to exhibit similar decreasing trend as observed in dielectric anisotropy. K_{11} near Cr–SmA transition ($20.5 \times 10^{-11} \text{ N}$) is found to be almost 1.5 times more than that observed ($14.0 \times 10^{-11} \text{ N}$) in 2TP-3'F-4NCS [14]. This is also more than that observed in a doubly fluorinated phenyl bicyclohexyl [34] and in a non-fluorinated hexylcyclohexyl isothiocyanatobenzene [35]. Since switching time is inversely proportional to K_{11} , faster response is expected in singly fluorinated compound.

3.4. Dielectric relaxation study

To see the dynamic response of the compound to an ac field, frequency dependent dielectric study was performed as a function of temperature in a gold coated cell. The frequency dependence of dielectric permittivities are shown in Figs. 7 and 8 only at some

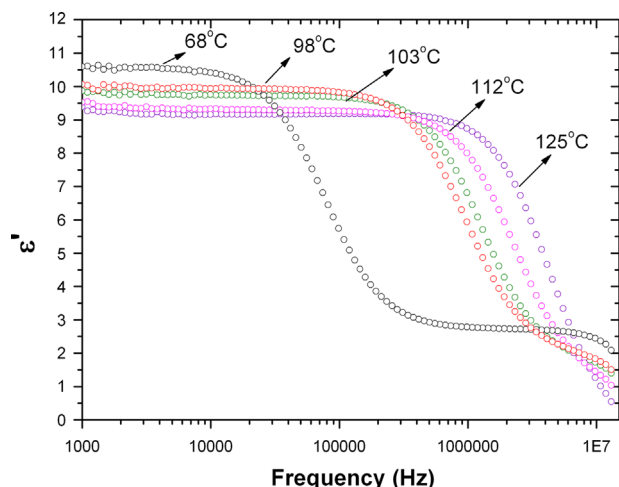


Fig. 7. Real (ϵ') part of dielectric permittivity of 2TP-3'F-4NCS as a function of frequency at some selected temperatures in gold cell.

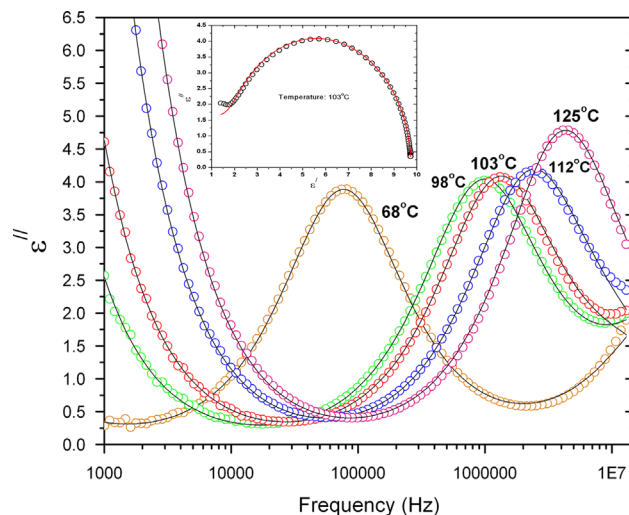


Fig. 8. Fitted dielectric absorption spectra at some selected temperatures in gold cell. Cole-Cole plot at 103 °C is shown in the inset.

selected temperatures for clarity. It is clear from Fig. 7 that the real part of dielectric permittivity remains almost constant till 200 kHz in the SmA phase as well as in the nematic phase. Considerable supercooling effect is observed and dielectric behaviour is different in the supercooled state. With temperature real dielectric constant is found to decrease from 10.6 (68 °C) to 8.8 (130 °C) in 2TP-3'F-4NCS, while in doubly fluorinated homologue it was found to increase from 16.3 (77 °C) to 18.8 (98 °C), then decreases to 12.9 (122 °C) [14]. Different behavior may be due to different phase behavior of the compounds.

Only one strong absorption process is observed in dielectric spectra as evident from Fig. 8. The ϵ'' peak height increases slightly with temperature in the smectic A as well as in the nematic phase and thus there are a larger number of free molecules (monomers) with a corresponding enhancement of the effective dipole moment at higher temperature [36]. Moreover, although no surface treatment or no external field treatment was made, natural molecular orientation in gold cell seems to be predominantly homeotropic because observed dielectric constant in low frequency (Fig. 7) is similar to that under high bias voltage (Fig. 5). However, in the supercooled SmA phase (68–102 °C), indication of existence of another relaxation mode beyond 10 MHz is present in the spectra which might be associated with molecular rotation around long axis, suggesting coexistence of homeotropic and homogeneous alignment of molecules in the cell. This could not be confirmed because of the limitation of measurement frequency of the impedance analyzer.

Relaxation frequencies are also found to increase with temperature. Assuming the relaxation behavior is a result of Cole–Cole type process, the complex dielectric permittivity was fitted with the following modified Cole–Cole equation [37] to get the actual values of relaxation frequency (f_c)

$$\epsilon^* = \epsilon' - i\epsilon'' = \epsilon_\infty + \frac{\Delta\epsilon}{1 + (i\omega\tau)^{1-\alpha}} - \frac{i\sigma}{\omega\epsilon_0}$$

where ω is the angular frequency ($\omega=2\pi f_c$), $\Delta\epsilon$ is the dielectric strength or increment, τ_0 is the most probable relaxation time related to the critical frequency f_c as $\tau_0=(1/2\pi f_c)$, α is a parameter responsible for symmetric distribution of relaxation times and σ is the conductivity related to motion of charge carriers. Fitting was made for two absorption processes—flip-flop mode and gold mode. Fitted curves are also shown in Fig. 8. As real and imaginary parts of dielectric constants are related through Kramers–Kronig relations, the Cole–Cole plot of the fitted spectra at 103 °C, as a

representative case, is shown in Fig. 8 as inset which shows that the fitting was quite good. Nature of the absorption process is found to be almost Debye type since in no case fitted α is more than 0.05, similar to that observed in doubly fluorinated compound. The conductivity (σ) of the cell is found to be 2.573×10^{-7} mho m^{-1} .

Relaxation frequency, assumed to be associated with rotation around short molecular axis (flip-flop mode), increases systematically with temperature, from 82 kHz to 2.56 MHz in SmA phase and in N phase it increases further from 2.81 MHz to 12.5 MHz, but in 2TP-3',3F-4NCS it was found to be much lower, varied from 510 kHz to 1.77 MHz. These values are lower than in cyanobiphenyls e.g. in 5CB it was 15.6 MHz [38]. This is expected since for rigid molecules f_c varies inversely with square root of moment of inertia [39] and present molecules have larger moments of inertia mainly because of large increase in their molecular mass compared to 5CB. Indeed, molecular mechanics calculation revealed that principal moments of inertia of 2TP-3'F-4NCS, 2TP-3',3F-4NCS and 5CB were respectively 68.27×10^{-46} , 1471.02×10^{-46} , 1538.24×10^{-46} kg m^{-2} ; 76.7×10^{-46} , 1550.0×10^{-46} , 1626.6×10^{-46} kg m^{-2} and 42.9×10^{-46} , 844.1×10^{-46} , 884.3×10^{-46} kg m^{-2} , where the first inertial axis is along the molecular long axis and the second one is along short molecular axis.

Increase of relaxation frequency with temperature suggests that it should obey Arrhenius law [37,40]. From a plot of $\ln(\tau)$ versus inverse temperature the activation energy of the thermally activated relaxation process was calculated and found to be 83.8 kJ mol^{-1} in SmA phase and 36.8 kJ mol^{-1} in N phase. In 2TP-3',3F-4NCS it was 35.2 kJ mol^{-1} [14]. Hence introduction of an additional fluorine atom decreases both the critical frequency and activation energy.

3.5. Optical birefringence and order parameters

Temperature variation of ordinary, extraordinary and average refractive indices (n_o , n_e , n_{av}) along with optical birefringence (Δn) in the nematic phase of both the compounds is shown in Fig. 9, no measurement was possible in the smectic phase of 2TP-3'F-4NCS. Although n_o is almost same, n_e in 2TP-3',3F-4NCS is found to be less than in 2TP-3'F-4NCS which may be due to less π -electron conjugation along the molecular axis because of the introduction of additional lateral fluorine atom as well as less order parameter. Both the compounds exhibit high birefringence, highest values being 0.373 and 0.357 in 2TP-3'F-4NCS and 2TP-3',3F-4NCS,

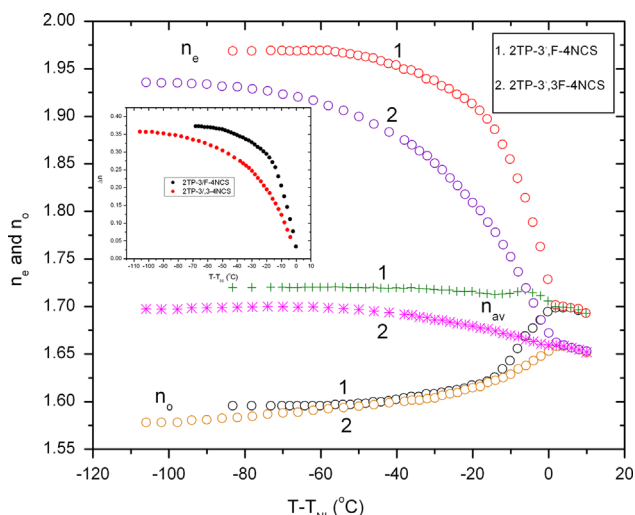


Fig. 9. Variation of n_e , n_o , n_{av} and Δn of 2TP-3'F-4NCS and 2TP-3',3F-4NCS as a function temperature.

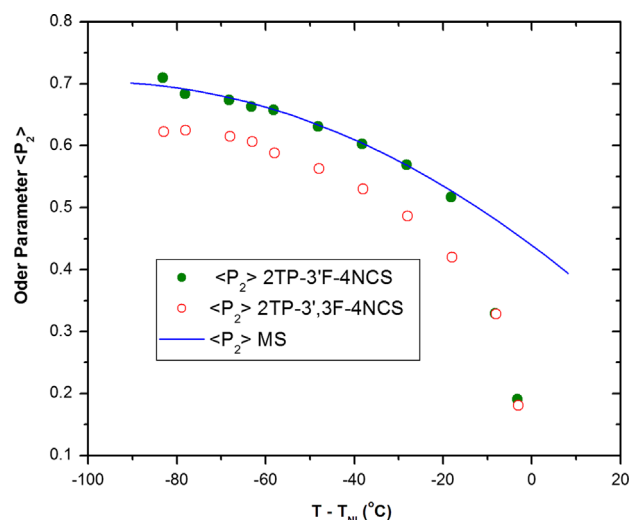


Fig. 10. Variation order parameters as a function temperature.

respectively. These values are comparable to reported values in nematic mixtures formulated using isothiocyanato terphenyls or isothiocyanato tolanes [1,16,41]. Although Δn decreases with temperature it is found to be greater than 0.3 till 164 °C in 2TP-3'F-4NCS and till 136 °C in 2TP-3',3F-4NCS. Commercially available high- Δn TFT-grade LC mixtures usually have $\Delta n \sim 0.2$. These two compounds are therefore expected to be very suitable for formulating high birefringence nematic mixtures.

In 2TP-3'F-4NCS measured densities are found to vary from 1.191 (90 °C) $g\ cm^{-3}$ to 1.151 $g\ cm^{-3}$ (110 °C) in SmA phase and from 1.142 $g\ cm^{-3}$ (120 °C) to 1.014 $g\ cm^{-3}$ (185 °C) in N phase. Because of the second lateral fluorine atom, 2TP-3',3F-4NCS is found to be less densely packed, observed densities being 1.087 $g\ cm^{-3}$ at 85 °C and 1.041 $g\ cm^{-3}$ at 185 °C.

Temperature variation of calculated principal molecular polarizabilities (α_o , α_e and α_{av}) is found to be similar to that of the refractive indices. Average value of α was found to be 28.73×10^{-24} cm^3 and 31.04×10^{-24} cm^3 respectively in the singly and doubly fluorinated compounds. Temperature dependence of orientational order parameter (P_2) for both the compounds is depicted in Fig. 10 wherein order parameters computed on the basis of Maier-Saupe mean field theory for calamitic nematogens have also been presented. In smectic A phase, as expected, order parameter is more (0.71 at 105 °C) than in nematic phase (0.67 at 120 °C). This is further less in 2TP-3',3F-4NCS being 0.62 at 85 °C. Thus the doubly fluorinated compound is not only less densely packed but orientationally less ordered as well.

4. Conclusions

Several physical parameters, important from application consideration, have been determined for a singly laterally fluorinated isothiocyanato terphenyl compound 2TP-3'F-4NCS which exhibits very broad range nematic phase (68 °C) in addition to a narrow smectic phase. Optical birefringence and order parameters of its doubly fluorinated homologue have also been determined. Contrary to common perception weak antiparallel correlation of molecules is observed in both the isothiocyanato compounds. Observed dielectric anisotropy, around 11, though less than cyano compounds, is strong enough to ensure a driving voltage suitable for thin ($< 2\ \mu m$) TFT based LC display cell. Value of splay elastic constant suggests that singly fluorinated compound will exhibit faster response. Flip-flop mode relaxation is observed lowest at 510 kHz in the doubly fluorinated compound which for the singly

fluorinated compound is 2.81 MHz. Thus the singly fluorinated compound excludes the possibility of undesirable energy absorption below MHz range applications. Above all both the compounds exhibit high birefringence, highest values being 0.373 and 0.357 respectively in the singly and doubly fluorinated compounds. Although Δn decreases with temperature it is found to be greater than 0.3 till 164 °C in 2TP-3'F-4NCS and upto 136 °C in 2TP-3',3F-4NCS. In addition both the compounds exhibit high value of order parameter in low temperature region. These two compounds are therefore expected to be very suitable for formulating high birefringence nematic mixtures for fast switching displays.

Acknowledgment

The authors like to thank W. Haase, Institute of physical Chemistry, TU Darmstadt, Petersenstr. 20, Darmstadt, Germany for active help and support.

References

- [1] S. Gauza, X. Zhu, W. Piecek, R. Dabrowski, S.T. Wu, J. Disp. Technol. 3 (3) (2007) 250.
- [2] M. Schadt, W. Helfrich, Appl. Phys. Lett. 18 (1971) 127.
- [3] K. Nishiyama, M. Okita, S. Kawaguchi, K. Teranishi, R. Takamatsu, SID Tech. Dig. 36 (2005) 132.
- [4] H.S. Hsieh, C.H. Chou, W.Y. Li, Proceedings of International Display Manufacturing Conference (2005) 622.
- [5] G. Harbers, C. Hoelen, SID Tech. Dig. 32 (2001) 702.
- [6] D.P. Resler, D.S. Hobbs, R.C. Sharp, L.J. Friedman, T.A. Dorschner, Opt. Lett. 21 (9) (1996) 689.
- [7] J.Y. Hardeberg, F. Schmitt, H. Brettel, Opt. Eng. 41 (10) (2002) 2532.
- [8] H.C. Lin, Y.H. Lin, Opt. Express 20 (3) (2012) 2045.
- [9] T.T. Ru, C.C. Yuan, R.P. Pan, C.L. Pan, X.C. Zhang, IEEE Microwave Wireless Compon. Lett. 14 (2) (2004).
- [10] J.L. Ferguson, SID Tech. Dig. 16 (1985) 68.
- [11] R.L. Sutherland, V.P. Tondiglia, L.V. Natarajan, Appl. Phys. Lett. 64 (1994) 1074.
- [12] N. Mizoshita, K. Hanabusa, T. Kato, Adv. Funct. Mater. 13 (2003) 313.
- [13] Y.H. Fan, H.W. Ren, S.T. Wu, Appl. Phys. Lett. 82 (2003) 2945.
- [14] D. Sinha, D. Goswami, P.K. Mandal, Ł. Szczucinski, R. Dabrowski, Mol. Cryst. Liq. Cryst. 562 (2012) 156.
- [15] S. Gauza, J. Li, S.T. Wu, A. Spadło, R. Dabrowski, Y.N. Tzeng, K.L. Cheng, Liq. Cryst. 32 (8) (2005) 1077.
- [16] S. Gauza, S.T. Wu, A. Spadło, R. Dabrowski, J. Disp. Technol. 2 (3) (2006) 247.
- [17] B. Jha, S. Paul, R. Paul, P. Mandal, Phase Transitions. 15 (1989) 39.
- [18] A.de. Vries, Mol. Cryst. Liq. Cryst. 10 (1970) 31.
- [19] B.R. Jaishi, P.K. Mandal, Liq. Cryst. 33 (2006) 753.
- [20] P.G. deGennes, Mol. Cryst. Liq. Cryst. 12 (1971) 193.
- [21] H.E.J. Neugebauer, Canadian J. Phys. 32 (1954) 1.
- [22] I. Haller, H.A. Huggins, H.R. Lilienthal, T.R. McGuire, J. Phys. Chem. 77 (1973) 950.
- [23] A. de Vries, Mol. Cryst. Liq. Cryst. 10 (1970) 219.
- [24] P. Sarkar, P. Mandal, S. Paul, R. Dabrowski, K. Czuprynski, Liq. Cryst. 30 (4) (2003) 507.
- [25] S. Haldar, S. Barman, P.K. Mandal, W. Haase, R. Dabrowski, Mol. Cryst. Liq. Cryst. 528 (2010) 81.
- [26] Hyperchem 6.03, Hypercube Inc., Gainesville, FL, USA.
- [27] A.J. Leadbetter, R.M. Richardson, C.N. Cooling, J. Phys. 36 (C1) (1975) 37 (Paris).
- [28] P.K. Sarkar, S. Paul, P. Mandal, Mol. Cryst. Liq. Cryst. 265 (1995) 249.
- [29] N.V. Madhusudana, S. Chandrasekhar, Pramana Suppl. 1 (1975) 57.
- [30] S. Biswas, S. Haldar, P.K. Mandal, K. Goubitz, H. Schenk, R. Dabrowski, Cryst. Res. Technol. 42 (10) (2007) 1029.
- [31] P. Bordewijk, Physica. 75 (1974) 146.
- [32] L. Bata, A. Buka, Mol. Cryst. Liq. Cryst. 63 (1981) 307.
- [33] B. Kundu, S.K. Pal, S. Kumar, R. Pratibha, N.V. Madhusudana, Phys. Rev. E: Stat. Nonlinear Soft Matter Phys. 82 (2010) 061703.
- [34] H. Ishikawa, A. Toda, H. Okada, H. Onnagawa, S. Sugimori, Liq. Cryst. 22 (1997) 743.
- [35] R. Dhar, A.S. Pandey, M.B. Pandey, S. Kumar, R. Dabrowski, Appl. Phys. Express 1 (2008) 121501.
- [36] N.V. Madhusudana, B.S. Srikanta, R. Subramanya, M. Urs, Mol. Cryst. Liq. Cryst. 108 (1984) 19.
- [37] J. Schacht, P. Zugenmaier, M. Buivydas, L. Komitov, B. Stebler, S.T. Lagerwall, F. Gouda, F. Horii, Phys. Rev. E: Stat. Nonlinear Soft Matter Phys. 61 (2000) 3926.
- [38] M. Gu, Y. Yin, S.V. Shivanovskii, O.D. Lavrentovich, Phys. Rev. E: Stat. Nonlinear Soft Matter Phys. 76 (2007) 061702.
- [39] H. Baessler, R.B. Beard, M.M. Labes, J. Chem. Phys. 52 (1970) 2292.
- [40] A.C. Diogo, A.F. Martins, J. Phys. 43 (1982) 779 (Paris).
- [41] M.D. Gupta, A. Mukhopadhyay, S.K. Roy, R. Dabrowski, J. Appl. Phys. 113 (2013) 053516.